E7.6-10.1 3.4
CR - 144485

DETECTION OF SOIL MOISTURE

AND SNOW CHARACTERISTICS FROM SKYLAB
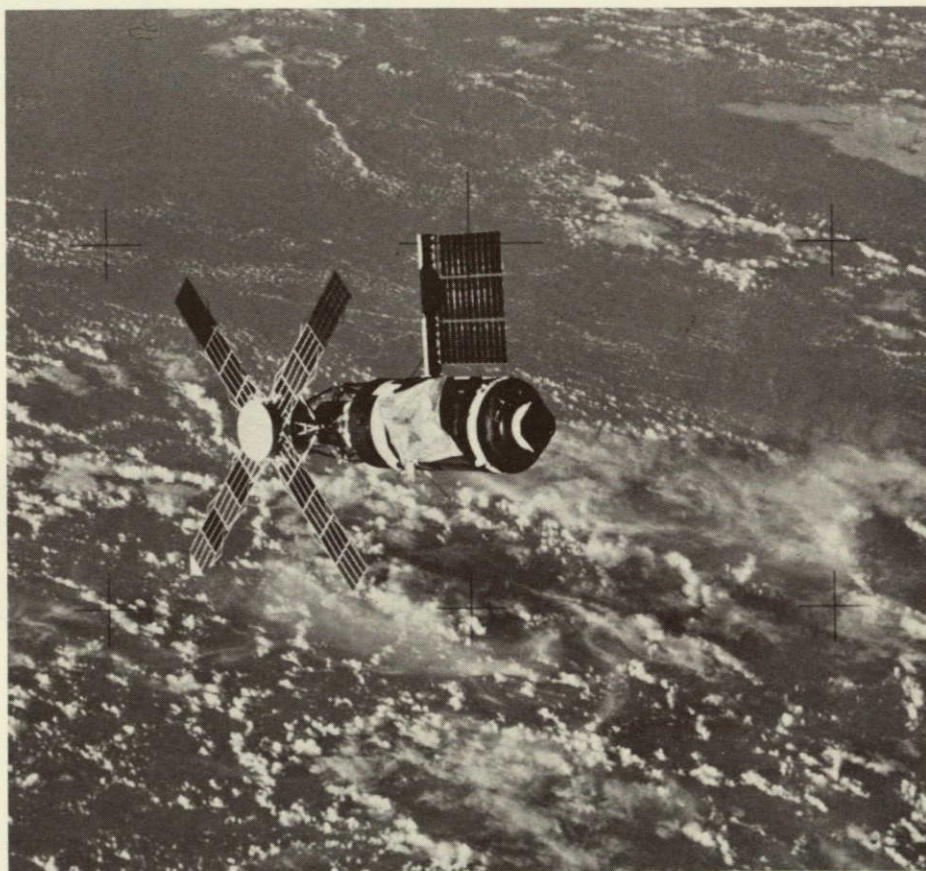
Joe R. Eagleman

Principal Investigator
NASA Contract NAS 9-13273

DETECTION OF SOIL MOISTURE

AND SNOW CHARACTERISTICS FROM SKYLAB

Joe R. Eagleman
Ernest C. Pogge
Richard K. Moore

With the assistance of:

Wen Lin
Norman Hardy
Richard Sloan
Surrenda Parashar
Charles Perry
Larry League
Margaret Engling

Atmospheric Science Laboratory
Space Technology Center, Center for Research, Inc.
University of Kansas
Lawrence, Kansas 66045

TABLE OF CONTENTS

Chapter I

BACKGROUND OF MICROWAVE MOISTURE MEASUREMENTS

Introduction

In the pursuit of understanding the world in which he
lives, man has reached into the depths of outer space itself
and has viewed the earth in a perspective never before pos-
sible. This age of sophisticated electronics has also pro-
duced varied instrumentation with which to extract earth re-
source data from orbital altitudes. Some devices, such as
ultra-violet and gamma ray instrumentation, are designed to
measure higher frequencies (shorter wavelengths) than our
human sensory mechanisms can detect. Others operate within
the visible spectrum (0.4-0.7 micrometers, μm) and include
most devices using photographic film. Still others operate
at wavelengths longer than our senses are capable of detect-
ing. These include instruments performing in the near-infra-
red (0.8-1.5 μm), the middle infrared (1.5-5.5 μm) and the
far-infrared (5.5-1000 μm) and the numerous radar and micro-
wave sensors (>1000 μm). Some systems readily detect a par-
ticular phenomenon, while others are "blind" to the identical
phenomenon.

Microwave backscatter and emission are both strongly de-
pendent on the moisture content of soil, vegetation and snow.
This comes about because of the relationship of microwave
backscatter and emission to the dielectric properties of the
scattering and emitting surface, and the relationship of these
dielectric properties to moisture content.

The dielectric constant of water at microwave frequencies
is quite large, as much as 80, whereas that of dry soil is
typically less than 5 and that of dry snow is less than 2.
Therefore, the water content of soil or snow can greatly af-
fect their dielectric properties. This suggests the applica-
tion of microwave remote sensors for monitoring soil moisture
content and snow properties.

Previous Investigations

In the mid-1960's, Kennedy (1968) and Edgerton et al.,
(1969) began the investigation of passive microwave sensors
for determination of soil moisture content. Numerous theo-
retical studies (Peake, 1959; Chen and Peake, 1961; Poe et al.,
1971; Stogryn, 1967; Fung et al., 1965; and Johnson, 1972)
and experimental studies (Schmugge et al., 1974; Jean, 1971;
Lee, 1974) have been conducted to measure soil moisture with
microwave radiometers. The radiometric results indicated
that under some conditions the soil moisture content can be
determined quite accurately and the passive microwave radio-
meter has high potential in this application.

Schmugge et al., (1974) reported a series of aircraft
flights over bare land using microwave radiometers in the
wavelength range of 0.8 cm to 21 cm. The results indicated
that it is possible to monitor soil moisture variations with
airborne microwave radiometer wavelengths and to determine
the distribution of soil moisture. It was shown that the
longer wavelengths were more sensitive to variations of soil
moisture content.

Sibley, (1973) has investigated the effects of vegetatio
on microwave emission. A theoretical model has been develope
for the apparent temperature of vegetated terrains for use in
soil moisture studies.

Lee, (1974), using a passive microwave radiometer system
of 1.41 GHz (21.13 cm. L-band) and 10.69 GHz (2.81 cm, X-band
for a field experiment has found that the L-band is more sen-
sitive to soil moisture variations than the X-band for all
surface types.

Another microwave remote sensor for soil moisture con-
tent detection is radar. The effects of soil moisture on the
radar return have been examined in the laboratory (Lundien,
1966) through the interpretation of airborne scatterometer
data (King, 1973), and by imaging radar (Waite & Mac Donald,
1970). Ulaby (1974) has shown that the radar response to
soil moisture content between 5 and 8 GHz is influenced by
surface roughness,microwave frequence and look angle. Ulaby
(1974-b) also has shown that the moisture content of the
soil strongly influences its dielectric properties at small
incidence angles (relative to normal) and the lower microwave
frequencies for vegetated surfaces.

King, (1973) and Dickey et al.,(1974) analyzed data from
13.3 GHz and 400 MHz scatterometers and found that for inci-
dence angles less than 40° the 13.3 GHz data showed a differ-
ence in backscatter from wet and dry fields of the order of
7 db. The averages of the various crop types were within a
spread of only 5 db.

In 1971, Poe et. al investigated the soil moisture content of a plot at the USDA's U.S. Water Conservation laboratory in Tempe, Arizona. This study encompassed #1, multiple wavelength microwave radiometric measurements (8.1 μm, 2.2 cm, 6.0 cm and 21.4 cm); and #2, dielectric constant measurements (8.1 μm and 2.2 cm), the numerical modelling of dielectric mixtures (soil, air water), and the emission characteristics of soils. This study minimized complicating features due to surface and lateral variations in the soils. Thus, the primary variables subject to measurements and analysis were the distribution of moisture and temperature within the soil.

The disagreement of measured and calculated temperature for 6.0, 2.2 and 0.81 cm was probably due to uncertainties in the near surface soil temperatures. Closer agreement at 21.4 cm was due to the greater skin depth, which implies that warm soil temperature in the first few centimeters had little effect on the 21.4 cm radiometric temperature.

Schmugge, Gloersen and Wilheit (1972 and 1974) used microwave radiometers to measure surface temperatures. Measurements were by a nadir viewing infrared radiometer operating in the 10 to 12 μ atmospheric windows. Agricultural test sites were located in the vicinity of Phoenix, Arizona; Weslaco, Texas; and the Imperial Valley, California. The majority of the selected fields were without vegetative cover and at least 400 meters on a side. In the Imperial Valley and Phoenix area four 15-cm soil samples were taken in each field to yield the

average soil moisture for the top 15 cm in the soil. More detailed surface truth data were available for flights over Weslaco, Texas. A surface sample one to three centimeters deep and a subsurface sample at a depth of 15 cm were taken. The study was conducted at frequencies of 1.42 GHz (21.1 cm), 4.99 GHz (6.01 cm), 19.35 GHz (1.55 cm) and 37 GHz (0.81 cm).

A linear regression analysis was performed on the brightness soil moisture data on each data set. In general, it was found that the correlation coefficient decreases with decreasing wavelength, as does the slope of the regression curve, indicating a greater sensitivity to soil moisture with longer wavelength radiometers.

The data presented indicated little change in the emission from soils with moisture contents less than 10 to 20% and above this point there appears to be a linear decrease at about 2°K per percent soil moisture. It has also been shown that both surface roughness and vegetative cover decrease the ability to sense soil moisture at least at 1.55 cm. It was also concluded that longer wavelength radiometers (6 and 21 cm) have greater sensitivity to soil moisture.

Using a Truck mounted radiometer, Edgerton and Treler, (1970) undertook to study various geological phenomena. The purpose of their study was to establish the microwave properties of representative rocks and minerals, and to examine the feasibility of utilizing microwave radiometry for various geological mapping problems. Microwave radiometric investiga-

tions were performed on 29 sites within nine localities of the Western United States. Field measurements were performed with dual polarized radiometers having observational wavelengths of 0.81, 2.2, 6.0 and 21 cm. Microwave brightness temperature measurements were used to determine the emissivities and physical characteristics of the materials. The authors determined that the characteristics included surface roughness, moisture content and specific gravity. It was also determined that a majority of the outcrops examined during the study were "distinctly non-specular" relative to the 0.81 cm observational wavelength and the corresponding emissivities were generally high (≥ 0.9). It was found that practically no correlation exists between moisture content of rough outcrops and the corresponding 0.81 cm emissivities. At the 21 cm scattering due to roughness was greatly diminished. This is evident as the 21 cm emissivities were low and the polarization differences were great. The low emissivities correlated closely with high moisture content in the outcrops.

On February 21 and March 1, 1971, NASA Goddard Space Flight Center performed airborne microwave radiometric measurements at 1.42, 4.99, 19.35, 37 and 94 GHz (λ, 21.4, 6.0, 1.55, 0.81 and 0.32 cm) over a portion of the Phoenix Valley, Arizona (Poe and Edgerton, 1971). The 1.42 and 4.99 GHz radiometers were pointed in the nadir position while the 37 and 94 GHz radiometers were aligned 45 degrees aft. The 19.35 GHz data were obtained with an imaging system which measures the

horizontally polarized brightness temperatures in the plane perpendicular to the direction of flight at 50° from nadir. It was found that atmospheric attenuation effects at 1.42, 4.99, 19.35 and 37 GHz were relatively unimportant, however, effects were important at 94 GHz.

The penetration of 1.42 and 4.99 GHz through alfalfa and wheat (25 cm and 15 cm, respectively) was noted in several cases. The penetration was noted only in cases where the underlying soil had substantial amounts of moisture in excess of 14 to 21 percent (dry weight basis). It was concluded that the lack of detectable penetration of vegetal cover over relatively dry soil was probably due to the lack of significant contrast in the emissivities of vegetal cover and dry soil. Further, the authors did not observe vegetal penetration with any consistency at higher frequencies. Estimates of the depth of penetration indicated the emission at 37 and 94 GHz is controlled by the moisture contained in the near-surface regions of soil. Values of correlation coefficients were consistently larger in magnitude at 1.42 and 4.99 GHz than at 37 and 94 GHz. Values obtained at 19.35 GHz for selected view angles varied widely.

Numerous hydrological studies employing various satellite sensor systems have been conducted. Their findings are quite encouraging. Edgerton, et al., (1968) indicated that the physical properties which are important when considering microwave emissions of snow interact in a very complex fashion. Experiments conducted on new snow showed that fresh, dry, low-density

snow is nearly transparent at microwave frequencies. Consequently, the brightness temperatures sensed under these conditions are primarily a function of the underlying materials. In old coarse-textured high-density snow, since layering is common and the individual snow grains are not necessarily small in comparison to observational wavelengths, scattering and interference phenomena occur. It may be possible to overcome these difficulties by utilizing longer observational wavelengths.

Ground based measurements (Edgerton, et al., 1971) have indicated that for dry snow over frozen soil the effective microwave emissivity decreases as the snow pack increases. At longer wavelengths, the decreases were less for the same snow pack. The effect of liquid water in the snow on microwave emission from snow has been investigated.

Schmugge, et al.., (1974) indicated that the effect of volume scattering in dry snow and firn becomes noticeable for free space wavelengths shorter than about 3 cm while at the longer wavelengths, 11 and 21 cm, scattering may not be an important mechanism. The rise in brightness temperature for wet snow indicates that it may be possible to detect the onset of snow melting by looking at brightness temperature differences between day and night passes over snow fields.

Chapter II

OBJECTIVES OF THE EXPERIMENT

Remote Sensing of Soil Moisture

The objective of the soil moisture experiment was to determine the feasibility of remote sensing of the soil moisture content of the earth's surface and near surface layers from the Skylab satellite. Water has the highest dielectric constant of all the naturally occurring materials. Soils have a very low dielectric constant at microwave frequencies. When varying amounts of water are added to the soil, the resulting mixture will have a dielectric constant proportional to the relative amounts of soil, water and air which are present. Since mixtures involving both water and soil material have dielectric constants in proportion to the amount of water, even small amounts of additional water may increase the dielectric constant of the mixture sufficiently for detection by remote sensors. The emissivity in microwave wavelengths of radiation is so strongly influenced by the dielectric constant of the emitting substance that the potential exists for remote sensing of soil moisture content by airborne or space sensors.

One of the major advantages of microwaves for soil moisture measurements is penetration. Whereas the signals for infrared and visible radiation that can be recorded by photo-

graphic sensors come from the very top layer of the soil, usually much less than a millimeter thickness, microwave signals come from a combination of the surface layer and deeper points within the soil. The depth of penetration depends on wavelength, with the longer wavelengths penetrating deeper than the shorter wavelengths. It also depends on the moisture content of the soil since greater penetration is possible for dry soils than for wet soils.

In addition to the influence of the soil moisture content on microwave emission, other factors such as vegetative cover and surface roughness may also affect the emissivity. Surface roughness and vegetative cover slightly modify the emission from the underlying soil by scattering and surface emission (Newton et al., 1974). The magnitude of the effect of surface roughness and vegetative cover depends on the wavelength of emission. Longer wavelengths have the advantage of being less influenced than the shorter wavelengths. In addition, the longer wavelengths suffer from less interference from atmospheric and weather phenomenon. In fact, wavelengths at 21 cm (L-band radiometers) are influenced very little by clouds and precipitation. While optical and infrared photographic images are produced from only the areas truly visible to the observer, microwave signals at longer wavelengths may come from beneath the vegetation from the soil surface and underlying layers beneath the immediate soil surface. Therefore,

the important capability of being able to remotely sense the moisture content of the subsurface layers beneath light vegetation exists for microwave sensors.

A Skylab soil moisture experiment was designed to determine the feasibility of using the microwave sensors on the Skylab satellite for determining the moisture content of the soil. Although Skylab has photographic and multispectral scanner sensors which were very useful in providing auxiliary information, the primary thrust of the soil moisture experiment concerned the use of microwave sensors for detecting soil mois ture. Microwave sensors on Skylab made measurements at two different wavelengths in the passive and active modes. Data were collected with an L-band passive radiometer which obtained brightness temperatures from large areas of the earth at 21 cm wavelengths. Sensors at 2.1 cm wavelength obtained measurements in both the active and passive modes. For the soil moisture experiment, the L-band radiometer, S194 sensor, obtained measurements from an area 115 km in diameter centered around nadir. The S193 sensor obtained measurements at 2.1 cm wavelength in both the active and passive modes and was operated at the 30° forward pitch angle with vertical-vertical polarization in the cross-track contiguous mode. While data were being collected by the Skylab microwave sensors, soil moisture samples were being collected in the field by ground crews. Samples were collected from the surface in every 2.5 cm depth down to 15 cm.

The object of the experiment was to collect detailed
soil moisture information for various layers so that the sen-
sitivity of microwave radiometers and scatterometers from
Skylab to soil moisture content could be determined. A suf-
ficient amount of data was collected to provide correlations
between the measurements made by the Skylab microwave sensors
and soil moisture content as well as data for testing the re-
sults of these correlations. The results suggest several ap-
plications of remote sensing techniques for determining soil
moisture content for agricultural and hydrological uses.

Snow Cover and Freeze-thaw Line

A very important factor in water resources management
in the upper Missouri and Mississippi River basins is the
amount of moisture stored in the plains snowcover. The snow
storage in the intermountain river basins of the Western
United States is also extremely important since the bulk of
the annual water yield for this area is derived from this
source. The ability to appraise basin yield prior to the melt
period is increasing in importance with the ever increasing
demand for water in the Missouri and Mississippi Basins. Of
paramount importance is the flood potential associated with the
plains snow-cover. In the recent past a number of the extreme
floods in both basins have resulted directly from snow-melt.
The ability to determine the amount of moisture stored in the

snow cover is crucial to determining the flood potential and to forecasting the magnitude of the resulting flood wave.

Because of the large geographical area involved and the wide variation in areal distribution characteristic of plains snow cover, it is practically impossible to establish a ground based sampling program capable of furnishing the quantity and quality of data required to properly assess the amount of moisture stored in the snow cover. During the melt period when time becomes a critical factor synoptic data for the entire snow covered area is necessary and cannot be obtained by any ground-based means.

A factor closely associated with the snow-cover in determining the hydrologic response of a drainage basin to snowmelt is whether the ground is frozen or unfrozen. Again this information is required over a large area for forecasting purposes and cannot be reliably obtained through ground-based collection programs. In both the assessment of moisture contained in the snow cover and the condition of the underlying ground the macroscale of the areal coverage dictates a comparable scale in the sensing or sampling program.

The application of remote sensing to the determination of the amount of moisture stored in the plains snow cover involved in this experiment or project had as an overall objective determining if this moisture assessment could be accomplished by remote sensors of the type operating on board Skylab during the SL4 portion of the mission. To determine

the amount of moisture stored in the snow cover requires the measurement of the areal extent of the snow cover and the areal variation of the water equivalent of the snow. The water equivalent is the depth of liquid water that would result from melting the snow and is a function of both the density and the depth of snow at a particular location.

The overall objective can be divided into the following separate items:

1. To determine the effectiveness of remote sensing in establishing the areal extent of snow cover.

2. To determine if remote sensing techniques can be utilized to obtain the depth and density of snow over large areas with sufficient accuracy to determine the areal variation of the water quivalent, or if the water equivalent of the snow cover can be determined directly.

The first item certainly can be accomplished by aerial or space photography provided cloud-free conditions exist, however, for flood forecasting purposes during the critical melt period the cloud-free constraint is not acceptable. Synoptic data for the entire snow covered area must be available frequently during this period.

Associated with the snow cover objective is the objective of determining the capabilities of the remote sensors to observe the advance and retreat of the freeze-thaw line during the winter period.

A secondary objective which would be pursued provided the two primary objectives discussed could be achieved was to investigate the possibility of determining the quality of the snow, that is the amount of water in crystalline form and also the capability of monitoring the heat content of the snow pack and the associated energy budget. This phase would be particularly important during the spring melt period. This capability would permit the determination of the time of melting and the rate of production of melt water which are important factors in the forecasting of the amount of runoff and the associated flood potential.

Data for the snow experiment were collected during SL4, while data for the soil moisture experiment were collected during SL2 and SL3. The experimental sites, data analysis and results are described in the following chapters.

Chapter III

EXPERIMENTAL SITES

Soil Moisture

Soil moisture experimental sites were established in es-
sentially two states, Texas and Kansas (Figure 1). The south-
ern sites were located in West Texas between Lubbock and San
Angelo for June and August missions and between Lubbock and
Hobbs, New Mexico for the September mission. The more north-
erly sites were located between Concordia and Emporia, Kansas
on June 13, 1973 and southeastern Kansas in September.

Texas

    The area of Texas which was selected as the test site for
June 5, 1973 and August 8, 1973 can be separated into essen-
tially two major landscape regions. The northern half of the
site is part of the region known as the High Plains. The most
striking feature of the High Plains is the very flat and level
character of the surface. This feature combined with well-
drained and relatively fertile sandy soil has permitted the
development of agriculture over most of the northern half of
the test site. The dominant crop in this part of the site is
cotton, however, lesser acreages of grain sorghum are grown
throughout the area.

    The southern half of the test site contrasts significantly
with the northern half. This section is characterized by rol-
ling and rough-broken topography. Much of the land shows the
results of periods of effective erosion. Relatively deep,
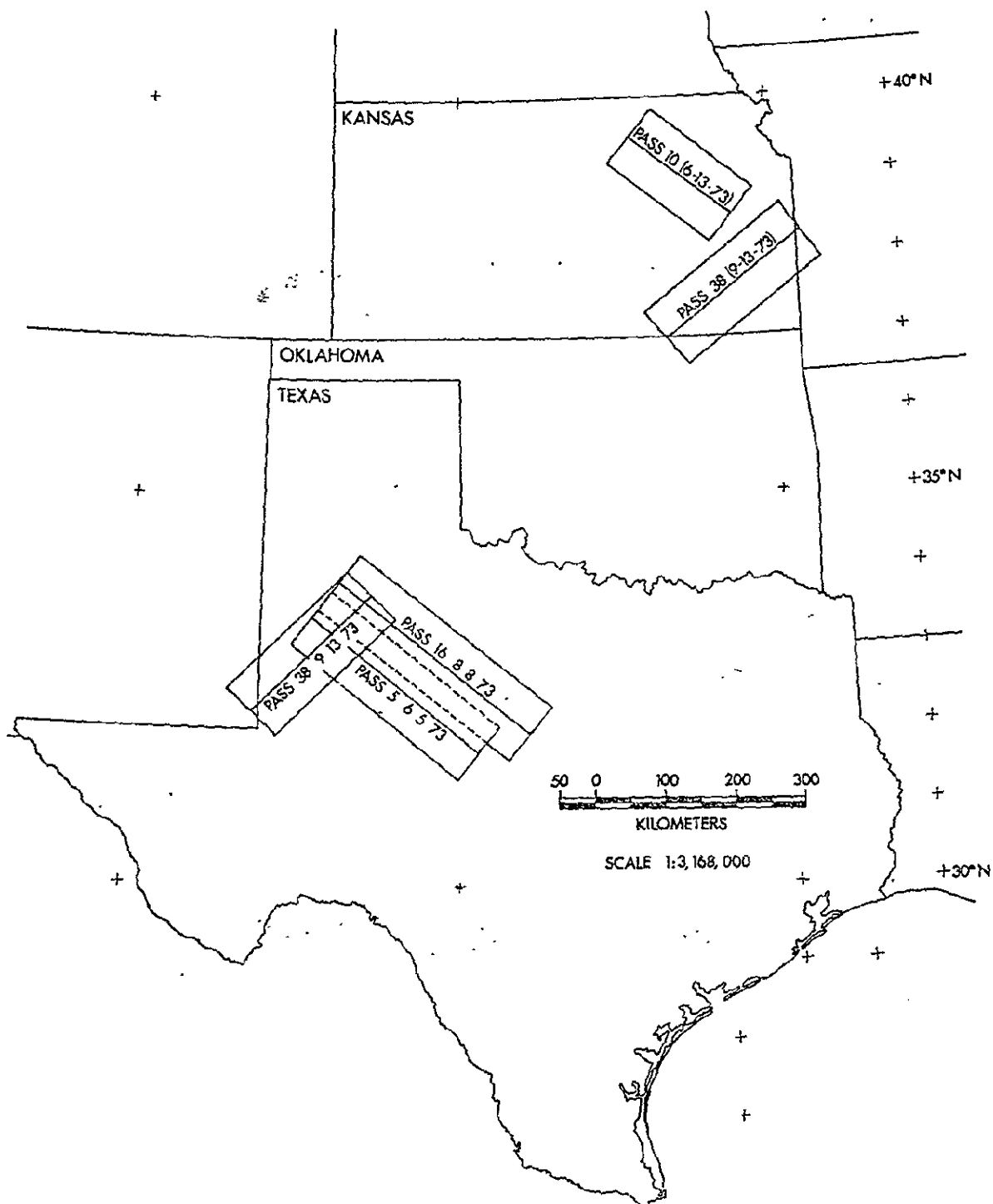
Figure 1 The location of the Texas and Kansas test sites used for the soil moisture experiment.

steep-sided arroyos are present locally as are small steeply sloping mesas with a flat resistant sandstone caprock. Because of the rugged character of the terrain, most of this section is uncultivated. The natural vegetation remains dominant over much of the landscape. This means that the vegetation is quite variable locally; however, the basic characteristics of vegetation tend to run throughout the area. Generally, the vegetation is rather shrubby, with the trees averaging about three meters in height and relatively dispersed. On very dry sites, the shrubs may be as low as 50 cm in height, but in spots of greater moisture availability may reach five meters. In most instances, the shrubs are underlain by a grass understory. Again, the grass is short (15 cm) on dry spots and as much as 50 cm in moist areas. Interspersed at various points throughout the area are various species of succulents, primarily cacti.

The site selected for the September 13, 1973 test is essentially perpendicular to the June-August test areas, but the landscape surrounding Lubbock is common to all missions. The eastern portion of the September mission overlaps to some extent with the northern portions of earlier sites. The primary differences from month to month in the area are varying stages of crop growth. In June the area was dominantly bare soil, but by September, heavy vegetation had transformed the landscape to the extent that little bare soil was visible. Moving to the southwest, the character of the test site changed rapidly

from cultivation to a relatively natural condition. The land surface is consistently flat across the entire test site, however, variations in the density of the vegetation and the character of the substrate are present along the site. The soil on the eastern end of the site is relatively uniform fertile sandy soil. Moving southwest the soil becomes sandier, oftentimes becoming dunes and ranging to a depth of 15-18 meters. Vegetation of these soils is rather sparse and is primarily composed of rather short and slender shrubs. Little ground cover is present and much of the surface is visible.

Toward the southwest end of the test site; vegetation and soil are somewhat different again. The land remains relatively flat. However, the soil in this area tends to be rather hard clay with significant numbers of pebbles and boulders in the soil matrix. The vegetation is quite different since there is a substratical ground cover of short drought resistant grass. The overstory of woody plants tend to be somewhat inconsistent in that densities are highly variable with relatively dense, open stands occurring at irregular intervals. Between the open stands individual plants occur in somewhat random fashion.

Kansas

Several passes across the state of Kansas provided the data base for soil moisture in this area. Data were collected for June 13, August 5, September 13 and September 18, 1973.

June 13 data were taken from Concordia to Emporia, Kansas,

across the region of the Flint Hills. This region is characterized by a rolling topography and in some parts rather substantial local relief. Over much of the region the soil is extremely rocky with gravel size material on the soil surface and throughout the soil profile. The vegetation of this area is almost exclusively mid-grass prairie with grasses potentially ranging from 50 cm to two meters. Most of the area is used as grazing range for beef cattle with a relatively small percentage set aside for cultivation.

August 5 data were taken along a track from the northwest corner of Kansas across Wichita and extending across Oklahoma and part of Arkansas. The soil moisture ground truth data were taken in an area surrounding Wichita, Kansas. This region is dominated by relatively flat topography and little local relief. Most of the vegetation of the area is small grain cultivated crops, mainly dominated by wheat. At the time of the Skylab III pass, more than half of the land area was bare ground, since the wheat land had been harvested and tilled. This cultivated zone grades gradually into a zone of natural grassland, which is primarily used for grazing. This zone is composed mainly of mid-grass with some evidence of shrub vegetation.

To the south and east of the August 5 pass, the September 18 pass begins. The flight line extends from southeast Wichita, Kansas toward Springfield, Missouri. Unlike the area of the August 5 pass, the land is largely uncultivated and is dominated by natural vegetation. Much short or medium grass

is present on the western half of the site. Shrubby vegetation is present also; however, some large deciduous trees occur locally. The deciduous tree cover increases eastward along the site. The topography of the test strip tends to be generally rolling with moderate local relief. Soils throughout the site tend to be more variable than within the other sites.

The five areas shown in Figure 1 served as the data base for the soil moisture experiment. The other two attempted data takes could not be used because of lack of corresponding ground truth and microwave data. The August 5 soil moisture data were collected in Kansas while the microwave sensors were operated over Oklahoma causing a mismatch of data. It was not possible to use the September 18 data in the final analysis because heavy rainfall began just after the Skylab data collection causing termination of the collection of soil moisture samples from the field. This left three data sets across Texas and two across Kansas for use in the soil moisture experiment.

Snow Cover and Freeze-Thaw Line

Six Skylab EREP passes were preliminarily scheduled for the analysis of snow cover and snow characteristics. The initial pass of Novermber 30, 1973, however, was aborted due to the absence of snow cover in the test site area. Skylab data were not available for the January 4, 1974 pass from Kentucky to New Brunswick nor from the January 12, 1974 transect from Texas to Montreal, Quebec. The three Skylab passes that obtained data for the snow study were those on January 11, January 14 and January 24, 1974.

The January 11 test site encompassed an area 30 nautical miles either side of a line from Amarillo, Texas to Clinton, Iowa. The S190B photography aided by information extracted from the NOAA/EDS Climatological Data showed that the snow cover extended from the Oklahoma panhandle northeastward into Iowa. However, the S190B revealed widely scattered patches of bare ground extending from northeast Kansas through northwest Missouri into Iowa. In addition, dense cirrus in Iowa and moderatley heavy stratocumulus in northeast Kansas and northwest Missouri were also observed. Four to six inches of fresh snow had fallen on January 9-10 in much of the test site area on top of a snow base from 4-7 inches. This resulted

22

in snow depths ranging from four inches in south central
Kansas to 12-13 inches in portions of southeast Iowa and north-
west Missouri. During the January period prior to this pass,
the Central United States remained under a high pressure air
mass of cP/cA origin. Maximum temperatures had not risen above
32 degrees F even as far south as Wichita, Kansas, while over-
night lows had frequently plunged below -20 degrees F in por-
tions of Iowa.

The January 14 (GT-30) Test site extended from Denver,
Colorado to Mankato, Minnesota. This run coincided with the
initiation of a pronounced warming trend in the test site
area which lasted for the rest of the month. The maximum tem-
peratures in Nebraska along the ground track generally ranged
in the mid-40's and increased to the mid-50's by January 16.
Maximum temperatures in Colorado floated from the mid-50's on
January 14 to as high as 71 in Boulder, Colorado by January 16.
A moderate cirrus cover extended from the Rocky Mountain
foothills into southwest Nebraska, but gradually dissipated
after reaching central Nebraska. Generally, no fresh snow had
fallen inside the test area since January 11. Snow depths
ranged from 4-8 inches, increasing northeastward along the track.

The January 24 (GT-33) test site area extended from north
central- northeast South Dakota into east central Iowa. This
pass took place well into the melt period. Consequently,
snow depths tended to vary from 0-4 inches in this area. Moder-
ate to dense cirrus clouds were located in the South Dakota
portion of the run, but Iowa skies were generally cloud-free.

Chapter IV

DATA BASE

Skylab Photography

Black and white and color photography was provided for each pass for which soil moisture data were collected. The multispectral camera (S190A) provided six simultaneous frames of imagery in a 70 mm format at approximately 1:285,000 in scale. The Earth Terrain Camera (S190B) provided a single image frame in 4.5 inch format at a scale of approximately 1:960,000. Additional details for these sensors are shown in Table I.

The imagery was at least partly cloud free in all cases. and some part of the pass was useable for detailed analysis. The June 5 pass across west Texas is cloud free over the northern half of the site. However, the southern half is totally cloud covered. The June 13 pass which crossed central Kansas is almost totally cloud covered so that it could not be used for extracting ground information. The August 5 pass provided good quality, relatively cloud free imagery in all bands. As such, the photographic data base proved to be a good source of vegetation land use and topographic information. Land-Use-Vegetation maps were completed for both the Kansas and Texas test sites for use in the microwave data analysis.

The August 8 pass across west Texas paralleled and overlapped the June 5 pass. The S190A 0.4-0.7 µm color imagery was quite dense and as such required extensive photo lab

TABLE I

Characteristics of the Skylab and Aircraft Photographic Sensors

System	Product	Wavelength (μ)	Resolution	Scale	Format	Coverage
MSC S190A	B&W IR	0.7=0.8	68 meters	1:2,353,620	70mm	169 km
		0.8-0.9	"	"	"	"
	B&W PAN	0.5-0.6	28 meters	"	"	"
		0.6-0.7	33 meters	"	"	"
	Color IR	0.5-0.88	57 meters	"	"	"
	Color	0.4-0.7	24 meters	"	"	"
ETC S190B	Color	0.4-0.7	15 meters	1:956,617	112mm	109 km
	Color IR 0	0.5-0.88	"	"	"	"
MSS S192	Tape	0.41-0.46	0.182mrdn.	1:771,213	Continuous Strip 109mm (3.5 in.)	69 km
	Film	0.46-0.51	260 sq. ft.			
	Tape	0.51-0.56	110 scan			
	Tape	0.56-0.61				
	Tape	0.62-0.67				
	Tape	0.68-0.76				
	Film	0.78-0.88				
	Tape	0.98-1.03				
	Tape	1.09-1.19				
	Tape	1.20-1.30				
	Film	1.55-1.75				
	Tape	2.10-2.35				
	Tape	10.2-12.5				
RC-8 Aircraft	Color	0.4-0.7	50 cm	1:16,183	228mm	4.6 km

manipulation to make it useable. The 0.5-0.88 μm color infra-red imagery was good quality, however, the magazine ran out of film and the test site was only partially covered by this band. S190B color data were not taken on this pass and as a result most of the land-use and vegetation interpretation was done from black and white photography of bands 0.5-0.6 μ and 0.6-0.7μ.

Good quality photography from all bands of the S190A and S190B sensors are available for September 13, 1973. From these images, good ground classifications could be developed. All of the Texas test area was cloud free as well as several miles to the northeast and southwest of the track.

Cloud cover at the time of Skylab data collection is shown in Figure 2 for the various dates and locations for the soil moisture experiment. The Texas site is the only one that was completely free of clouds and this occurred on only one day, September, 13, 1973. The Skylab data were collected through varying degrees of cloudiness for the other passes.

For the snow experiment, the January 11, 1974 photographic data were received in the form of S190B 0.4-0.7 μm color trans-parencies only. Since most of the pass was cloud free, this imagery was useable for the purpose of providing ground support information. Interpretations from these data carried as far as possible with respect to judgements relating to snow char-acteristics. Similarly, good information is available for January 14 as all bands are of good quality and all are avail-able.

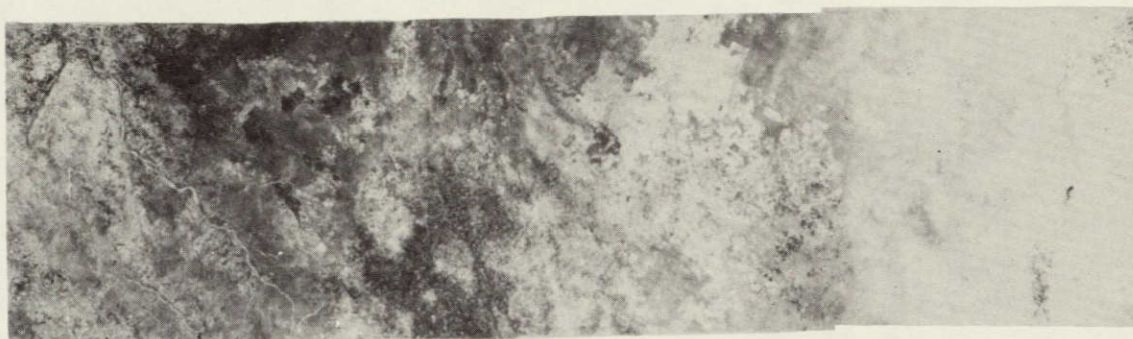Texas-June 5, 1973

Kansas-June 13, 1973

Texas-August 8, 1973

Figure 2   S190A .6-.7 micron photographic mosaics showing
            cloud conditions for the five data sets for the
            soil moisture experiment.

Texas-September 13, 1973

Kansas-September 18, 1973

Figure 2. S190A 0.6-0.7 μm image mosaics showing cloud conditions for five Skylab passes

However, only half of the track of January 24 is cloud free. Fortunately, the northwest end of the track is clear and of sufficiently good quality to permit interpretation.

Skylab S194 L-band Radiometer

The S194 microwave sensor on the Skylab satellite is an L-band radiometer operating at a 21 cm wavelength. This absolute microwave-radiometric sensor utilizes a fixed planar array antenna oriented toward nadir. It records thermal radiation at 21 cm wavelength and measures absolute antenna temperature. This radiometer utilizes a calibration scheme referenced to a fixed hot and cold load input (EREP Users Handbook).

The half-power beam width of the S194 sensor is 15°. The 15° solid cone centered about the vertical axis corresponds to the angular width of the beam between the half-power points of the antenna pattern. The 15° angle will encompass a swath width (resolution cell size) of 60 nmi at the orbital altitude of 235 nmi (Sensor Performance Report). The first null of the major lobe of the antenna pattern is at 36° which encompasses a swath width of 145 nmi. About 90% of the energy is contained within the major lobe. The radiometric measurements made by this sensor are influenced to the greatest extent by the brightness temperature of the surface material contained within the half-power beam width giving a footprint size of 60 nmi or 115 km.

The radiant energy received by the antenna is sampled at such a rate as to ensure a minimum of 97% ground coverage overlap. Because of this, the distance on the ground between centers of two consecutive resolution cells is about 2 nmi. The ground coverage provided by the S194 sensor across the Texas site is shown in Figure 3. The precision of the measurements made by the radiometer is about 1°K.

In SL2 and SL3, the L-band radiometer collected seven sets of data (Table II) for the soil moisture experiment over the Kansas and Texas test sites. All the data were taken in the morning at mode 1 with sun elevations ranging from 29.9 in pass 10 to 77.9 in pass 5 while Skylab was over the test sites.

Skylab S193 RADSCAT Sensor

The S193 microwave sensor on Skylab consisted of three systems--an altimeter, a radiometer and a scatterometer. All three systems shared the same hardware. The altimeter could only be operated when the radiometer or scatterometer were not operating. The radiometer and scatterometer could be operated either concurrently or separately. The passive radiometer and the active scatterometer sensors are called the S193 RADSCAT. The specifications and characteristics of the equipment are contained in the documentation provided by General Electric Company and NASA (EREP Users Handbook).

The Skylab RADSCAT instrument operated at a frequency of 13.9 GHz (2.16 cm wavelength). It used a parabolic antenna which provided a two degree pencil beam at the half-power
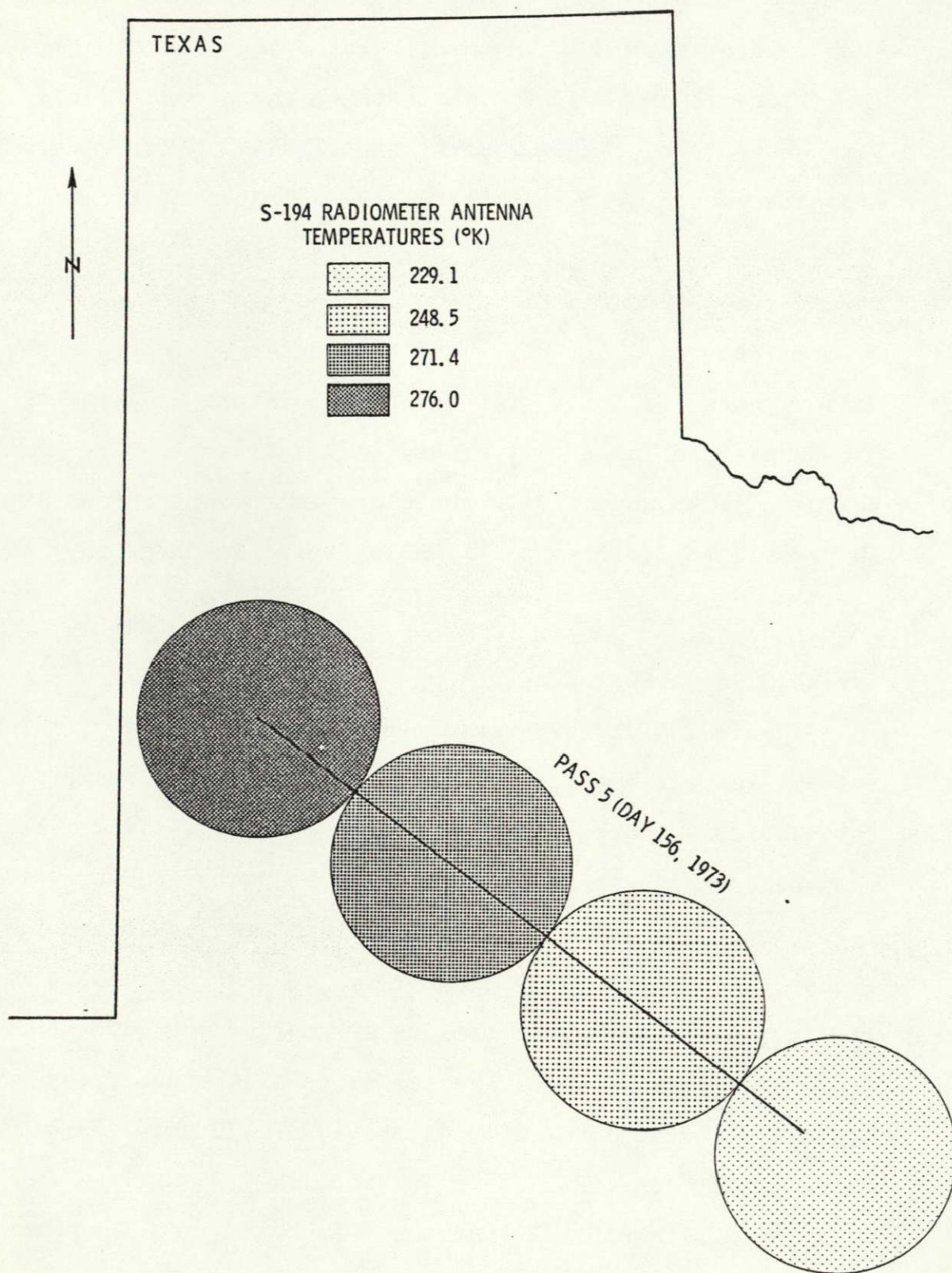
Figure 3 The antenna temperature, location and size of the footprint of the S194 radiometer across the Texas test site.

TABLE II

Skylab S194 Data Collected for the Soil Moisture Experiment.

Mission	2	2	3	3	3	3	3
pass	5	10	15	16	38	38	48
Date	6-5	6-13	8-5	8-8	9-13	9-13	9-18
Time over test site (GMT)	18: 0:49.51 18: 1:38.20	13:51:22.74 13:51:57.59	16:37:44.35 16:37:58.30	16:4:30.99 16:5:14.66	17:57:25.06 17:58: 0.40	17:59:21.15 17:59:51.95	15:57:59.26 15:58:36.90
Test site	Texas	Kansas	Kansas	Texas	Texas	Kansas	Kansas
Altitude (nm)	237.9 237.6	234.4 234.7	235.3 235.3	236.0 236.1	229.2 229.3	228.8 228.9	
Sun elevation	74.8 77.9	29.9 31.4	56.2 57.1	48.7 51.2	58.9 58.5	56.3 55.3	42.2 42.7
mode	1	1	1	1	1	1	1

point. The antenna is mechanically scanned to provide measurements at various angles relative to nadir. Several scan modes and various transmit-receive polarizations are provided to study the sensitivity of the terrain.

. The S193 RADSCAT system could be operated in the following basic modes:

1) In-Track Non-Contiguous (ITNC). The scatterometer and the radiometer are used jointly in this mode. In this mode, overlapping measurements are made at angles of $0°$, $15°$, $29°$, $40°$ and $48°$ between the antenna pointing direction and the vertical at the space craft. The distance between the centers of each set of measurements is about 100km. The measurements at each angle are made for four transmit-receive polarization pairs (HH, HV, VH and VV) in the scatterometer and for both vertical and horizontal polarizations in the radiometer. The object of this mode is to view the same target at five discrete angles to study the variations in radar backscattering coefficient and radiometer brightness temperature with incidence angle. This mode is intended primarily for use over a homogeneous terrain (such as the ocean) where the measurements made at discrete targets some 100 km apart could be meaningful. The precision of measurements made in this mode is better than in the contiguous modes because of relatively larger integration time for each measurement.

2) Cross-Track Non-Contiguous (CTNC). In this mode, the scatterometer and the radiometer were again used concurrently. Measurements were made at the same angles of incidence but

perpendicular to the track so they were spaced approximately 100 km rather than overlapping. The antenna in this mode could be moved either to the left or the right or both left and right of the satellite track. The polarizations were the same as in the ITNC mode.

3) In-Track Contiguous (ITC). The scatterometer and the radiometer were used almost concurrently in this mode. Measurements were made at the same angles as before for the scatterometer and at intermediate angles for the radiometers. The measurements were spaced approximately 25 km. Data in this mode were taken for only one transmit-receive polarization pair for the scatterometer and one polarization (the same as the receive polarization for scatterometer) for the radiometer.

A target cell viewed at 48° in a scan overlaps a cell viewed at 48° in the previous scan because of the rapid scan of the mode. The amount of overlap between successive scans is a function of incidence angle and is greater at higher angles and decreases as the incidence angle approaches nadir. At nadir, a gapping rather than an overlap occurs. On successive scans as the vehicle progresses, virtually the entire path was viewed from 48° down to the lower angles (near about 15.6°). The beam width of the antenna corresponds to a target cell of 11.1 km diameter at nadir for the scatterometer and 15.2km diameter for the radiometer at nadir.

4) Cross-Track Contiguous (CTC). In this mode the radiometer and scatterometer could each be operated either individually or concurrently. In this mode, the antenna swept in the

roll plane, both to the left and to the right of an initial-
ized point. The measurements were made at 12 points over a
22° angular range about the center point. The center point
could be vertical or tilted ahead or to the side by 15°, 30°
or 40°. The sub-mode chosen dictated whether the measurements
being made were all radiometer, all scatterometer or half of
each. Due to the rapid scan, not all possible polarization
pairs are allowed. The cross-polarized combinations (HV or VH)
are not allowed in this mode. The measurements for vertical
transmit-receive (VV) and horizontal transmit-receive(HH) pol-
arizations were made alternately. This mode is also called
the mapping mode and was primarily intended for land targets.
It comes closest to radar or radiometer terrain mapping.

The precision of the radiometer (1σ) varied with the op-
erative mode but was in the neighborhood of $1°K$. The precision
of the scatterometer measurement also varied with mode (Sensor
Performance Report) and was usually between 5 and 7% (about
0.25 db).

The S193 scatterometer was designed to measure radar
backscattering coefficient, $\sigma°$, for different angles of inci-
dence and polarization pair combinations (HH, VV, HV and VH).
The S193 radiometer measures apparent radiometric antenna tem-
perature as a function of incident angle and for different
polarizations. The S193 RADSCAT sensor illuminates a 11.1 (SCAT)
or 15.2 (RAD) km cone at nadir when flying at an altitude of 235
nautical miles. A complete analysis of the footprints as a

function of orbit height, velocity and pointing accuracy of the antenna is given by Sobti (1973).

The S193 instrument was operated at a forward pitch of 29.4° in the CTC mode with VV polarization for most of the passes for the soil moisture experiment. A comparison of the ground coverage in relationship to the S194 sensor is shown in Figure 4. The antenna excursion extended about the initialized point 11.375° to the left and right. During one scan cycle, a total of 24 data measurements were recorded, which included 12 data values for both the radiometer and scatterometer. Data were taken for only one polarization pair (VV or HH) for both the radiometer and scatterometer.

During SL2 and SL3, the S193 microwave sensor obtained five sets of data for the soil moisture experiment over Texas and Kansas test sites. Only three of the five data sets were comparable since the other two data sets were taken at a 40.1° pitch angle with one of these having vertical polarization and the other horizontal polarization (Table III).

Aircraft Photographic and Microwave Data

Supplementary information for the soil moisture experiment was obtained from the AAFE RADSCAT underflight of June 5, 1973. This flight was flown from latitude 31.51°, longitude 99.68° to latitude 33.44°, longitude 101.81° which covered a distance of approximately 190 miles across the Texas test site (Figure 5). This track was nearly the centerline of the area to be investigated by Skylab II pass 5 on June 5, 1973.
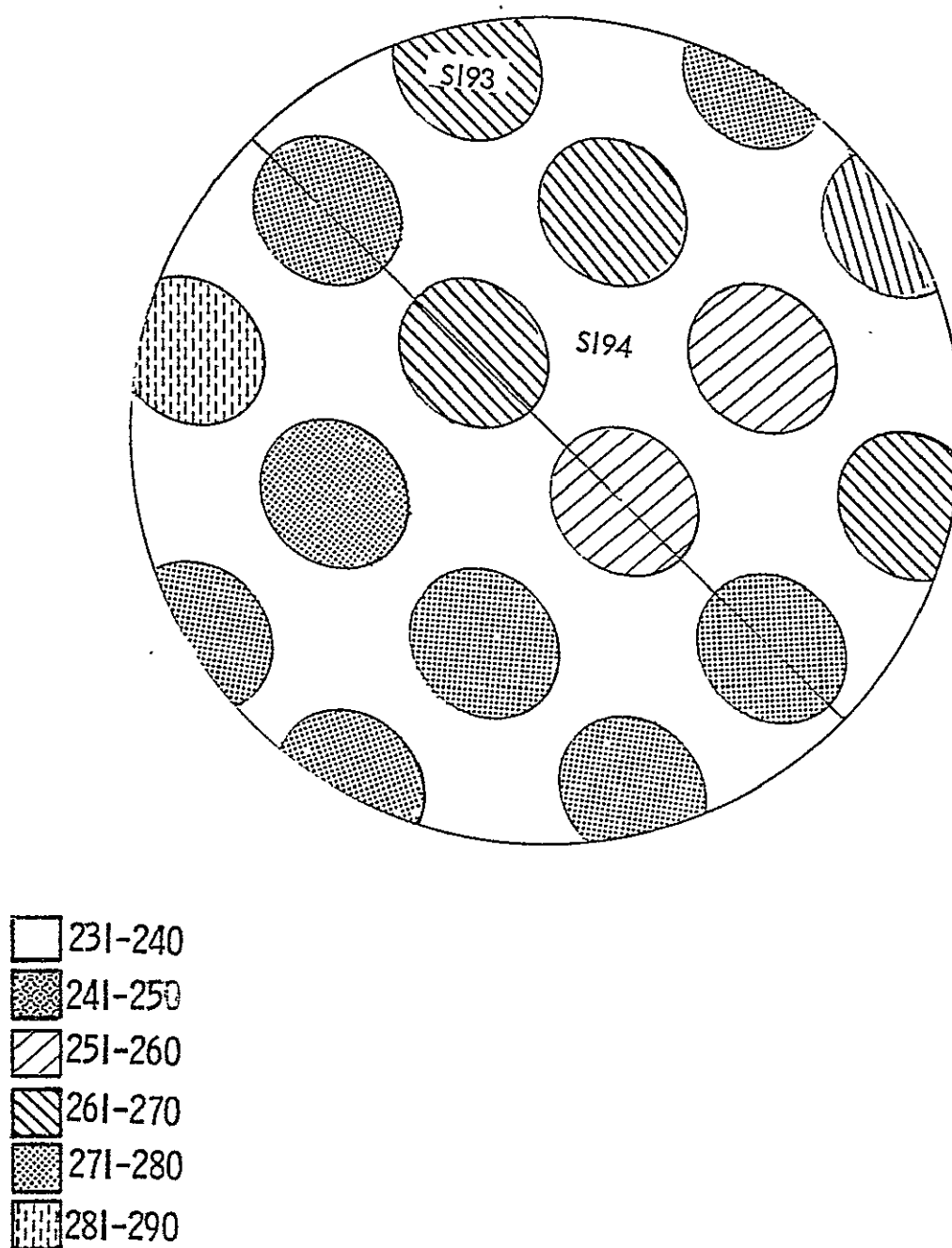
Figure 4   A comparison of the S193 and S194 radiometer foot-
prints.

TABLE III

S193 RADSCAT DATA FOR SOIL MOISTURE EXPERIMENT

Pass	5	15	16	38	38
Date	6-5-73	8-5-73	8-8-73	9-13-73	9-13-73
Mode	CTC	CTC	CTC	CTC	CTC
Pitch angle	29.4°	29.4°	29.4°	40.1°	40.1°
Roll angle	0	0	0	0	0
Polarization	VV	VV	VV	VV	HH
Test site	Texas	Kansas	Texas	Texas	Kansas
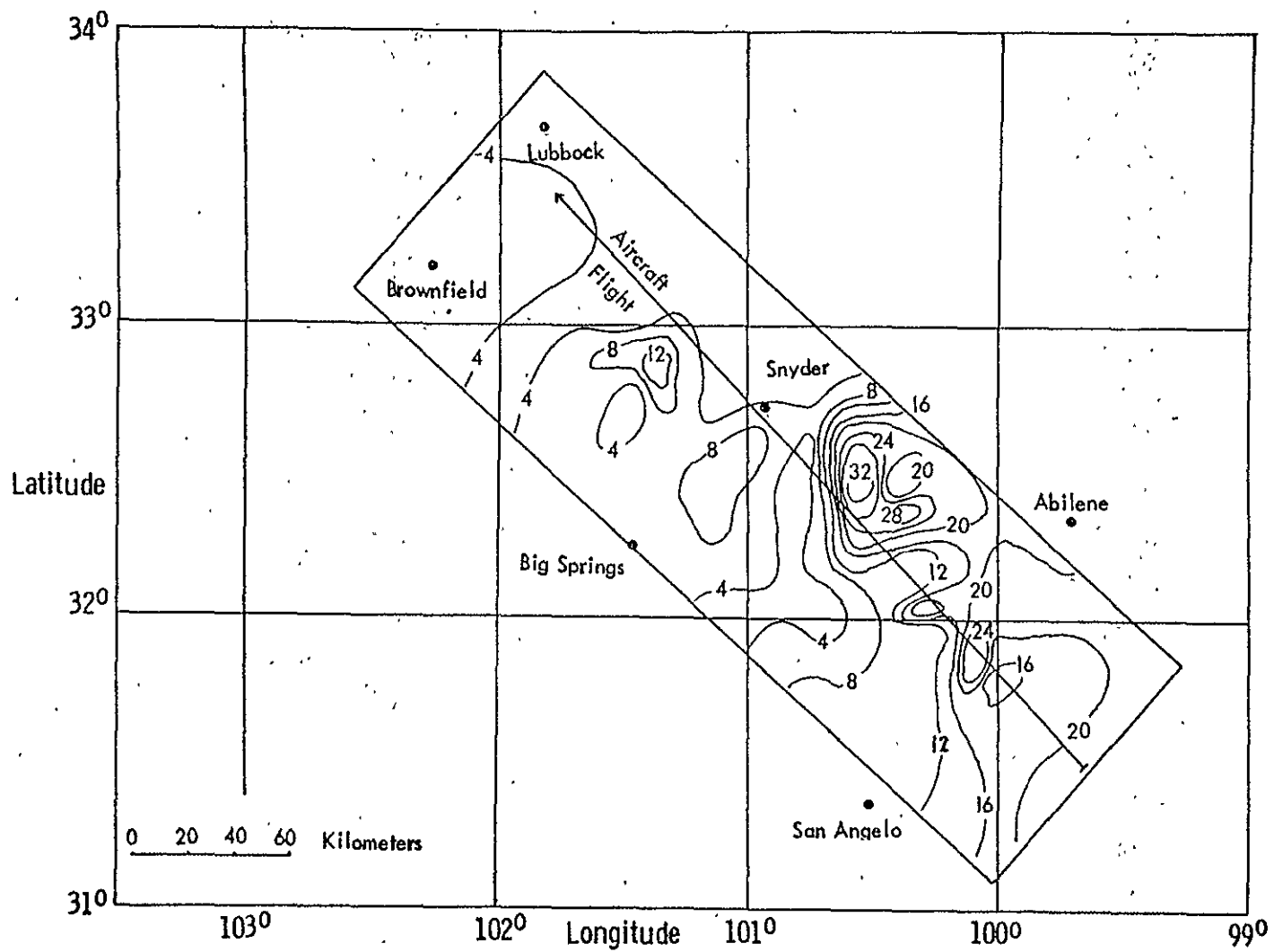
Figure 5. The flight path for the supporting aircraft data across the Texas test site in June, 1973 and soil moisture distribution throughout the test site.

39

The aircraft was a NC130B which was to be flown at an altitude of 10,000 feet, plus or minus 1000 feet. Terrain elevation at the beginning of the flight was approximately 1500 feet. As the flight progressed to the northeast, terrain elevation increased to almost 3200 feet. During the flight the actual altitude ranged between 9000 and 7300 feet. The ground speed of the aircraft averaged approximately 167 knots or 281 feet per second. Due to varying cross winds the cross angle of the aircraft ranged between 13.8 degrees to the right to 9.2 degrees to the left in order to maintain a flight direction of approximately 322 degrees. Altitude and cross angle reflect movements of the aircraft's pitch and yaw, but no measurements were taken for roll. Therefore movement along the longitude axis of the aircraft was assumed to be zero. On board the aircraft were a RADSCAT system operating at the same wavelength as the S193 RADSCAT and a vertical RC8 camera system. Due to the variance of height above the ground level, the scale of the aerial color photography ranged between 1:19,500 and 1:16,900. The film used was number SO-397 and the camera used a six inch lens with a 2-A skylight filter. Photographs were taken every 34 to 37 seconds throughout the flight, giving forward overlap of each frame. Also, it was apparent from adjoining frames that the subpoint of the camera system was ahead of the aircraft giving a slight obliqueness to the photographs. This factor remained nearly constant throughout the flight.

The principal aircraft instrument used for the soil moisture experiment was the S193 RADSCAT. This instrument is a passive radiometer and active scatterometer operating at 13.9 GHz, 2.1 cm wavelength, that was operated in the vertical polarization mode. The antenna has a half-power beam width of 1.8 degrees and this beam was directed approximately 30 degrees from nadir behind the aircraft. An eliptical footprint was obtained with major and minor radii of 150 and 130 feet for an altitude of 7300 feet, and 190 and 160 feet for 9000 feet. The time lag between the two components of the RADSCAT was about 10 microseconds. Even though the aircraft's velocity was 281 feet per second, the footprint of the radiometer and scatterometer differed by only 0.00281 foot. Therefore, the values obtained by the radiometer and scatterometer are representative of the same area of land. The RADSCAT recycles in as short a time as 0.4 second and as long as one to two seconds. These times allowed between 50% and 0% footprint overlap. The data sample contained 6054 points with an average distance of 166 feet between mid-points.

A comparison of the characteristics of the various microwave sensors and the complete data sets which could be used in the final analysis for the soil moisture experiment is shown in Table IV.

TABLE IV

Microwave Data Sets used in the Soil Moisture Experiment

Sensor	S194 Passive Microwave Radiometer	S193 Active Microwave Scatterometer	S193 Passive Microwave Radiometer	Aircraft Active Microwave Scatterometer	Aircraft Passive Microwave Radiometer
Frequency (GHz)	1.4	13.9	13.9	13.9	13.9
Wavelength (cm)	21	2.1	2.1	2.1	2.1
Normal Altitude (km)	435	435	435	2.5	2.5
Half-Power Beam Width (Degree)	15.0	2.02	1.56	1.8	1.8
Half-Power Footprint Diameter (km)	115	13x16	17x21	0.09	0.09
Pitch Angle (Degree)	Nadir	29.4	29.4	29.4	29.4
Data Sets Available	5	2	2	1	1

Soil Moisture Data

The Skylab soil moisture experiment was conducted over test sites located in western Texas and eastern Kansas. The sites were approximately 300 to 400 km in length and 120 km in width. During the time of data collection from Skylab, soil samples were being collected from the test sites. Samples were taken for each 2.5 cm depth down to 15 cm at intervals of approximately 6 km along one route (pass 5 and pass 10) or two somewhat parallel routes (pass 15 and pass 16 and pass 38) through the test sites. Location of the soil moisture sites are shown in Figures 6 to 11. Soil samples were collected from 42 to 120 different locations for the different Skylab passes with samples from six different depths at each location. After collection of the soil samples in tin containers, they were taken to the laboratory where they were weighed and dried so that the percentage of moisture in the soil was determined on a weight basis. The actual measured values of soil moisture content at the locations shown in Figures 6 through 11 are given in Appendix I for the 2250 soil samples.

Soil Moisture Distributions in the Test Sites

The soil moisture content of sample sites were obtained along the Skylab track for all missions for relating to the measurements of the Skylab sensors. Although the distribution of samples in the test sites were carefully devised before going to the field, the coverage of sensors was so large that

43

TEXAS SITE (6-5-73)

SOIL SITE MAP

Lubbock

Abilene

San Angelo
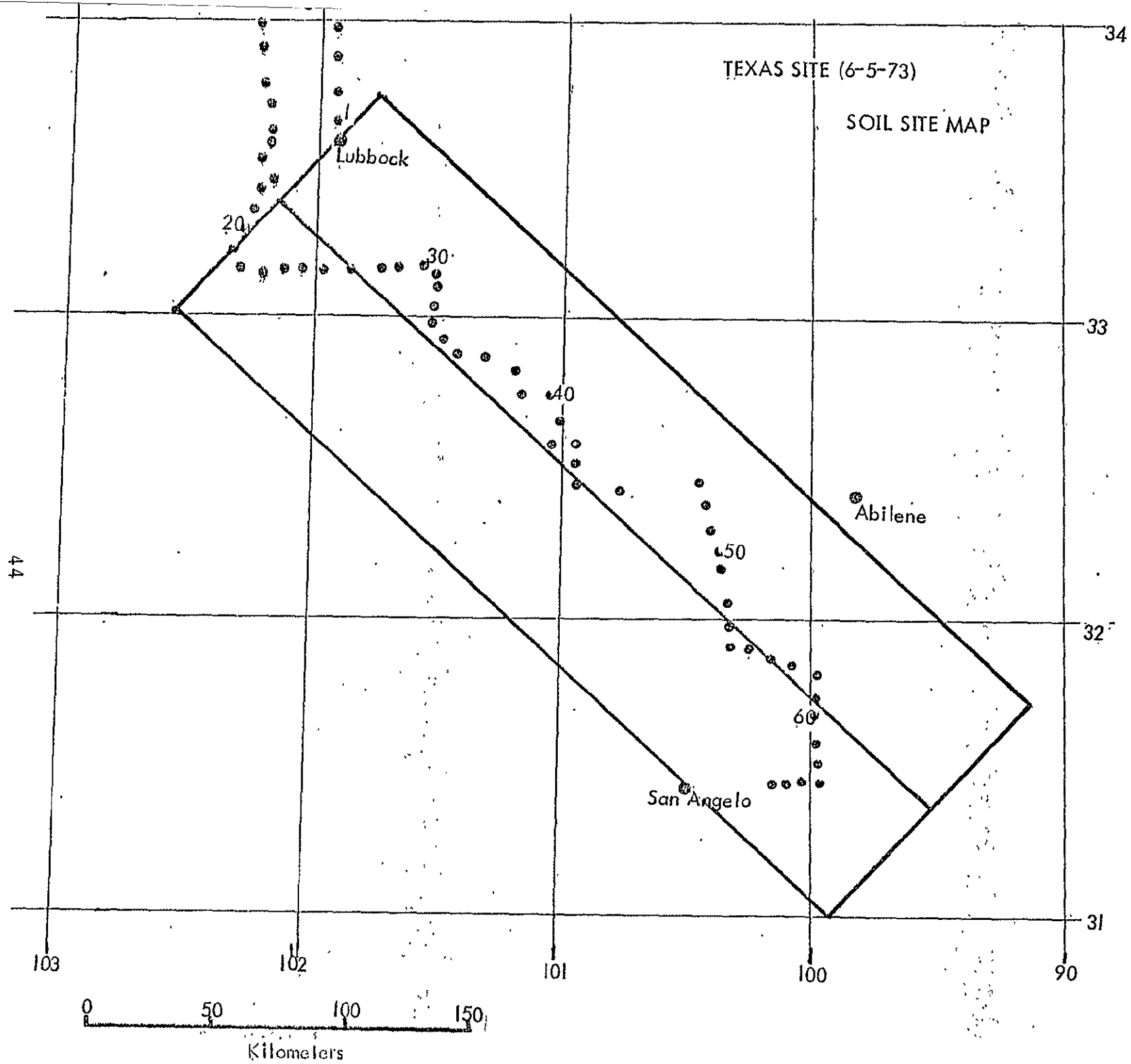
Figure 6   The location of the soil moisture sampling test sites in Texas in June 5, 1973.

44

Kilometers

Kansas site (6-13-73)

SOIL SITE MAP

Topeka

Abilene

Emporia

Scale

0   20   40
kilometer

Figure 7 The location of the soil moisture sampling sites
in Kansas on June 13, 1973.

45
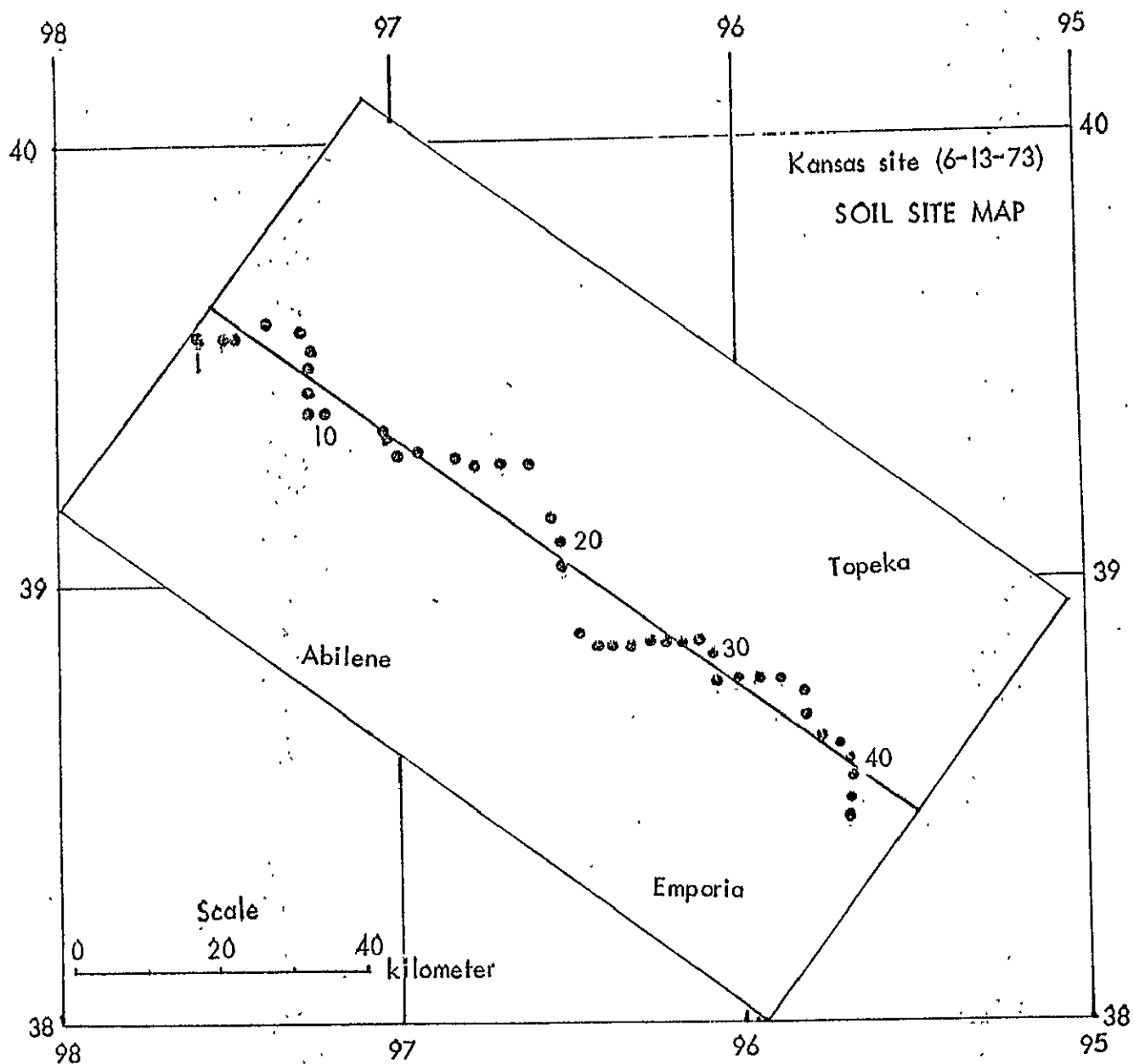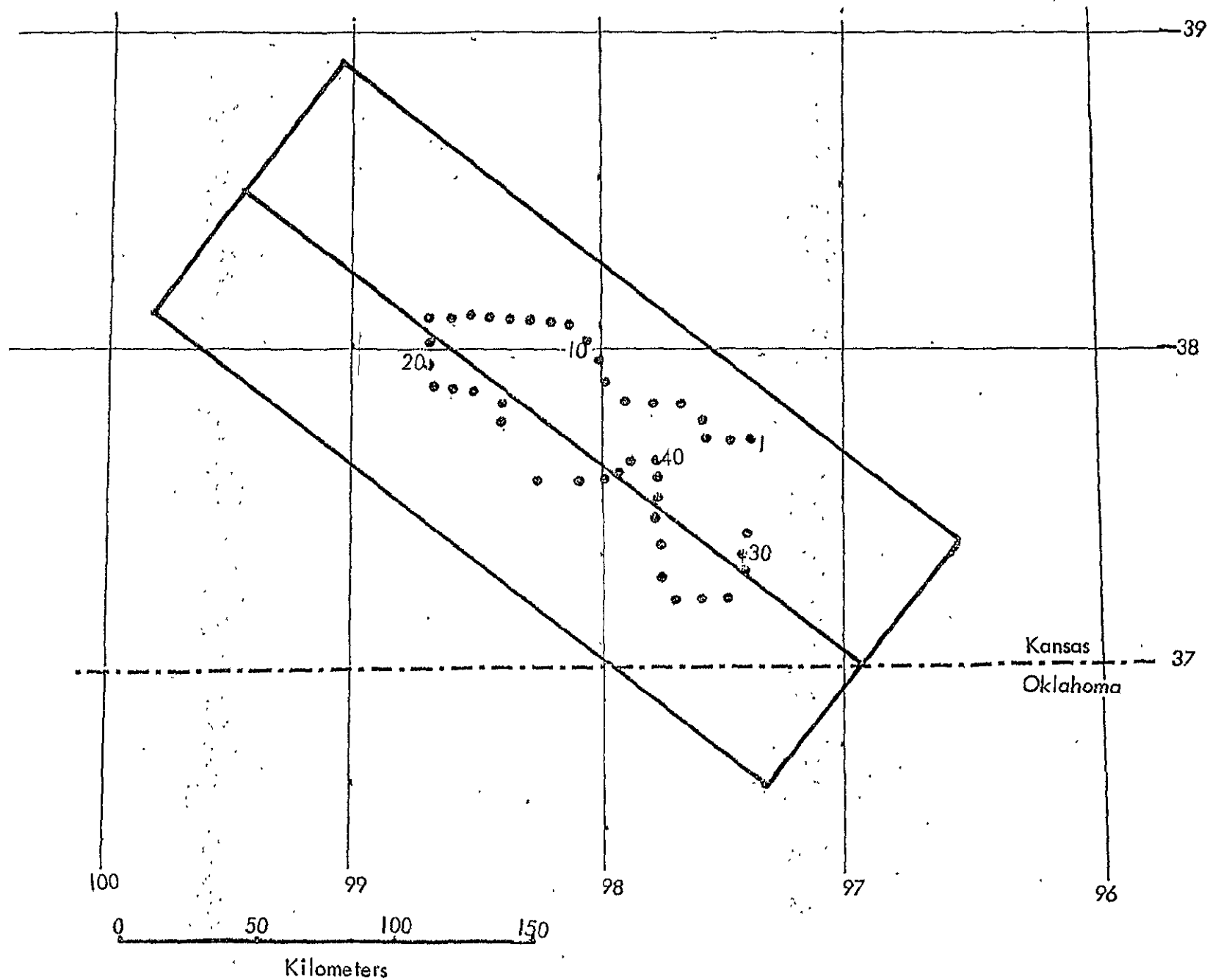
Figure 8 The location of the soil moisture sampling sites in Kansas on August 5, 1973.

TEXAS SITE (8-8-73)

SOIL SITE MAP

Lubbock

50

50

40

60

30

70

80

20

Abilene

10

San Angelo

1

Figure 9 The location of the soil moisture sampling sites in Texas on August 8, 1973.

33

32

31

102

101

100

99

0   50   100   150

Kilometers

47

Figure 10 The location of the soil moisture sampling sites in Texas on September 13, 1973.

TEXAS SITE (9-13-73)

SOIL SITE MAP

Lubbock

Hobbs

Big Spring

Kilometers

48

KANSAS SITE (9-13-73)

SOIL SITE MAP

Figure 11   The location of the soil moisture sampling sites
in Kansas on September 13, 1973.

49
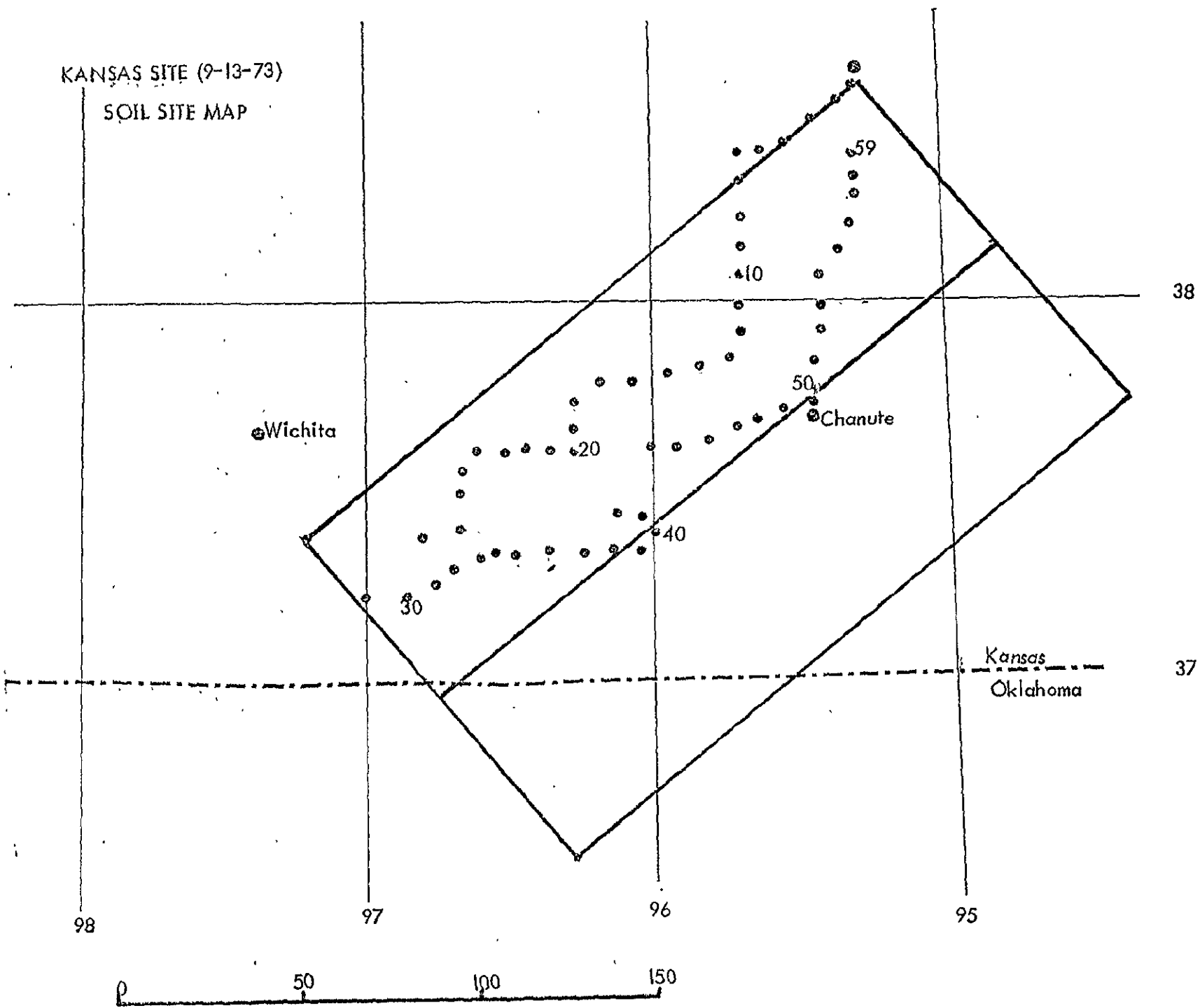
samples could not cover the entire area. Also all the soil

samples could not be taken in the same day. In addition,

thunderstorms in the summer are very localized. As a result,

distribution of soil water content can vary considerably in

short distances. Therefore, it has been found necessary to

apply the techniques of climatic water balance calculations

to improve the ground truth information on the geographical

distribution of soil moisture in the test sites.

The climatic water balance technique required the calcu-

lation of potential and actual evapotranspiration from meteoro-

locical parameters. Thus, the soil moisture storage and run-

off could be determined by these calculations for various soil

types.

The methods used in this investigation were developed by

Thornthwaite (1948), and Eagleman (1971). These methods are

simple to use and produce good results. Thornthwaite's equa-

tion can estimate the daily rate of potential evapotranspira-

tion (PE) from mean daily temperature. This PE rate is adjus-

ted by a factor which varies with the day of year and the lati-

tude of the station (Thornthwaite and Mather, 1957). The ac-

tual evapotranspiration at any location depends upon PE, pre-

cipitation and the availability of soil moisture and can be

calculated (Eagleman, 1971). The available water which is

the amount of water between wilting point and field capacity,

varies with different soils, Table V (Salter and Williams, 1965).

The soil type of each station was determined from county soil

TABLE V

Available Water Data for the Top 12 in. of Soil Sum-
marized as Means per Textural Class (After Salter
and Williams, 1965).

Textural Class	FC (% H₂O)	WP (% H₂O)	AW (in.)
Sand	6.7	1.8	0.79
Loamy Sand	17.9	5.1	2.15
Fine Sandy Loam	25.6	9.5	2.56
Silt Loam	35.3	12.7	2.82
Clay	39.4	22.1	1.93

survey maps and other sources. A computer program (FORTRAN IV) has been developed for these calculations. The inputs of the program are monthly temperature, daily temperature, daily precipitation, soil type, initial value of soil moisture, and latitude of each station. The daily variation of soil water storage in the upper six inches of soil depth was then computed for 61 stations (Figure 12) from May 1 to September 13, 1973 in Texas and New Mexico, and for 57 stations (Figure 13) from July 19 to September 18, 1973 in Kansas.

In order to be of value for comparison with Skylab data, the moisture content of the upper 15 cm layer had to be partitioned into each of the separate 2.5 cm layers. This was accomplished by using the moisture profile from the sites where soil moisture measurements were available. It was assumed that the moisture profile at the calculated sites was the same as that at the nearest measured site.

As a check on the validity of this procedure, the measured and computed values of soil water content in the upper 15 cm of soil depth were compared for the stations which had soil moisture measurements as well as meteorological data for calculations, Figure 14. The correlation coefficient is 0.87 and the averages of the measured and computed soil water are 9.50% and 9.36% respectively. The largest individual difference is less than 4% with most of the differences less than 2%. Therefore, this is a useful technique for obtaining more complete coverage of ground truth information for each test

Figure 12 The location of weather stations that were used
to provide supporting ground truth information
for the Texas passes.
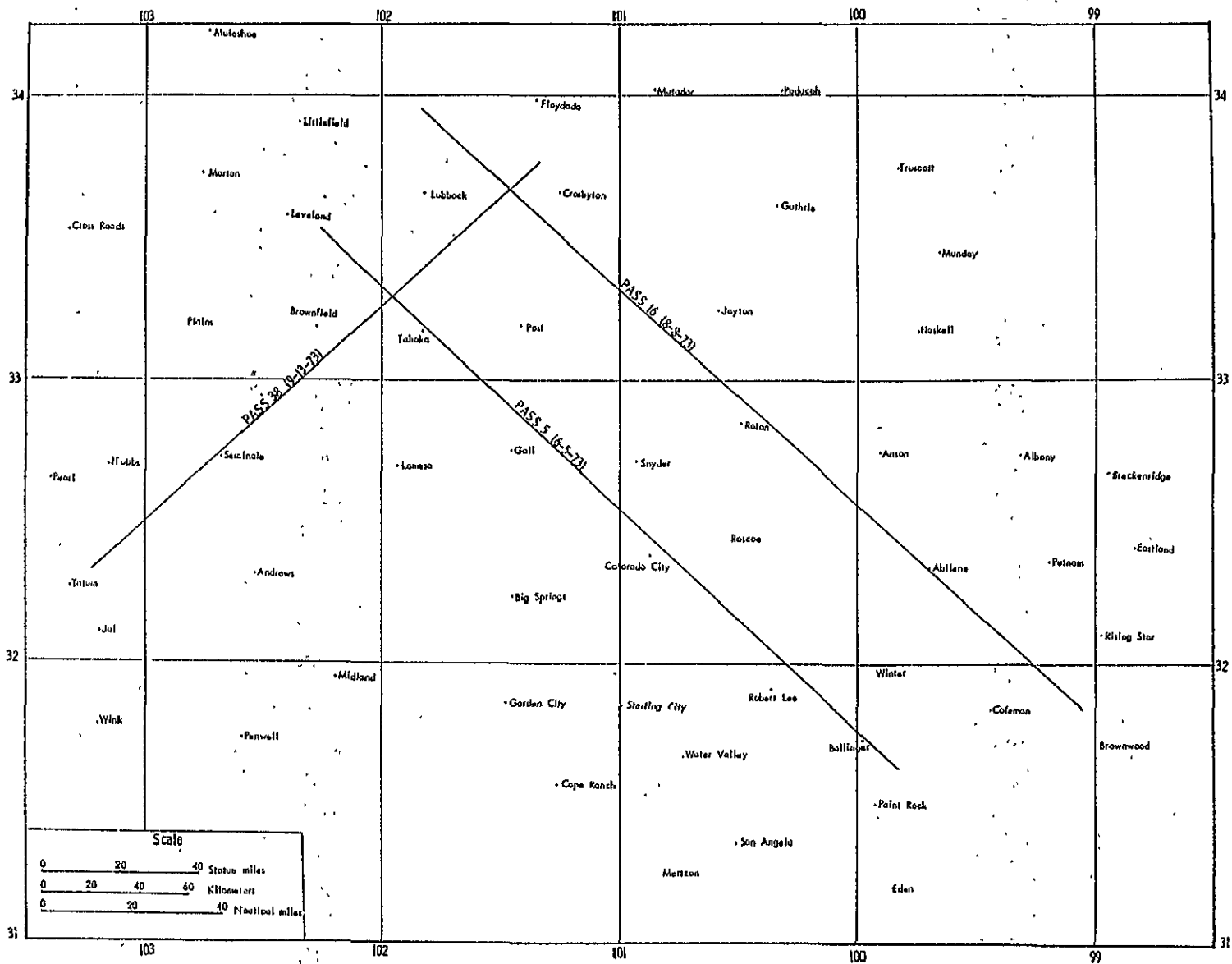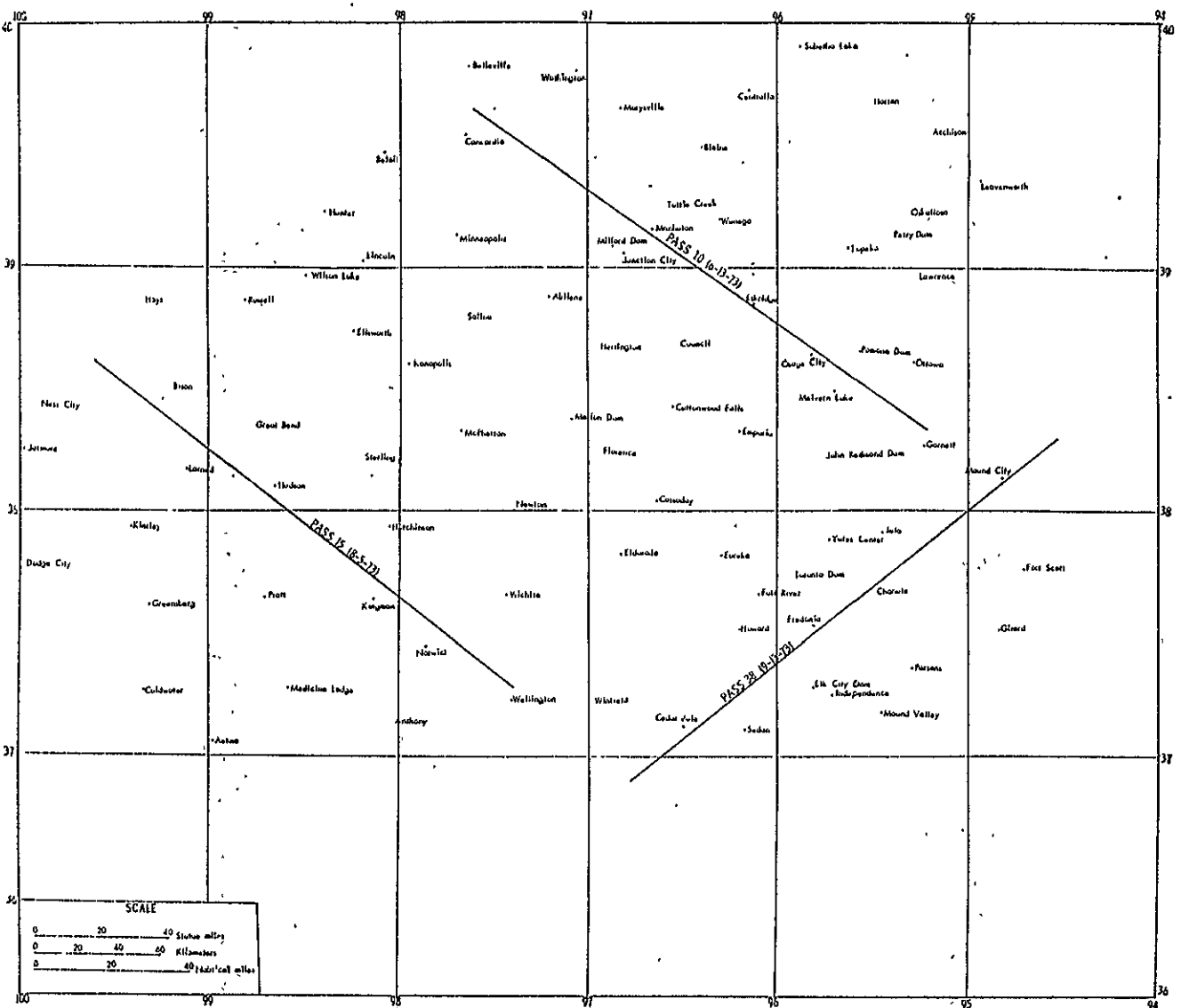
Figure 13 The location of weather stations which were used for supporting ground truth information for the Kansas passes.
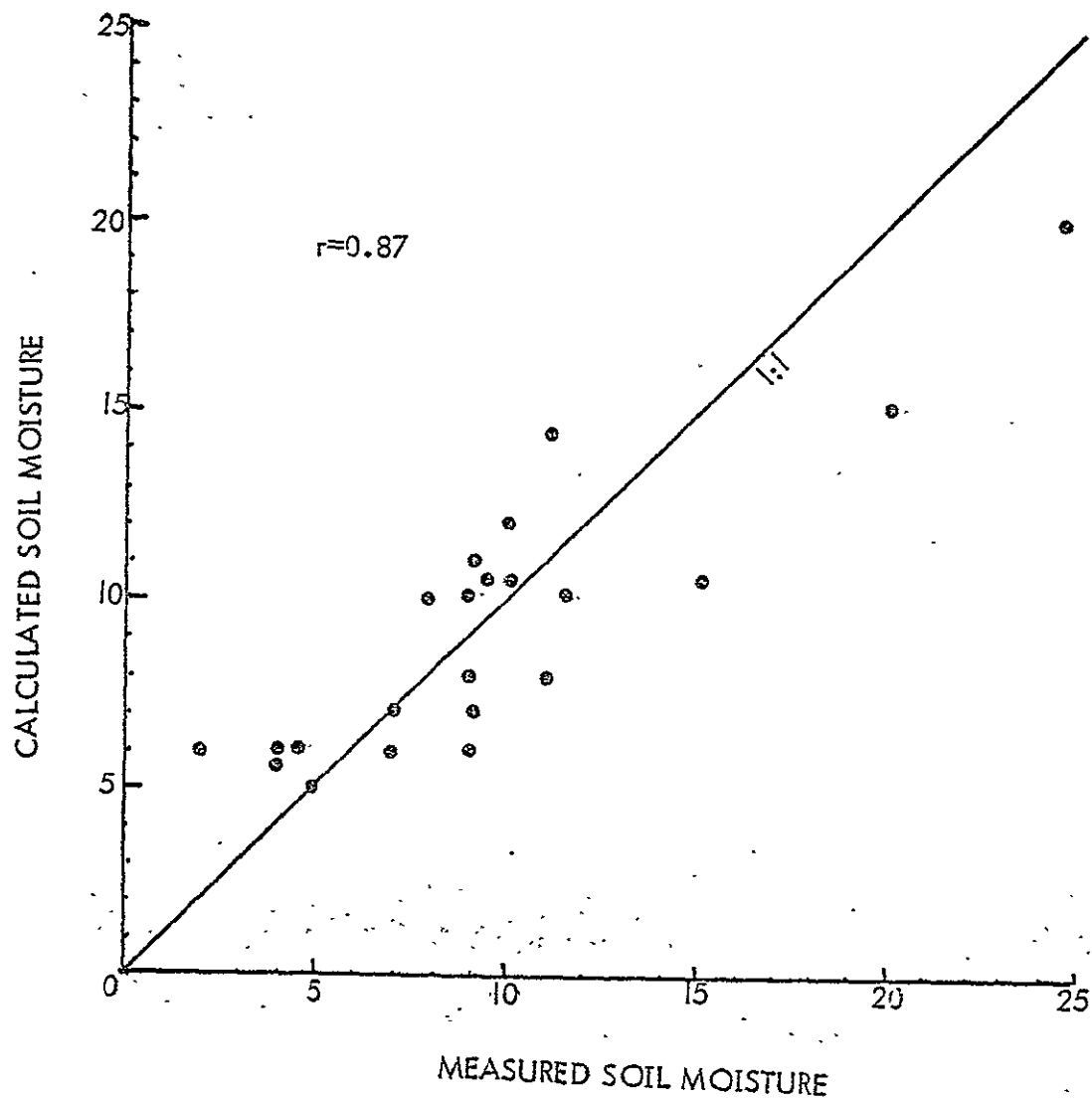
Figure 14 A comparison of the measured soil moisture content
with the calculated soil moisture content.

site and also for adjusting all moisture measurements to the exact time of Skylab data collection.

In pass 5, Skylab flew over the Texas test site from 2:00:30 pm to 2:02:00 pm, local time. The soil samples were taken from 8:30 am, June 5, to 12:30 pm, June 6, 1973. There was no rainfall after Skylab passed this area or before the soil samples were taken. The soil water content of the first 2.5 cm of soil depth in percentage by weight is plotted in Figure 15 for the 66 sites where soil moisture was measured and for the additional 48 stations where soil moisture was calculated. The geographical distribution of soil moisture over the entire test site was obtained from a computer program using the technique of weighted linear trend surface, which is based on distance for weight and a least squares solution for each grid intersection. Figure 16 shows the same soil moisture distribution contoured for every 5% interval.

In pass 16, Skylab passed over the test site from 10:04:00 am to 10:05:30 am, local time. The 720 soil samples from 120 locations were taken from 8:30 am, August 7, to 12:30 pm, August 9, 1971. There was 0.04 to 0.08 inches of rainfall in the early morning of August 8 in the northwest part of the test site. According to the water balance calculations and the distribution of rainfall, 3% to 6% of soil water content was added to the first 2.5 cm of 18 soil samples which were taken from Tahoka to Lubbock in the evening of August 7. The soil water content of the first 2.5 cm of soil depth in percentage by weight was then calculated for the entire site

56

Figure 15 The geographical distribution of soil moisture content throughout the Texas test site on June 5, 1973 as computed by fitting a least squares trend surface to the data points.
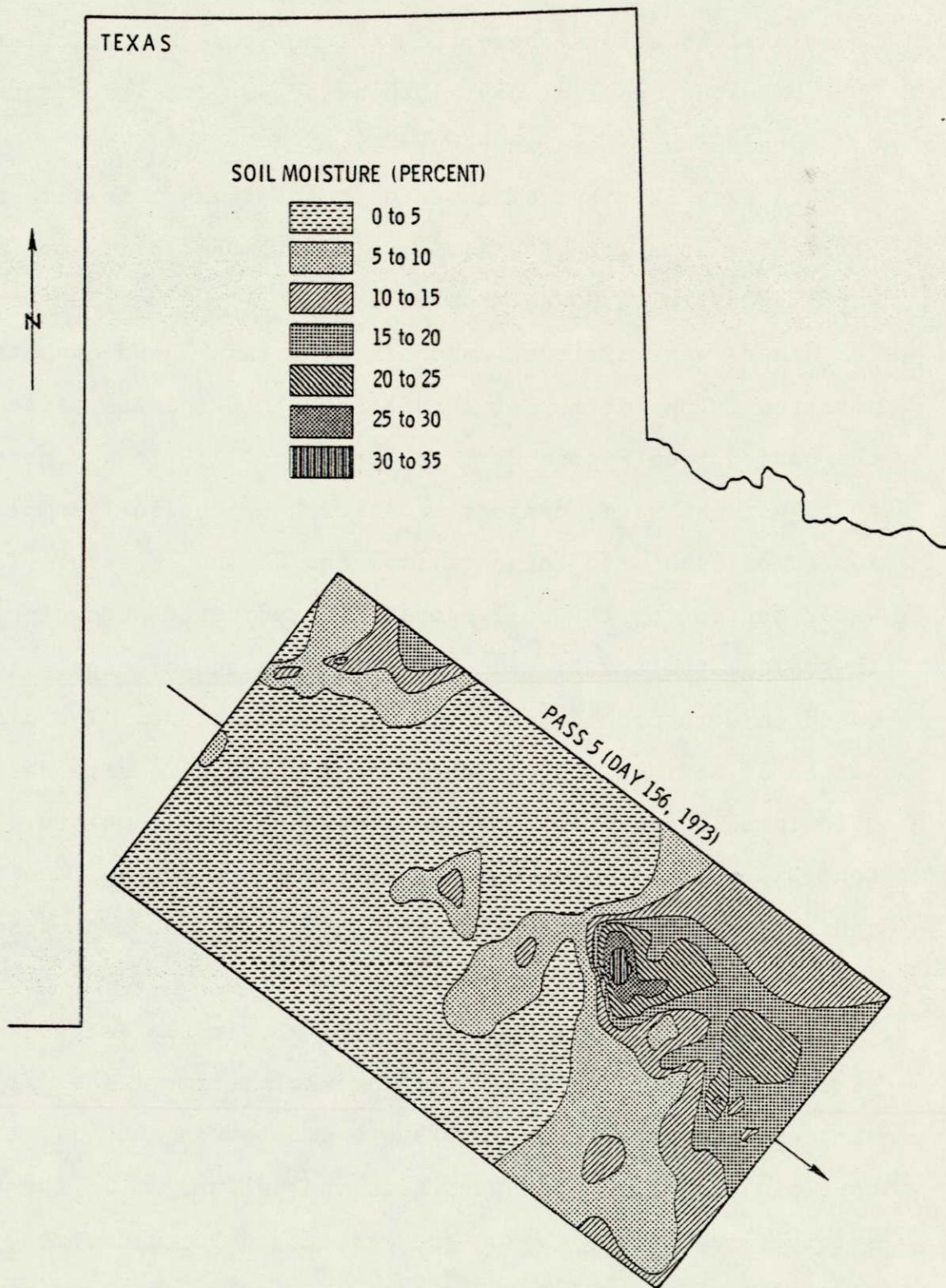
Figure 16 The geographical distribution of soil moisture
content throughout the Texas test site on June 5,
1973.

based on the 120 soil moisture measurement locations and 48 additional locations where the soil moisture was calculated. Thus, the geographical distribtuion of soil moisture content was obtained as shown in Figure 17.

In pass 38, Skylab passed over the Texas test site from 11:57:00 am to 11:58:30 am, local time. The soil samples were taken from 8:30 am, September 8 to 12:00 pm, September 10. There were different amounts of rainfall and evapotranspiration in the different locations within the test site in the period from September 8 to September 13. It was necessary to adjust the water content as measured by the soil samples for comparison with the data from the Skylab sensors. The water content of the soil samples was adjusted according to the calculated actual evapotranspiration and precipitation based on data from the nearest weather stations. The distribution of soil moisture content over the entire site was then calculated based on the 86 locations where soil moisture content was measured and the 35 stations where the soil moisture content was calculated. The resulting distribution of soil moisture is shown in Figure 18.

In pass 10 Skylab collected data over the Kansas test site from 7:51:22 am to 7:57:57 am, local time. The soil samples were taken from 8:30 am to 4:30 pm on June 13, 1973. Several local thundershowers occurred on June 12 in the test site before the Skylab and ground truth data collection, resulting in very high soil moisture levels. Soil moisture
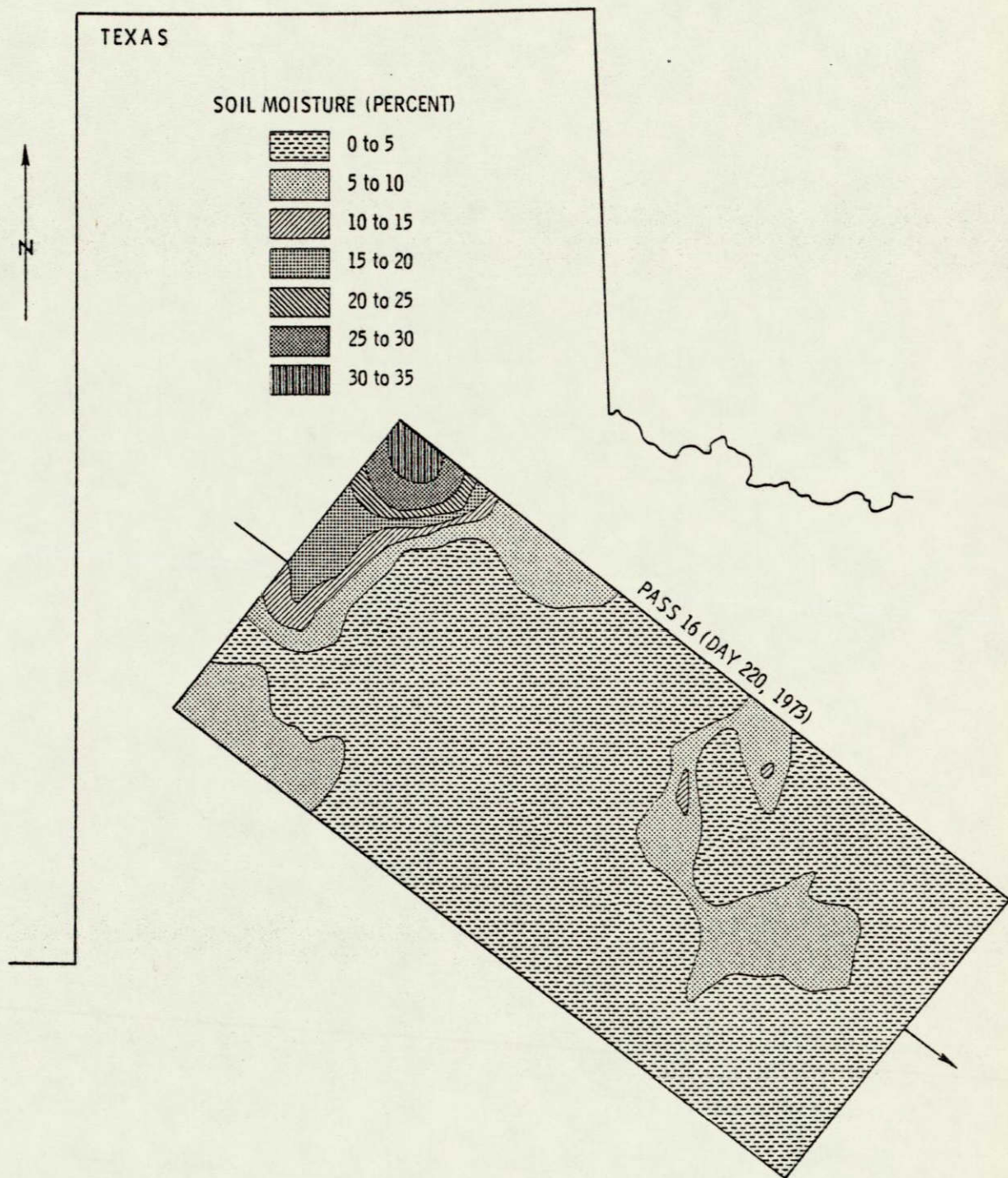
Figure 17   The geographical distribution of soil moisture
content throughout the Texas test site on August
8, 1973.
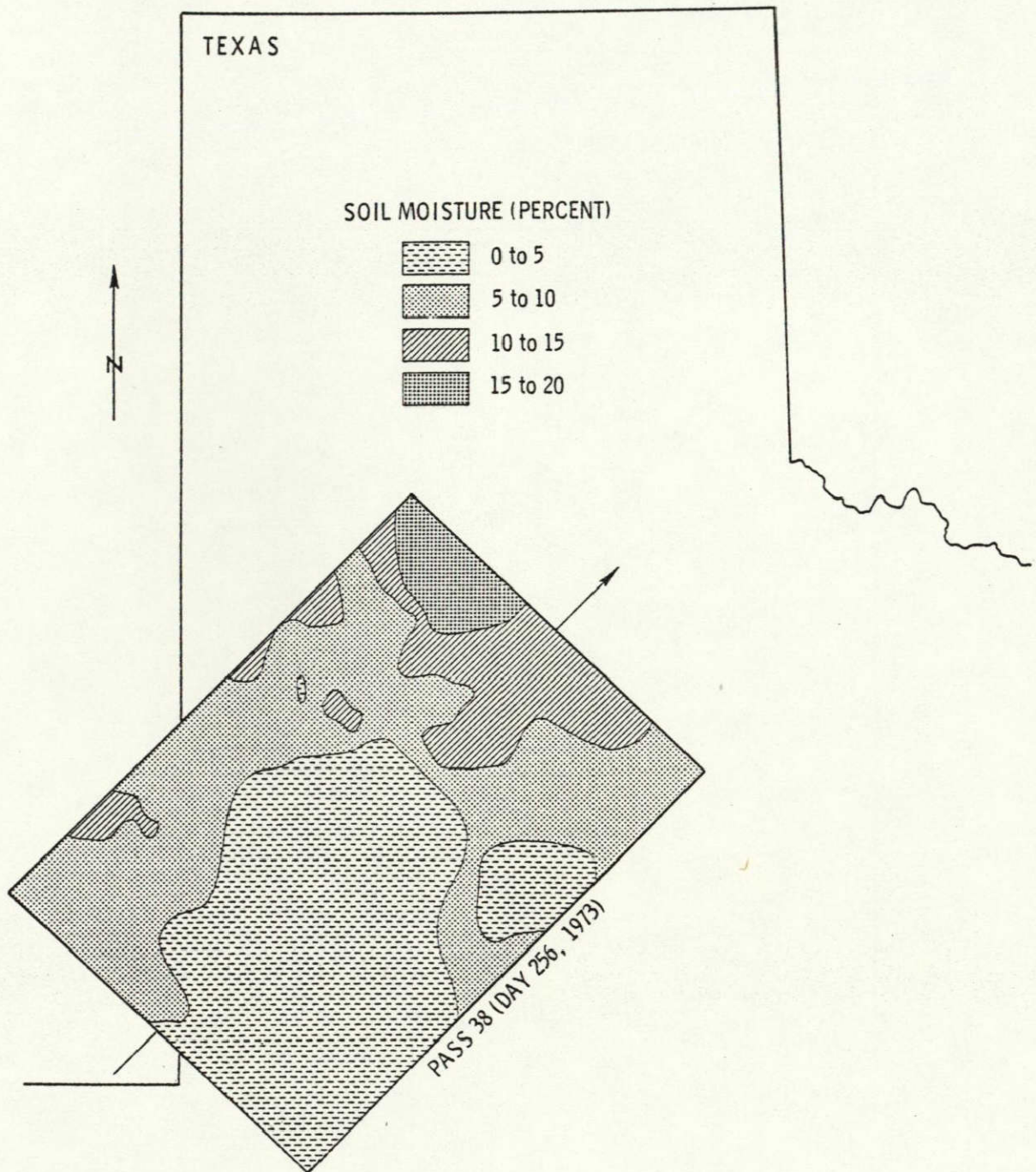
Figure 18   The geographical distribution of soil moisture
content throughout the Texas test site on Sept-
ember 13, 1973.

content was measured at 42 locations throughout the test site. The distribution of soil moisture content over the whole test site (Figure 19) was computed based on these measured values and 37 stations where the soil moisture content was calculated by the water balance technique.

For the Kansas test site, Skylab pass 15 collected data for the soil moisture experiment from 10:37:10 am to 10:38:10 am, local time. The soil samples were taken from 8:30 am, August 5 to 12:00 pm, August 6. There was no rainfall after Skylab passed this site or before soil samples were taken. The water content of the soil was so low that the actual evapotranspiration rate was negligible in the period from August 5 to August 6 so that no adjustments of measured soil moisture were necessary. The ground truth data for this pass included 42 soil sites where the moisture content was measured and 36 stations where calculations were completed for obtaining the soil moisture distribution patterns over the whole test site as shown in Figure 20.

In pass 38, Skylab collected data over the Kansas test site from 11:59:21 am to 11:59:51 am, local time. The soil samples were taken from 10:00 am, September 13 to 5:00 pm, September 14. There were heavy local thunderstorms before the Skylab and ground truth data collections. Therefore, the variation of soil moisture content in the site was rather great and all 59 locations of soil samples were located in the west side of the test site as shown in Figure 11. It was necessary
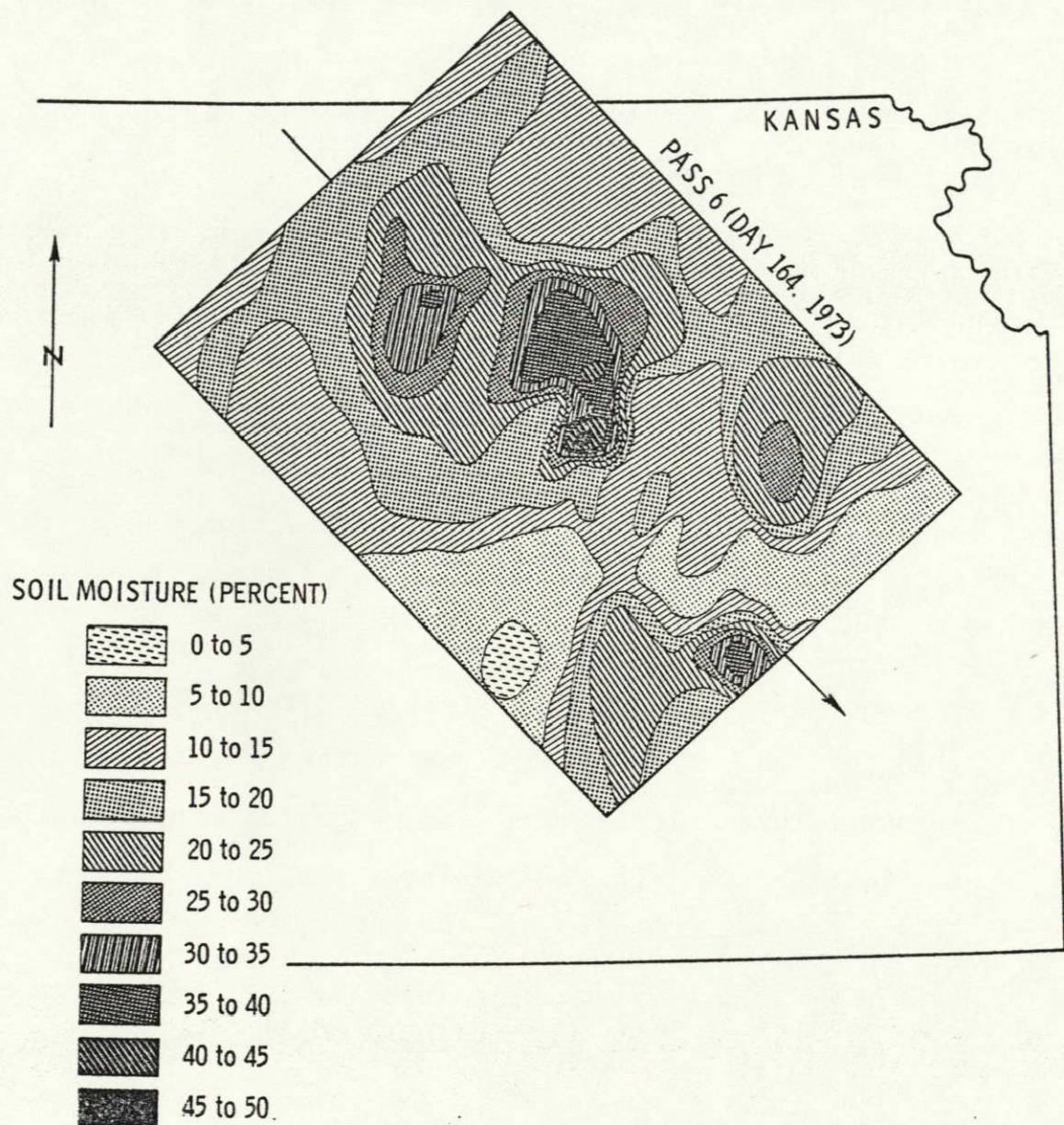
Figure 19   The distribution of soil moisture content through-
out the Kansas test site on June 13, 1973.
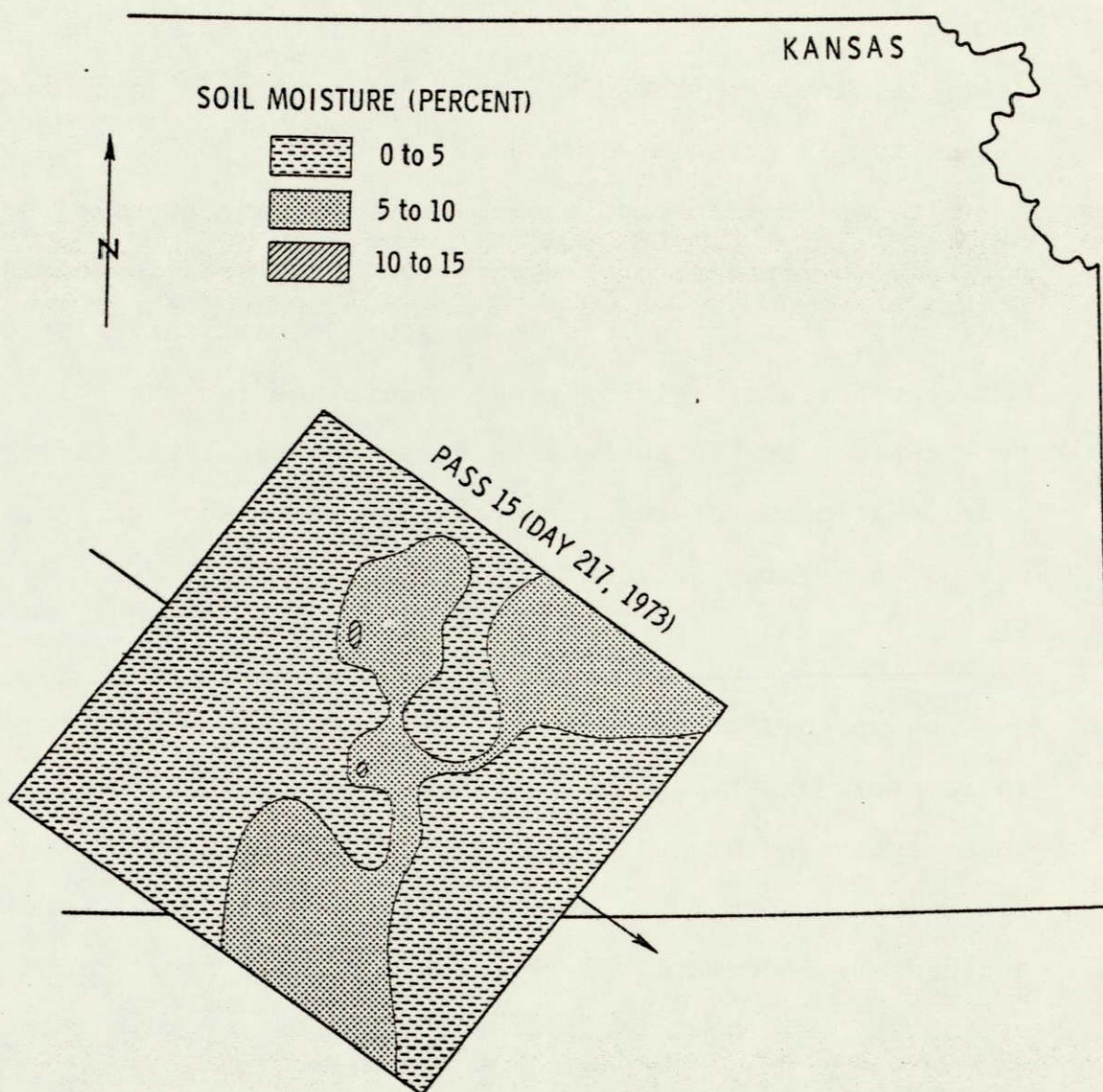
Figure 20 The distribution of soil moisture content through-
out the Kansas test site on August 8, 1973.

to calculate the soil moisture content in the east side of the test site by the water balance technique. Thus, the distribution of soil moisture content over the entire test site was determined as shown in Figure 21 based on 59 measured values and 39 calculated values.

It can be seen from the previous illustrations of soil moisture variations for the different data sets in Kansas and Texas that wide variations in moisture conditions existed. This was very fortunate, giving ideal conditions for the soil moisture content of the surface and near surface layers of the earth. Response of the different Skylab sensors will be discussed in a later section.

Vegetation and Land-Use Data

While collecting quantitative soil moisture data for the radiometric experiments, other types of information of a less quantitative nature were also gathered. During the course of field work, photographs of the vegetation were taken and height and density information were gathered on the basis of best estimates. All of these pieces of information were then assembled in the laboratory.

In order to understand the contribution of vegetation and land use to Skylab measurements, a vegetation land-use map was generated for the two test sites. These maps were prepared from the S190A and S190B vertical color photography, supplemented by ERTS imagery and ground truth photographs taken during the soil moisture sampling missions. Figure 22 shows the map
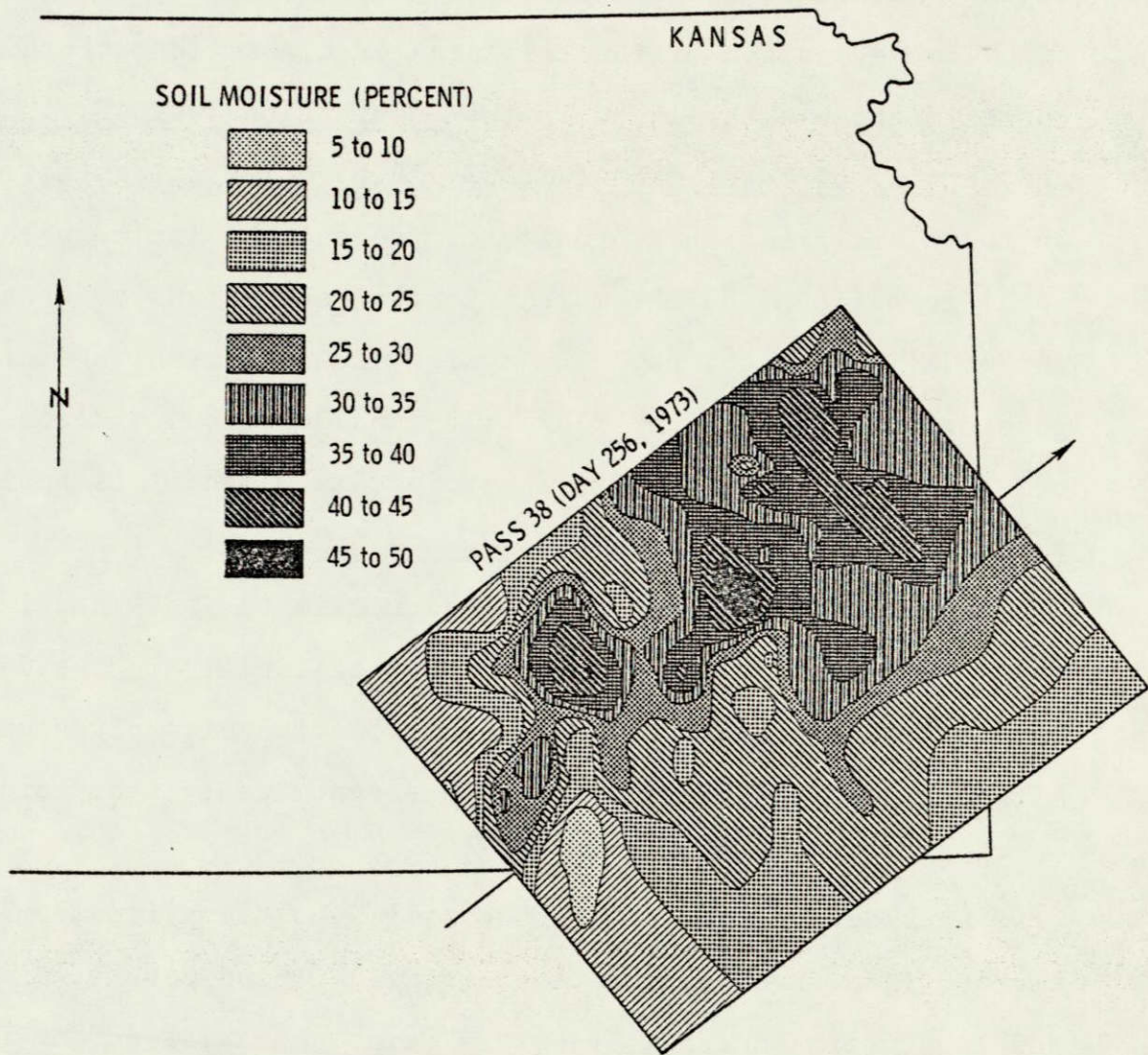
Figure 21   The distribution of soil moisture content through-
out the Kansas test site on September 13, 1973.

for the June 5, 1973 Texas test area and Figure 23 shows the vegetation and land use in the Kansas test site based on the August 5, 1973 data. Table VI describes in some detail vegetation characteristics of each category on the maps.

The vegetation of the test area is classified according to the methods established in the International Classification and Mapping of Vegetation (UNESCO, 1973). The categories used in the classification are units of vegetation, including both zonal formations and the more important and extensive azonal and modified formations. The system is based upon vegetation physiognomic rather than floristic considerations and considering the nature of the Skylab project to which it is applied, this is quite appropriate.

Supplementary terms referring to climate, soil and landforms are included in the names and occasionally in the definitions, where they help the identification of a given unit. Although most units are defined physiognomically, they broadly indicate environmental conditions.

Considering the specific details, the classification is divided into five major categories: (i) Closed Forest, (ii) Woodland, (iii) Scrub, (iv) Dwarf-Scrub and Related Communities, (v) Herbaceous Vegetation.

The relative amounts of each vegetation type within each footprint of the S193 and S194 Skylab sensors was determined. The percentage of each type of vegetation within each footprint was determined by utilizing a Hewlett-Packard calculator-
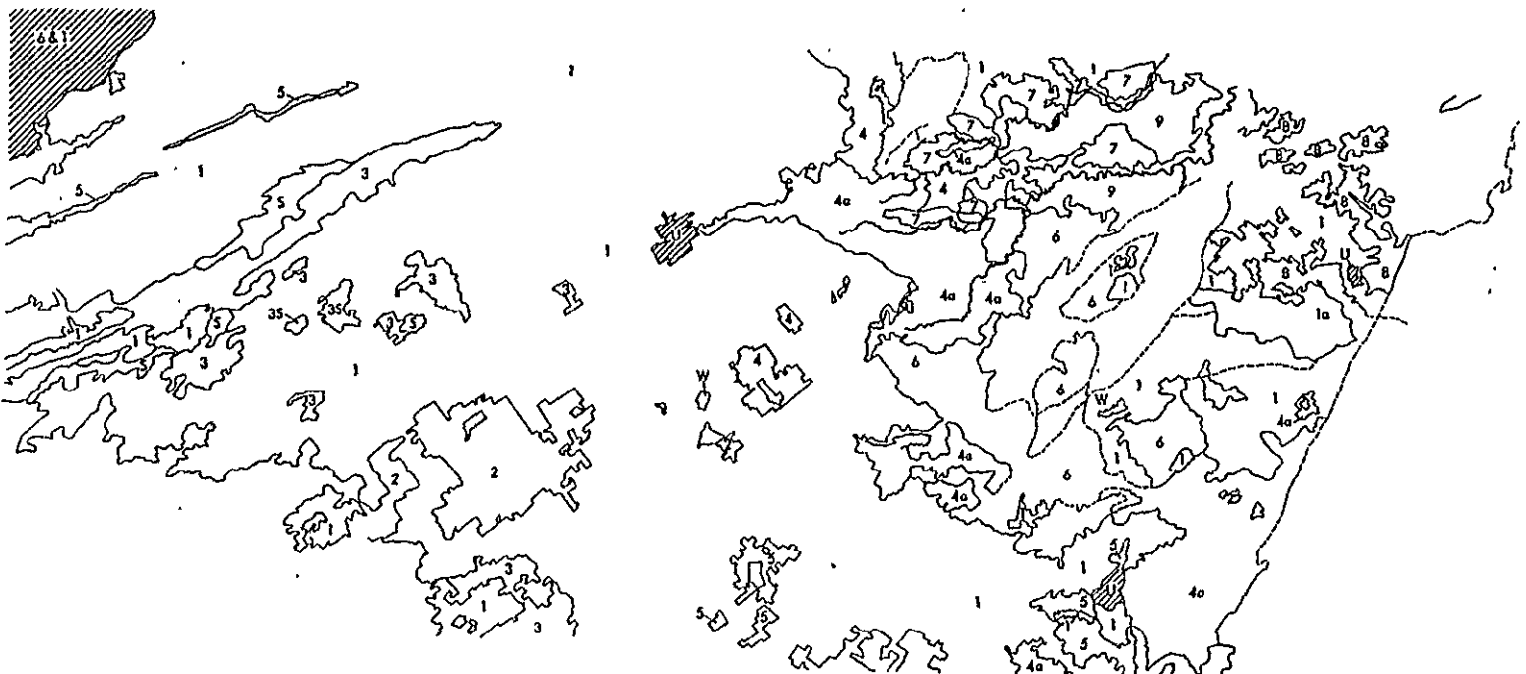
Figure 22 Type of vegetation in the Texas site on June 5, 1973. Numbers refer to map catagories and are described in the accompanying tables.
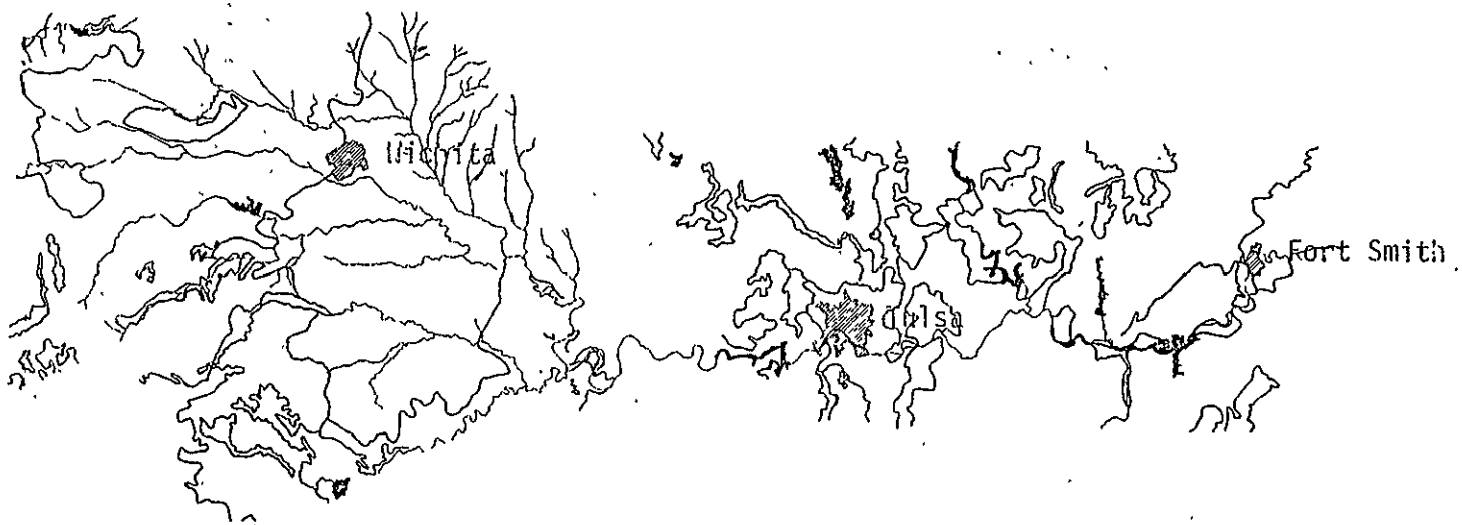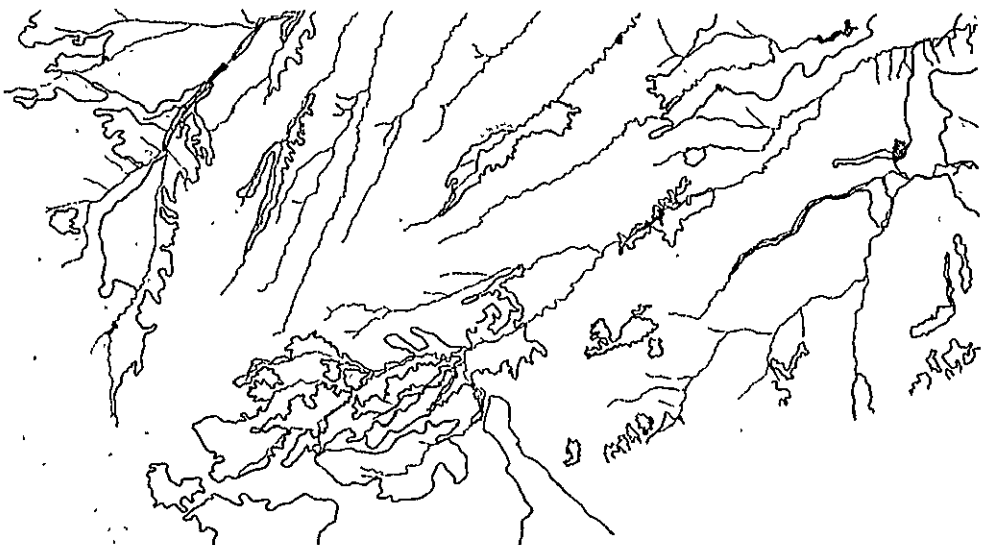
Figure 23 Type of vegetation in the Kansas test site on August 5, 1973.

69

Table VI

Vegetation-Land-Use Map Categories

Map Categories	UNESCO Formula	Description
1	V-D-2b	Dominantly bare ground, some emergent shoots of cotton and grain sorghum less than 5 cm in height.
1a	V-D-2b	Same as above; variations due to soil type differences.
2	V-C-3c	Short grassland; dominant graminoid growth forms are less than 50 cm tall. Woody synusia of shrubs covering less than 10% of the areas.
3	V-C-6a	Short grass communities practically without woody synusia.
4	V-B-3c	Medium tall grassland; dominant graminoid growth forms are 50 cm to 2 m tall; woody synusia of broad leaf diciduous shrubs covering 10% or less.
4a	V-B-3c(1)	Same as above, but total plant coverage per unit area is significantly less.
5	V-D-2b(2)	Mainly anual low forb communities less than 1 m tall.
6	V-B-3c(2)	Medium tall grassland; dominant graminoid growth forms are 50 cm. to 2m tall; woody synusia of broad leaf diciduous shrubs covering 10-40%.
7	III-C-2a	Xeromorphic (sub-desert) shrubland without succulents. Open stands of shrubs with various xerophytic adaptions. Mainly less than 2 meters tall.

Table VI (cont.)

Map Category	UNESCO Formula	Description
8	III-B-3a(1)	Temperate deciduous shrubland. Moderately dense scrub with more or less continuous grass under story. Shrubs 2 to 3 m tall. Grass less than 50 cm tall.
9	III-B-3a(2)	Temperate deciduous shrubland. Essentially the same as category 8, but the percentage of shrub coverage is lower and individual plants are more widely separated.
9a	III-B-3a(3)	Same as above, but much less total vegetative cover, i.e., more bare soil.
S		Bare saline soils, often found in dry channel or depressions.
W		Water.
U		Urban.

digitizer system. Therefore, detailed vegetation information was available for understanding the performance of the microwave sensors.

Snow Cover and Freeze-Thaw Line Data

In general, two significant factors minimized the data base uable for SL-4 analysis. Most noteworthy of these was the inadvertent modification of the S193 instrument through astronaut error. The abrupt removal of the antenna cap on S193 augmented the radiometer footprint to essentially horizon-to-horizon size. Though the active microwave portion (scatterometer) did not suffer the identical fate, a substantial alteration in footprint size and shape did occur.

The collection of suitable ground truth fared somewhat better. Sufficient advance notice for ground truth collection, however, was received only for the January 11 pass. On this date, a special data collection by NWS personnel was taken in Kansas and extreme northwest Missouri. No collections of this nature were taken for January 14 or January 24. In spite of this setback, sufficient data was obtained from contour maps supplied by the River Forecast Office (RFC) in Kansas City, Missouri for the January 14 test area. The data extracted from RFC contour maps on January 24 is sparse, and it has been determined that the density of observations will not support any conclusions generated from this data set.

The following is a list of data available for analysis:

A. January 11, 1974

    1. Site: Amarillo, Texas to Clinton, Iowa

    2. Skylab Data Available:

        a. S190B: frames 44-60

            1) Time GMT start: 17:34:34.3

            2) Time GMT stop: 17:36:13.6

            3) Coordinates @ start: 36:57.5N 99:14.6W

            4) Coordinates @ stop: 40:35.8N 92:55.3W

        b. S192: channels 9, 10, 15, 16, 18, and 21

            1) Time GMT start: 17:35:47.9

            2) Time GMT stop: 17:43:58.0

        c. S193

            1) Time GMT start: 17:34:47.3

            2) Time GMT stop: 17:36:0.04

            3) Coordinates @ start: 37°32' 98°19'

            4) Coordinates @ stop: 40°10' 93°49'

        d. S194

            1) Time GMT start: 17:34:40.19

            2) Time GMT stop: 17:36:12.42

            3) Coordinates @ start: 37°12'N 98°51'W

            4) Coordinates @ stop: 40° 34'N 92°59'W

    3. Ground Truth Available:

        a. special data collection taken by NWS for Kansas
            and NW Missouri only

        b. other sections of track have snow depth only
            from CD's; water equivalent data not available.

B. January 14, 1974

    1. Site; Denver, Colorado to Mankato, Minnesota

    2. Skylab Data Available:

        a. S190A: frames 119-132

            1) Time GMT start: 17:01:0.1146

            2) Time GMT stop: 17:03:10.1992

            3) Coordinates at start: 38:58.5N 105:21.8W

            4) Coordinates at stop: 43:21.3N 96:27.0W

        b. S190B: frames 81-105

            1) Time GMT start: 17:00:45.8

            2) Time GMT stop: 17:03:15.6

            3) Coordinates @ start: 38:26.9N 106:14W

            4) Coordinates @ stop: 43:32.3N 96:01.2W

        c. S193S

            1) Time GMT start: 17:01:07.43

            2) Time GMT stop: 17:02:19.5

            3) Coordinates @ start: 39°15' 104°50'

            4) Co rdinates @ stop: 41°44' 100°02'

        d. S194

            1) Time GMT start: 17:01:20:11

            2) Time GMT stop: 17:03:07.18

            3) Coordinates @ start: 39°43'N 104°02'W

            4) Coordinates @ stop: 43°16' 96°37'

    3. Ground Truth Available:

        a. data obtained from River Forecast Center Operational Charts, including snow depth and water equivalent for entire track.

C. January 24, 1974

    1. Site: South Dakota and Iowa

    2. Skylab Data Available:

        a. S190A: frames 349-360

            1) Time GMT start: 17:56:32.2

            2) Time GMT stop: 17:58:22.1

            3) Coordinates @ start: 45:04.9N 99:14.7W

            4) Coordinates @ stop: 41:46.1N 91:07.4W

        b. S193S: not processed from tape

        c. S194

            1) Time GMT start: 17:56:31.90

            2) Time GMT stop: 17:58:12.01

            3) Coordinates @ start: 45°05'N 99°15'W

            4) Coordinates @ stop: 41°46'N 91°07'W

    3. Ground Truth Available:

        a. sparse data obtained from River Forecast Center
           Operational Charts

CHAPTER V

THEORETICAL BASIS FOR THE DETECTION OF
GROUND MOISTURE CHARACTERISTICS FROM SPACE

Introduction

The need to make measurements over a large area in a short
time has increased the role of remote sensing techniques in sci-
entific study. An effort is being made to measure the character-
istics of earth's surface by airborne and/or spaceborne remote
sensors. A number of different sensors, both active and passive
are being utilized to gather information about the significant
features of the earth. The active systems transmit their own en-
ergy and measure the energy reflected or scattered by the target.
Passive systems measure the energy emitted by the target. Some
of these systems operate in the microwave region of the electro-
magnetic frequency spectrum. The all weather day/night opera-
tional capability of microwave sensors is particularly useful for
repeated and timely coverage.

The S194 and S193 radiometers are passive systems and mea-
sure antenna temperature. The antenna temperature is related to
the brightness temperature which is dependent on the emissivity
and thermometric temperature of the target. The S193 scattero-
meter is an active system and measures the radar backscatter co-
efficient, σ°, of the target that is related to the reflection
coefficient of the target. Both reflection coefficient and emis-
sivity depend on the electrical properties of the target. The
electrical properties of most of the targets change significantly
with moisture.

Scatterometer Theory

The radar scatterometer is an instrument designed to measure the radar scattering coefficient σ° (radar cross-section per unit area as a function of the illuminated incidence angle Θ measured from the vertical). The signals radiated by the transmitter of the radar are re-radiated by the ground and received back at the radar. The power incident at the receiver input terminals is given in terms of radar operating parameters by the classical radar equation:

$$P_r = \frac{P_t G_t G_r \sigma \lambda^2}{(4\pi)^3 R^4} \tag{1}$$

where:

P_r = radar receive power appearing at the receiver input terminals, in watts
P_t = transmitter power, in watts
G_t = transmitter antenna gain
G_r = receiver antenna gain
σ = target cross-section, in square meters
λ = radar wavelength, in meters
R = radar range, in meters

The received radar signal is made up of component signals scattered from numerous small scatterers and simultaneously observed by the radar. Thus, the average power received by radar is the sum of the powers received from the individual scatterers.

If there are n scattering elements in a region illuminated at one time by a radar, the radar equation becomes (assuming $G_t = G_r = G$):

$$P_r = \sum_{i=1}^{n} \frac{P_t G^2 \lambda^2 \sigma_i}{(4\pi)^3 R_i^4}$$

or

$$\bar{P}_r = \frac{P_t G^2 \lambda^2 \sigma^\circ \Delta A}{(4\pi)^3 R^4}$$

where $\bar{P}_r$ is the average returned power and $\sigma°$ is the differential scattering coefficient.

Thus $\sigma°$, the radar scattering coefficient can be written as:

$$\sigma° = \frac{(4\pi)^3 \, R^4 \bar{P}_r}{G^2 \lambda^2 \Delta A \, P_t}$$

where the gain, G, and the wavelength, λ, are the parameters of the radar. The range, R, depends on the experiment and the area, ΔA is determined by the radar and the experiment.

The value of $\sigma°$ for a particular target depends on the polarization, wavelength and angle of the incident wave. In addition, $\sigma°$ also depends upon the target, surface roughness and subsurface structure. $\sigma°$ for a target can be found experimentally by utilizing a radar scatterometer. A number of simplified theoretical models are available to compute the value of $\sigma°$ for different types of target. For example, the analytical expression for the polarized scattering coefficients for a weakly perturbed dielectric plane are given by:

$$\sigma°_{VV} = 8K^4 \sigma_1^2 \; \left| R_V \cos^2\Theta + (1+R_V)(1-\frac{1}{\epsilon_r})\sin\Theta \right|^2 \; W_f(2K \sin\Theta, 0)$$

and:

$$\sigma°_{HH} = 8K^4 \sigma_1^2 \; \cos^4\Theta \; |R_H|^2 \; W_f(2K \sin\Theta, 0)$$

where $K = 2\pi/\lambda$ and W_f is the two dimensional Fourier transform of the surface correlation coefficient of the perturbed plane. R_V and R_H are Fresnel reflection coefficients for vertical and horizontal polarization respectively. σ_1 is the standard deviation of the small scale surface height variation. VV corresponds to vertical receive-vertical transmit polarization and HH corresponds to horizontal receive-horizontal transmit polarization.

λ is the wavelength. Thus, the value of σ° depends on the reflection coefficient which in turn is related to the dielectric properties of the target. The above expressions are only applicable when there are small perturbations in the surface roughness on the wavelength scale.

This example of the theory was given for the very simplified model based on perturbation theory. This model applies only to surfaces slightly rough compared with the wavelength, so it is not truly applicable to many natural surfaces at 2 cm wavelength. It is shown here only as an illustration of the theories that may be applied. The subject of radar scattering theory has a rich literature, but most of it is not directly applicable here because of the assumption nearly always made that the scatter is from the rough boundary between two half spaces. In fact, most natural areas cannot be easily represented by simple rough surfaces, for they contain vegetation, structures made by man, and even natural structures like cliffs that are not amenable to the theories. When these objects are present, volumetric scatter must be considered, particularly for vegetation covered surfaces and for bare surfaces dry enough to permit penetration of the signal to volume scatterers within the soil.

The model shown illustrates the two essential features of the physics of scattering even though it is not in a detailed sense applicable to most surfaces. That is, it shows that the scattered signal depends both on the surface roughness and on the dielectric properties of the surface (or of volume scatters).

The Fresnel reflection coefficients for horizontal and

vertical polarizations are given respectively by:

$$R_H = \frac{\cos\Theta - \sqrt{\varepsilon_r - \sin^2\Theta}}{\cos\Theta + \sqrt{\varepsilon_r - \sin^2\Theta}}$$

$$R_V = \frac{\varepsilon_r \cos\Theta - \sqrt{\varepsilon_r - \sin^2\Theta}}{\varepsilon_r \cos\Theta + \sqrt{\varepsilon_r - \sin^2\Theta}}$$

where Θ is the angle of incidence and ε_r is the complex dielectric permittivity.

The dielectric properties of water at two temperatures are shown in Figure 24 (Hoekstra and Delaney, 1974). K' is the real part and K" is the imaginary part of the complex permittivity. The value of the dielectric constant can be as high as 80 and that of the imaginary part as high as 40 at certain frequencies. The complex dielectric constant of silty clay for 10% water content at 24°C is shown in Figure 25. The dielectric constant of dry soil is typically less than 5. Therefore, the water content of a soil greatly affects its dielectric properties.

Available studies have shown that the relative dielectric constant (with respect to vacuum) of soil increases with increasing moisture content. Variations in the real and complex part of the dielectric constant as a function of water content at 2.2 cm wavelength are shown in Figures 26a and 26b respectively (Poe et.al, 1971). A number of formulas such as given by Rayleigh, Bottcher, Weiner and Pierce are available to compute theoretically the dielectric properties of mixtures if the dielectric properties of its constituents are known. Such values computed by using formulas given by Bottcher and Rayleigh are shown in Figures 26a and 26b. These
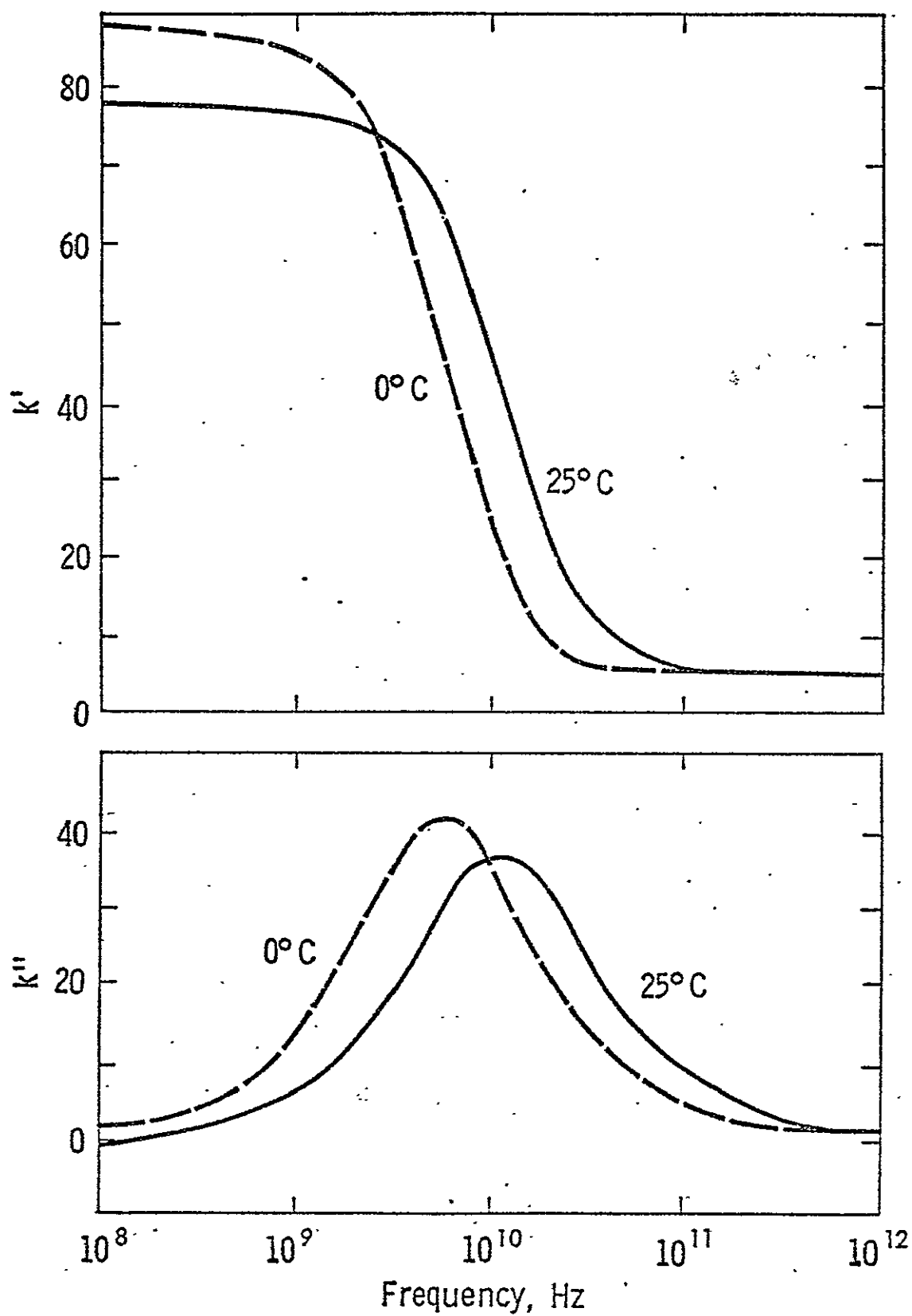
Figure 24   The dielectric spectrum of water at two temperatures
(after Hoekstra and Delaney, 1974).
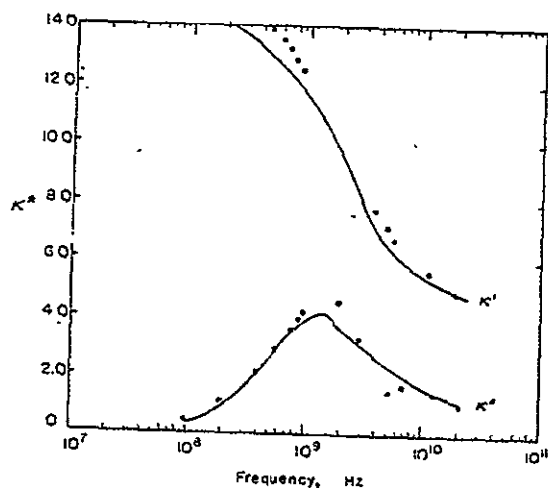
A
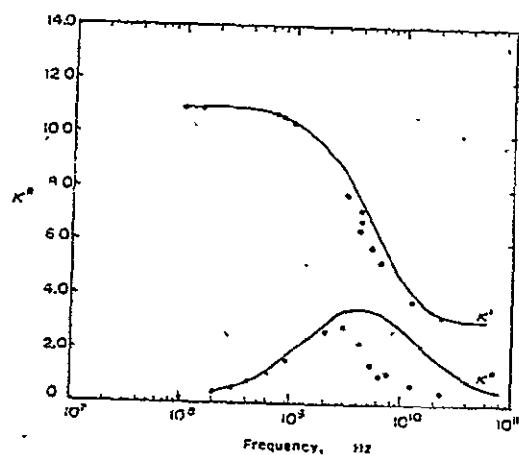
B

Figure 25. The complex dielectric constant of silty clay at a
moisture content of 10% by weight. The solid lines
are curves generated by fitting two debye type dis-
persions to the experimental points at 24°C (A) and
-10°C (B).(After Hoeksta and Delaney, 1974).

Figure 26 Dielectric constant (2.2 cm) showing the real part (A) and imaginary part (B) versus percentage soil moisture (after Poe et. al, 1971).

83
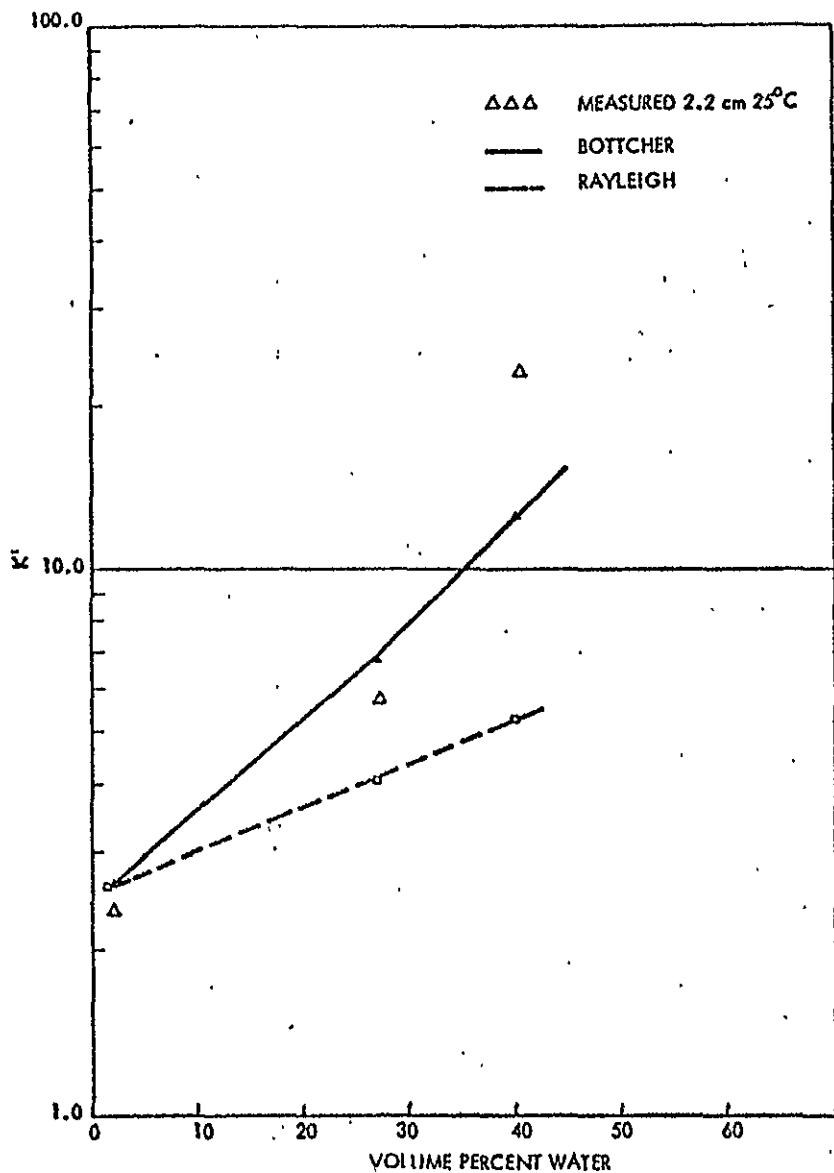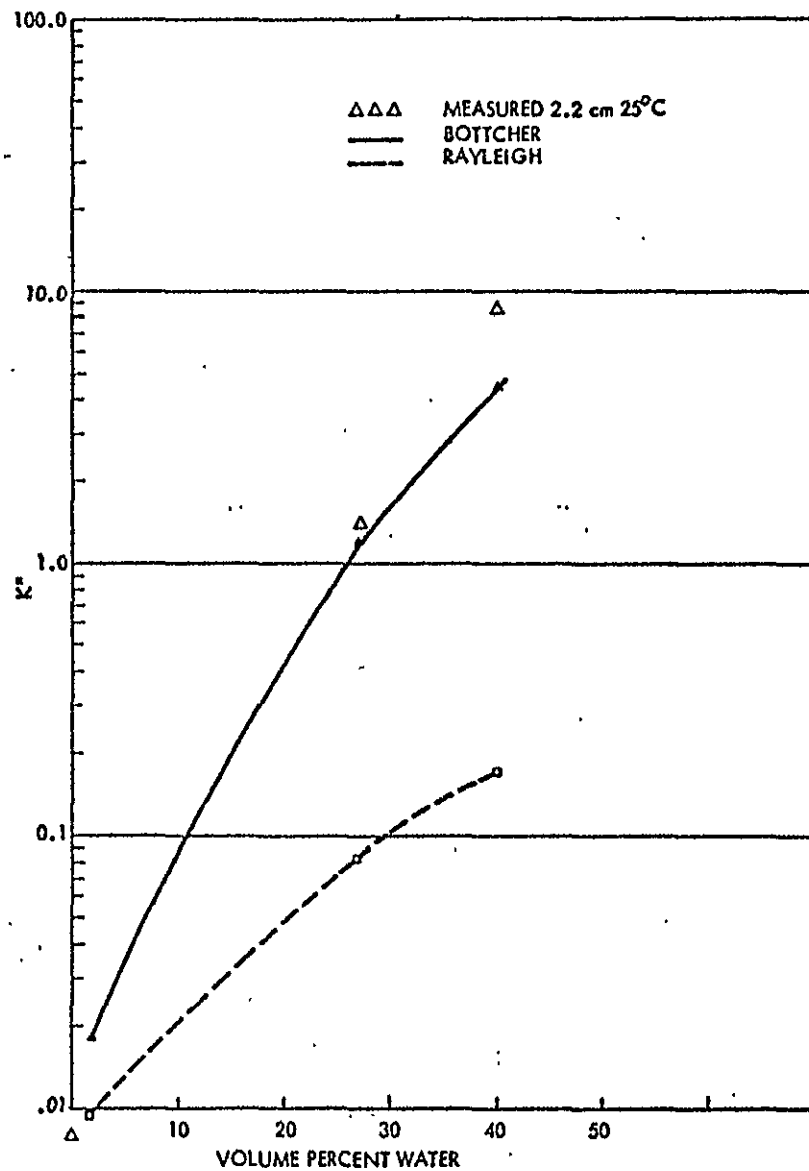
theoretical formulas are useful in inter- and extra-polating experimental measurements. An excellent comprehensive summary of dielectric properties of soils as a function of moisture content is given by Cihlar and Ulaby (1975).

It should be pointed out that the dielectric properties of soil not only change with water content but also are dependent on the temperature, density of soil and the soil type.

Radiometry Theory

It is well known that any object emits (and absorbs) electromagnetic energy in different parts of the frequency spectrum. The relationship between the frequency of emittance (or absorption) and amount of energy emitted (or absorbed) is given by Plank's Black-Body Radiation Law.

The temperature equivalent to the energy measured by a radiometer is termed the Apparent Temperature. In a practical situation, a radiometer viewing the surface of the earth measures contributions from surface emission, emission by the intervening atmosphere and in turn absorbed by the atmosphere (some part) and the atmosphere-emitted radiation reflected by the surface in the direction of the radiometer.

The apparent temperature of a surface when measured by the radiometer at an angle Θ from the vertical, given by Skolnik(1970):

$$T_{aj}(\Theta) = L(\Theta) [T_{Bj}(\Theta)+T_{sj}(\Theta)] + T_{atm}(\Theta) \qquad (1)$$

In the above equation, "j" stands for vertical or horizontal polarization. $L(\Theta)$ is the atmospheric transmittance determined by atmospheric absorption between the surface and the radiometer in

the direction Θ. $L(\Theta)$ can be written as:

$$L(\Theta) = \exp\left[-\sec\Theta \int_0^H \alpha(z)\ dz\right] \tag{2}$$

$T_{atm}(\Theta)$ represents the direct contribution from the atmosphere and is given by:

$$T_{atm}(\Theta) = \sec\Theta \int_0^H T_{air}(z)\ \alpha(z) \cdot \exp\left[-\sec\Theta \cdot \int_z^H \alpha(z')dz'\right]dz$$

$$\tag{3}$$

Equation (3) gives the emittance by the atmosphere and subsequent attenuation by the intervening atmosphere.

Other parameters appearing in equations (1), (2) and (3) are defined as follows:

$\alpha(z)$ = The atmospheric attenuation coefficient per unit length at an altitude of z.

$T_{air}(z)$ = Thermometric temperature of the atmosphere at an altitude z above the surface.

H = Height of radiometer from which the measurement is made.

$T_S(\Theta)$ = The atmospheric emitted radiation reflected by the surface of the earth in the direction of the radiometer.

$T_B(\Theta)$ = Brightness temperature of the surface of the earth.

$= \epsilon_m T$

ϵ_m = Emissivity of the surface.

T = Thermometric temperature of the surface.

The parameters which influence the radiometric measurement are (i) atmospheric effects, (ii) surface emissivity.

Atmospheric effects

The atmospheric effects influence the radiometric measurement through L, T_S and T_{atm}. All these three variables are dependent on atmospheric attenuation coefficient α. α represents contributions from oxygen, water vapor, rain and clouds. If α equals 0, L = 1, and $T_S = T_{atm} = 0$. Both T_S and T_{atm} are caused by atmospheric emission, and for a black body in thermodynamic equilibrium, the absorption coefficient is equal to the emission coefficient. Thus, under the clear sky conditions and operating at frequencies in the "windows" of the absorption spectrum, the effect of L, T_S and T_{atm} can be reduced considerably. Usually if meteorological information is available, L and T_{atm} can be calculated and T_S can be inferred approximately.

The effect of the atmosphere may be significant if clouds and rain are present. If the atmosphere were not an emitter, the signal received from the ground would be attenuated; since the antenna temperature T_a is just the strength of the received power flux expressed in temperature instead of watts/m^2, this would mean that the observed temperature would be less when clouds intervene. Since the atmosphere does emit in an amount proportional to its absorption, the reduced signal from the ground is combined with both the direct cloud emission and the downward emission that has been scattered from the ground. If the emissivity of the ground is low, as it is over water, the signal from even a moderately attenuating cloud is strong enough not only to compensate for the loss in ground signal due to attenuation but actually to raise the observed signal strength; thus the temperature

observed over a cloudy ocean may well be tens of degrees higher
than when the sky is clear. On the other hand, if the brightness
temperature of the ground exceeds the physical temperature of the
cloud, as it does over dry warm land, the effect of clouds is to
reduce the observed signal. In the extreme case of attenuation
exceeding a few dB, the observed signal is almost entirely from
the cloud and is at the physical temperature of the cloud.

For soil moisture measurement, the brightness temperature of
the ground may be either lower than that of the cloud (high mois-
ture content with little vegetation) or higher than that of the
cloud (low moisture content). In the high moisture case, cloud
attenuation tends to raise the observed temperature, leading to
an underestimate of the soil moisture. In the low moisture case,
cloud attenuation lowers the observed temperature, leading to
an overestimation of soil moisture. This effect can be quite sig-
nificant at the S193 frequency (13.9 GHz), but at the S194 fre-
quency, (1.4GHz) the cloud attenuation, and indeed attenuation in
heavy rain, is insignificant.

Surface emissivity

The emissivity of the surface is related to the scattering
behavior of that surface integrated over the upper half-space.
According to the law of thermodynamic continuity, the emitted
energy = absorbed energy = incident energy - reflected energy.

The emissivity of a target is given for a flat surface by:

$$E_p = (1 - |R_p|^2)$$

where p corresponds to the appropriate polarization (vertical or
horizontal).

When the surface is not flat, the emissivity must be calcu-
lated by taking into account the angular variation of the emis-
ison in both polarization.   Here we must replace the above equa-
tion by:

$$\varepsilon_p(\Theta_0) = 1 - \frac{\sec\Theta_0}{4\pi} \int [\sigma_{pc}(o,s) + \sigma_{pp} o,s)] d\Omega_s$$

where $\sigma_{pc}(o,s)$ is differential scattering coefficient for a wave
from direction Θ_0 scattered in direction s, with incident polari-
zation p and scattered polarization c and $\Theta_{pp}(o,s)$ is the same
where both polarizations are p. These σ's are functions of both
roughness and dielectric properties of the ground.

The emissivity is very sensitive to soil moisture. For ex-
ample, the emissivity of very dry soil is about 0.95. The emis-
sivity of calm water is about 0.4-0.6 for most microwave frequen-
cies. At 13.9 GHz, the difference in brightness temperature be-
tween dry soil and 17% soil moisture is about 56°K. The effec-
tive emissivity at 21.4 cm wavelength as a function of water con-
tent is shown in Figure 27.   Included in this figure is the em-
issivity calculated by using theoretical formulas given by Bottcher,
Weiner and Pierce for different form factors F. Figures 28 and 29
show the brightness temperature versus soil moisture curve at 21.1
cm wavelength for two different test sites (Schmugge et.al, 1972).

Discussion

As is evident from above, the dielectric properties of a
medium influence the radar scattering coefficient and the radio-
meter emissivity in two ways: a) through the Fresnel reflection
coefficient and b) the effective depth in the medium responsible
for the backscattered or the emitted energy.
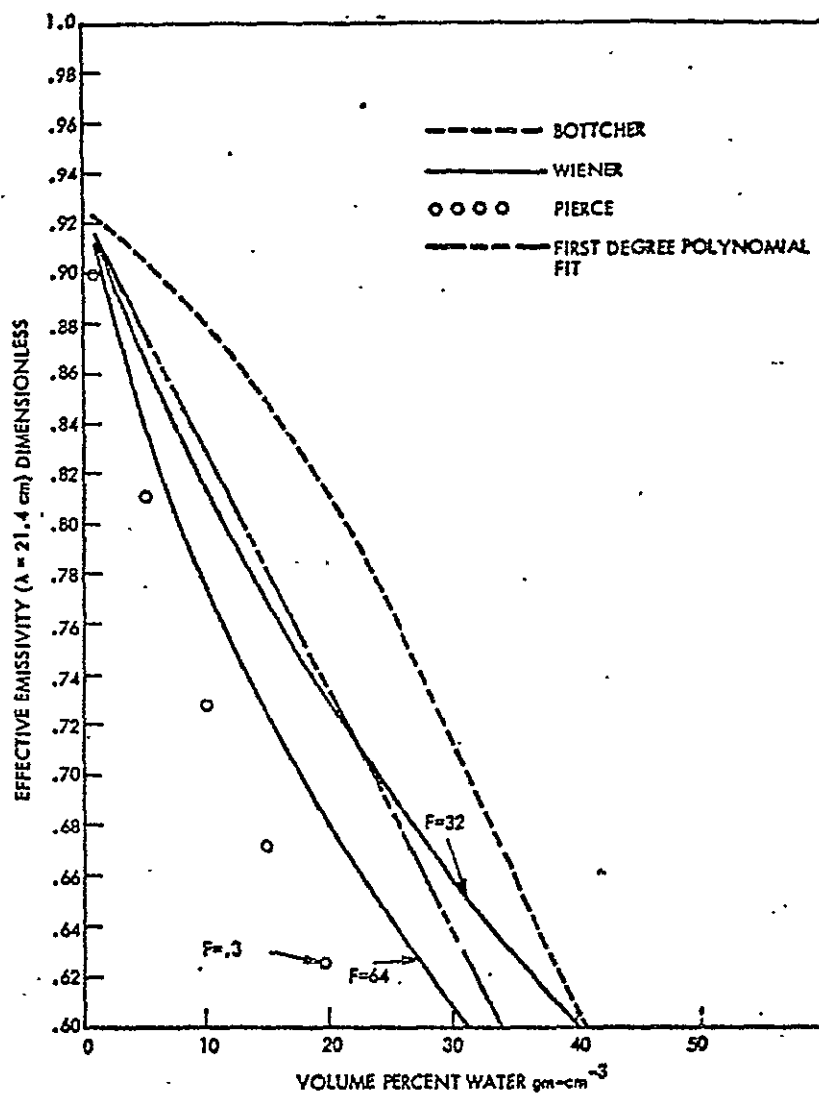
Figure 27 Effective emmissivity versus the volumetric moisture
content for a wavelength of 21.4 cm , 30° view angle,
horizontal polarization (Poe, et. al, 1971).
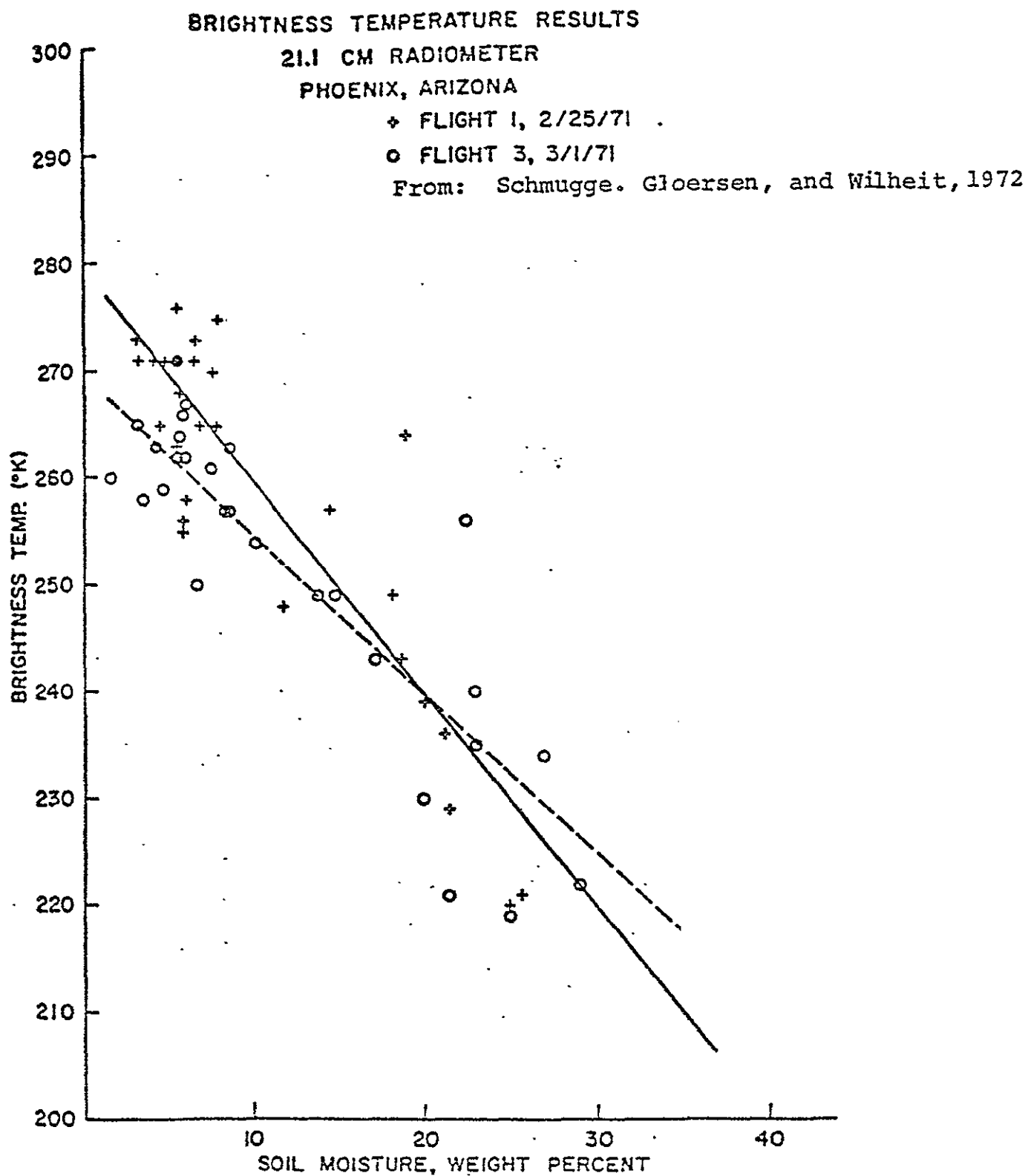
Figure 28   Brightness temperature at 21.1 cm wavelength versus
            soil moisture from Phoenix, Arizona (after Schmugge,
            et. al, 1972).

BRIGHTNESS TEMPERATURE RESULTS
21.1 CM RADIOMETER
IMPERIAL VALLEY, CALIFORNIA
FLIGHT I, 2/25/71
+ EARLY PASS
O LATE PASS

From: Schmugge, Gloersen and
Wilheit, 1972
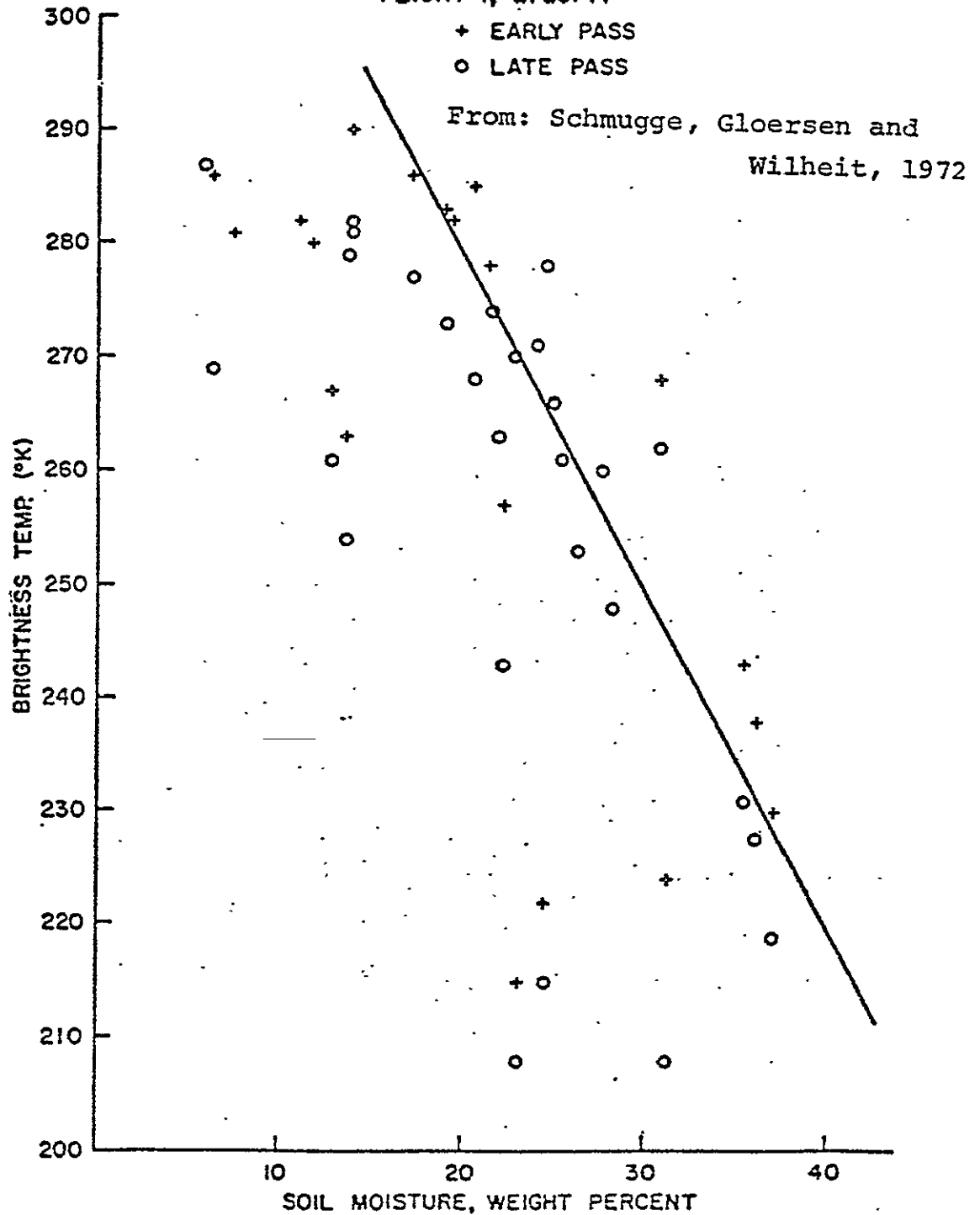
Figure 29 Brightness temperature at 21.1 cm wavelength versus
soil moisture from the Imperial Valley (after Schmugge,
et. al, 1972).

Thus, any changes in the dielectric properties and thereby in soil moisture should be evident in the radiometric and scatterometry measurements. It should be pointed out that these measurements are also affected to a large extent by the surface roughness and any vegetation cover. The effect of soil moisture and the roughness on these measurements have to be separated. Also, needing to be established, is the amount of surface penetration and the effect of subsurface structure. The ultimate utility of these measurements for detecting ground moisture depends on how well the moisture effects can be separated from other effects. Thus, the task is of establishing parameters such as frequency, polarization and angle which are optimum in detecting ground moisture. The measurements made while operating with these optimum parameters will be more sensitive to any variations in soil moisture than to other factors such as surface roughness.

Chapter VI

ANALYSIS AND RESULTS OF THE SOIL MOISTURE EXPERIMENT

S190A and S190B Photographic Interpretations

Portions of the S190A photography have been studied in detail to determine what features can be seen for each of the six bands. The bandwidths and related information are as follows:

Researu Serial No.	Bandwidth(μ)	Film Type	Filter
15	0.7-0.8	IR Aerographic B&W Type EK2424	CC
08	0.8-0.9	IR Aerographic B&W Type EK2424	DD
11	0.5-0.88	Aerochrome IR color Type 2443	EE
02	0.4-0.7	Aerial color (high resolution) type SO-356	FF
06	0.6-0.7	Pan-X aerial B&W type SO-022	BB
10	0.5-0.6	Pan-X aerial B&W type SO-022	AA

Frame 169 for the September 13, 1973 Texas site was studied using the aerial color .4-.7 μ and the Aerochrome IR color .5-.88 from the transparencies. The other four filter types were enlarged to approximately 11 x 11 prints. No attempt was made to determine each and every tonal change on the photos, however, a great deal of general information was obtained. Frame 169 included much of the 9-13-73 Texas site (Figure 30). Therefore, topographic maps, field notes and aerial photography were available for identification of many features.
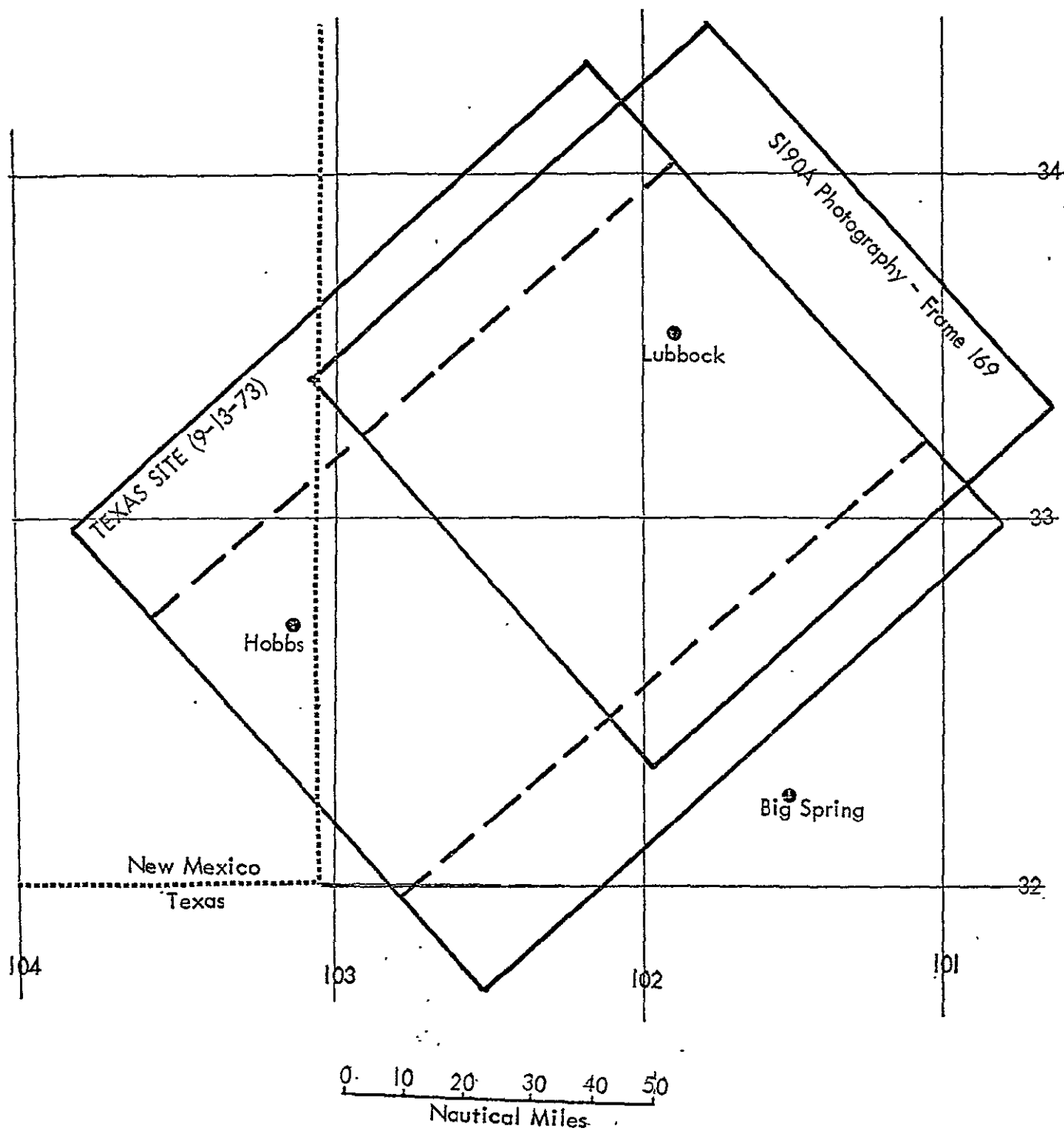
Figure 30 The location of frame 169 S190A image which was used for photographic interpretations.

C.2

General Tonal Change

General color variations in the aerial color .4-.7 μ
range from black in the north to red in the south. The low-
lands appear dark gray with the south-central regions of the
photo showing a lighter red color.

The IR color .5-.88 μ has excellent color contrast. The
upland area to the north of Lubbock is a very dense red in
comparison to the west and south of Lubbock which is light
green with a small amount of red visible.

Excellent tonal contrast is also visible on the black and
white .6-.7 μ band. The area to the north and northwest of
Lubbock and also immediately surrounding Lubbock appear black
to dark gray. The central portion of the photo is a mixture
of black and dark to light grays. The southern portion of the
photo is the lightest, appearing light gray to white. The
lowlands are dark gray.

The black and white .5-.6 μ band shows less general con-
trast. The overall tonal quality is dark to medium gray with
the lightest area being east of Brownfield. The lowland and
the area north of Lubbock are the darkest grays.

The IR black and white (bands .7-.8 and .8-.9 μ) are very
similar to each other. The uplands are in generally light
gray to almost white in contrast to the dark gray lowlands.
Large apparently non-cultivated areas stand out on the upland
as dark gray areas.

Cities

Cities show up a light gray color on the aerial color and the color IR. Cities ranging in size from Lubbock (130,000) to Post, Texas (4,600) may easily be seen. On the aerial color band, some of Lubbock's major streets are visible plus about half of the interstate loops around the city. The major streets are not visible in the IR color band and only a small portion of the interstate loop can be seen.

On the black and white aerial band, cities still appear light gray. Lubbock is easily visible on both photos but smaller cities such as Staton, and Levelland, Texas are more visible in the .5-.6 band as they stand out against the darker background. Some of the major streets stand out on both photos but the interstate loop is better seen in the .5-.6 band.

Black and white IR bands show cities as medium gray. Where cities are surrounded by a light background they are easily visible but next to medium or dark gray backgrounds, they can no longer be seen. On both bands the major street patterns in Lubbock show up well. Seven east-west and seven north-south streets are visible but the interstate loop does not show up. The Texas. Tech. campus is visible as a dark gray rectangle in both photos.

Roads

Roads are not easily visible in the aerial color and color IR bands but some major roads such as west of Lamesa and south-west of Brownfield can be detected. The aerial B&W bands have

the same problem. Some major roads can be followed for a short distance then they fade out as the background changes, however, the Lubbock airport is visible as well as an airstrip between Brownfield and Levelland. A major road in the dissected lowland southeast of Post, Texas can easily be seen. Secondary roads can be traced as section lines in some areas.

On the B&W IR bands some major roads such as Highway 82 from Brownfield to Lubbock and Highway 84 running NW-SE through Lubbock stand out better than in any of the other bands. The roads are dark gray and therefore fade out on the dissected lowland. Secondary roads and section lines are not as clear as in the B&W aerial bands.

Lakes and Streams

On the aerial color band two lakes (White River Lake and Illusion Lake) appear very black but most lakes are hard to see. More easily seen are the color changes of the landscape surrounding the lakes. Two areas appear very white and are apparently areas of high salt content (Mound Lake and an area near Cedar Lake). Major streams on the dissected lowland show up as light brown but tributaries can not be seen.

The IR color band shows White River Lake, Illusion Lake and Rich Lake as dark blue with other lakes being medium blue. The same two white areas also appear in IR color bands. Major streams show up as light green to white in color.

The B&W aerial bands show the same three lakes as in the

color IR band except the lakes are black. The other lakes are medium gray generally with white borders around them. The two white areas are easily seen in the .5-.6 μ band but in the .6-.7 band they are less distinct due to other very light areas in the photograph. Major streams appear white and many tributaries can be seen in both aerial B&W bands.

Almost all lakes appear black in IR B&W bands. Many more of the smaller lakes can be detected than in the other bands. Streams, however, do not show up as well but the major streams can be traced. Few if any tributaries can be seen.

Cultivated and Non-Cultivated

In the aerial color band, cultivated areas range from black in color in the north to various shades of red farther south. Field work indicated the predominant crops in this region are cotton, grain sorghum and corn. Non-cultivated areas appear medium to dark gray and are predominately grassland or grassland and shrubs. Aerial photos revealed that some very light red areas, such as around Mound Lake, are sand dunes.

The color IR band shows cultivated regions ranging in color from deep red north of Lubbock to medium and light green throughout the rest of the photograph. Non-cultivated areas are dark green in color. Frame 028 of the June 5, 1973 mission also provides an excellent opportunity to examine fields of cotton and grain sorghums in the color IR and B&W IR bands. Figure 31 shows the spectral reflectance characteristics for cotton under conditions of moderate and high soil moisture.
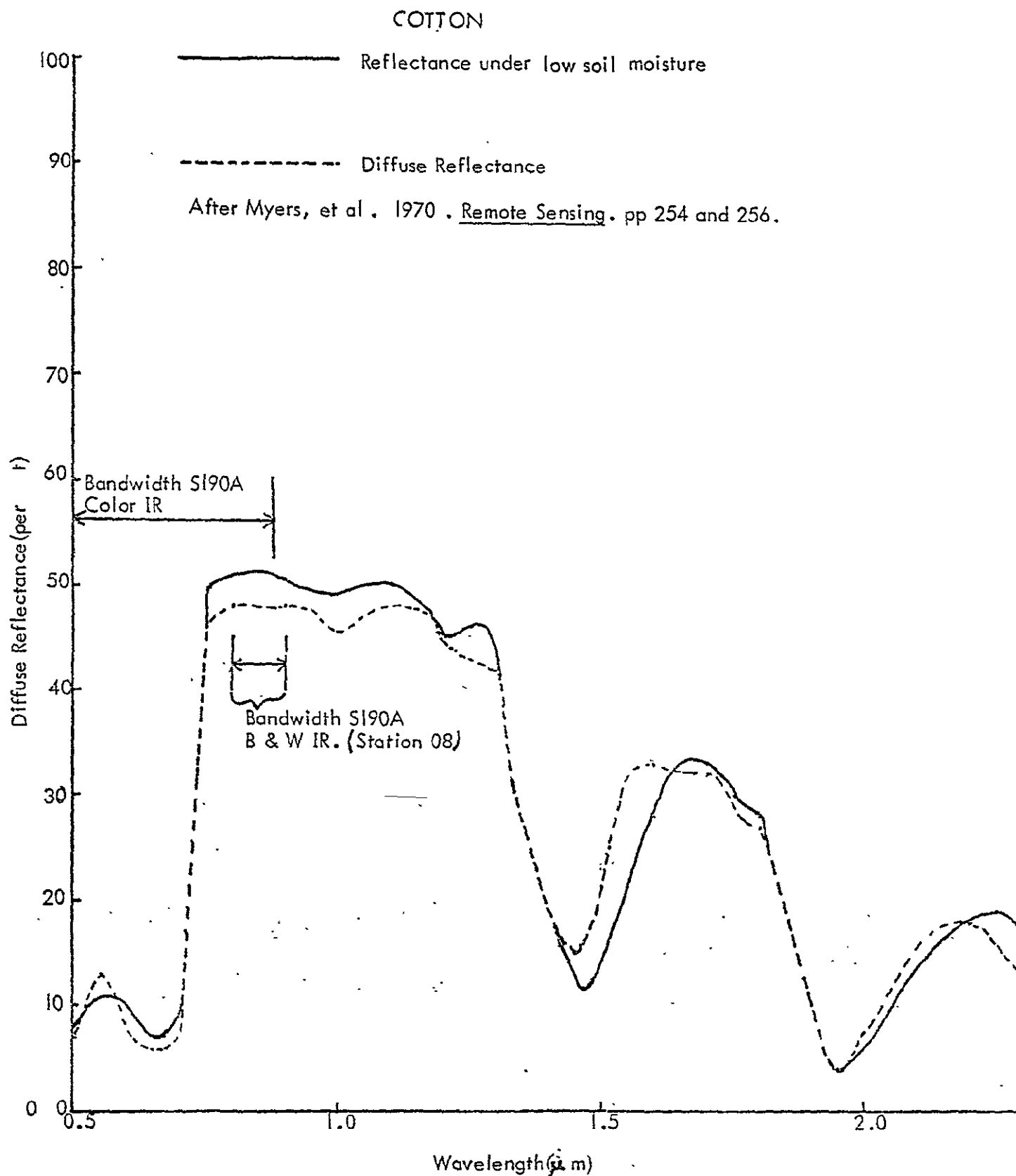
COTTON

Figure 31 The diffuse reflectance from cotton at various
wavelengths (after Meyers et. al, 1970).

It is readily seen that reflectance in the red and near infra-red is extremely high. This is observable on the color IR where cotton fields show up as intense reds and on the B&W IR bands where cotton appears as brighter fields. Similarly, on the Pan-X band (0.5-0.6) cotton is seen as very black fields, which from the curve is what would be predicted.

Cultivated areas range from black to almost white in the B&W Pan-X aerial band and therefore smaller tracts of non-cultivated land are more difficult to detect. The non-culti-vated lowlands and uplands are dark gray. Large upland tracts can be separated from cultivated areas but not as easily as in the aerial color and color IR.

Since the B&W aerial band (0.5-0.6) is an overall medium to dark gray, although some non-cultivated areas can be seen, this band is not as good for distinguishing between cultivated and non-cultivated areas. However, the IR B&W bands are excel-lent for distinguishing the two. Non-cultivated areas appear as smooth dark gray tones in contrast to a medium to light gray cultivated area.

Local Relief

Local relief is not easily detected on the aerial color band. The escarpment separating the cultivated upland and the dissected lowland is visible as a color change from light red to medium gray but the exact dividing line is often hard to see. Local relief on the dissected lowland does not stand out very well but due to color changes from gray to black the

circular depressions on the northern upland are easily seen.

The detection of local relief on the color IR band is about the same as in the aerial color band, however, the escarpment is more easily seen as a dividing line between the light green upland and the dark green lowland. Local relief is poor on the dissected lowland and only a few upland circular depressions stand out and only then as color changes from gray centers to the red fields surrounding the depressions.

The black and white aerial bands have the best visible local relief. The actual boundary between the upland and lowland is not as clear as in the B&W IR bands but the dendritic drainage pattern leading off the escarpment is very visible. The depressions stand out as pocket marks all over the northern part of the photo.

The B&W IR bands show little or no local relief. The depressions are not visible nor are the dissected lowlands. The escarpment is seen as a color contrast from a light gray upland to a dark gray lowland. Some streams can be seen leading away from the escarpment on the lowland side.

Clouds

Scattered cumulus clouds covered part of the test site on June 5, 1973. On the aerial color and color IR bands clouds are about the only white objects, therefore, they stand out quite clearly. They also stand out well in the aerial B&W (.5-.6) band since the background is medium to dark gray, however, they are not as easily seen as in the aerial color and color IR bands.

The aerial B&W band (.6-.7μ) and the two IR B&W bands are not good for detecting small scattered cumulus clouds. There are some scattered and apparently thin clouds in the south-central portion of the photos. In these three bands only the shadows of the clouds show up on the landscape, however, in the southwest portion of the photos, the individual scattered cumulus clouds are larger in diameter so the clouds as well as the shadows may be seen.

Soil Types

June 5, S190A photography (Frames 9-27 &28) of the Texas and New Mexico border areas displays a significant amount of soil information. Included in these photos are Roosevelt and Lea Counties, New Mexico and Cochran, Yoakum, Hockley and Terry Counties in Texas. These particular counties are of interest since certain soil associations tend to be well delineated on the color and B&W IR bands (Figure 32). Amarillo loamy sands and sandy loams are well delimited on this imagery with respect to adjacent deep sand associations. Various soil characteristics are shown in Table VII. From this table it can be seen that essential variations are quite small and significant overlap in variable values is present.

Soil Moisture and Precipitation Analysis
On S190A Imagery (0.7-0.9 Microns)

Two Skylab photos were analyzed for the detectability of soil moisture. Soil moisture should be detectable in the reflective IR-portion of the spectrum. This moisture should

Figure 32   Different types of soil which can be identified on
the S190A photography.

TABLE VII. Some Soil Characteristics in the Texas Test Site.

Soil	Surface Depth	USDA Texture	Permeability	Water Available
			inches/hr.	inches/in.
Amarillo fine sandy loam	0-10 in.	Fine sandy loam	0.75 - 2.0	0.125
Amarillo loam	0-8 in.	Loam	0.5 - 1.5	0.150
Amarillo loamy fine sand	0-12 in.	Loamy fine sand	1.0 - 2.0	0.83
Brownfield fine sand	0-14 in.	Fine sand	1.5 - 3.0	0.67
Tivoli fine sand	0-72 in.	Fine sand	1.0 - 4.0	0.67
Abilene clay loam	0-18 in.	Clay loam	0.2 - 0.6	0.16-0.18

After: (1) USDASCS Survey Series 1960, No. 17, March, 1964

(2) USDASCS Soil Survey Series 1960, No. 15, March, 1964

appear as dark swaths on the point resulting from local thunderstorm precipitation.

Figure 33 was taken on August 5, 1973 over south-central Kansas using the 0.7-0.8 micron band. Figure 34 was taken on June 5, 1973 over the Lubbock, Texas area using the 0.8-0.9 band. Both photos show the amounts of precipitation that occurred during the five days prior to overflights and the average moisture content for the first inch of soil along the soil sample route.

For the June 5 Texas site all the precipitation values shown occurred on June 2. Precipitation values range from .08 inches at Tahoka to .83 inches at Lorenzo. None of these locations reveal any detectable tonal changes caused by precipitation. The Slaton area with .50 inches is darker than most areas of the photo yet the Abernathy and Lorenzo areas received more precipitation, .58 and .83 inches, respectively, but have a lighter tone. Although moisture swaths are not visible one should take into account that the rain gauge stations are widely scattered and that the precipitation occurred three days prior to the Skylab overflight.

Thirty-six soil samples taken within 24 hours of overflight reveal a moisture range in the first 2.5 cm of soil from .7% to 21.1%. Where the moisture changes significantly, break points are shown as dashed lines on the figures. Looking north of Lubbock on Figure 34, the average moisture values are 4.1%, 21.1%, 5.1%, .7%, 13.5% and 2.4% yet there is little
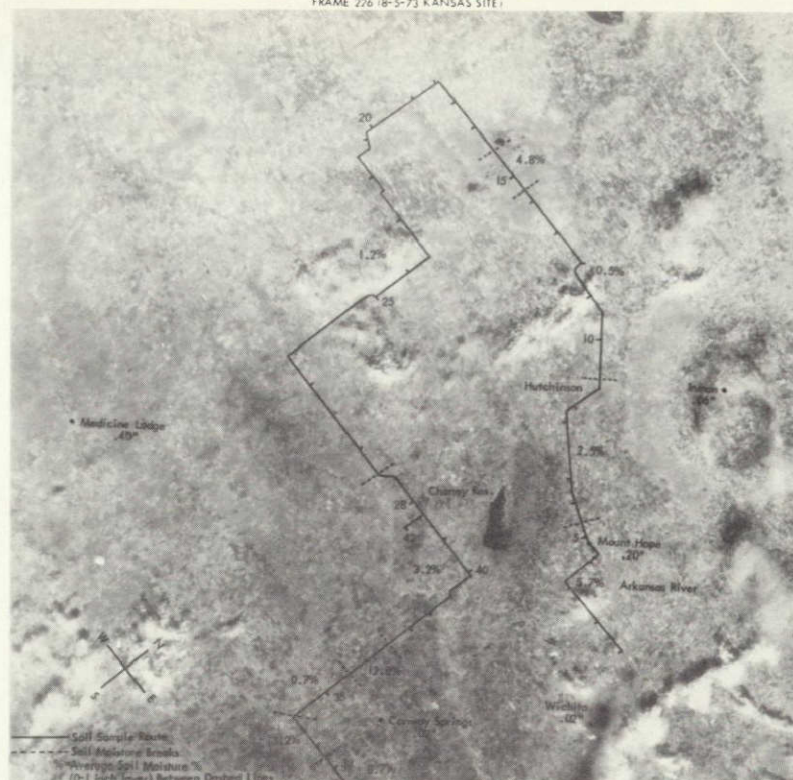
Figure 33   Soil moisture variations plotted on S190A black and white infrared photography, .7-.8 microns.
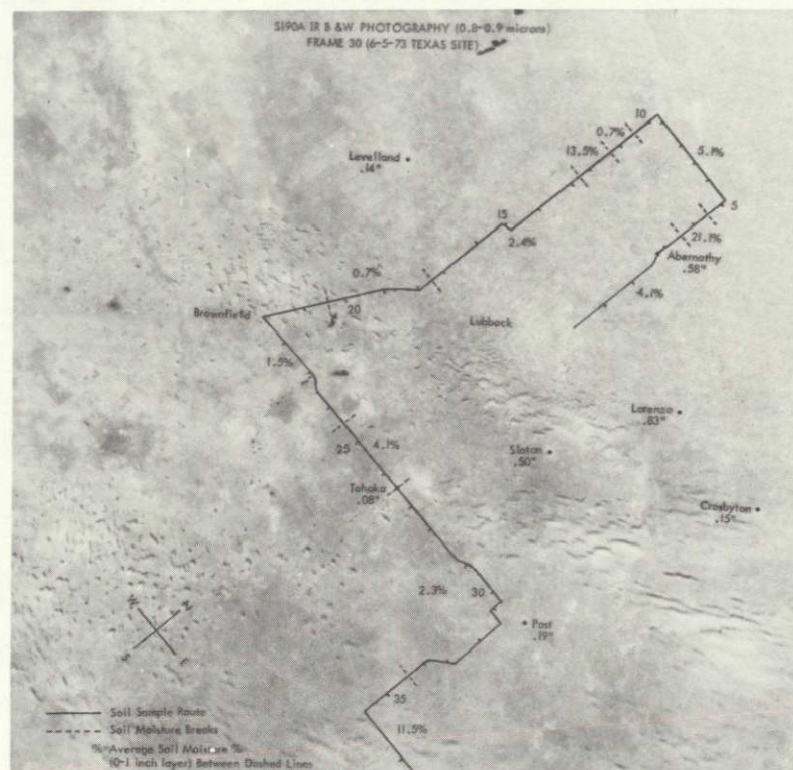
Figure 34   Soil moisture values plotted on S190A black and white infrared photography, .8-.9 microns.

detectable tone variation in this area. Similarly throughout the photo moisture changes do not coincide with tonal changes. This may be due in part to the low moisture contents observed. Most of the moisture values are less than 5.0%. However, this does not account for the lack in tonal change for the 13.5% and 21.1% values.

For the Ausust 5 Kansas site, (Figure 33) all of the precipitation values shown occurred on August 2 with the exception of the Medicine Lodge value which occurred on August 1. Precipitation values range from .02 inches at Wichita and Conway Springs to .4 inches at Medicine Lodge. As on the Texas photo, none of these locations reveal any detectable tonal changes caused by precipitation. The Medicine Lodge area with .4 inches is lighter in tone than the Conway Springs area with 0.2 inches. Once again, although moisture swaths are not visible one should take into account that most of the precipitation was negligible and occurred three and four days prior to overflight.

Soil sample sites 1-28 and 33-42 appear in the Kansas photograph. Soil samples taken from these sites within 24 hours of overflight reveal a moisture range in the first 2.5cm of soil from .7% to 12.8%. Tonal variation is greater than in the Texas photo yet these variations do not seem to coincide with the moisture changes. Once again, the moisture content is generally less than 5.0%. However, in the bottom portion of the photo the moisture values are 12.8%, .7%, 2.3% and 8.7%,

yet there is no noticeable tone change as these moisture values change.

It was concluded that small soil moisture and precipitation variations were not detectable as tonal variations on the S190A IR B&W photography. Some light tonal areas contained high precipitation, .83 inches, and high moisture content, 21.1%, while another light tonal area contained only .02 inch of precipitation and as little as .7% moisture. Similar variations were observed in dark tonal areas. This inconsistency may be caused by a lapse of three to four days from the time precipitation occurred until the photographs were taken and by the fact that in the first inch of soil the measured soil moisture was generally less than 5%.

From the point of view of soil moisture, non-microwave imaging sensors may not have the same potential as microwave sensors. However, the infrared bands of both the S190A and S192 sensors have been successfully, though to a limited extent, employed in segregating areas where soil moisture varies significantly from that of adjacent areas. An excellent sample of this is illustrated in Figure 35 in which the Abilene clay loam, a very fine grained soil with significant water capacity, can be identified on the black and white infrared and color infrared bands of the S190A, and the B&W IR of the S192, (0.7-0.8 μm, 0.8-0.9, 0.5-0.88 and 0.7-0.8 μm, respectively). Similarly, an area of medium grained, highly permeable sand, interdigitated with less permeable sandy loams is present along the border
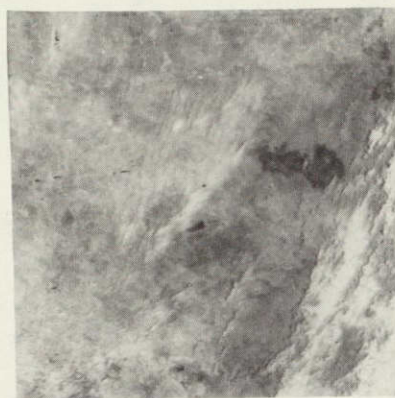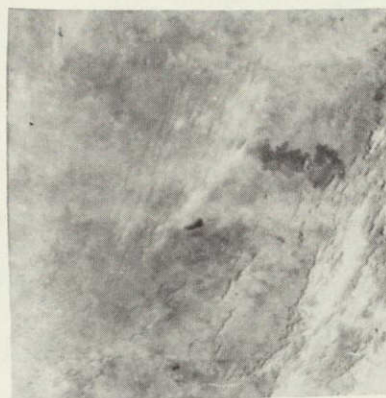
a.   0.7 - 0.8   b.   0.8 - 0.9

c.   0.70 - 0.88

d.   1.55 - 1.75

Figure 35. S190A IR photographs (a and b) showing the Abilene Clay Loam as a dark irregular zone near the right center of the frame, and S192 MSS Imagery showing the same area (c and d). Note that the soil variation does not show on the 1.55 - 1.75 μm imagery. (All bandwidths are indicated in micrometers.)

between Texas and New Mexico. These permeable sands again are displayed on the infrared images (Figure 36).

In view of the interpretations of the Skylab imagery and the known soil moisture characteristics of the test sites, it can be tentatively concluded that spectral resolution is of significantly greater importance than spatial resolution for detecting general soil moisture variations. However, the relatively poor spatial resolution of the black and white infrared bands tends to cause boundary zones to be very indistinct. This unfortunately causes the imagery to yield a continuously changing view. Therefore, for mapping purposes greater spatial resolution is essential.

In general, however, direct measurement of soil moisture variation by optical and MSS data is impossible in areas of moderate to heavy vegetation cover. In these situations, inferences relating to long term moisture availabilty must be made on the basis of the vegetative densities. This means that quantitative soil moisture information cannot be gathered from optical or MSS data.

Good quality, high resolution optical and MSS can be used more effectively in conjunction with microwave sensors in order to increase the accuracy of soil moisture measurements by using imagery as a means of providing vegetation type and density information and using a thermal band to collect and assemble surface temperature. These data can be used in conjunction with microwave sensors to provide sound moisture information as well as land-use and vegetation information.

Figure 36. S190A black and white infrared photograph showing
the permeable sands which are present over much of
this region of the high plains. Note the lighter
image density of the sands in contrast to the
darker loams and sandy loams by which they are
bounded.

111

Quantitative information can only be secondarily extrac-
ted from multispectral camera data in the form of densitomet-
ric measurements. Therefore, MSS data in both digital and
image form can provide more useful information. Data can be
extracted readily for selected areas with substantially great-
er accuracy than densitometric measurements from photographic
transparencies.

Examination of the available MSS bands indicates that a
narrow band of approximately 0.7 to 0.88μ is the most likely
to produce useable soil moisture information. Shorter wave-
lengths are adversely affected by the atmosphere and as a re-
sult show a great deal of haze. On the other hand, longer
wavelengths (1.55 to 1.75 μ) appear to be best suited for
showing vegetation details, but show little effect due to soil
moisture. Figure 35 shows the contrast between 0.70 to 0.88μ
MSS images and 1.55 to 1.75μ MSS images.

Considering the problem of spectral signatures, it must
be noted that spectral signatures in all likelihood do exist.
Based on Figures 35 and 36 it can be readily seen that signif-
icant spectral variations are present. While, from these ex-
amples it is obvious that spectral responses to different
soils and soil moisture conditions show considerable variabil-
ity, the lack of time sequential imagery over a specific test
site prevents detailed sun angle or seasonal studies.

Turning briefly to the problem of spatial resolution and
scale versus spectral resolution, various arguments can be

112

presented to support improvements in both. However, from the point of view of accurate land classification schemes, there are definite advantages in improved spectral resolution. This permits more accurate identification of vegetation types and soil types, better determination of range conditions and general vegetation vigor. On the other hand, for mapping purposes, good spatial resolution is absolutely essential. Boundaries between various vegetation types or soil types must be displayed as realistically as possible since natural boundary zones are normally transitional or gradational and good resoltuion is essential if confusion on the part of the interpreter is to be eliminated. Ideally, the spatial resolution of any given spectral band should be no worse than thirty meters.

S192 MSS Analysis

An initial investigation was conducted using the S192 MSS 10.5 to 12.2μ thermal band. Data used in the study were those obtained from Skylab IV, pass 81, on January 11, 1974. This pass collected data from southwest to northeast across the Kansas test site. The S192 thermal channel data were available for a section of the pass between Wichita and Topeka, Kansas.

Surface data were obtained for snow depth, water equivalent, maximum temperatures and minimum temperatures in the study area. There were 40 stations within the east site with various weather data. In addition, the National Weather Service cooperated in obtaining additional measurements during

the Skylab pass on January 11 for snow depth and water equivalent.

The general weather pattern of the study area indicated a slight gradient from north to south. However, there were a few instances in which the weather pattern was interrupted--warmer air from the south formed pockets toward the southern portion of the study area and there were also noticeable pockets of deeper snow around the towns of Cassody and Alta Vista, Kansas.

Contour maps of the four ground truth parameters were prepared by Surface II (a computer mapping program), using a nearest neighbor search. Overlays have been used for a visual comparison of the meterological and hydrological parameters with the thermal channel in addition to various statistical comparison

Processing of S192 Computer Compatible Tapes

Computer Compatible Tapes (CCT) from the S192 sensor were processed using the KANDIDATS IDECS facility at the Space Technology Center. This facility allows the user to interact with the processing of digital images.

The tapes received contain data for approximately 50 seconds of sensor operation. The start time listed on the tapes is 11:17:43:58.0 and the stop time is 11:17:35:47.9. The start time matches with information in the header record. Before processing began, an attempt was made to locate the area covered by the sensor. The ancillary blocks of several

scanline data sets were examined to determine the latitude and longitude of the scanlines. The following locations, rounded to the nearest second, were obtained for the test site.

	Scanline #88	#2039	#2930
Space Craft Nadir	lat 37°52'18" long-97°45'57"	38°38'17" -96°28'55"	38°58'56" -95°52'56"
Center First Pixel	38°15'28" -97°48'44"	39° 1'31" -96°31' 8"	39°22' 4" -95°55'18"
Center Center Pixel	38° 4'39" -97°23'38"	38°50'24" -96° 5'45"	39°10'49" -95°30' 8"
Center Last Pixel	37°42' 7" -97°22' 4"	38°27'52" -96° 4'46"	38°48' 5" -95°29'10"
Azimuth	54°	55°	55°

The CCT were copied on a diskpack for use by KANDIDATS.* Only channel 9 (band7) and channel 21 (band 13) were copied due to disk storage limitations. Channel 21 is a low sample rate (1240 points per scanline) channel of band 13, 10.2-12.5 microns. Channels 9 and 10 form a high sample rate pair (2480 points per scanline) of band 7, .78-.88 μ. By copying only channel 9, we obtain low sample rate data for band 7.

The CCT also contained channels 19,15,16 and 18. Channel 10 was essentially the same as channel 9 since channels 9 and 10 make a high sample rate pair of band 7. Channels 16 and 15 make a high sample rate pair for band 13. Although these channels were not processed in detail, it was noted that they showed an unexpectedly high number of under-range counts. Channel 18 is a low sample rate of band 2, .46-.51μ, and also

. *Kansas Digital Image Data System

showed a high number of over-range counts.

Processing of the digital images for band 7 and 13 consisted of the following steps:

1. Compression of the image.
2. Equal probability quantizing of the compressed image.
3. Convolution with a rectangular pulse, a type of low pass filtering.

Compression of the image was performed by sampling every fourth point per scanline and every fourth scanline. This resulted in a 16 to 1 reduction in the size of the image and allowed the image to be displayed and analyzed.

Quantizing of the compressed image removed the bias from the data and increased the range of values. The quantizing was such that each resulting data value has an equal probability of occurring. The resulting quantized image was quite grainy so a rectangular convolution was performed to smooth the data.

The results of the processing were displayed by several methods. To observe the original data, the compressed image was displayed on and photographed from the IDECS black and white television screen. Both band 7 and 13 were photographed in this way and a mosaic was made of the photographs. The compressed band 7 and the compressed, quantized and convolved band 13 were printed on a line printer to form a grey map. The final method of display uses the IDECS to level-slice the convolved band 13. The four slices were each displayed in a different color and photographed from a color television

screen. Again, a mosaic was made with the photographs. The colors used were red, yellow, green and blue, with red representing low counts and blue high counts.

Scanline straightening of the image was not performed for display purposes since this operation is very time consuming. The original counts from the CCT were displayed. Each count may vary in value between 0 and 255. For each data point, the count can be converted to radiance measure by the following equation:[1]

$$R = A_o + C * A_1$$

where:

   R = Absolute radiance
   A_o, A_1 = Calibration coefficients
   C = Count value

For the area under study, the calibration coefficients are:

	A_o	A_1
Band 7	-.395	.2561
Band 13	.295	.154

These coefficients are taken from the CCT header record.

Radiance values may be converted to an effective temperature by use of the inverse of the following function:

$$R(T) = I_G \int_{\lambda_1}^{\lambda_2} \frac{C_1 * G(\lambda) \, d\lambda}{\lambda^5 * EXP \, (14388/\lambda T) - 1}$$

[1] Earth Resources Production Processing Requirements for EREP Electronic Sensors, PHO-TR 524 REV A, Change 1: NASA, 1974, pp 5-17 to 5-19.

117

where:

$$\lambda = \text{Wavelength in } \mu m$$
$$C_1 = 11909 \text{ Watts-}\mu^4/\text{cm}^2\text{-STER}$$
$$T = \text{Temperature in } °K$$
$$G(\lambda) = \text{Spectral response for band 13}$$
$$I_G = 1/\int_{\lambda_1}^{\lambda_2} G(\lambda) \, d$$
$$R(T) = \text{Radiance for given temperature.}$$

The resulting radiance is therefore a measure of the effective temperature across the band pass. This temperature is not the physical temperature most commonly thought of but a comparison to a black body temperature. The original count values were used in this analysis rather than conversion to radiance measure and then to effective temperature.

Thermal infrared image interpretation

Mosaics of the imagery from the red band and the thermal band have been assembled. The red band has been used primarily as means of reference for purposes of locating points on the thermal band imagery. Some problems were encountered in interpretation of the imagery. Major variation in topographic features, cities or climatic variations were limited for this pass over almost complete snow cover. This was verified by interpretation of S190B photography and aircraft photography, as well as by ground truth information gathered from a number of weather stations in the area.

A comparison between the S190B and a color enhanced image of the Topeka, Kansas area made from the S192 thermal channel data is shown in Figure 37. The lack of geometric similarity
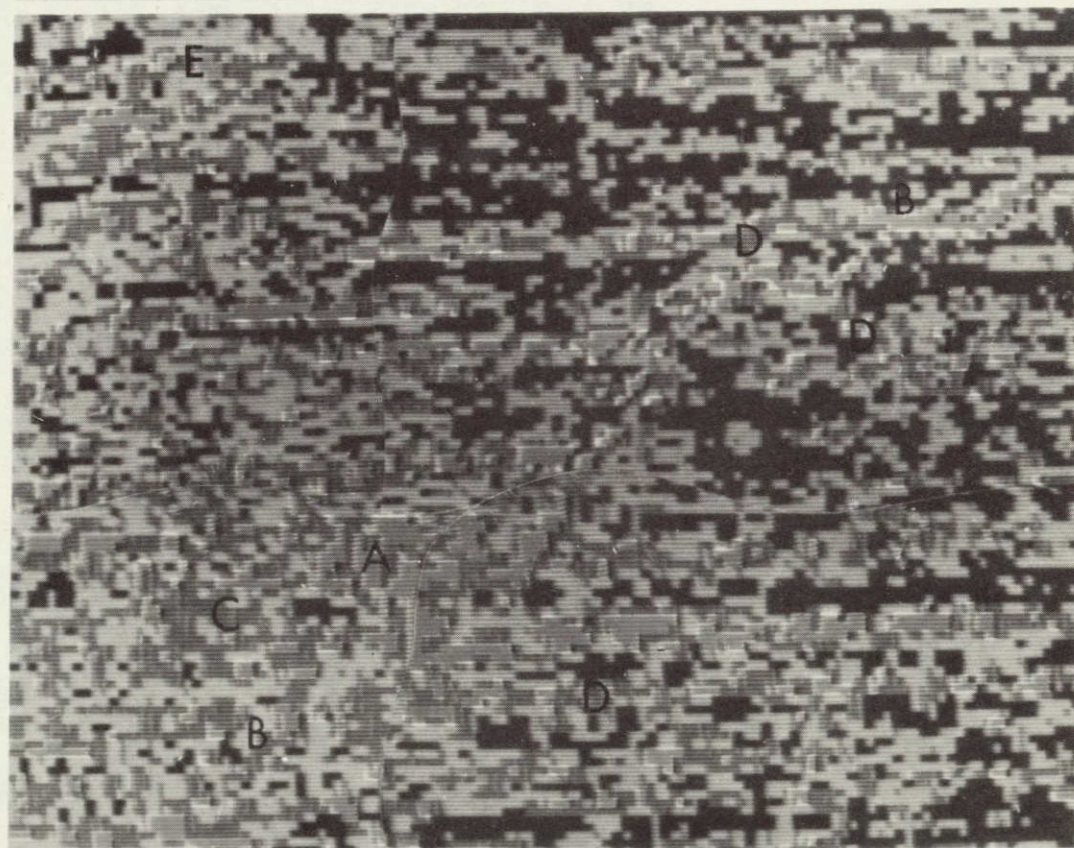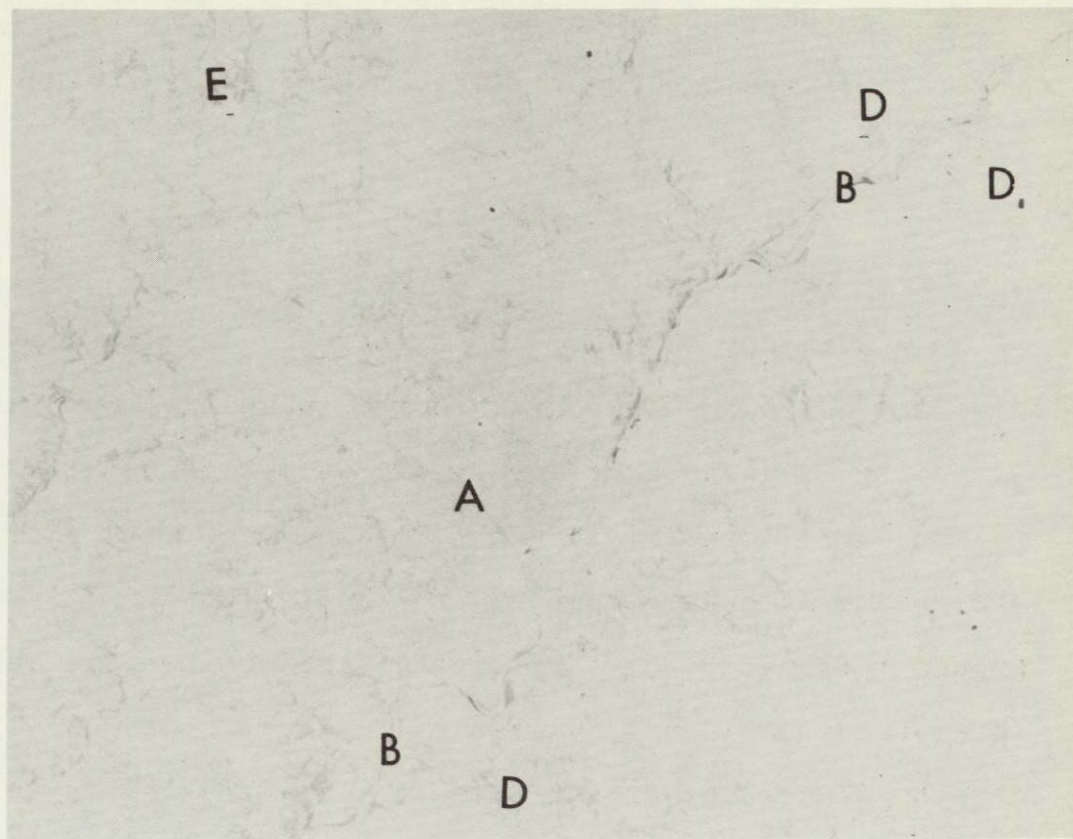
Figure 37   Comparison of S190B (upper) and S192 thermal data
for Topeka, Kansas and vicinity, January 11, 1974.

119

is due to the uncorrected scan lines. Close examination of this area immediately permits the interpreter to identify certain major features. Topeka (A) can be more readily distinguished from its background on the thermal channel than on the color photography. Similarly, the Kansas River (B) is also immediately obvious. Both features are identified in blue on the thermal output. To the immediate southeast side of Topeka is an area of apparently warmer temperatures (C); this area is identified on the mosaic in green. While this area seems somewhat coherent and related to the city of Topeka, ground information of sufficient detail to support such an interpretation is not available.

Looking at other smaller areas it is possible to relate isolated points on the thermal channel to their counterparts on the photograph. Several small stream channels can be distinguished on local areas along their lenghts (D). Although in almost all cases the streams are frozen and covered with snow, there appears to be an influence of the stream bands upon the signal. Such a situation may be due to a lack of snow on steep surfaces and differential heating of snowy and bare surfaces. Other areas such as (E) can also be distinguished on the thermal channel as on the photography. These are steeper slopes and hill tops which have been swept clear of snow and are therefore more susceptible to heating.

In general, it is possible to detect major landscape features with minimal difficulty. Small streams can be detected

occasionally, however, this is probably dependent upon their being sufficiently incised that the banks do not retain significant depths of snow. Other features are not immediately detectable on this set of data; however, it is quite likely that this is due to the relatively low and uniform temperatures within the test area. It is quite possible that in an area of greater temperature range and surface diversity, the sensor would show more local features and regional trends.

Thermal infrared correlations with snow characteristics

Variations in snow depth throughout the study area are shown in Figure 38. The contours generated by the Surface II mapping program vary from 6 to 10 inches of snow. The actual data values measured at the individual locations varied from 4 to 11 inches. The Surface II program calculates values and fits a surface to individual data points. Although the thermal infrared data is much more detailed, comparisons were attempted between the generated surface for snow depth and S192 thermal infrared data points. The surface trend mapping for the limited number of stations having snow depth information (18 locations) generated 518 data points for the entire test site.

The thermal infrared data, on the other hand, consisted of about 350,000 individual data points for the test site. These data had to be generalized because of the coarseness of the ground truth data. The individual thermal data points together with their coordinates were fed into the Surface II mapping

SNOW DEPTH: JAN. 11, 1974
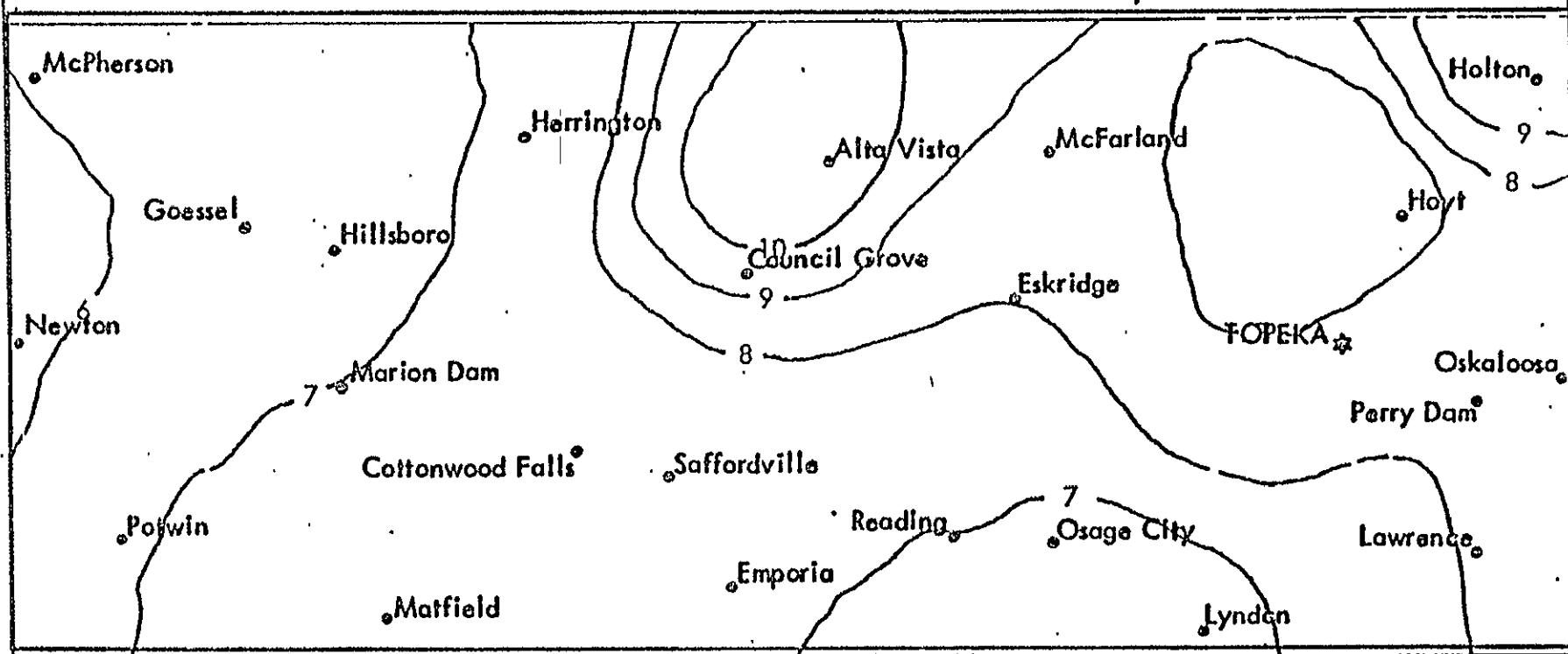
STATIONS FOR WHICH DATA HAS BEEN OBTAINED

Data Source: U.S. Department
of Commerce, Climatological
Data, January, 1974

N

Scale 1:1,000,000
1 inch equals approximately 16 miles
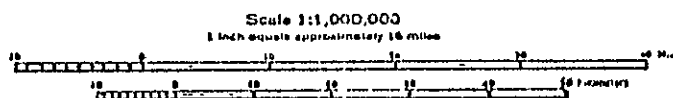
CONTOUR INTERVAL - 1 INCH

Contours obtained by Surface II
Graphics System; Kansas
Geological Survey

Figure 38   Snow depth contours and location of measurements
in the test site on January 11, 1974.

122

program which averaged the data down to 518 data points. The
conical nature of the thermal infrared scanlines was circum-
vented by using the location of the individual data points
in the plotting program. This allowed a correlation between
snow depth and the thermal infrared data for the 518 grid
points which were uniformly spaced throughout the test site.
The scatter diagram for the 518 data points is shown in Fig-
ure 39. Increasing snow depths gave lower thermal infrared
counts as anticipated, although the correlation coefficient
is quite low, -0.12. A similar comparison between water e-
quivalent within the snow cover and thermal infrared data is
shown in Figure 40. The relationship is somewhat better with
a correlation coefficient of -0.28.

Figure 41 shows the scatter diagram relating maximum
temperature within the test site to thermal infrared data.
Most of the weather stations are between 15 and 30 miles a-
part. When considered in light of the much smaller resolu-
tion of the thermal infrared system, it is obvious that great
generalization has taken place. Therefore, much of the
detail which is present in the scanner data can be interp-
reted. A prime example of this problem is the city of Topeka,
which shows up as a cold spot from the temperature distri-
bution, but as a warm area on the S192 scanner output. This
anomalous situation is created by the fact that the scanner
is reading the temperature of the city of Topeka in detail,
while the weather station is located at the airport, a location
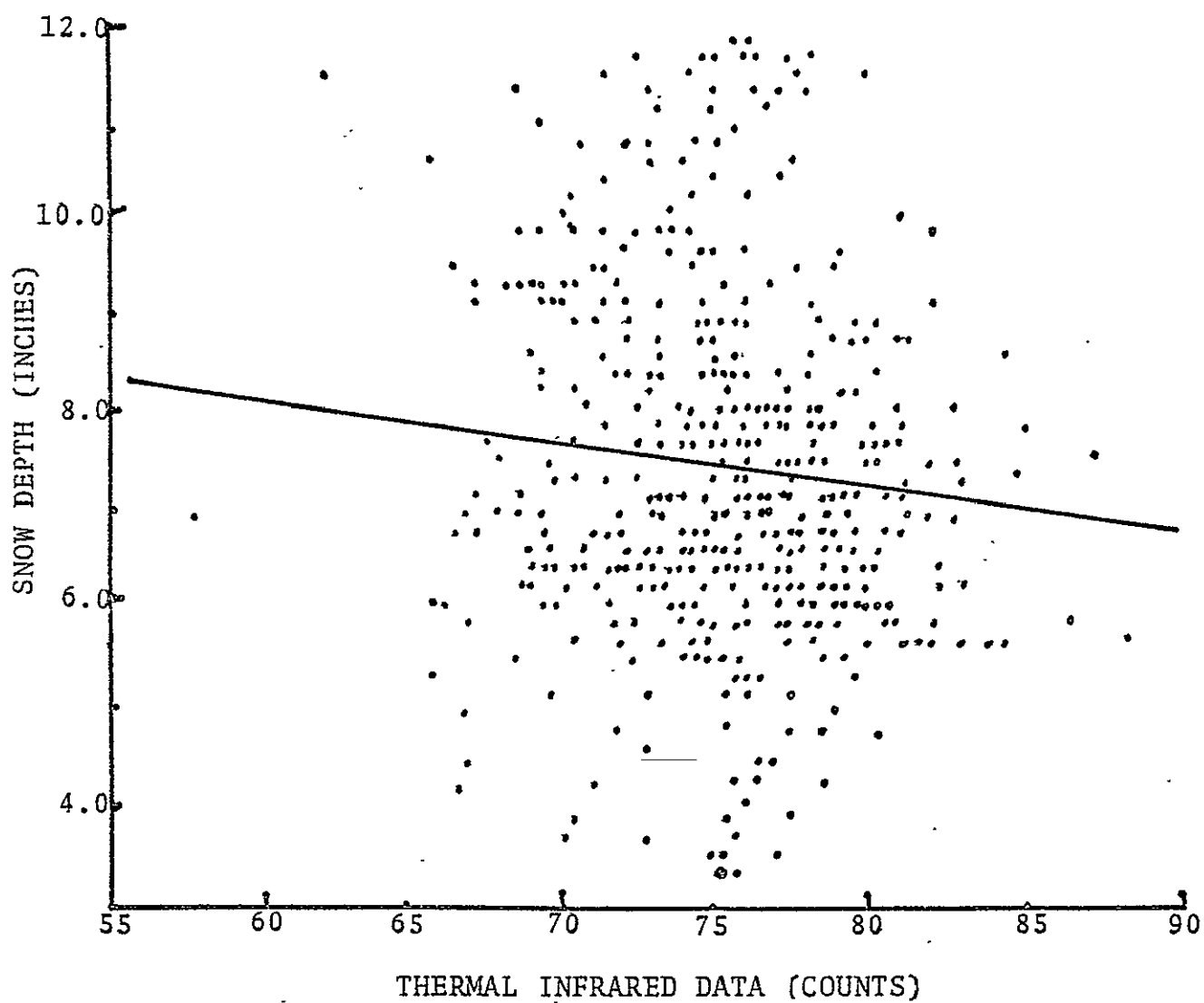
Figure 39   Scatter diagram relating snow depth to S193 thermal
infrared data.
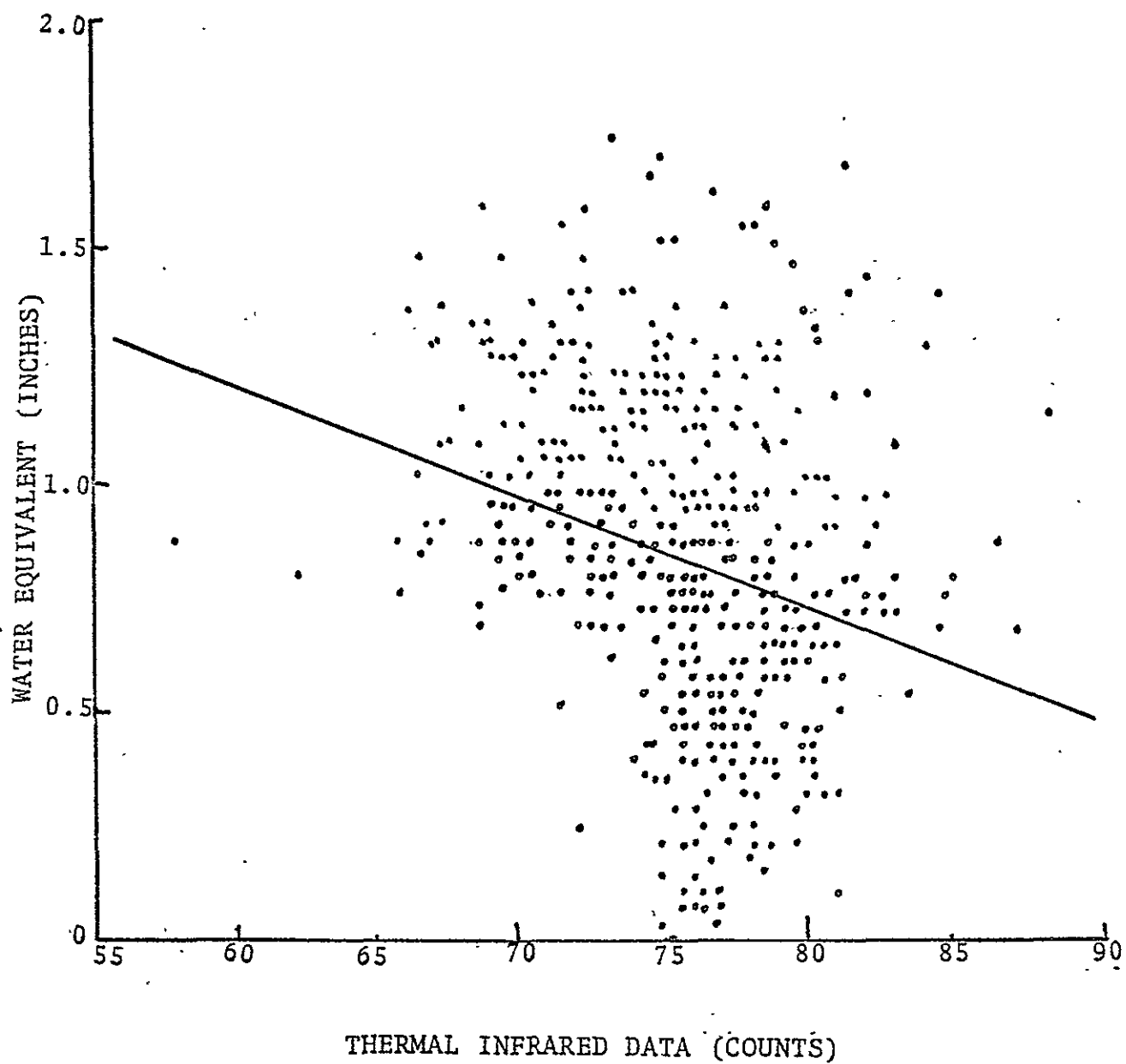
Figure 40   Scatter diagram relating the water equivalent in
snow to S192 thermal infrared data.
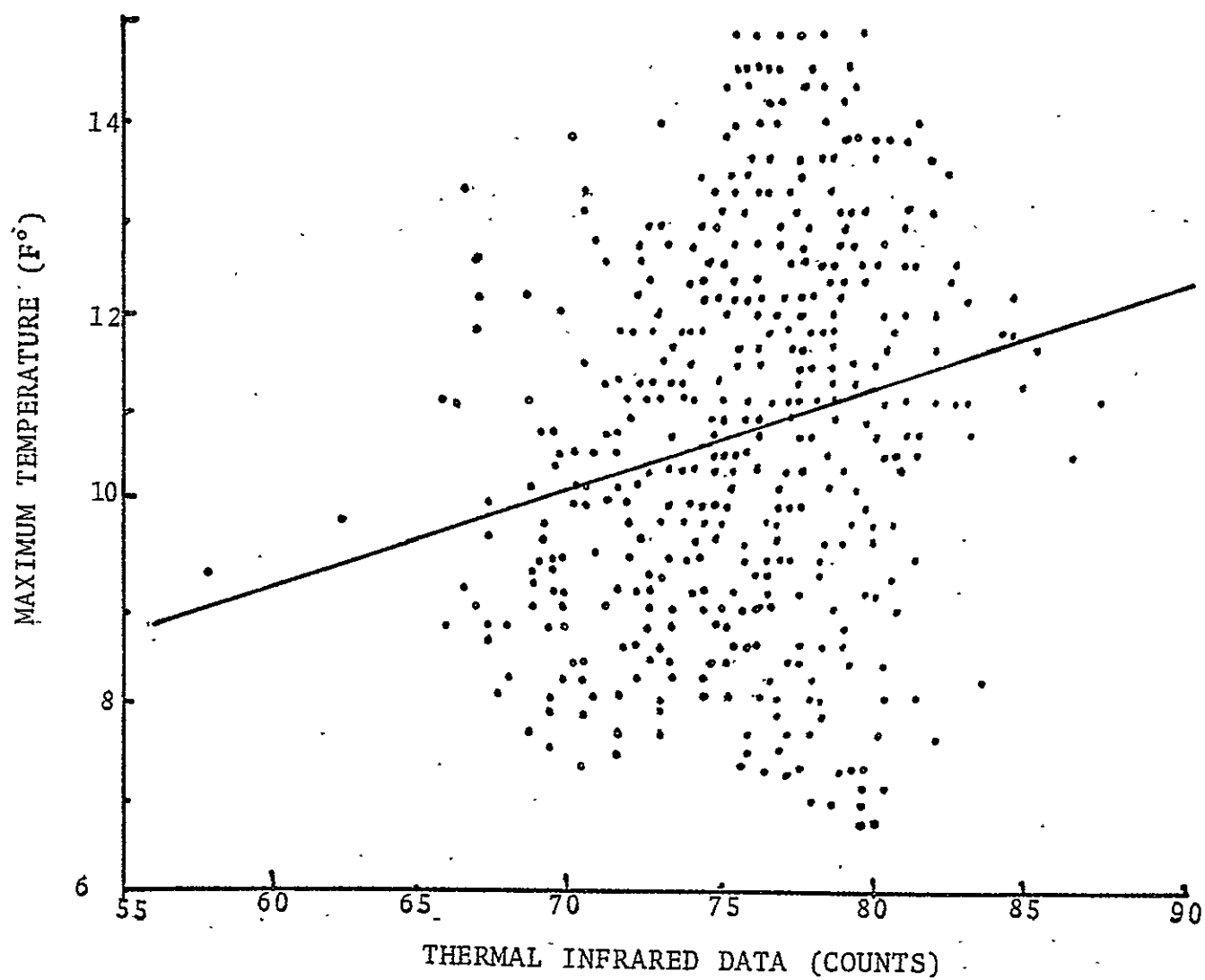
Figure 41   Scatter diagram relating the maximum measured
temperature with the S192 thermal infrared data.

which has, on the basis of previous data, been shown to be colder than the surrounding landscape. Similarly, this situation may occur throughout much of the test area, as one weather station cannot represent all of the local variations. For this reason, a good correlation cannot be expected between the thermal infrared data and ground temperature. For these data, the S192 data may be so much more detailed than the ground data that comparisons are impossible. A very detailed snow mapping and surface temperature measurement program would be required to match the resolution of the S192 sensor and provide a sound basis for testing the response of the instrument.

S193 data analysis

Although five sets of data were collected for the soil moisture experiment, only two sets of S193 data were comparable; pass 5 over the Texas site and pass 38 over the Kansas site. Pass 15 would also have been comparable except that the soil moisture samples were taken in southeast Kansas and the S193 instrument started to collect data in Oklahoma. Therefore, the soil moisture data did not match the Skylab data and could not be used in the analysis.

The data from pass 5 over Texas is a very good data set, because it satisfied the original requirements for the soil moisture experiment and covered the whole test area. Antenna temperatures in the test site ranged from 240°K to 286°K and scatter coefficients from -8.0 to -11.0 dB. The distribution

patterns of antenna temperature and scatter coefficient are shown in Figures 42 and 43.

Although the radiometer and scatterometer data were analyzed for individual footprints these figures were developed to show the general distribution of the radiometric temperature and the backscatter coefficient. They were generated by computing a least squares trend surface for the individual data points located throughout the test site.

During pass 16, data were collected by the S193 microwave sensors over the southeastern part of the Kansas test site, where soil moisture content was lower, one to eight percent by weight in the layer from the surface to 2.5 cm. Therefore the range of data were smaller than those for pass 5, -9.5 to -11.3 dB for the scatter coefficient and 280°K to 287°K for the antenna temperature. In addition, a gap of two sweeps occurred at the south part of the test site (Figure 44). This figure also shows the individual values of the scatter coefficient for this pass.

In pass 38, the S193 microwave system collected data at 40.1° pitch angle over the two test sites, with vertical polarization for the Texas site and horizontal polarization for the Kansas site. Data from the S193 instrument covered about one-third of the Texas test site. The antenna temperatures varied from 271°K to 287°K and the scatter coefficients ranged from -8.7 to -13.0 dB. For the Kansas test site with soil moisture content greater than in the Texas test site, the
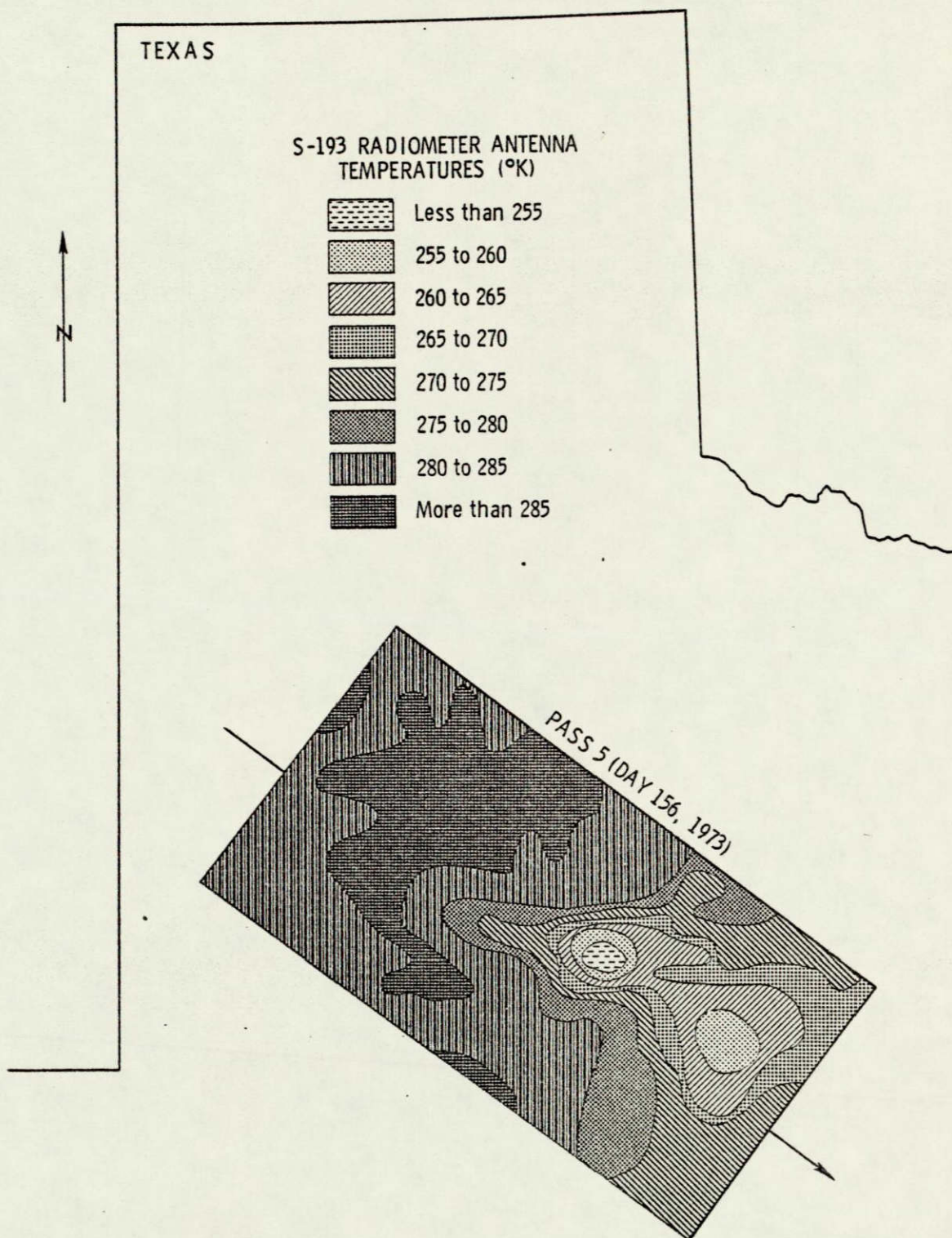
Figure 42   The distribution of S193 radiometric temperature throughout the Texas test site on June 5, 1973.
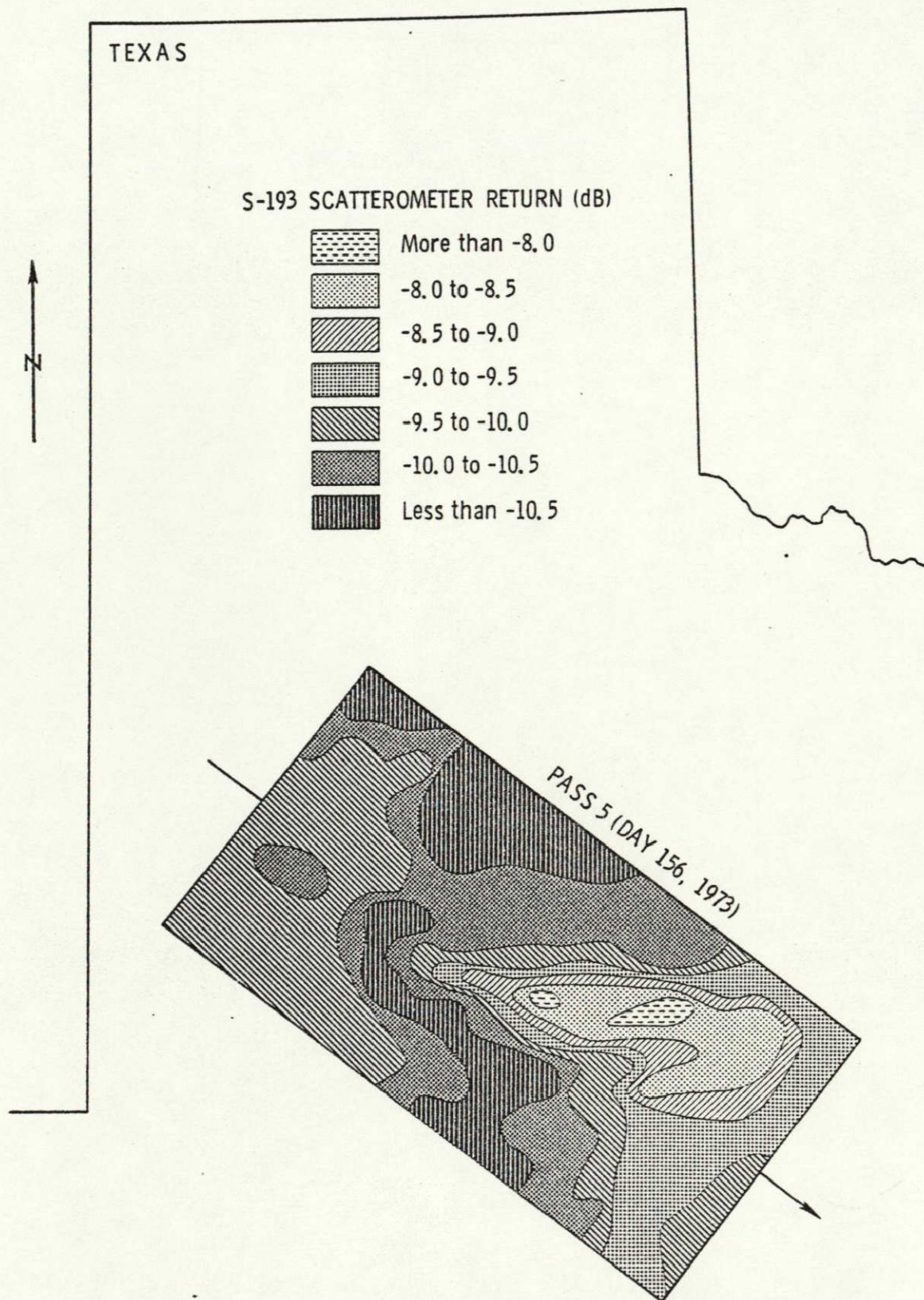
Figure 43 The distribution of S193 scattering coefficient
throughout the Texas test site on June 5, 1973.

Figure 44   The location of data points for the scattering
coefficient showing the data skip in the Texas
test site on August 8, 1973.

antenna temperatures ranged from 250°K to 272°K and the scatter coefficients from -8.5 to -11.5 dB.

For the S193 sensor at 0° roll and 29.4° pitch forward, the radiometer footprint was about 17 x 21 kilometers in size whereas the scatterometer footprint was about 13 x 16 km. The location of each of the S193 footprints was plotted and an overlay was made for the soil moisture content distribution (Figure 15) to determine the soil moisture content within each footprint for comparison and correlation. If individual footprints covered an urban area or large lake, these data were not included in the analysis.

Relationship Between Soil Moisture and S193 Data

The relationship between the S193 radiometric temperature and the soil moisture content and scatter coefficient as a function of soil moisture content are shown in Figures 45 and 46 for pass 5 through the Texas test sites. These data obtained for a forward pitch of 29.4° and vertical-vertical polarization gave a correlation coefficient of -0.91 between the S193 antenna temperature and soil moisture content and a correlation coefficient of 0.53 between the S193 scatterometer and soil moisture content. The soil moisture content in both cases is the moisture in the upper 2.5 cm of soil. The correlation between the 2.1 cm passive radiometer and soil moisture content is quite good and is considerably better than the correlation with the scatterometer as shown in these figures.

The same type of analysis is shown in Figures 47 and 48
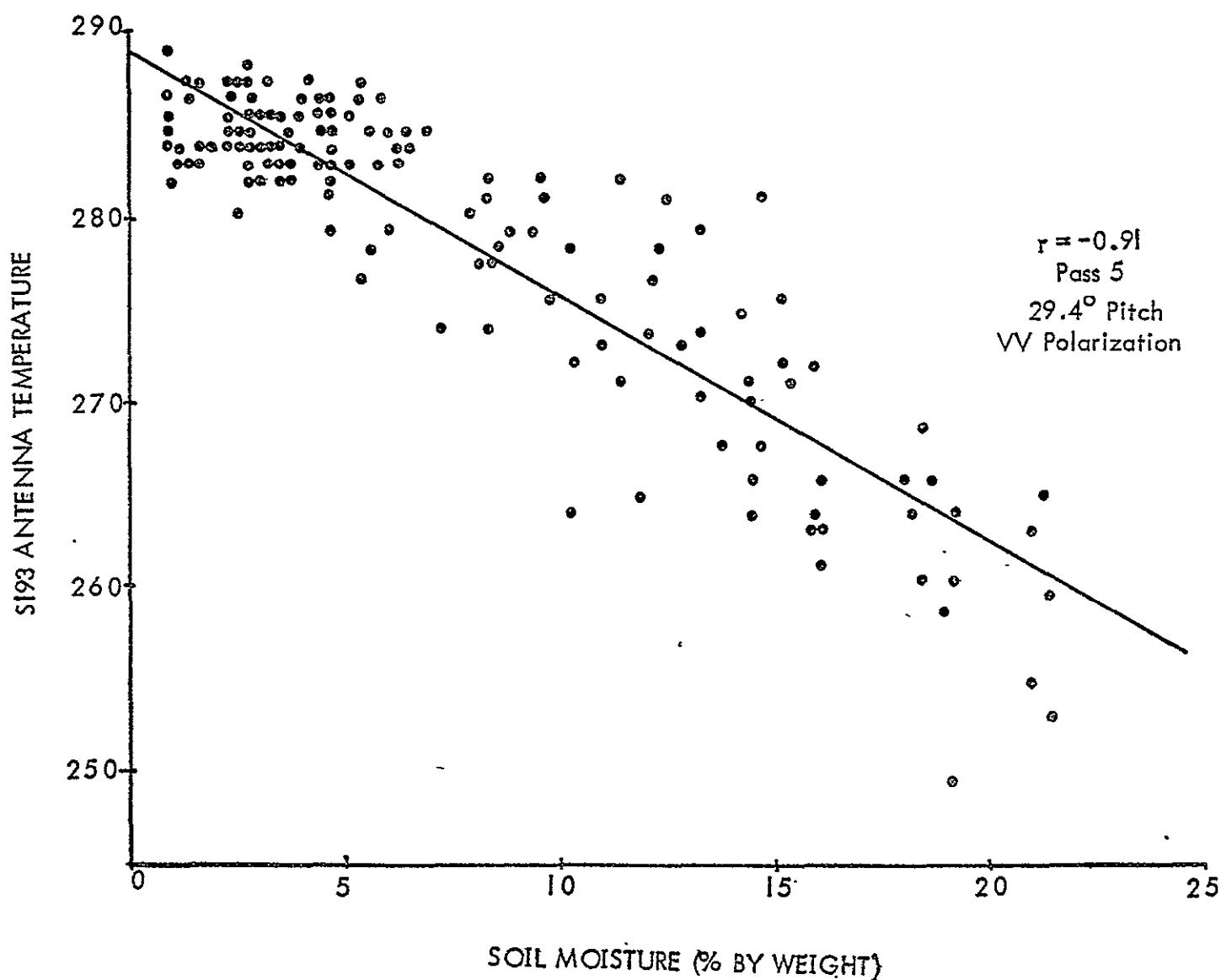
Figure 45   The S193 antenna temperature as a function of soil
moisture content for pass 5.

Figure 46   The S193 backscatter coefficient as a function of
soil moisture for pass 5.
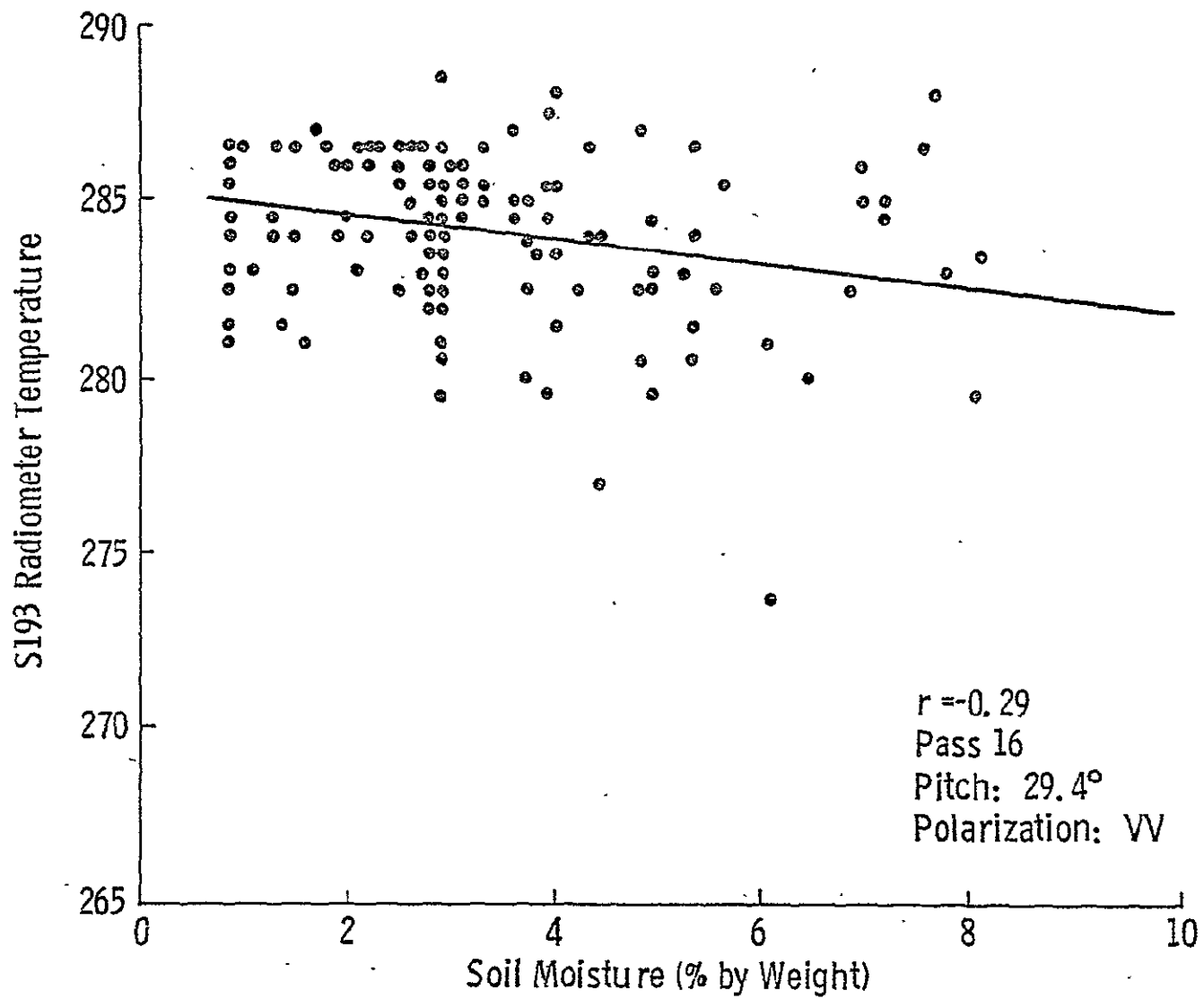
Figure 47   The S193 radiometric temperature as a function of
             soil moisture for pass 16.
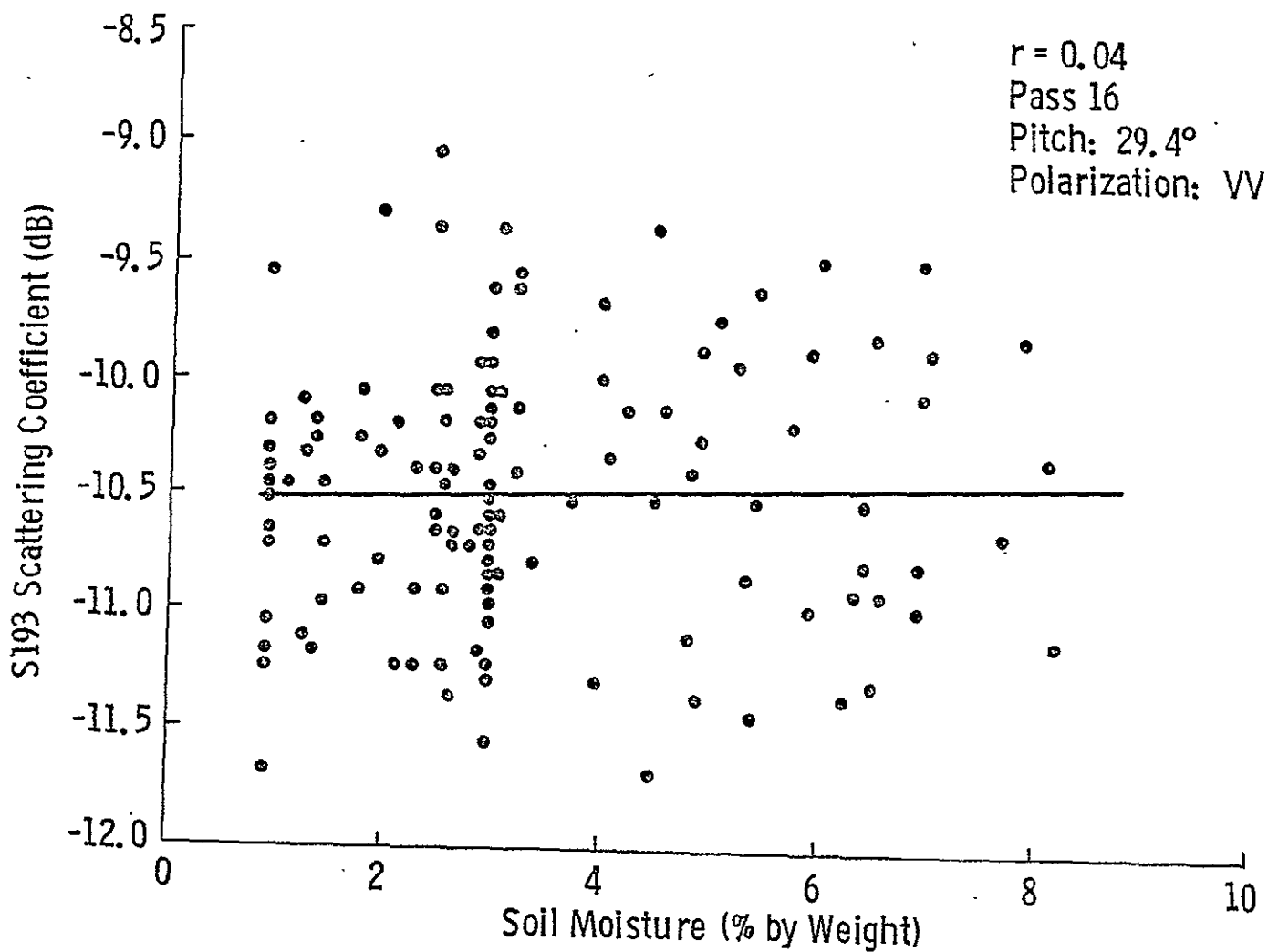
Figure 48 .The S193 scattering coefficient as a function of soil moisture for pass 16.

for pass 16 on August 8, 1973 over the Texas test site. At this time, the soil moisture variations were much smaller and all of the moisture contents were less than 10%. Since the variations were much less than for pass 5, the correlations could not be expected to be as good. Figures 47 and 48 show that the correlation between the S193 radiometric temperature and soil moisture content for pass 16 was -0.29 and the correlation coefficient between the S193 scatterometer and soil moisture content was only 0.04. In addition to the small range of soil moisture values, the water in dry soils below the wilting point is held very tightly by the soil particles. The absorbed state of the liquid water at very low moisture content would cause it to have a smaller influence on the dielectric constant. The lack of response of microwave sensors at very low soil moisture levels has also been noted by Schmugge, et. al, (1974).

Since there are slight variations in the incidence angle between the center and the edges of this test site which amount to about two degrees for the forward pitch mode at 29.4°, the influence of angular variations was investigated by plotting data from these central four lines from the microwave sensor as a function of soil moisture content as shown in Figures 49 and 50 for pass 5. This improved the correlation coefficient for the passive radiometer from a value of -0.91 to -0.95 and for the scatterometer, from 0.52 to 0.75. This indicates that small variations in incidence angle are more important for the
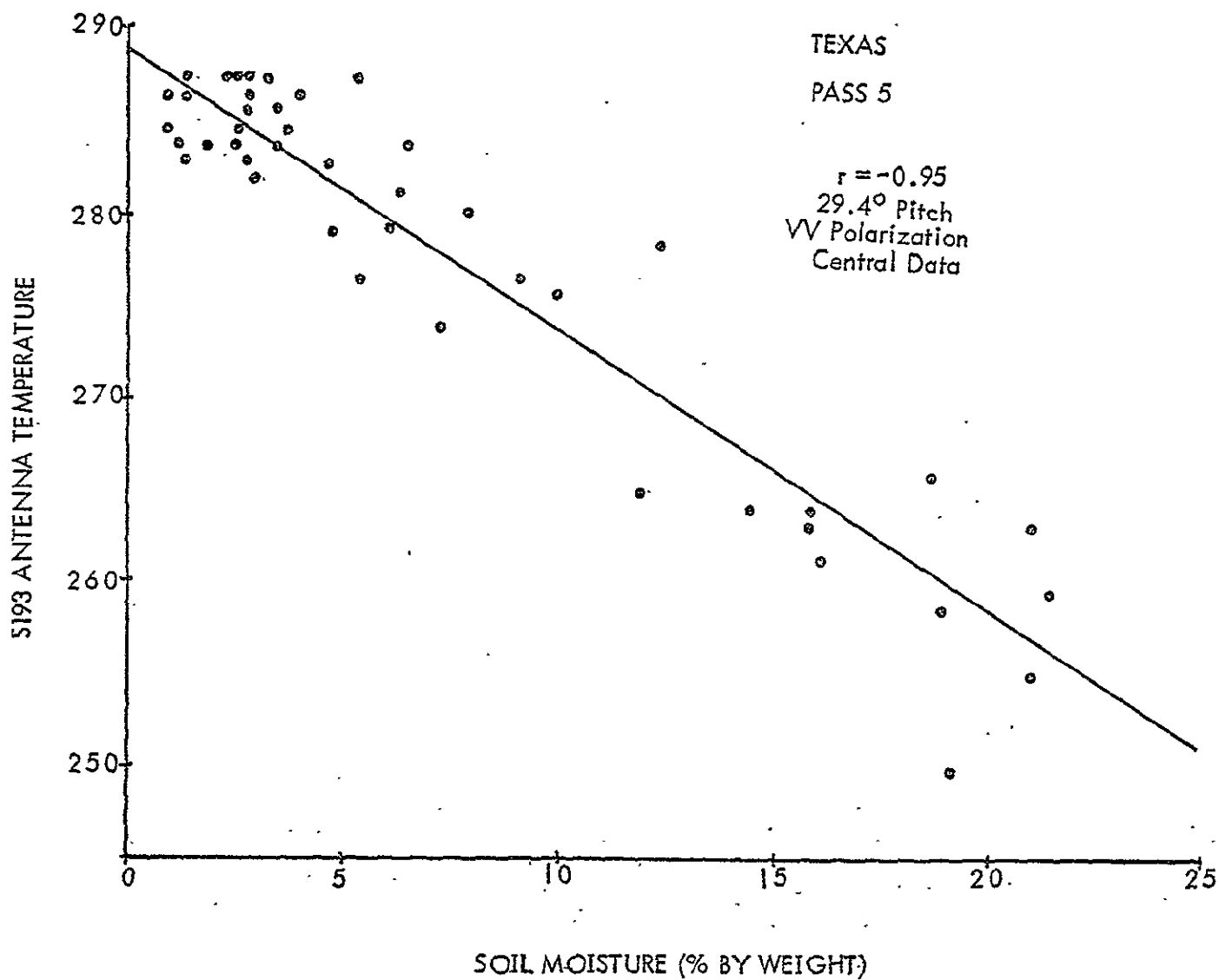
Figure 49   The S193 radiometric temperature as a function of soil moisture for the central four lines of data.
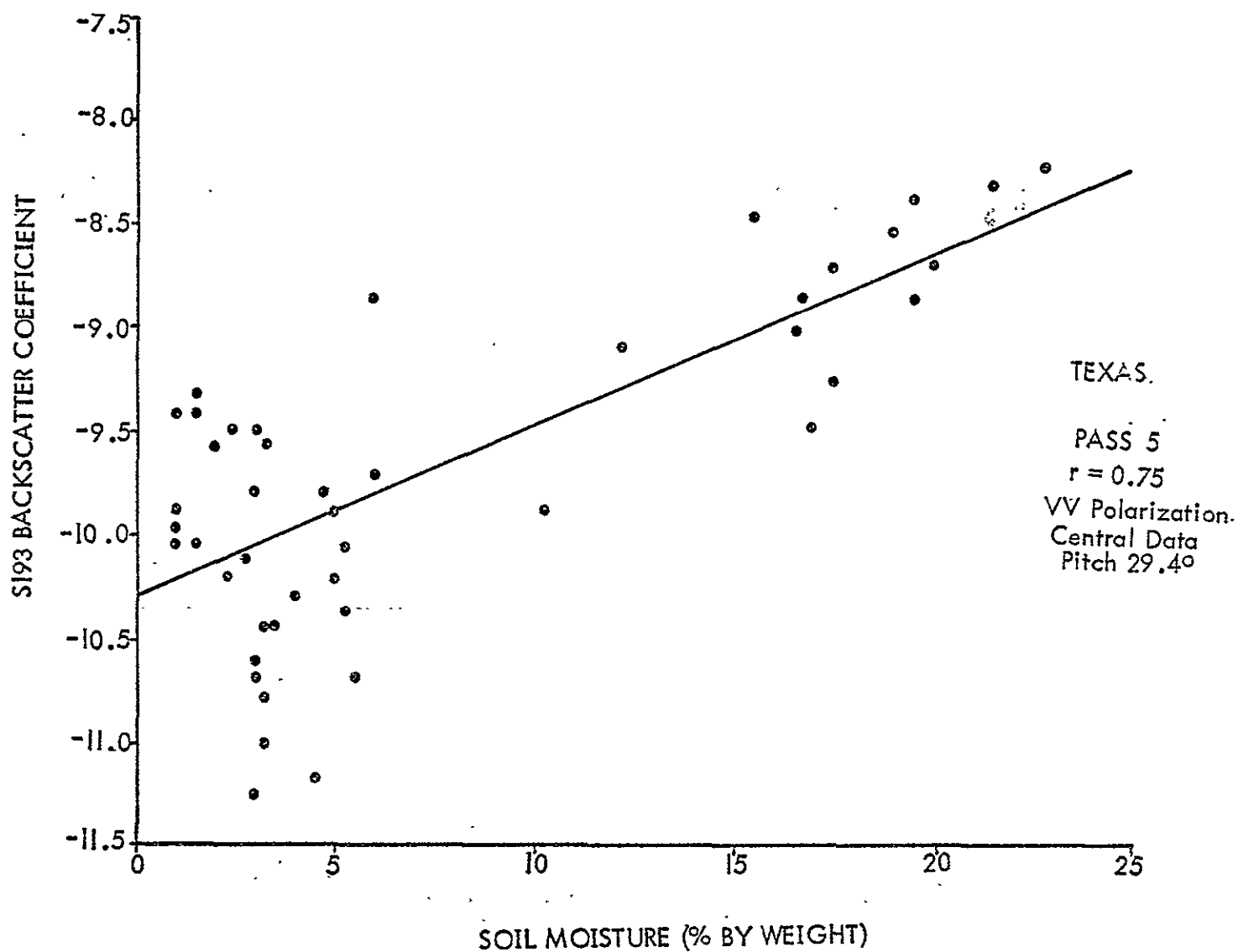
Figure 50   The S193 backscatter coefficient as a function of
soil moisture for the central four lines of data
for pass 5.

scatterometer return than for the passive radiometer. The small improvement in the radiometer correlation probably results from more accurate ground truth near the center of the test site rather than effect of angle on the performance of the sensor.

During pass 38 the S193 sensor at 0° roll and 40.1° pitch forward produced a 14 x 22 kilometer footprint for the scatterometer and a 20 x 29 km footprint for radiometer. The individual footprints of the S193 RADSCAT were analyzed for pass 38 for the relationship between soil moisture content and the passive and active microwave data in a manner similar to those for pass 5.

The S193 data over the Texas site were collected with vertical-vertical polarization. The plots of antenna temperature and scatter coefficients with soil moisture content are shown in Figures 51 and 52. The correlation coefficients are -0.69 and 0.72 for the radiometer and scatterometer, respectively.

The data sets for the Kansas site were plotted as shown in Figures 53 and 54. There were low correlation coefficients for both the scatterometer and radiometer, 0.14 and -0.34. Surface roughness and vegetative cover may contribute to these poor correlations at this pitch angle. In addition, Lee (1974) has found that roughness has less effect on vertical polarization measurements than on horizontal polarization.
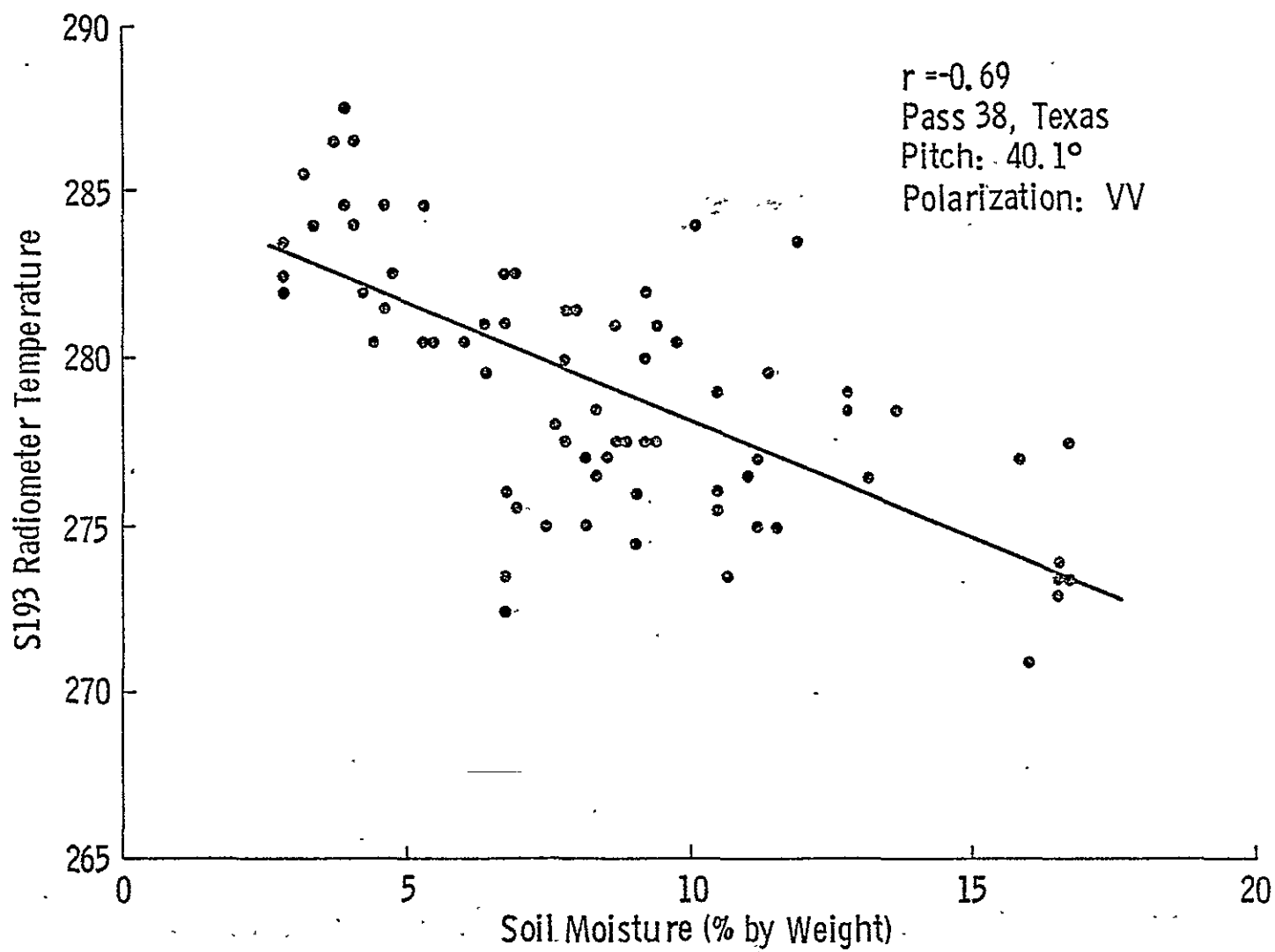
Figure 51   The S193 radiometric temperature as a function of
             soil moisture for pass 38   across the Texas test
             - site.
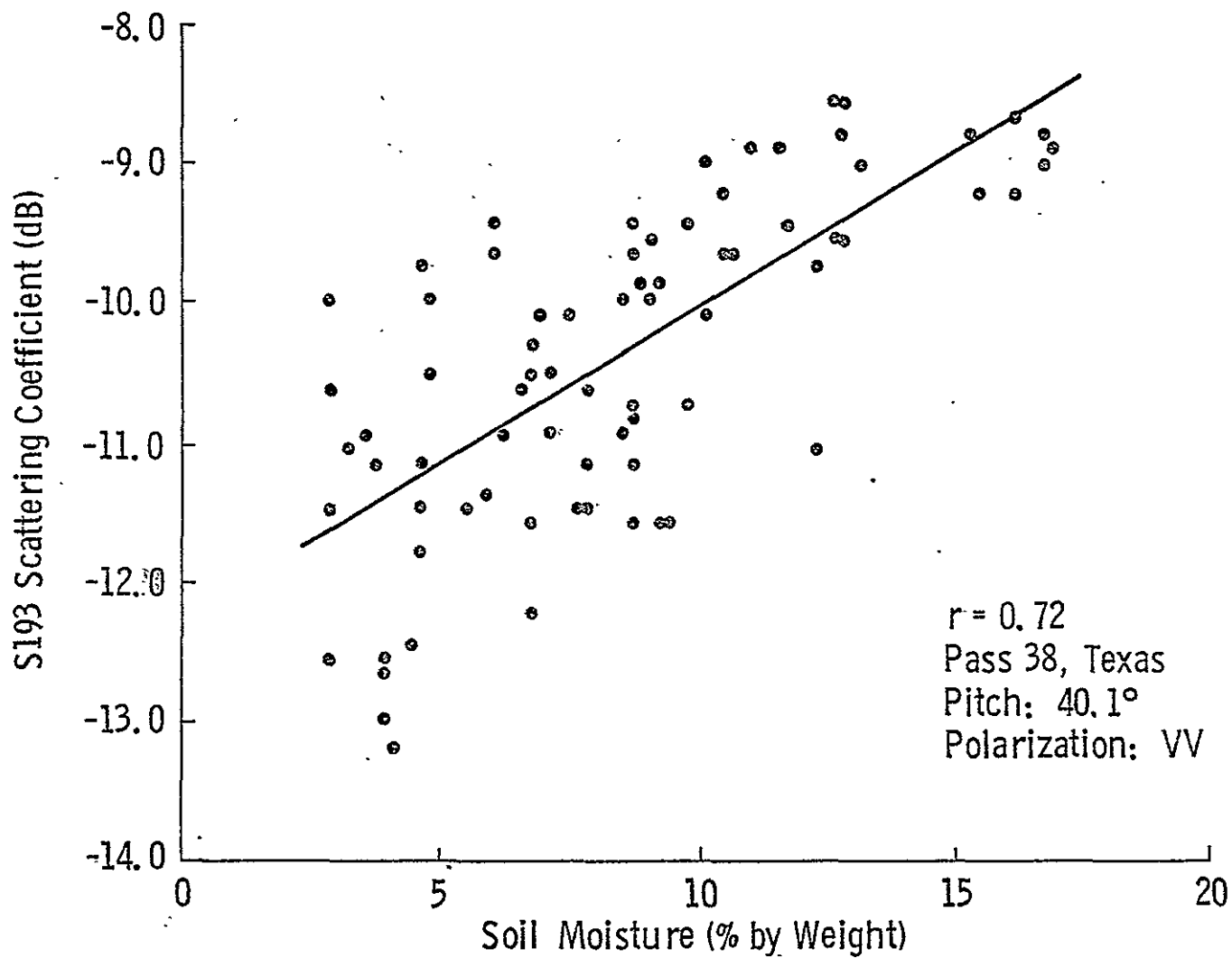
Figure 52 The S193 scattering coefficient as a function of
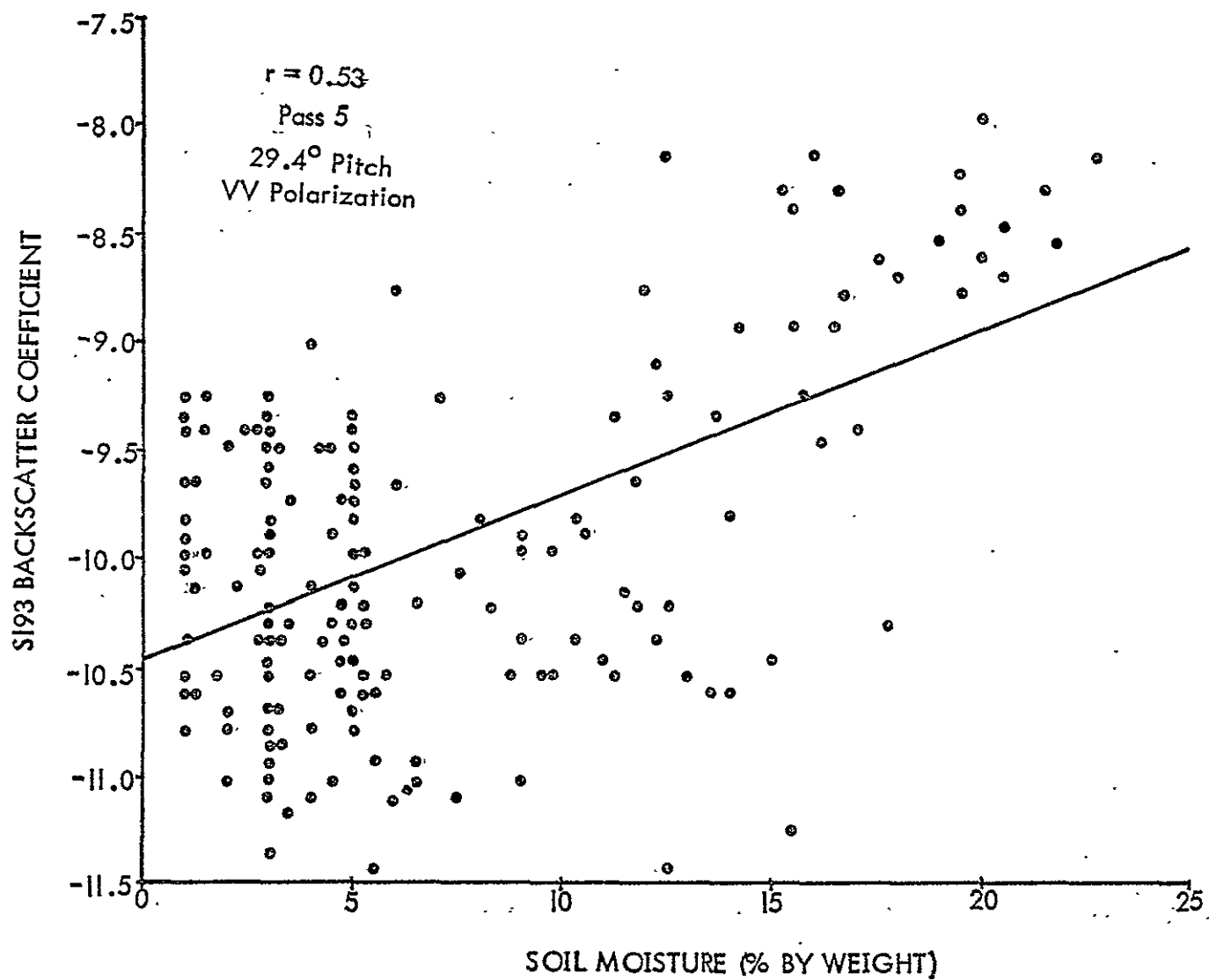soil moisture for pass 38 across Texas.
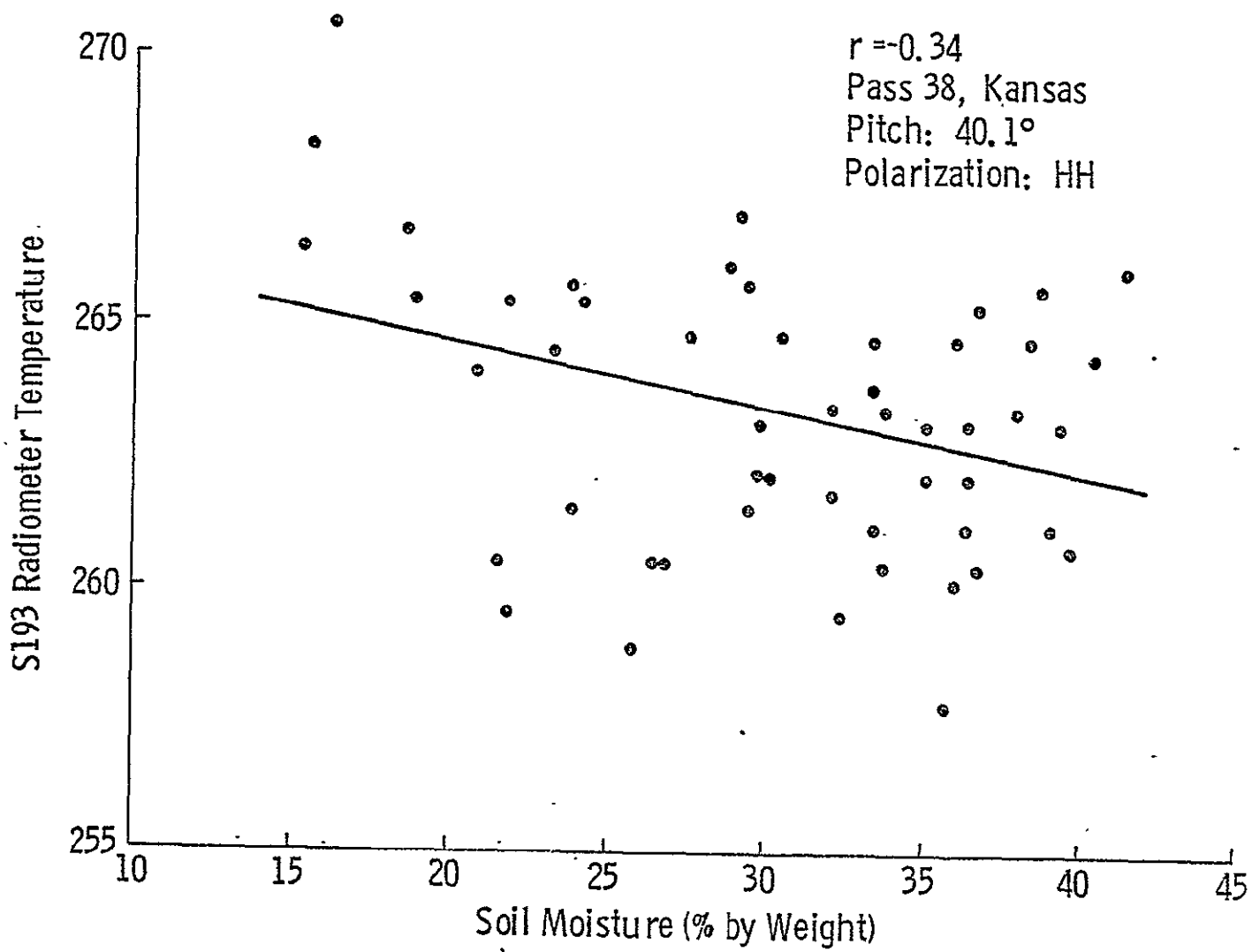
Figure 53 The S193 radiometric temperature as a function of
soil moisture for pass 38 across the Kansas test
site.

Figure 54   The S193 scattering coefficient as a function of
soil moisture for pass 38 across the Kansas test
site.
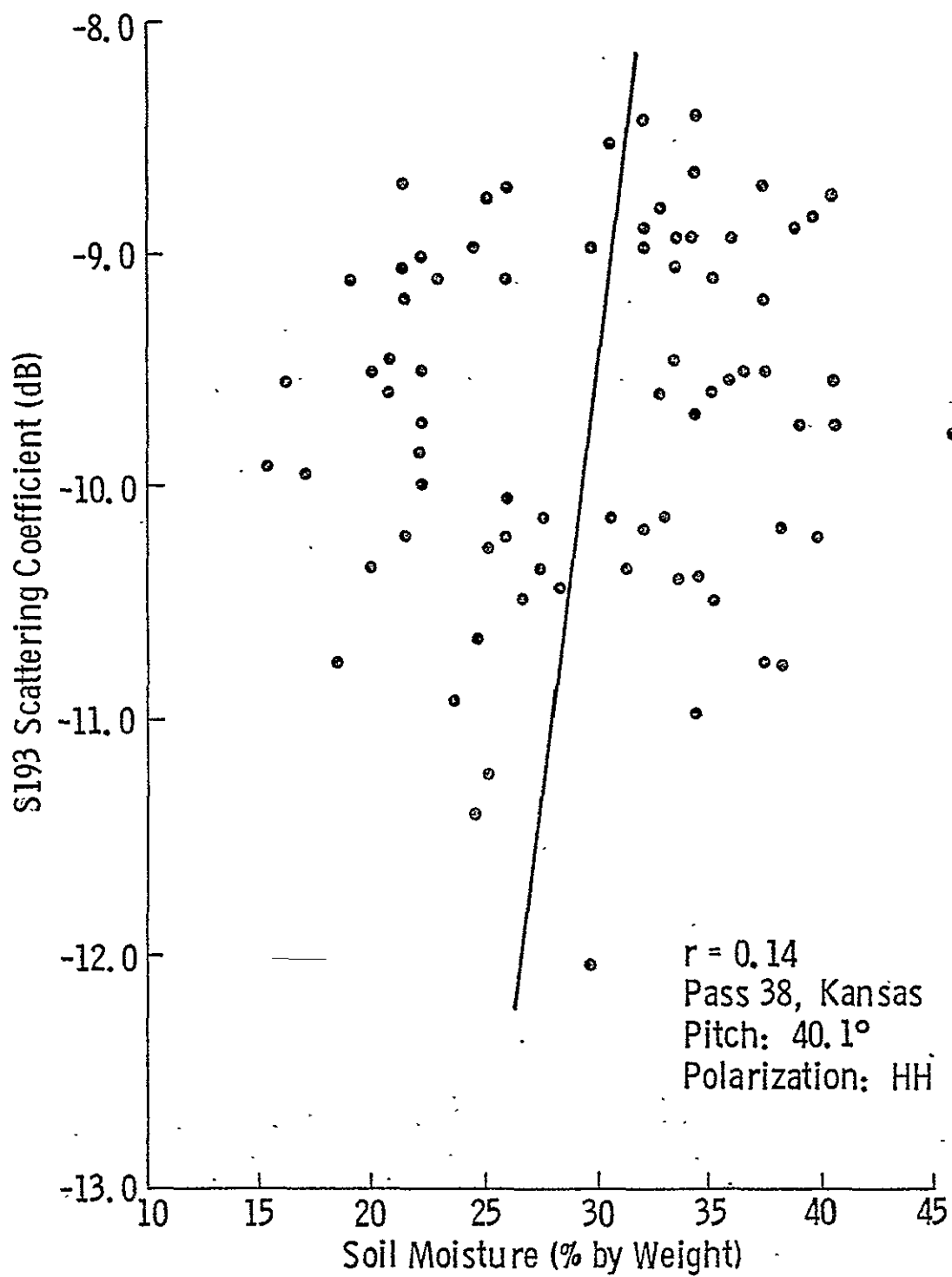
Composite Data S193 Microwave System

Since some of the S193 data were taken with various pitch angles and polarizations, fewer of the data sets are comparable than for the S194 sensor; however, two of the passes, 5 and 16, were taken at the same pitch angle and polarization (29.4° forward pitch and vertical-vertical polarization). These data were combined to determine the composite relationship between the S193 passive radiometer and soil moisture content. This relationship is shown in Figure 55. When these two passes are combined, the resulting correlation coefficient was -0.93 for the central four data lines which should represent the best data base for analysis. This result obtained by combining data across Texas on June 5 and August 8, 1973, indicates that the S193 passive radiometer has a potential for remote sensing the moisture content of the upper 2.5 cm of soil. Although this sensor operating at 2.1 cm wavelength is more sensitive to the amount of vegetative cover and the amount of cloud cover than the S194 instrument, it has the advantage of a smaller resolution cell so that more detail can be obtained.

A similar analysis for the S193 active scatterometer is shown in Figure 56. The resulting correlation coefficient when the data from pass 5 and pass 16 are combined is -0.72. These data also represent the center four lines of data through the test site. While this correlation coefficient is not as good as for the passive radiometer operating at the same wavelength, it is much better than the correlation for some of the individual passes.
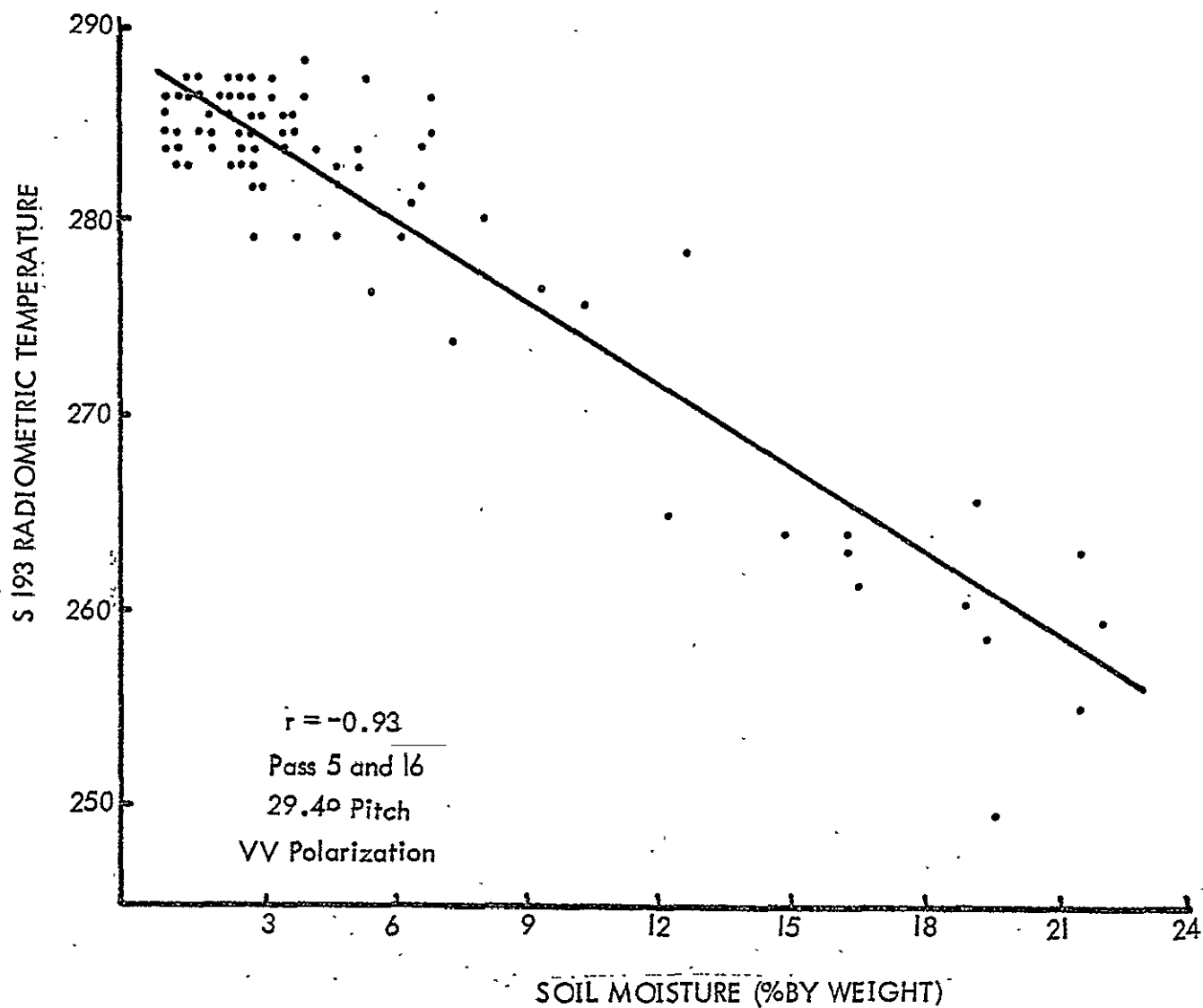
Figure 55 The composite relationship between S193 radiometric
temperature and soil moisture content for passes
5 and 16 across the Texas test site.
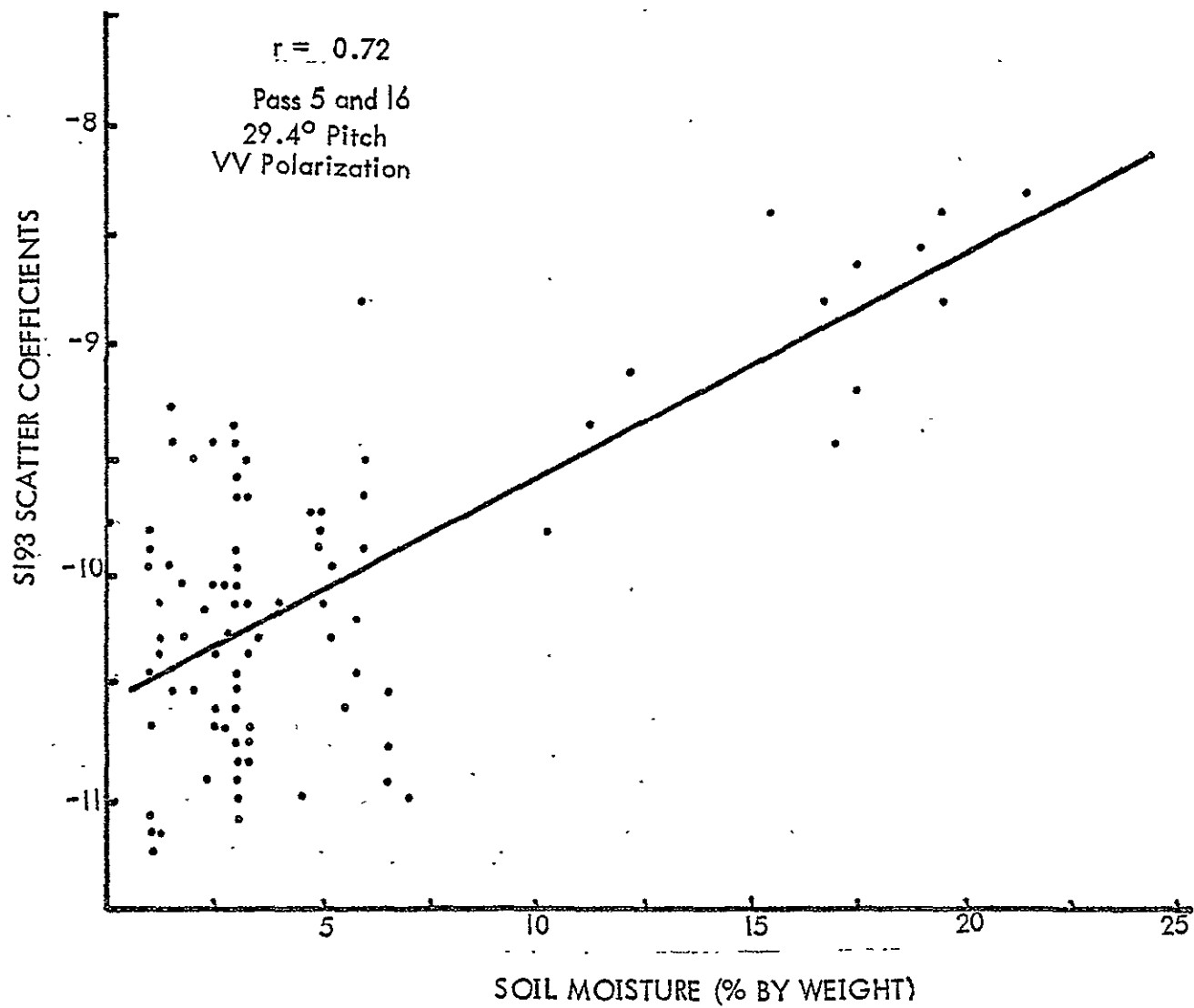
Figure 56   The composite relationship between S193 scattering
coefficient and soil moisture for passes 5 and 16
across the Texas site.

S194 Radiometric Data Analysis

The corrected antenna temperature of the S194 21 cm radiometer was used for evaluation of the response to soil moisture of the earth. The maximum and minimum temperatures of each pass over the test sites are shown in Table VIII. Since the reported spacecraft pitch and roll angles were unstable during pass 15 over the Kansas site, almost all fields of view of the S194 antenna missed the Kansas site (Table IX). Thus, this set of data could not be used in the analysis for the soil moisture experiment. Pass 48 over the Kansas test site could not be used because of rainfall immediately after the Skylab data collection which terminated soil moisture measurements. Therefore, five out of seven sets of S194 radiometric data were analyzed for response to soil moisture content.

Table VIII

Pass	5	10	15	16	38	38 38	48
Date (1973)	6-5	6-13	8-5	8-8	9-13	9-13	9-18
Test Site	Texas	Kansas	Kansas	Texas	Texas	Kansas	Kansas
Maximum T	276.0	254.3	273.0	274.0	271.0	228.8	225.0
Minimum T	229.1	232.1	250.0	251.7	249.1	218.8	220.0

Relationship Between Soil Moisture
and S194 L-band Radiometric Data

The response of the S194 L-band radiometer to the moisture content of the soil was analyzed by determining the soil moisture content within each of the S194 footprints which

Table IX

S194 EPHEMERIS DATA

PROJECT
MISSION 3   ORBIT 15   4-DPCA-1-15-82-A-R11   SITE 0
SENSOR S194-LBR   RECORDING FORMAT PCHNRZL-180BPS   FLIGHT DATE 5 AUG 73

START TIME 16 HR 37 MIN 2.14 SEC   STOP TIME 16 HR 37 MIN 58.30 SEC

GMT	ALT (NM)	LAT.	LONG.	Z-LV PITCH	Z-LV YAW	Z-LV ROLL	BETA	SUN ELEV.	FIELD OF VIEW LAT	FIELD OF VIEW LONG.
16:37: 2.14	235.370	39.351	-100.868	360.0	360.0	360.0	3.4	53.5	39.357	-100.895
16:37: 3.13	235.369	39.315	-100.802	0.0	0.0	0.0	3.4	53.6	39.324	-100.829
16:37: 4.12	235.368	39.280	-100.742	360.0	360.0	360.0	3.4	53.6	39.285	-100.763
16:37: 5.11	235.357	39.244	-100.676	360.0	360.0	359.9	3.4	53.7	39.244	-100.703
16:37: 6.10	235.365	39.208	-100.610	359.9	359.9	359.7	3.4	53.8	39.195	-100.643
16:37: 7.09	235.363	39.173	-100.549	359.9	360.0	359.9	3.4	53.8	39.173	-100.577
16:37: 8.09	235.362	39.137	-100.483	0.0	0.0	0.1	3.4	53.9	39.145	-100.511
16:37: 9.08	235.361	39.098	-100.423	0.0	0.0	0.1	3.4	54.0	39.109	-100.445
16:37:10.07	235.350	39.063	-100.357	360.0	360.0	359.9	3.4	54.0	39.065	-100.384
16:37:11.06	235.358	39.027	-100.291	359.9	359.9	359.7	3.4	54.1	39.013	-100.324
16:37:12.05	235.357	38.991	-100.231	359.5	360.0	359.6	3.4	54.1	38.964	-100.264
16:37:13.05	235.356	38.956	-100.165	359.4	0.0	359.7	3.4	54.2	38.931	-100.198
16:37:14.04	235.355	38.920	-100.104	359.6	0.0	359.8	3.4	54.2	38.906	-100.132
16:37:15.03	235.354	38.881	-100.038	359.9	0.0	359.9	3.4	54.3	38.881	-100.066
16:37:16.02	235.353	38.846	-99.978	0.0	360.0	0.0	3.4	54.4	38.854	-100.000
16:37:17.01	235.351	38.810	-99.912	359.8	0.0	359.9	3.4	54.5	38.807	-99.940
16:37:18.01	235.349	38.774	-99.852	359.6	0.0	359.8	3.4	54.5	38.758	-99.879
16:37:19.00	235.348	38.735	-99.786	359.6	0.0	359.8	3.4	54.6	38.722	-99.819
16:37:19.99	235.347	38.700	-99.725	359.8	0.0	359.9	3.4	54.7	38.695	-99.753
16:37:20.98	235.346	39.664	-99.659	360.0	0.0	360.0	3.4	54.7	39.670	-99.687
16:37:21.97	235.345	33.626	-99.599	0.1	360.0	0.0	3.4	54.8	38.640	-99.621
16:37:22.97	235.344	38.590	-99.539	0.0	0.0	0.1	3.4	54.9	38.604	-99.561
16:37:23.96	235.342	38.555	-99.473	0.1	0.1	0.2	3.4	54.9	38.579	-99.495
16:37:24.95	235.341	38.516	-99.412	360.0	360.0	359.9	3.4	55.0	38.519	-99.440
16:37:25.94	235.340	38.480	-99.346	359.9	359.9	359.7	3.4	55.0	39.464	-99.379
16:37:44.35	235.317	37.791	-98.199	360.0	360.0	359.9	3.4	56.2	37.794	-98.226
16:37:45.35	235.316	37.755	-98.138	359.9	359.9	359.7	3.4	56.3	37.744	-98.171
16:37:46.35	235.315	37.717	-98.077	360.0	360.0	359.9	3.4	56.3	37.720	-98.105
16:37:47.34	235.313	37.678	-98.017	0.0	0.0	0.0	3.4	56.4	37.689	-98.039
16:37:48.34	235.312	37.643	-97.957	360.0	360.0	360.0	3.4	56.5	37.648	-97.979
16:37:49.33	235.311	37.604	-97.896	9.8	5.8	351.7	3.4	56.5	37.269	-97.951
16:37:50.33	235.309	37.566	-97.836	25.9	12.6	341.5	3.4	56.6	37.000	-98.418
16:37:51.33	235.308	37.527	-97.770	10.8	3.8	354.2	3.4	56.7	37.547	-98.011
16:37:52.32	235.307	37.489	-97.709	338.6	356.8	5.7	3.4	56.7	36.951	-96.765
6:37:53.32	235.306	37.453	-97.649	325.4	1.6	0.3	3.4	56.8	35.676	-94.974
16:37:54.31	235.305	37.415	-97.589	350.6	0.5	0.1	3.4	56.8	36.929	-97.012
16:37:55.31	235.303	37.376	-97.528	2.5	359.9	359.9	3.4	56.9	37.525	-97.709
16:37:56.31	235.302	37.338	-97.468	5.3	359.7	359.8	3.4	57.0	37.640	-97.814
16:37:57.30	235.301	37.299	-97.407	2.7	359.7	359.7	3.4	57.1	37.448	-97.605
16:37:58.30	235.300	37.264	-97.347	358.8	359.9	359.7	3.4	57.1	37.187	-97.314

ORIGINAL PAGE IS
OF POOR QUALITY

149

were 115 km in diameter. This was accomplished by preparing

a circular overlay for use with the soil moisture distribu-

tions generated by the computer as shown in Figure 15. The

S194 weighted brightness temperature from every 7 km along the

flight track was compared with the appropriate average percen-

tage of soil moisture content within the circular area of 115

km diameter. Scattergrams for the three passes over the Texas

site and two passes over the Kansas site for the upper 2.6 cm

of soil depth are shown in Figure 57. The correlation indices

of the second degree curve ranged from -0.99 to -0.95. There

is obviously a very good relationship between the weighted

brightness temperature from the L-band radiometer and the soil

moisture content for all five sets of data. These correlation

coefficients were obtained by using all data points as if they

were independent. Analysis of independent samples (see page

158) shows, however, that the correlation is indeed extremely

good.

In order to verify that the high correlations obtained

between the radiometric temperature and soil moisture content

were not the result of a third factor, comparisons were made

for the soil moisture-radiometric temperature over similar

terrain with changing moisture patterns. Two passes, 5 and

16, were chosen for further comparison of S194 brightness temp-

erature and soil moisture content. These two passes were par-

allel to each other over the Texas site (Figure 58). The S194

brightness temperature and soil moisture content are shown in

Figure 59. For pass 5 on June 5, soil moisture contents in-

creased from northwest to southeast, with a reversal for pass
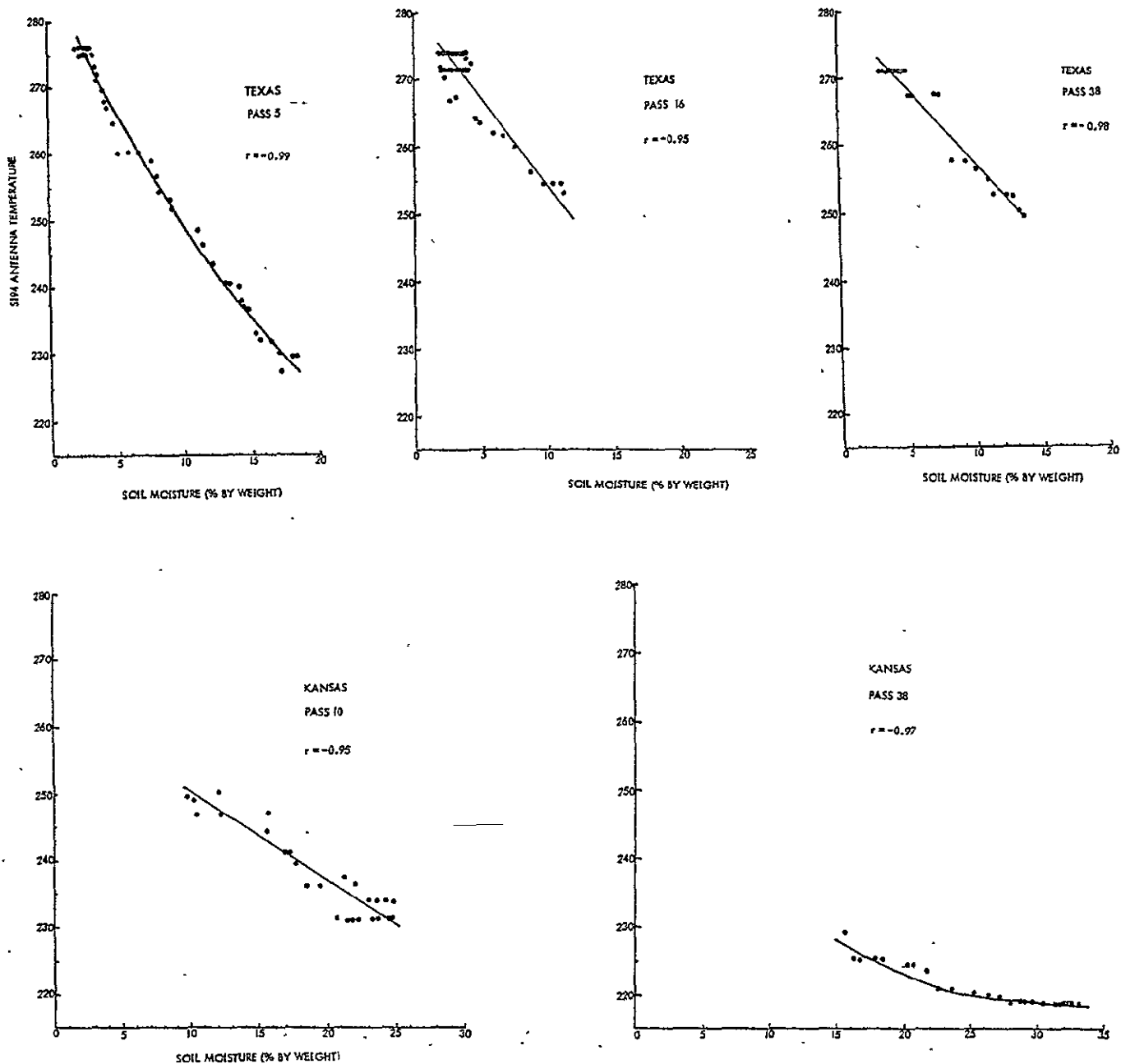
Figure 57   The relationship between the S194 brightness temp-
            erature and soil moisture content for the five
            separate data sets.
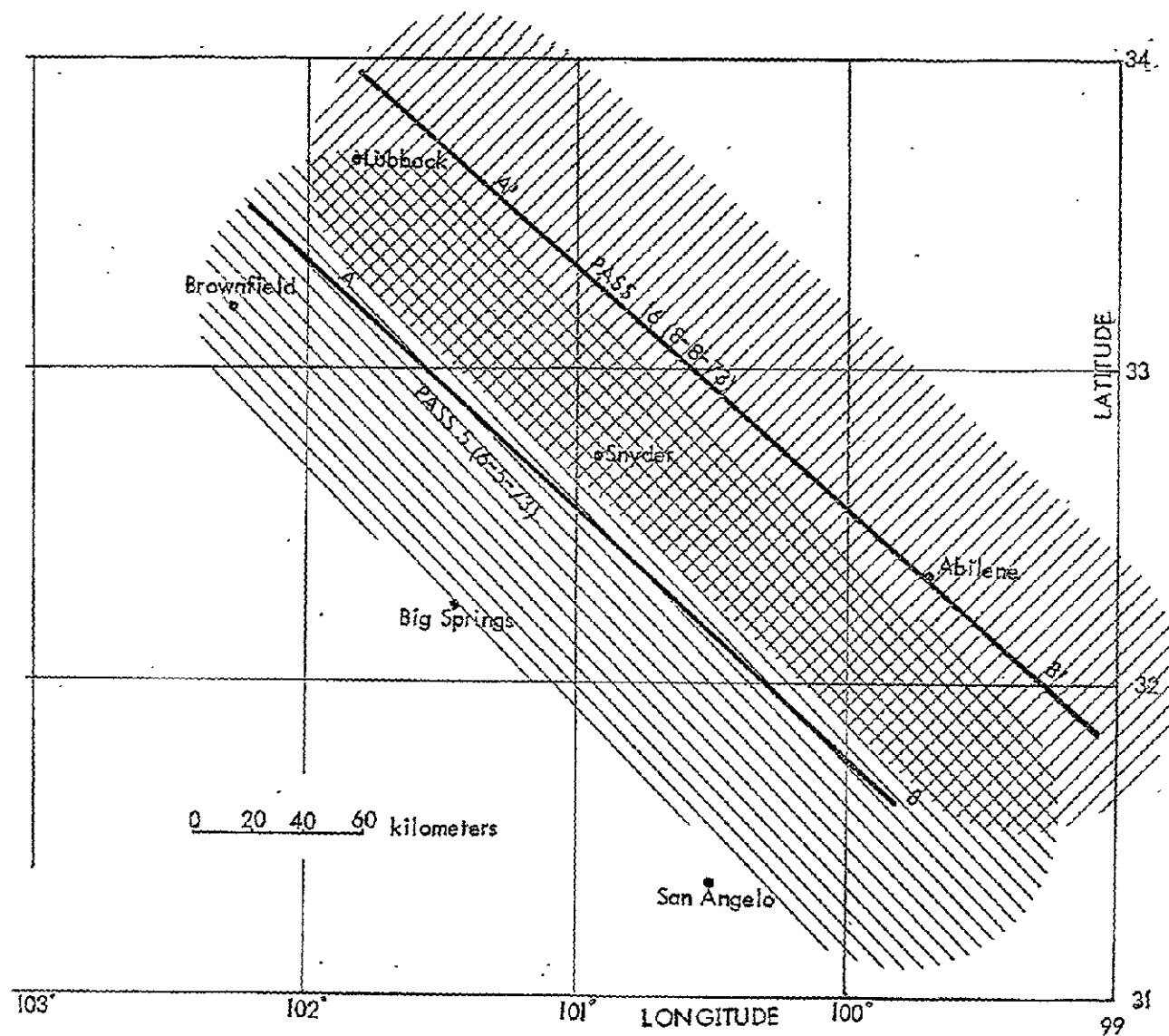
Figure 58   The location of the Skylab passes across Texas on
June 5 and August 8, 1973.

152
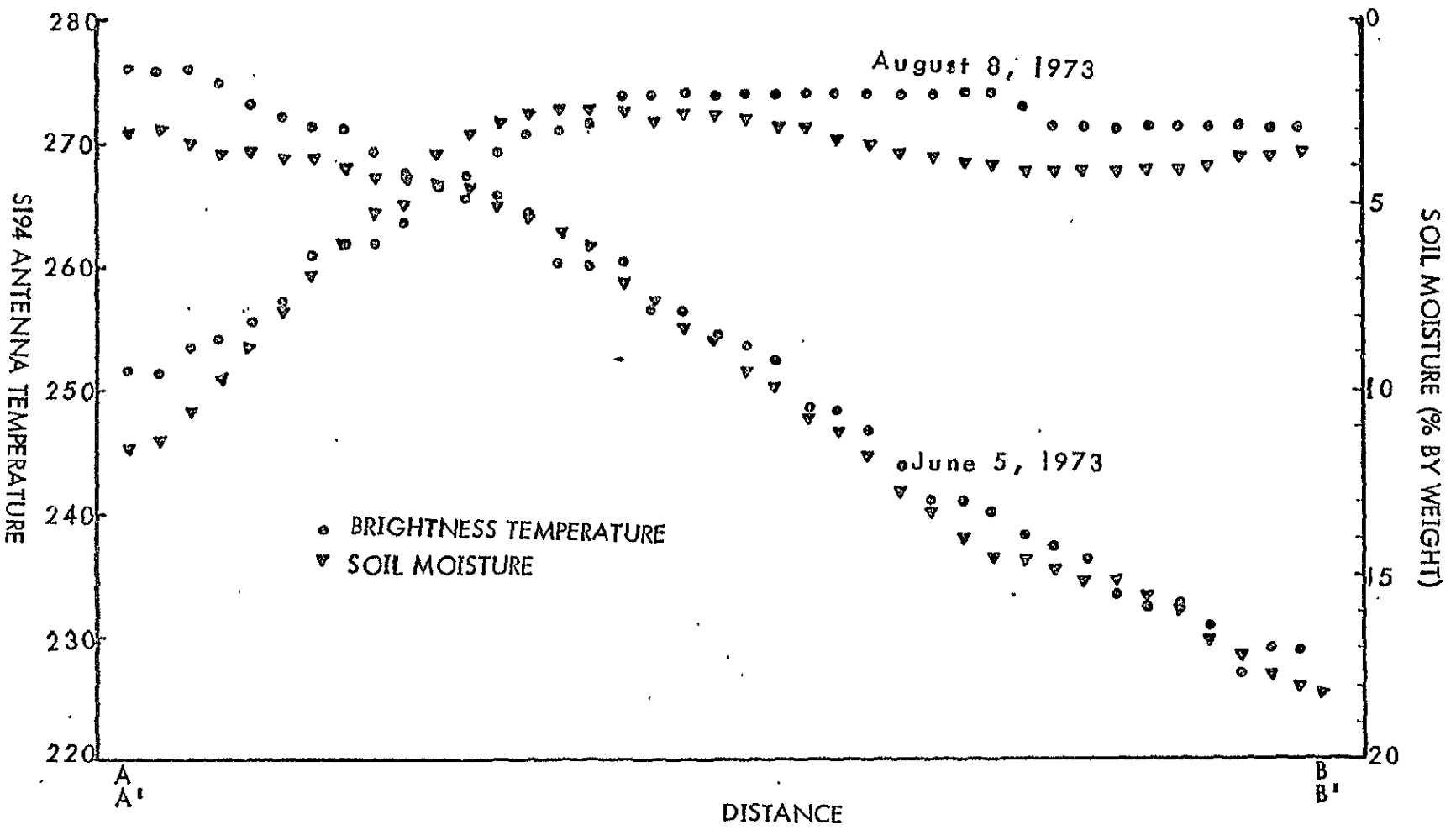
Figure 59   Variations of SI94 antenna temperature and soil
moisture content across the Texas site on June
5 and August 8, 1973.

153

16 so that decreasing soil moisture contents occurred from northwest to southeast. This provides convincing evidence that the radiometric brightness temperature was responding to soil moisture content, since the distribution patterns of soil moisture were quite different for the two passes over similar soil types and vegetation patterns.

In order to further investigate the relationship between the S194 weighted brightness temperature and soil moisture content at various depths below the surface, data have been plotted and correlation coefficients have been calculated. Table X compares the correlation coefficients for various depths for two of the data sets. The surface 2.5 cm depth gave the best correlation with the weighted brightness temperature for four of the five data sets with the pass five data over Texas giving a slightly higher correlation for the top five cm depth. Since four of the five data sets gave a higher correlation for the first 2.5 cm depth, the following analysis will concentrate on the soil moisture content in the upper 2.5 cm of soil.

Since more return from the ground may come from near the center of the footprint in comparison to the edges, revised soil moisture contents in the S194 footprint circle of 115 km diameter were computed by weighting the soil moisture content by the appropriate antenna pattern factors (Sensor Performance Report-S194, NASA, 1974). The weighted soil moisture contents correlated with the brightness temperatures of the S194 radiometer are shown in Figure 60 for pass five in Texas and pass 38 in Kansas. The correlation indices are -0.99 and -0.97 for

Table X

CORRELATION BETWEEN SKYLAB L-BAND RADIOMETER
AND SOIL MOISTURE

Soil Moisture Layer (cm)	Pass 5- Texas Correlation Coefficient	Pass 38-Texas Correlation Coefficient
0-2.5	-0.991	-0.973
2.5-5.0	-0.990	-0.959
5.0-7.5	-0.951	-0.938
7.5-10.0	-0.923	-0.952
10.0-12.5	-0.885	-0.954
12.5-15.0	-0.880	-0.955
0-5.0	-0.993	-0.968
0-7.5	-0.987	-0.960
7.5-15.0	-0.899	-0.954
0-15.0	-0.966	-0.957
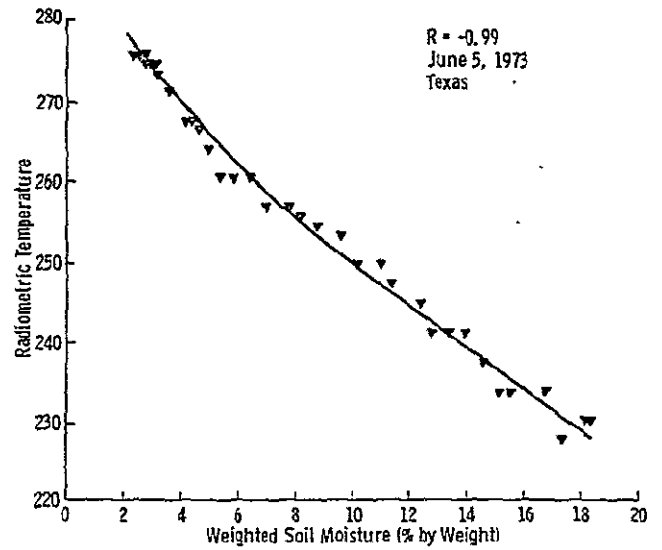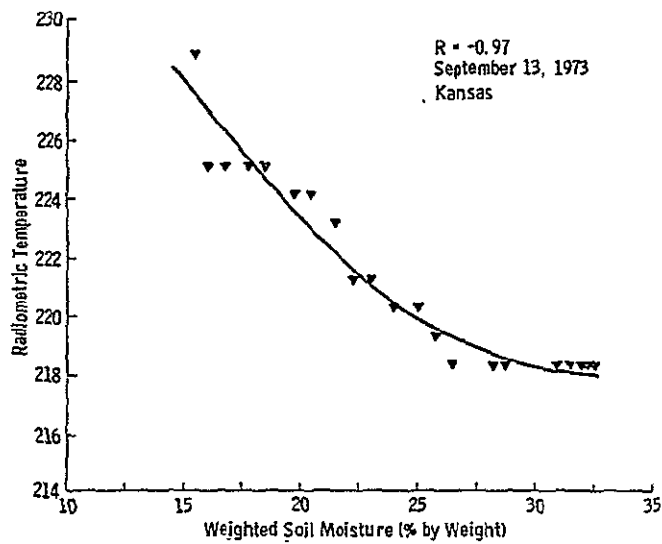
Figure 60 Correlation of the radiometric temperature with the soil moisture content as weighted by the antenna pattern.

pass 5 and pass 38, respectively. These correlations are so
similar to those obtained by the previously determined average
soil moisture content over the whole footprint circle that it
was concluded that it was unnecessary and impractical to use
such weightings.

Composite Relationship From Five Sets of Data

Since the five data sets were taken at different times
of the year and different places, the differences in ground
temperature among the five data sets varied form 1°C to 5°C as
estimated by air temperature. While the near surface ground
temperature has large fluctuations at low moisture contents
and clear skies at midday, the soil temperature below the sur-
face is closer to fluctuations of air temperature. Due to
the greater skin depth of the S194 radiometer, the probable
error of the estimated ground temperature had little effect
on the S194 radiometer temperature (Poe and Edgerton, 1971).
For comparison and combination, the weighted brightness temp-
eratures were adjusted to a ground temperature of 300°K by
the following procedures.

The brightness temperature measured by a downward looking
microwave radiometer is given by:

$$T_B = L(\varepsilon T_g + T_{sc}) + T_u$$

where L is the atmospheric transmittance, ε is the target emis-
sivity, T_g is the ground temperature, T_{sc} is the upward scat-
tered radiation and T_u is the upward emission by the atmosphere.
For a plane surface model, T_{sc} can be expressed in terms of

the downward emitted radiation T_d and the surface reflectivi-
ty, $r = 1-\varepsilon$:

$$T_{sc} = (1-\varepsilon)T_d$$

At 1.4 GHz (S194 frequency), L and T_u at nadir were cal-
culated to be about -.993 and 2°K, respectively (Eagleman and
Ulaby, 1974). T_d includes downward emitted atmospheric radi-
ation as well as galactic radiation and is estimated to be a-
bout 7°K. Attenuation by clouds in this frequency range is
very small (Benoit, 1968) and hence can be neglected. There-
fore, the adjusted-weighted brightness temperature was obtain-
ed by:

$$T_b = T_B + 0.993 \cdot \varepsilon(300-T_g)$$

The five data sets were combined to form a composite re-
lationship between the adjusted brightness temperature and
moisture content of the upper 2.5 cm layer of soil as shown in
Figure 61. Correlation index for the second degree curvilin-
ear relationship is -0.96. This relation is quite good con-
sidering the various differences between the soil and vege-
tation characteristics for the different data sets.

For the half-power footprint of 115 km diameter, the
footprint overlap from one measurement point to the next was
approximately 92%. The independence of the data points is,
therefore, of concern if all the data are used in the analy-
sis. Independent footprints based on the half-power footprint
of the S194 were also analyzed to see what effect this would
have on the correlations (Figure 62). There were three
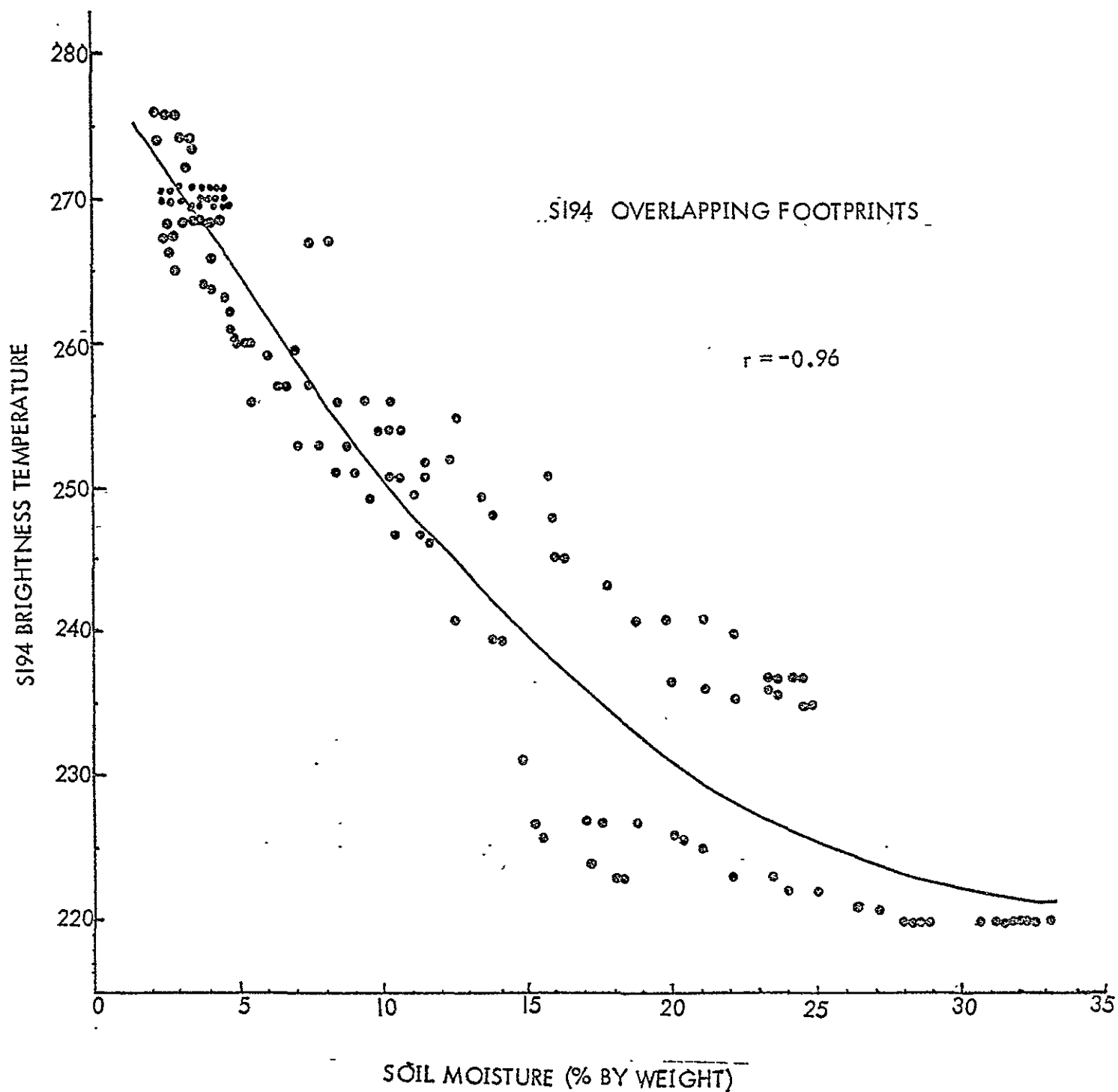
Figure 61 The composite relationship between the S194 bright-
ness temperature and soil moisture content for the
five data sets using overlapping footprints.
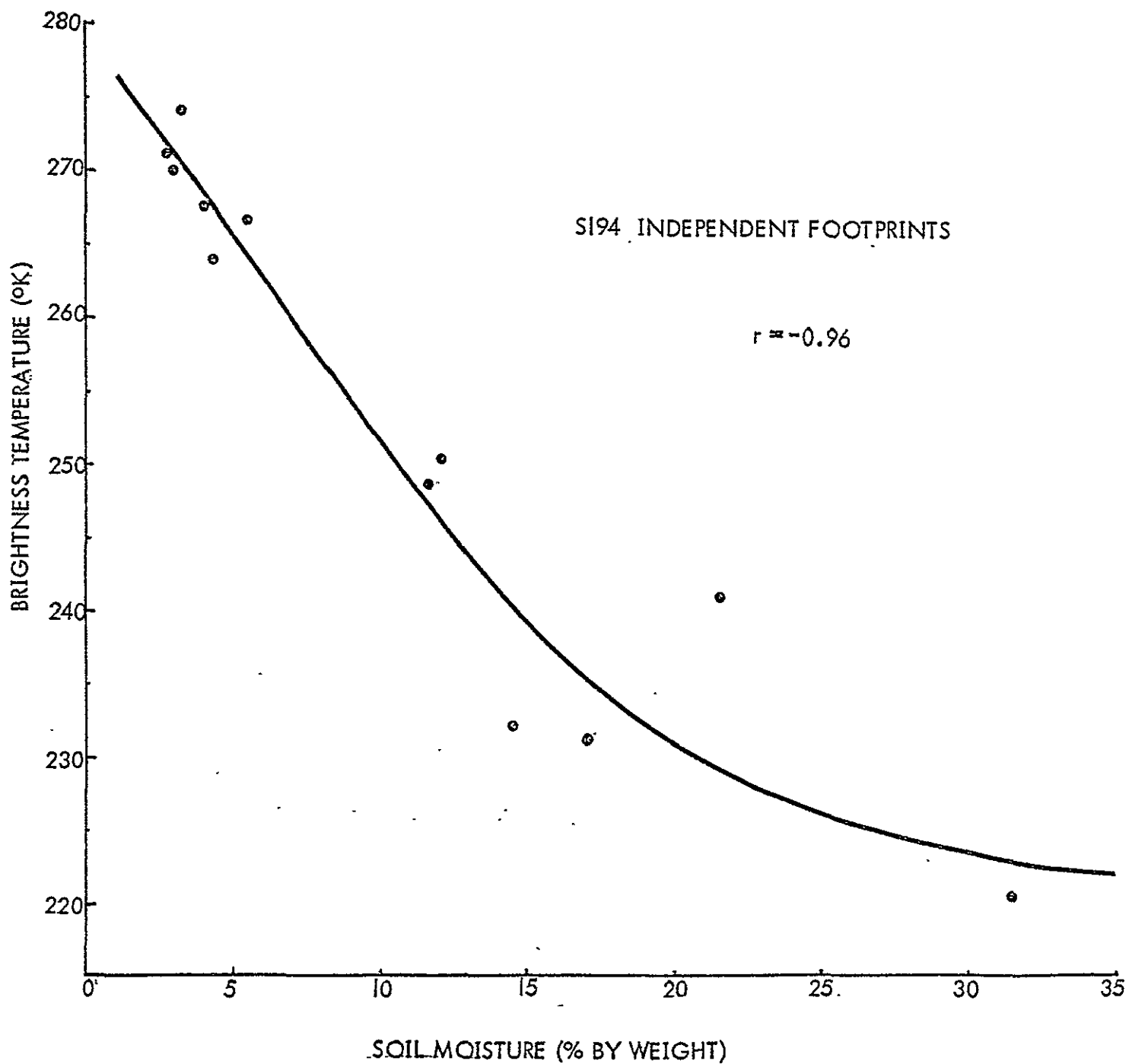
Figure 62   The composite relationship between the S194 bright-
           ness temperature and soil moisture content for the
           five data sets using independent footprints.

independent footprints for pass five and 16, two for pass 10
and four for pass 38. These 12 independent samples also re-
sulted in a correlation index of -0.96. Therefore, the high
correlations cannot be discounted on the basis of overlapping
footprints.

Vegetation Effects

The amount of vegetation cover has been shown to influence
the capability of passive microwave radiometers to detect soil
moisture (Newton, et al., 1974 and Lee, 1974). The effect of
vegetation-shielding of soil moisture varies for different
radiometer wavelengths. The S194 radiometer should be less
affected by vegetation than higher frequency radiometers, al-
though there were indications of slight vegetation effects in
the S194 radiometric response during the different passes.

Vegetation cover modifies the soil emission through scat-
tering, attenuation and augmentation of the original emission
due to the presence of vegetation and emission from it. Sibley
(1973) has made extensive theoretical studies on the effect
of vegetation on radiometric data and has developed apparent
temperature models incorporating the vegetation effects for
the natural terrain. In this model of apparent temperature of
terrain as a function of soil moisture content, the thermal
emission of soil and vegetation only were considered.

Sibley's model for a smooth surface and uniformly vegeta-
ted surface was used to calculate the effect of vegetation
cover of various heights on the S194 radiometric temperature.

Figure 63 shows a comparison of the radiometric temperature variations for different soil moisture content and heights of vegetation. A canopy volume of 3% was assumed for the volume occupied by plant material for the various heights. Even though the composite data gave a correlation of -0.96 between radiometer temperature and soil moisture content there are slight differences between the different passes that may be related to vegetation. The three Texas passes for June, August and September are displaced in the direction of more vegetation cover as the growing season progresses. The June and September passes across Kansas do not have this pattern, however. There are several possible explanations for this. The winter wheat in Kansas provides more cover than many crops in Texas during the early part of the growing season. The June 13 data are also probably the least reliable of the five data sets. In addition to cloud cover over the Kansas test site, precipitation occurred in parts of the test site close to the time of Skylab data collection. Even though precipitation and evapotranspiration adjustments were made to the measured soil moisture, the data could not be expected to be perfect. Errors here would be expected to cause a low correlation rather than a displaced curve, however. Another possible explanation arises from the abnormally high temperatures observed for the cold load #1 and #2 for pass 10 (Sensor Performance Report-NASA, 1974) It was concluded in the sensor performance evaluation, that this should not affect the quality of the data,
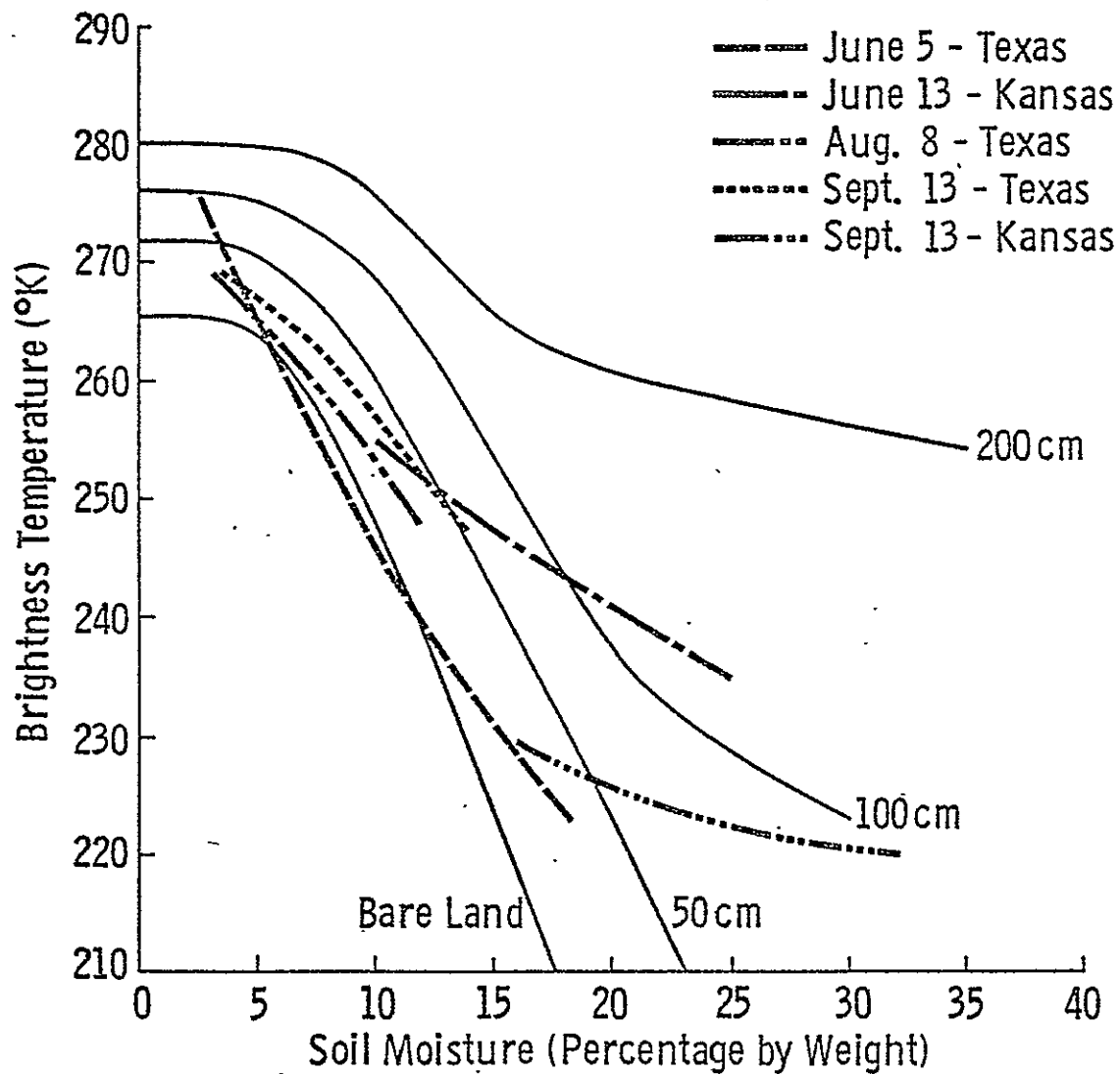
Figure 63   Comparison of the radiometric temperatures for
different soil moisture content and height of
vegetation for the five Skylab data sets.

but the comparison shown in Figure 63 lends some doubt, since abnormally high radiometric temperatures would also explain the difference observed for the June 13 data. Even so, the maximum discrepency in radiometric temperature between the different passes is about 15°K which corresponds to 5% soil moisture. It is worth noting that this difference arises when comparing different passes and the composite of the five data sets still gave a very high correlation (-0.96). It was concluded, therefore, that the S194 passive radiometer was very sensitive to soil moisture content even under varying vegetation, atmospheric and soil conditions.

Analysis of Aircraft Microwave Data

The soil samples were taken on the average about 2.5 miles apart and the aircraft microwave data were taken about every 165 feet. Therefore, the ground truth was very coarse in comparison with the aircraft data. Microwave data were obtained across the Texas test site with an active and passive microwave system operating at 2.1 cm wavelength at an angle of 30° with vertical-vertical polarization. It was decided that a visual inspection of the flight path be conducted to compare the soil moisture map with the aerial photograph to detect any gross errors. A discrepancy was found in an eight mile segment about one-half of the way through the flight from point A to B in Figure 64. The computer generated map for June 5, 1973 in Texas (Figure 16) depicts a gradient from high
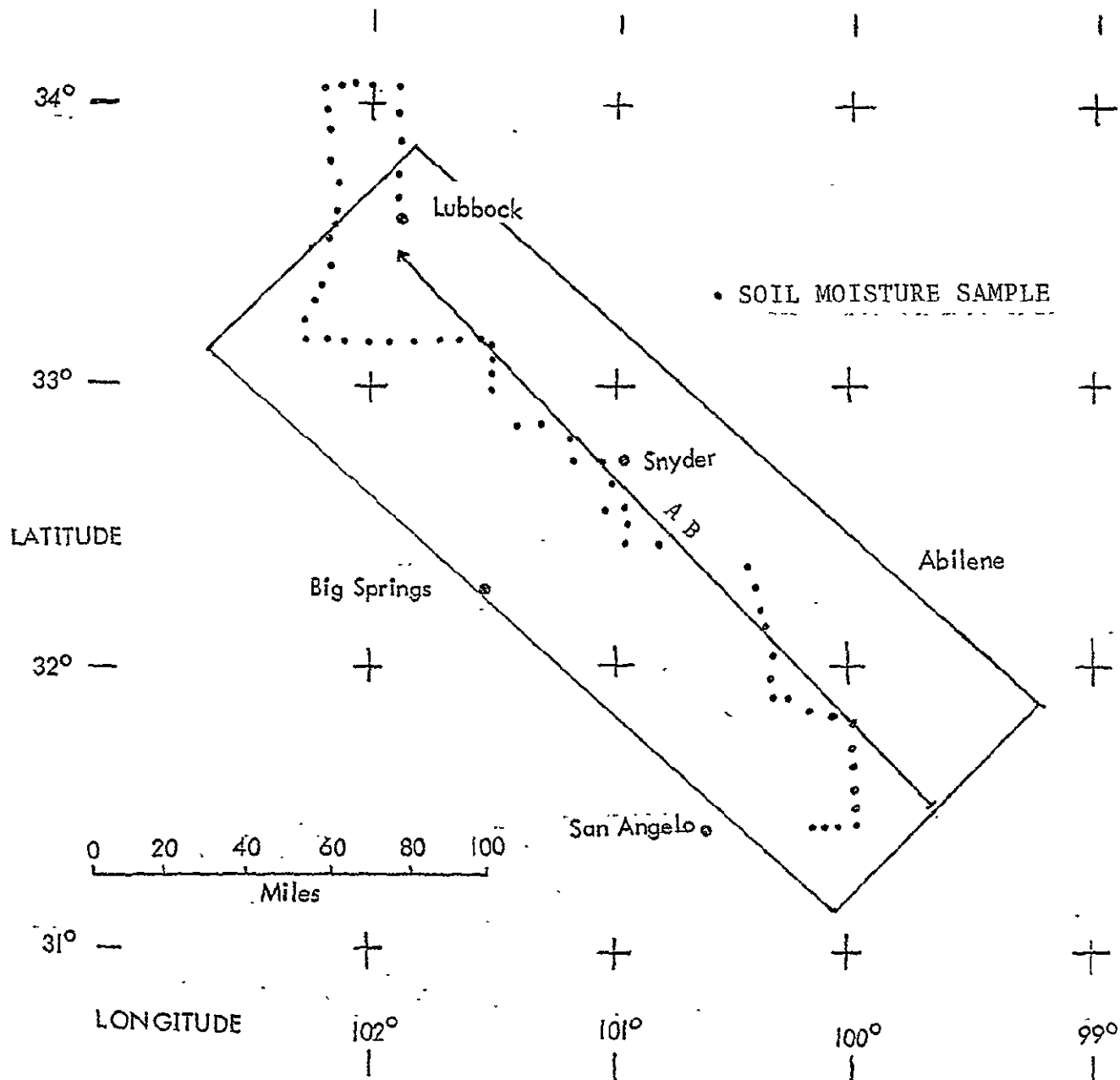
Figure 64 The location of the aircraft flight pass in comparison to the locations of the soil moisture sampling sites.

to low moisture values in this area. The aerial photographs clearly revealed wet fields with some standing water through most of the segment and then an abrupt change to dryer conditions within one to two miles. The closest soil sample to segment AB was at least five miles away. This segment was, therefore, not included in any of the aircraft data analysis. No other contradictions could be detected from the aerial photographs.

The next step was to correlate the aircraft microwave data with the soil moisture. Correlations were computed by calculating the best fit least squares first and second degree equations.

Given the aircraft's altitude and cross angle, the angle from nadir of the sensor, and the time that the data was taken, by simple geometry the location of the footprint for that data could be found on the aerial photograph. Using this procedure, data points were taken from terrain which was used as range land only. The vegetation covering this type of land was fairly homogeneous throughout the entire flight. A random selection of points throughout the flight was correlated to the soil moisture values for the points for both the radiometer antenna temperature and the scatterometer coefficient. Correlation coefficients were low, -0.15 for the radiometer and 0.13 for the scatterometer. (Figures 65 and 66)

It was noted that large fluctuations occurred in the data

Figure 65 The relationship between soil moisture and the 2.1 cm radiometric temperature obtained by the aircraft over range land.

Figure 66 The relationship between soil moisture and 2.1
cm scattering coefficient obtained by the air-
craft over range land.

as the aircraft moved short distances. Two plots of all the data, one for the scatterometer and one for the radiometer were generated by the computer showing sensor measurements along the entire flight path to investigate these fluctuations. For the radiometer antenna temperature fluctuations of 10 to 20°K were noted to occur over bodies of water. Another correlation was run for the radiometer using the average antenna temperature for fifty data points. The fifty points covered approximately 1.5 miles on the ground. Individual data values showing very large fluctuations were ignored and the average computed from those remaining. These correlations were not much better than the first, -0.17 for the radiometer and -0.30 for the scatterometer. Indeed, the slope of the line for the scatterometer correlation was negative which was opposite the expected relationship since with an increase in moisture an increase in the scatter coefficient should occur.

Since the aircraft measurements are for very small areas further refinements in the data analysis were necessary. The best results were obtained for bare cultivated fields for 50 data point averages. Since over 70% of the land in Texas in June was under cultivation, 50 data point averages were computed by the same procedure as before and for an average to be considered for the correlation at least 75% of the points had to come from cultivated fields. The resulting correlations showed considerable improvement for both the

radiometer and scatterometer. Figure 67 shows the scatter diagram for the radiometer data with a correlation coefficient of -0.69.

The scatterometer data, however continued to have a low correaltion (-0.27) and the persistant negative slope, Figure 68. From all of the correlations conducted it was evident that other factors besides soil moisture were affecting the 2.1 cm scatterometer data. A correlation was run between the radiometer and the scatterometer data for individual points to see if the sensors were reacting similarly to the same footprint. A correlation of -0.11 indicated that the sensors were reacting differently to the same area.

In order to try to further understand the response of these microwave sensors, a qualitative study of the reaction of the sensors to the terrain features was conducted by plotting the sensor's measurements on the aerial photographs. Figure 69 depicts the sensors' reaction to a section early in the flight just east of Ballinger, Texas. From point A to A' there is a transition from cultivated land to range land; but there is little change in both sensors which should mean little change in moisture from one area to another. On the other hand there is a significant change from B to B'. The ground looks equally wet in either field but different crops are growing in the two fields. At point C the footprint of the sensors crosses the river and opposite reactions are noted with the radiometer indicating the low temperature from
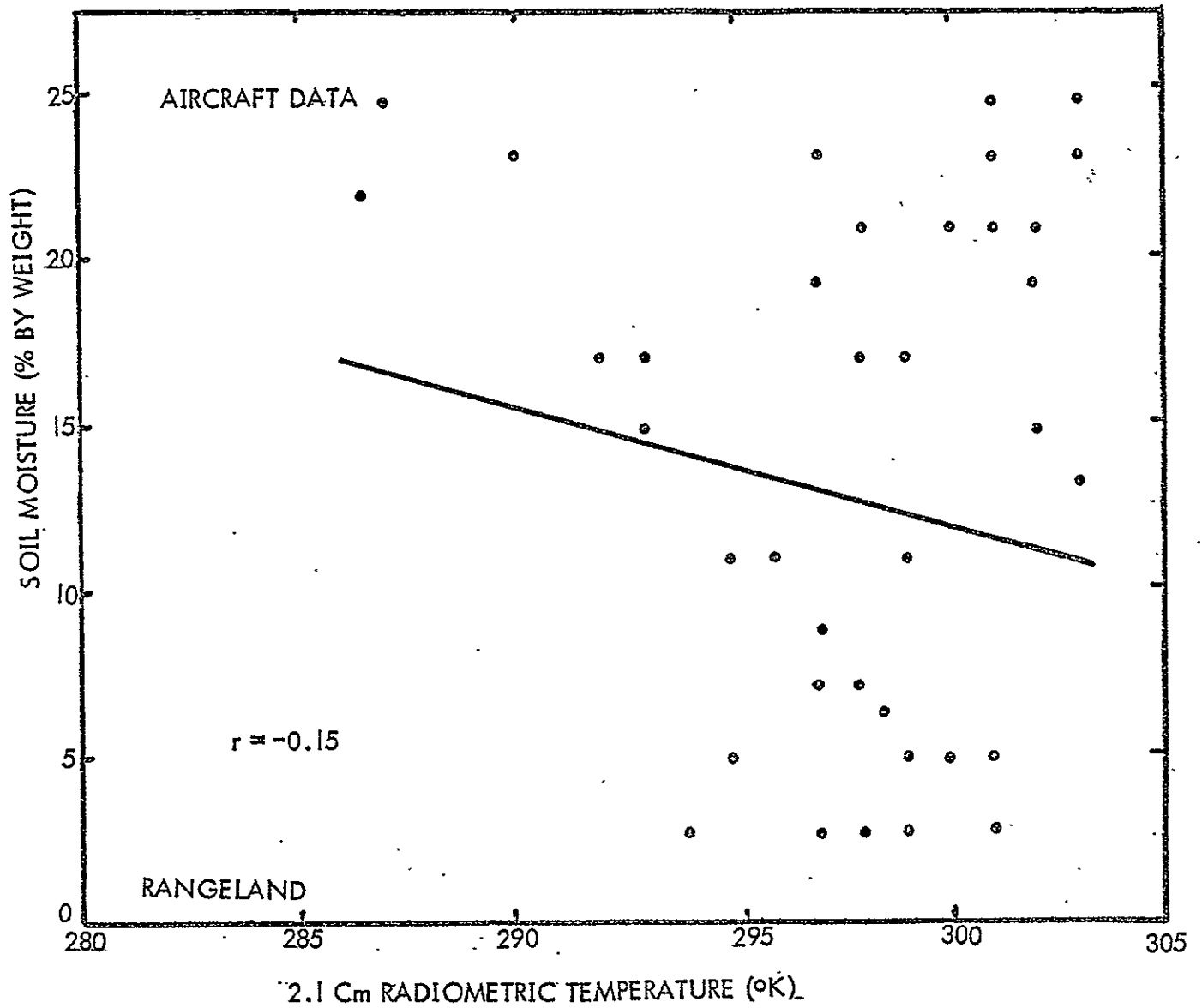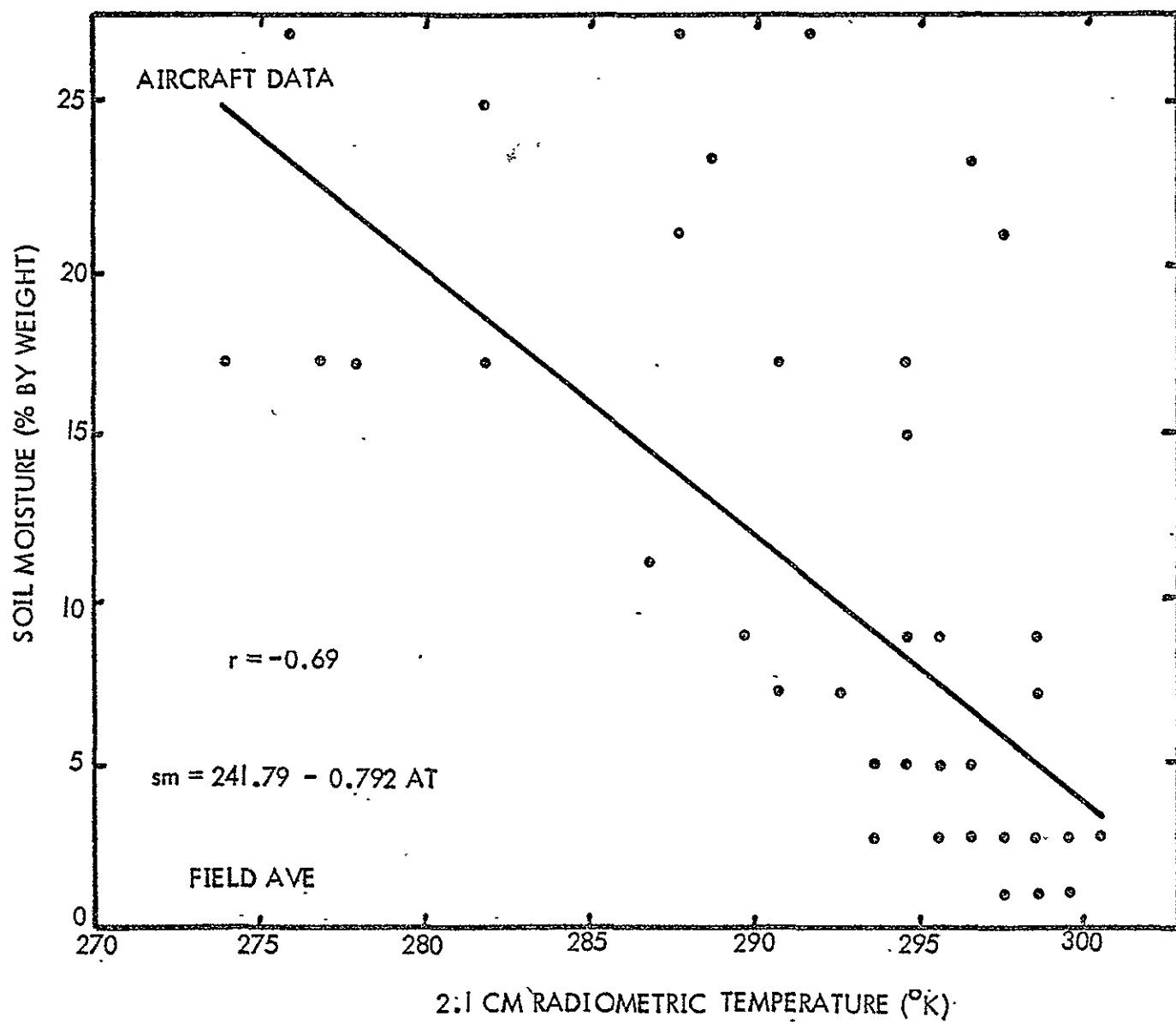
Figure 67   The relationship between soil moisture and 2.1 cm radiometric temperature obtained by the aircraft over bare cultivated fields.

171
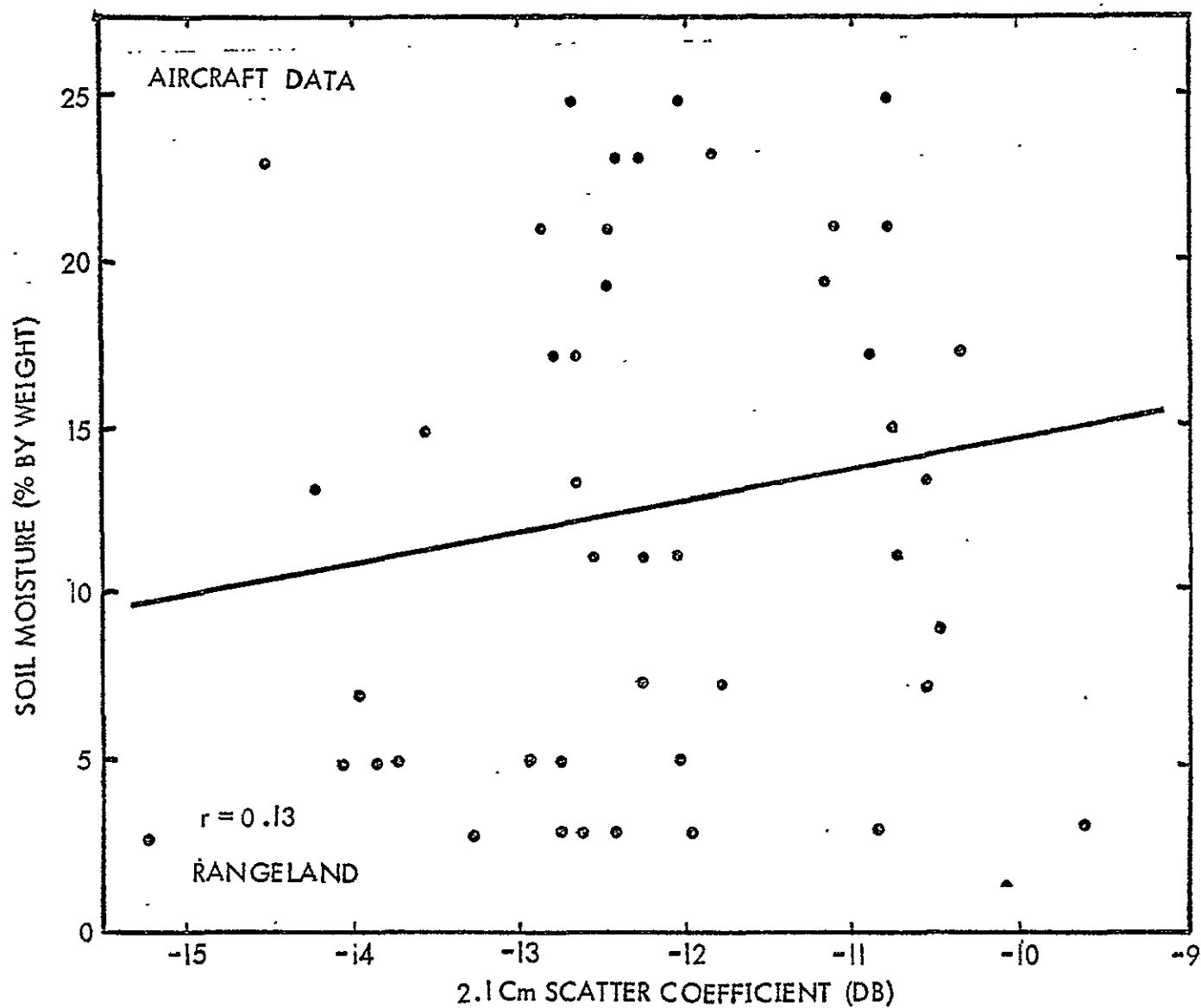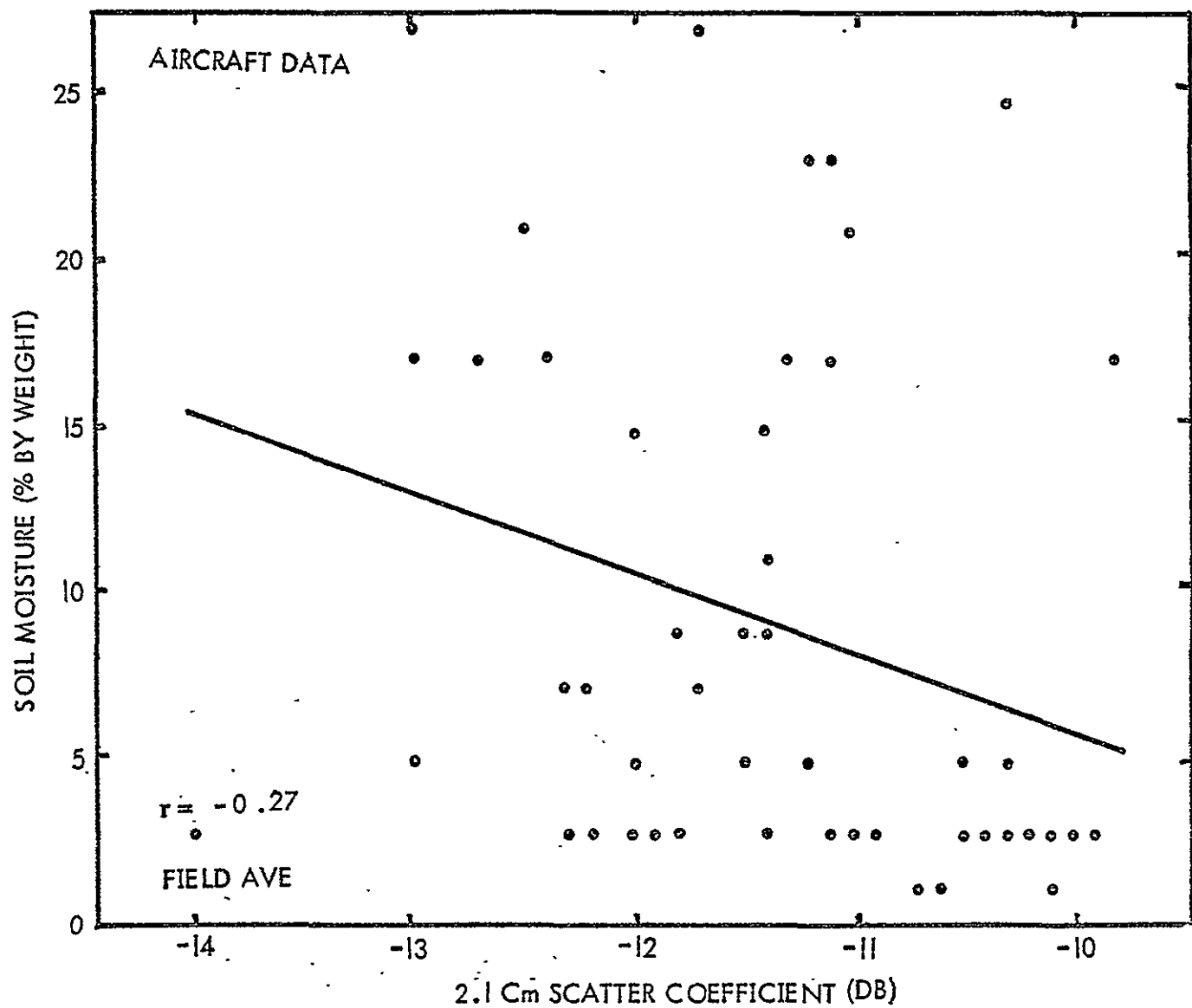
Figure 68 The relationship between soil moisture and the
2.1 cm scattering coefficient obtained by the
aircraft over bare cultivated fields.
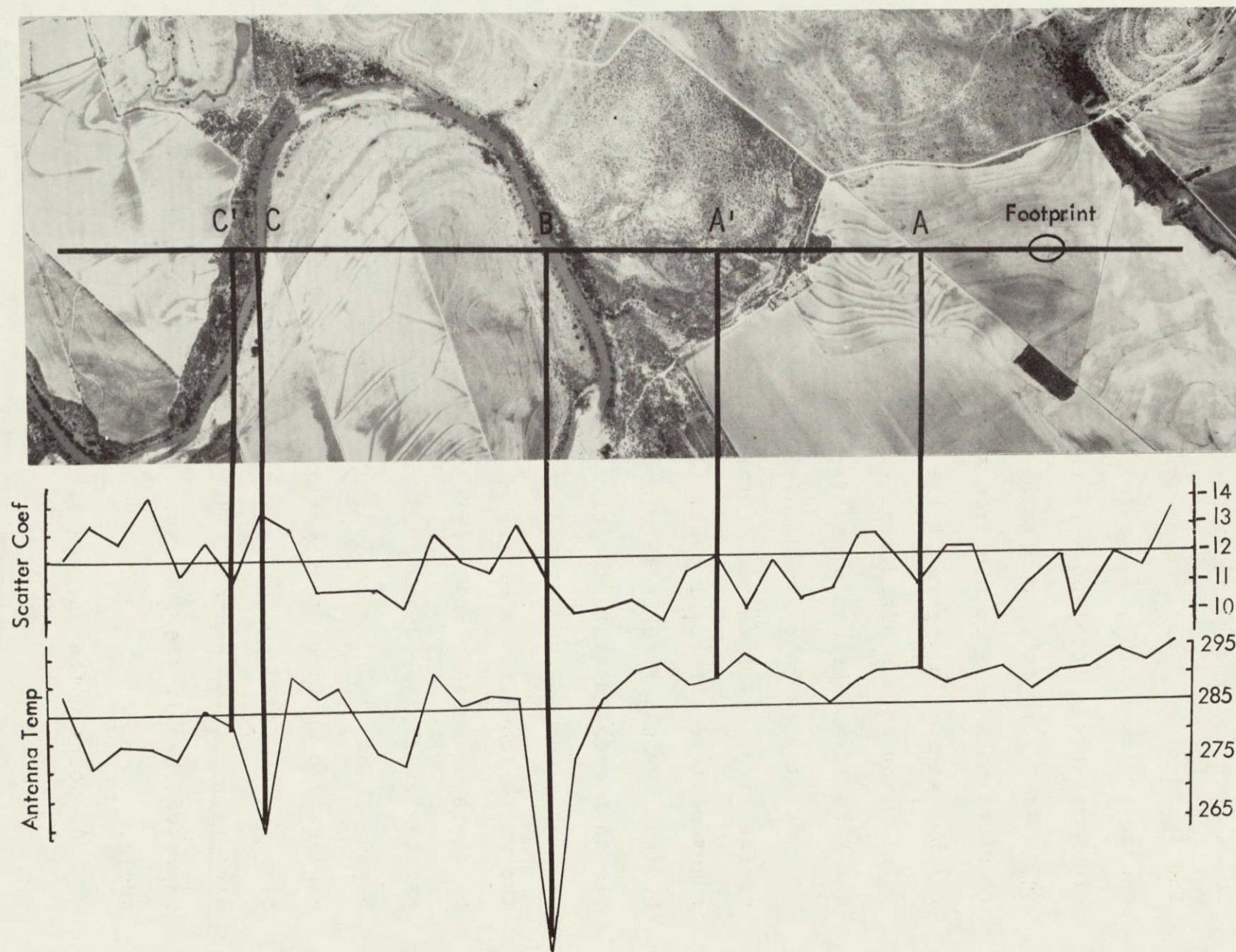
Figure 69 The variation of antenna temperature and scattering coefficient over particular terrain features.

the water but less return for the scatterometer. This would be expected as the water surface is smooth and nearly all of the incident energy is reflected away from the sensor. At the point immediately following the river, C', opposite reactions are again received. Perhaps the radiometer detected the warmer, dry trees along the bank while the scatterometer received much more return from the trunk, branches and leaves of the trees. In Figure 70 the values obtained at and around point D can be explained similarly. Fluctuations between C and D could not be explained from the photographs.

Point E is in a field which is located on the flood plain of the river. The center of the field looks wetter than the edges next to the river bank. A possible explanation would be that the water table is closer to the surface in the middle than right next to the river where the surface is slightly higher due to the natural levee. The radiometer detected the wetter conditions of the middle of the field. The scatterometer, however, only registered two points at the wettest portion of the field and then remained consistent until point F gave values that would indicate lower moisture. The only explanation would be that the orientation of the rows of the crop in the field, possibly wheat, is parallel to the look direction of the sensor. Therefore, less return would be expected than if the rows were perpendicular to the look angle.

At point G the antenna temperature drops, similar to
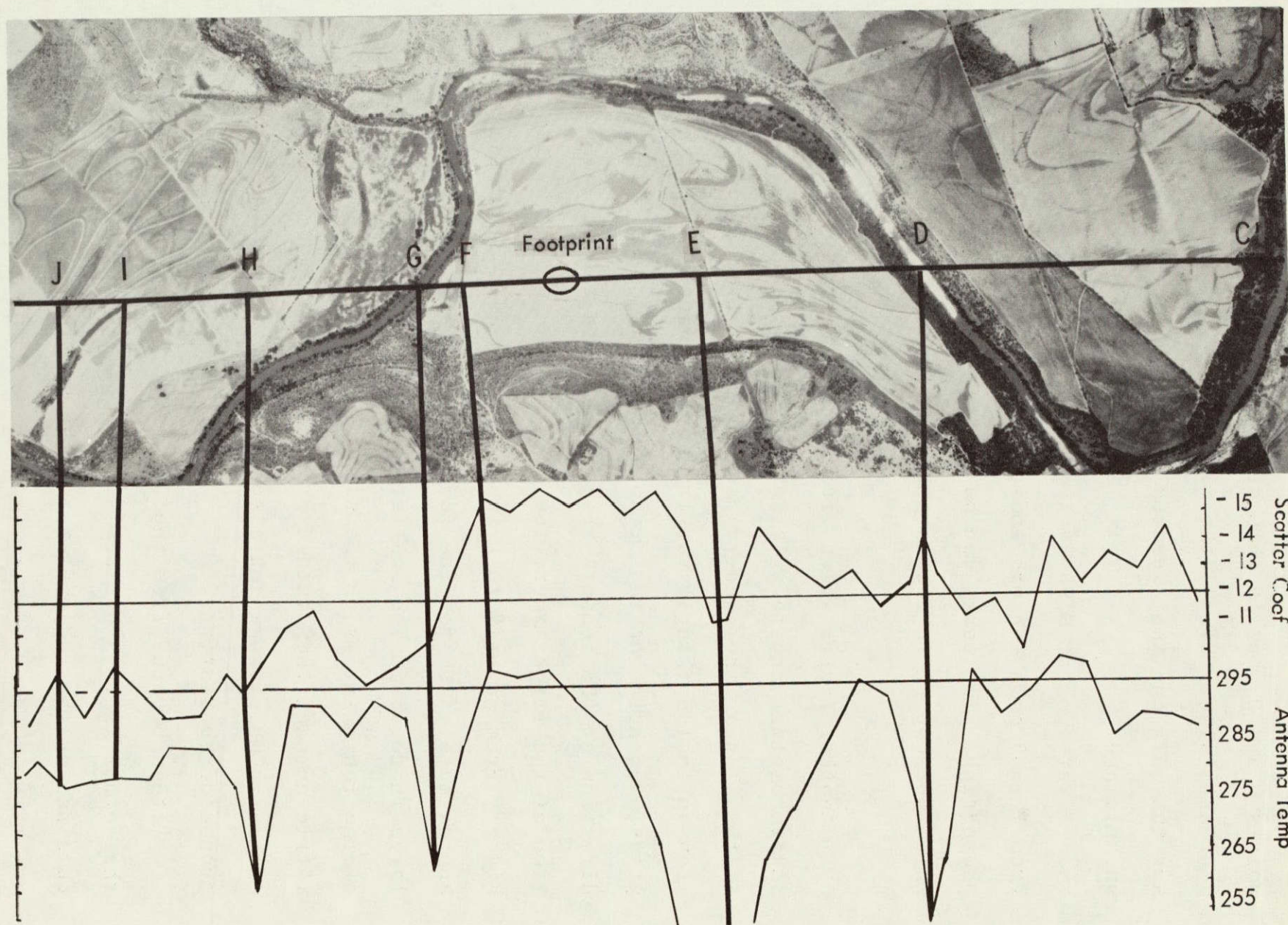
Figure 70   The variations of antenna temperature and scatter-
ing coefficient obtained by the aircraft over
rivers and other types of terrain.

points C and D, but in this case, the scatterometer reading decreases also. Of all the river crossings investigated this was the only one that reacted in this manner and it remains unexplained.

A wet spot at H was detected by the radiometer and from I to J both sensors indicated wet conditions as does the photograph. Two peaks can be seen in the scatterometer data which correspond to free standing water in the field.

Another factor which greatly affects the return of the scatterometer, and to a lesser extent the antenna temperature, is the slope of the land. A slope of thirty degrees could mean an incident angle varying between ninety and thirty degrees, depending on the orientation of the slope with the look direction of the sensor. Figure 71 is in the northwest portion of the flight where the high plains are cut by the Brazos River. From point K to L the slope has been determined to be approximately 10° for the four data points investigated. A large increase in the scatterometer return results once all of the footprint is on the slope. A decrease in the radiometric antenna temperature probably detects the slight increase in moisture which also is reflected in the slight increase of vegetation.

It is obvious from the analysis of the aircraft data that other factors besides soil moisture affect the values obtained by the radiometer and the scatterometer. These
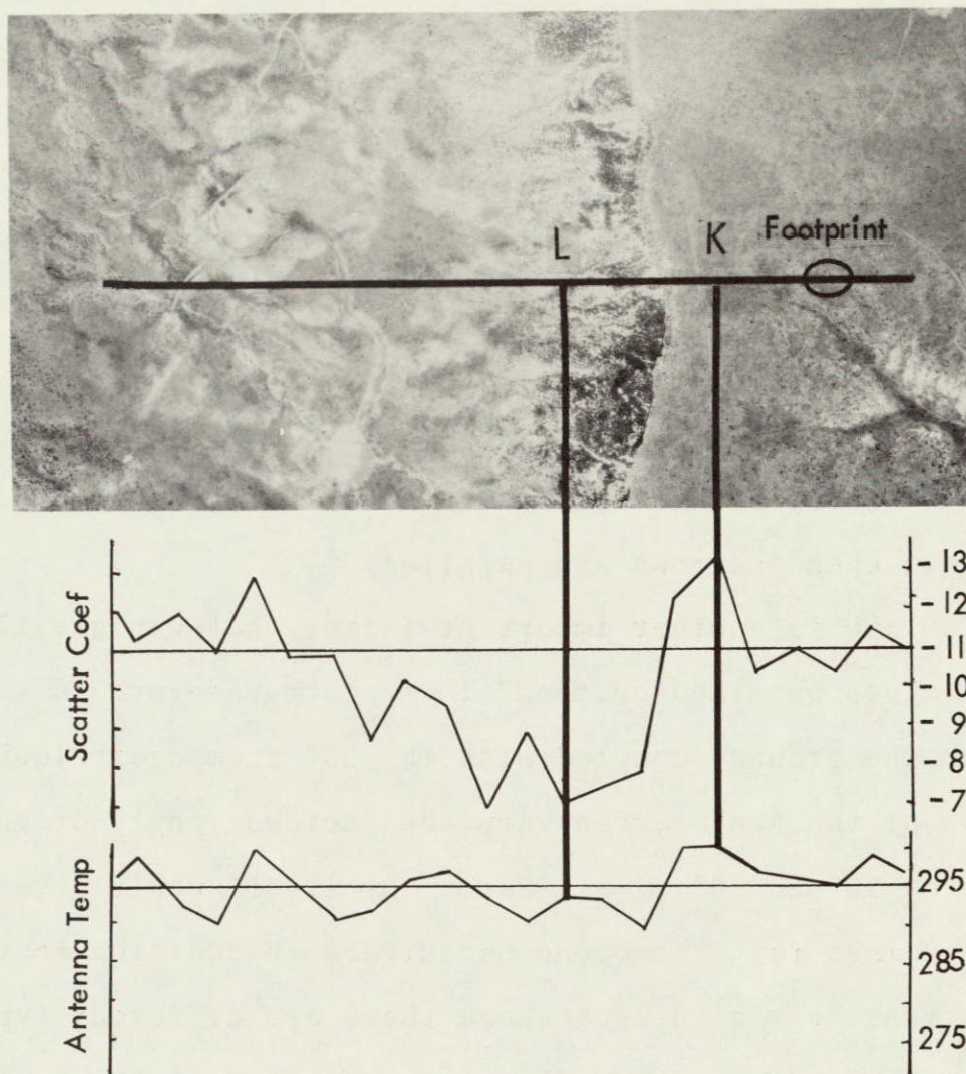
Figure 71   The variations of antenna temperature and scatter-
ing coefficient obtained by the aircraft with
changing topography.

fluctuations are of the magnitude to completely mask the effects of soil moisture. The scatterometer was more susceptible to this than the radiometer. These factors need to be investigated further in order to understand how much each contributes to the total response of the instrument.

Vegetation types and orientations are factors which can subtract or add large amounts to the values received by the scatterometer. Trees and large bushes tend to increase the amount of return in most cases. In addition, smaller vegetation, such as corn, milo or wheat has a larger return when the rows are perpendicular to the look direction of the sensor than when the rows are parallel.

Slope is another important factor that can greatly affect values obtained by the 2.1 cm scatterometer. A slope of 30° on the ground, coupled with the 30° from nadir look direction of the sensor, can vary the incident angle of the sensor from 90° to 30°. This factor by itself would give different readings for a homogeneous surface in addition to the complications from a surface where there are different types of vegetation and varying soil moisture content. Slope also affects the radiometer, but to a lesser degree.

Surface texture can be an important factor in returns from the scatterometer. It has been shown in the examples that water surfaces which were smooth along the rivers reflected the incident energy and therefore diminished the return. Other surface textures will also affect the amount of the return with very rough surfaces having more return than plowed

fields and those more than smooth disked fields. Also, soil texture should be considered, since clay soils will have different emissivities and reflectivities than sandy loam soils, for example.

The results of these qualitative investigations and the raw correlations show that better results were obtained with the radiometer than with the scatterometer. Also with the scatterometer correlations, the persistent negative slopes indicate that better understanding of the scattering process of soil moisture in the region of lower moisture is needed. The radiometric measurement of soil moisture is affected less by the various factors mentioned above. Since the aircraft microwave instrument senses such a small area on the surface, greater detailed ground truth would be necessary for an accurate assessment of the capabilities of this system.

Skin Depth Calculations

Since the thickness of soil providing the electromagnetic radiation to be measured by remote sensors varies with moisture content and incident angle, microwave response to water content in a constant thickness of the soil is subject to this influence. The return of an active radar and the image of a passive radiometer depend largely on the complex dielectric constant of the ground and incident angle. It is important, therefore, to consider the skin depth of electromagnetic radiation in the ground which can be computed from

a knowledge of the dielectric properties of soil and water.

The presence of water in most earth materials causes high attenuation of microwave radiation. Microwave radiation will, therefore, penetrate deeper in places where there is lower liquid water. The attenuation as a function of water content is valid for a large range of soil types but for relatively few of the other soil characteristics (Hoekstra and Delaney, 1974).

The exact nature of the influence of the water content of soil on the complex dielectric constant has not been well defined since slightly different results have been obtained by various investigators. Therefore, the several measurements of soil dielectric constant (Wiebe, 1971, Newton et.al, 1974 and Teschanskii, et. al, 1971) are shown in Figures 72 through 75. Each of these have been used to compute the skin depth. The skin depth of each soil sample from the Texas test site on June 5 was computed using the definition of skin depth (δ) as the following equation:

$$\int_{o}^{\delta} \alpha(z)dz = 1$$

where z is depth of soil and α is attenuation coefficient in nepers per meter.

The skin depths of the 66 moisture profiles for the June 5, 1973 pass over the Texas site were computed by considering cumulative attenuation of soil layers 0.1 cm thick for the Skylab S194 sensor, Figure 76. For the S193 sensor, the skin
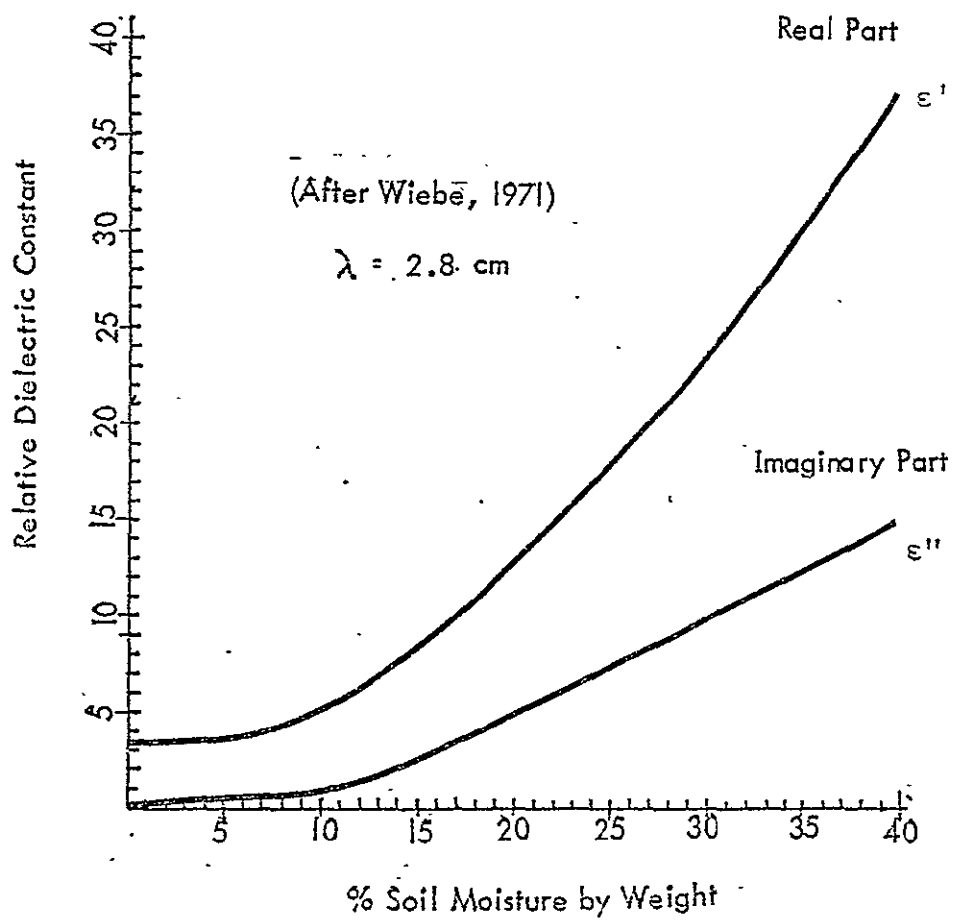
Figure 72   The relative dielectric constant as a function of
soil moisture (after Wiebe, 1971).
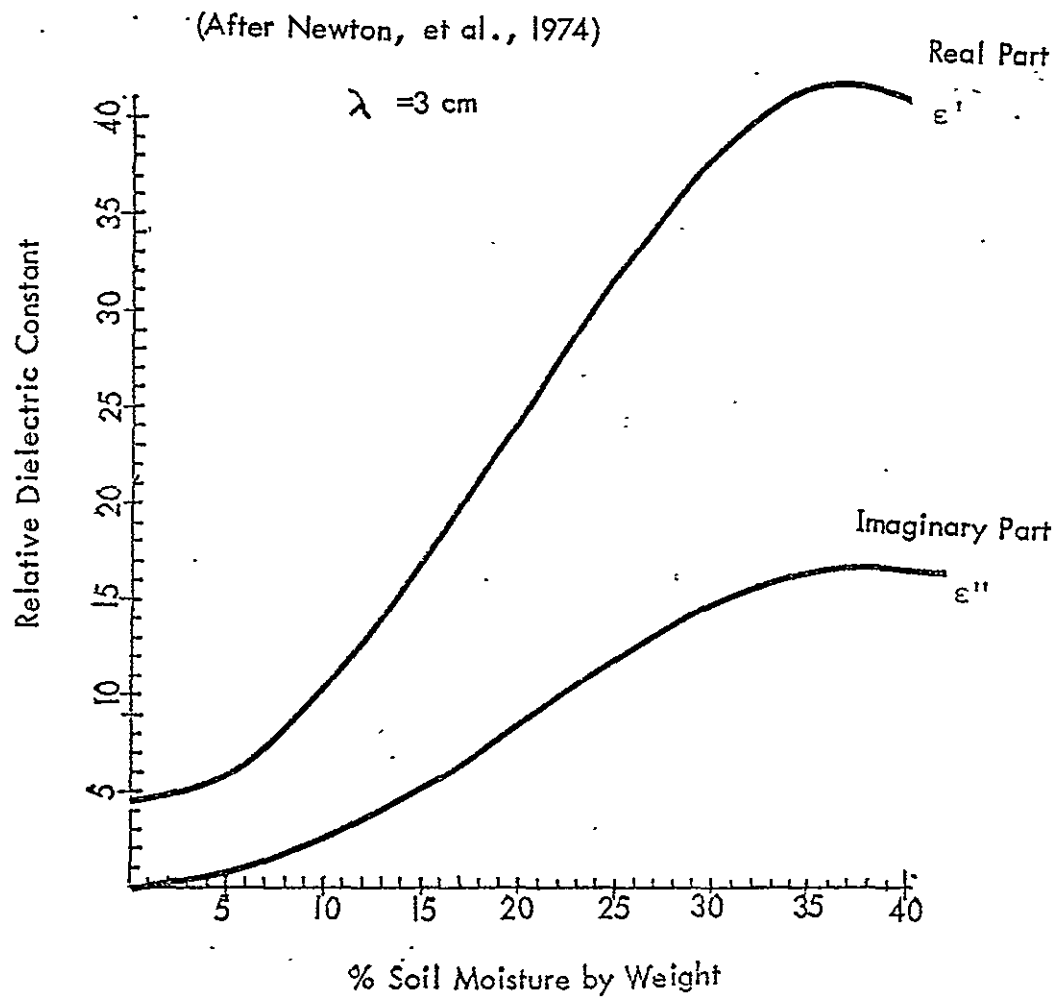
Figure 73   The relative dielectric constant as a function of
soil moisture (after Newton, et. al, 1974).
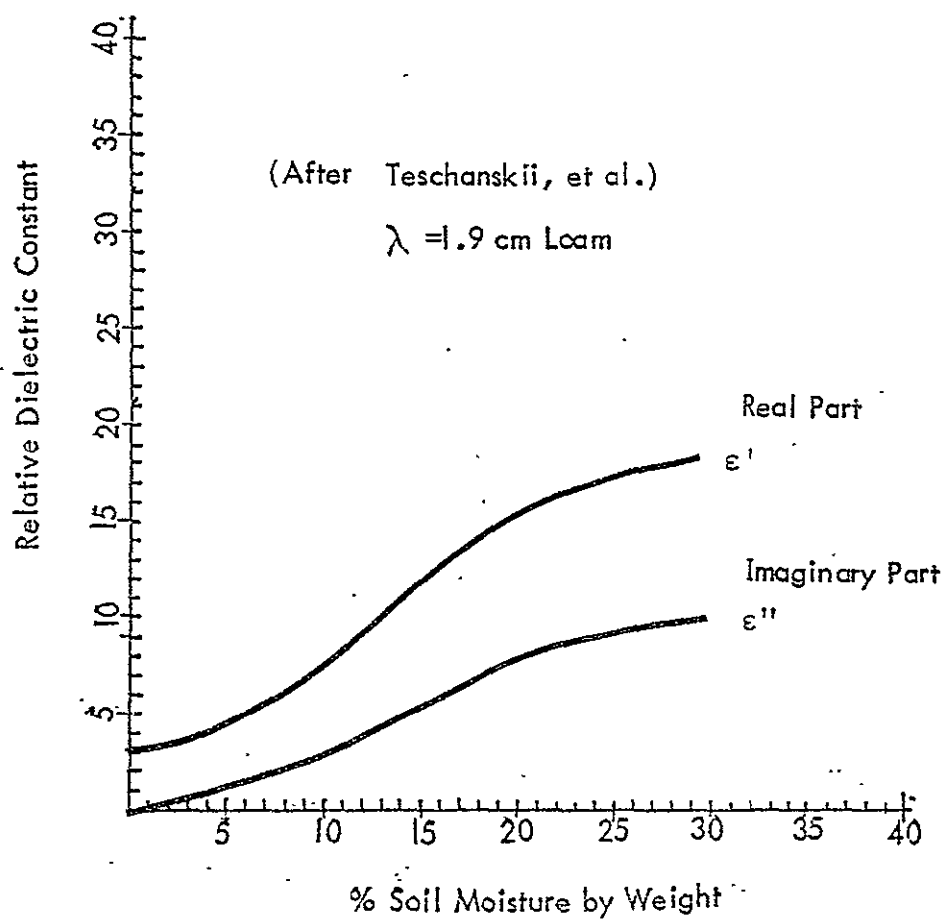
Figure 74   The relative dielectric constant as a function of
soil moisture for a wavelength of 1.9 cm (after
Teschanskii, et.al).
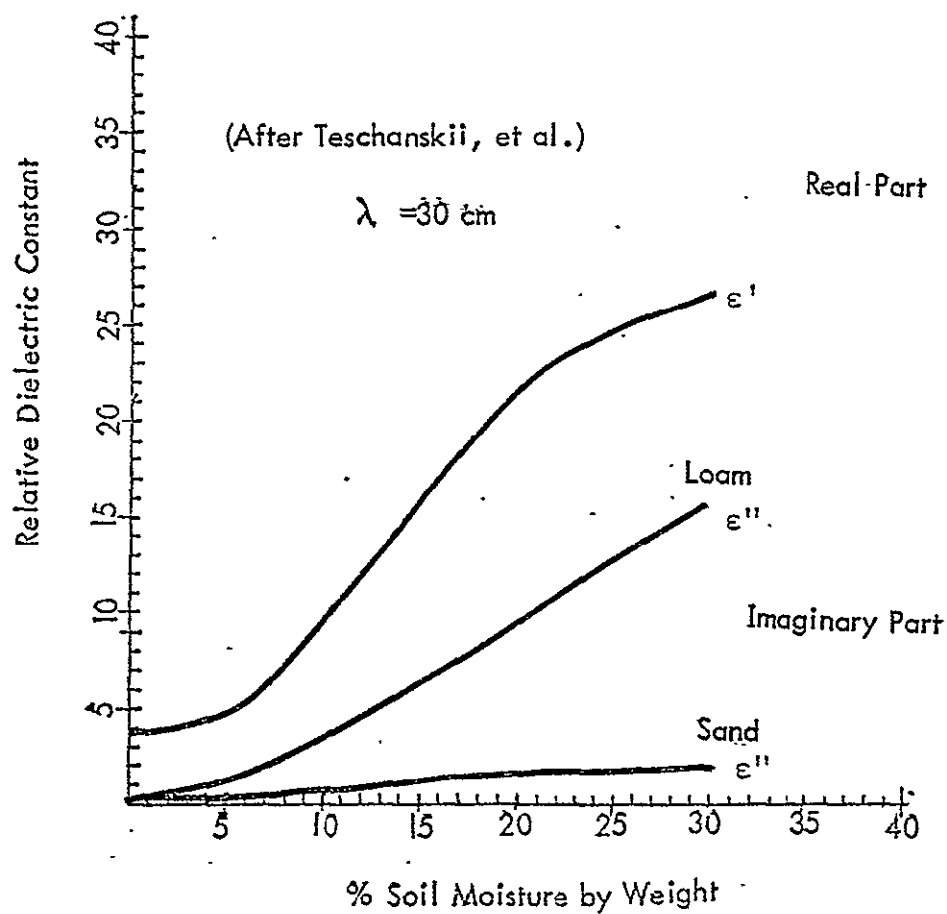
Figure 75   The relative dielectric constant as a function of
            soil moisture for a wavelength of 30 cm (after
            Teschanskii, et.al).
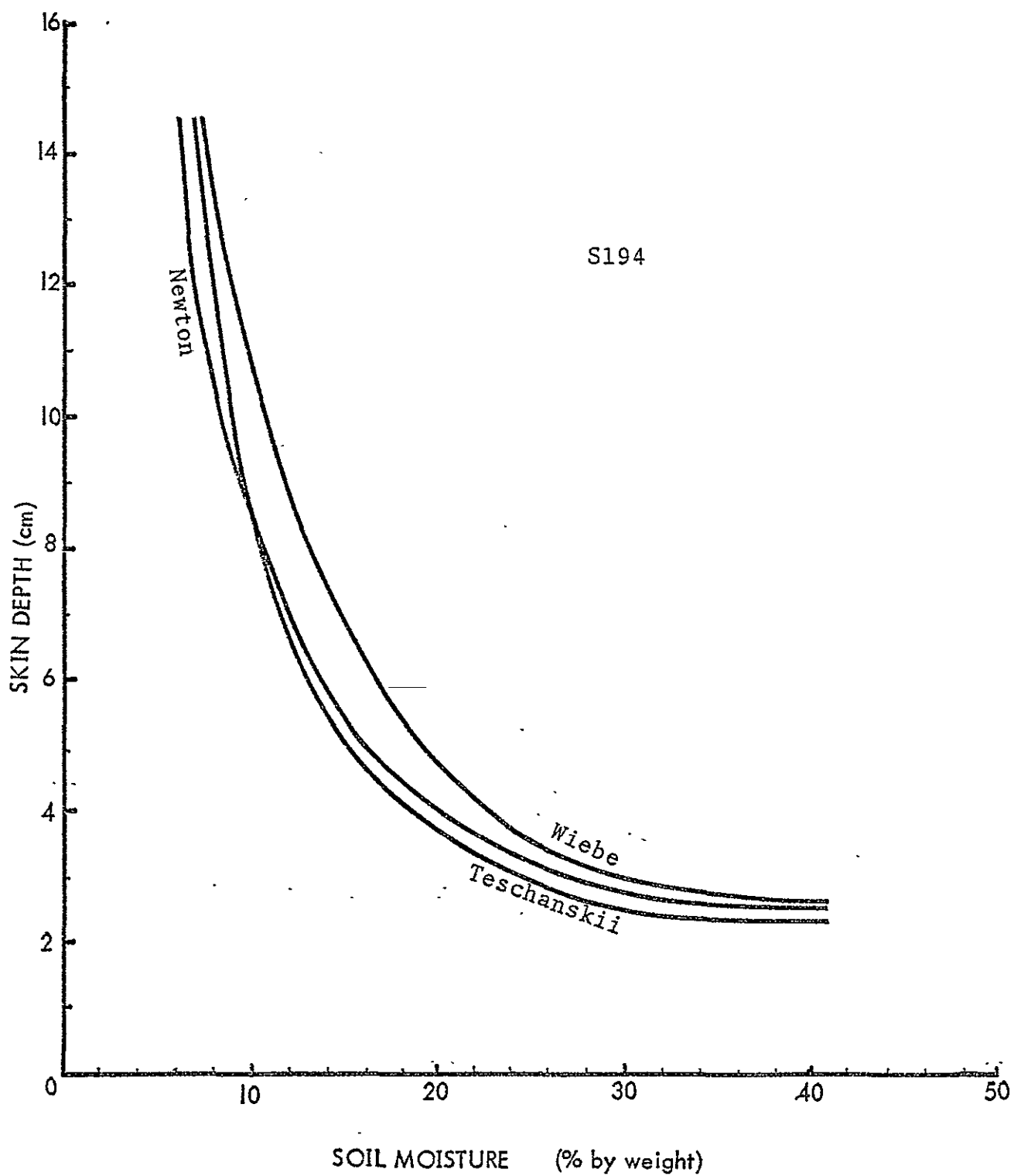
Figure 76   The calculated skin depth for various amounts of soil moisture for the S194 radiometer.

depth was calculated using Snell's law of refraction with the results shown in Figure 77. These calculations are helpful in understanding the relationship between the microwave sensors and the moisture content at various depths within the soil. For the S194 radiometer, the radiation emitted from the soil is coming primarily from the first 2.5 cm if the soil is wet and from the first 15 cm if the soil is very dry. Correlations between the S194 radiometric temperature and the experimentally determined soil moisture content of various layers have been best for the first 2.5 cm for four Skylab passes and for the first 5 cm for the fifth pass.

As expected, the skin depth of the shorter wavelength S193 instrument is not as great as for the S194 for the same moisture content as shown in Figures 76 and 77. Radiation is emitted from the first 2.5 cm of soil for all moisture contents except very dry soils. Radiation from wet soils comes from an even shallower layer. These figures indicate that the experimental data from Skylab might have been expected to correlate better with the 0 to 15 cm average soil moisture for some of the drier dates for the Texas test site. However, the lower sensitivity of the microwave sensors to moisture content below about 5% probably precludes obtaining this type of result from experimental data.

Figure 77   The claculated skin depth for various amounts of
soil moisture for the S193 radiometer.

Comparison of the Skylab Microwave Sensors

An accurate comparison of the various microwave sensors
on Skylab is complicated by the different resolutions of the
sensors. The analysis of the aircraft data has indicated that
the soil moisture sampling network was much too coarse for
these data. The S193 analysis may also be affected by this
same factor. Each S193 footprint had from one to three soil
sampling sites within it, while the S194 footprints had as
many as thirty five different sample sites in one footprint.
Although this limitation of the data was minimized by using
computer calculated surfaces of the geographical distribution
of soil moisture, other means of comparison seem warranted.

The June 5, 1973 data across the Texas test site serve
as a good basis for comparison since both S193 and S194 data
were obtained with fairly good variations in soil moisture
content across the site. These variations along with the S194
antenna temperature variations were illustrated in Figure 59
which showed the antenna temperature decreasing in response
to soil moisture increases across the test site. Figure 78
compares the variation in antenna temperature of the S194 and
S193 radiometers for the same data set. The S193 radiometer
also decreased somewhat as the moisture increased across the
test site, but not as much as the S194.

In an effort to make quantitative comparisons between
the two passive radiometers and the active scatterometer, the
data for the various footprints of the S193 sensor were
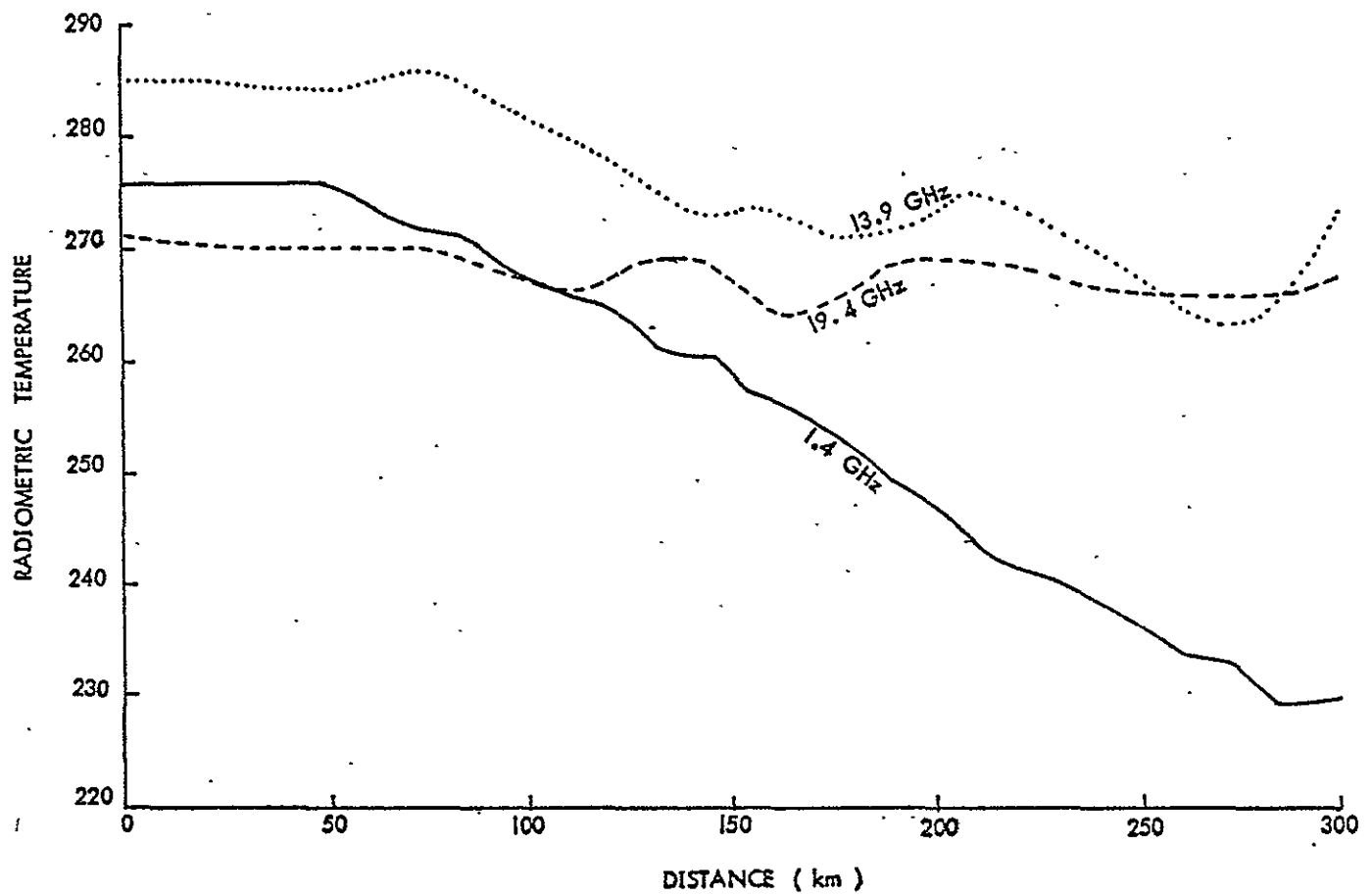
Figure 78 Variations of the S193 and S194 radiometric temp-
erature across the Texas test site of June 5, 1973.

averaged for the same large area as for the S194 sensor and then correlated with the average soil moisture throughout this area. Figure 79 shows the results of this analysis. The S193 scatterometer gave the poorest relationship with no uniform variation with moisture content of the soil and a correlation coefficient of 0.63. Both the S193 and S194 passive radiometers show a decrease in antenna temperature with increasing soil moisture content with correlation coefficients of -0.988 for the S193 and -0.996 for the S194.

It can be concluded from these data that passive radiometers have more potential for accurate measurements of soil moisture than the active systems. While both the 2.1 and 21 centimeter passive radiometers show good response to soil moisture, the longer wavelength seems to have the greater potential because of less influence from clouds and vegetation. Also from Figure 79 the longer wavelength radiometer has a perfect straight line relationship to soil moisture for moisture contents greater than 4% and has a range in antenna temperature of 47°K compared to a range of only 16°K for the S193. Therefore, noise in the system would be a much smaller problem for the longer wavelength radiometer.

The conclusions regarding the scatterometer must be more equivocal. The correlation with soil moisture, as indicated above, was less than for the radiometers. However, observations using ground-based sensors have been made (Ulaby, 1974) since the S193 operational parameters were selected and these
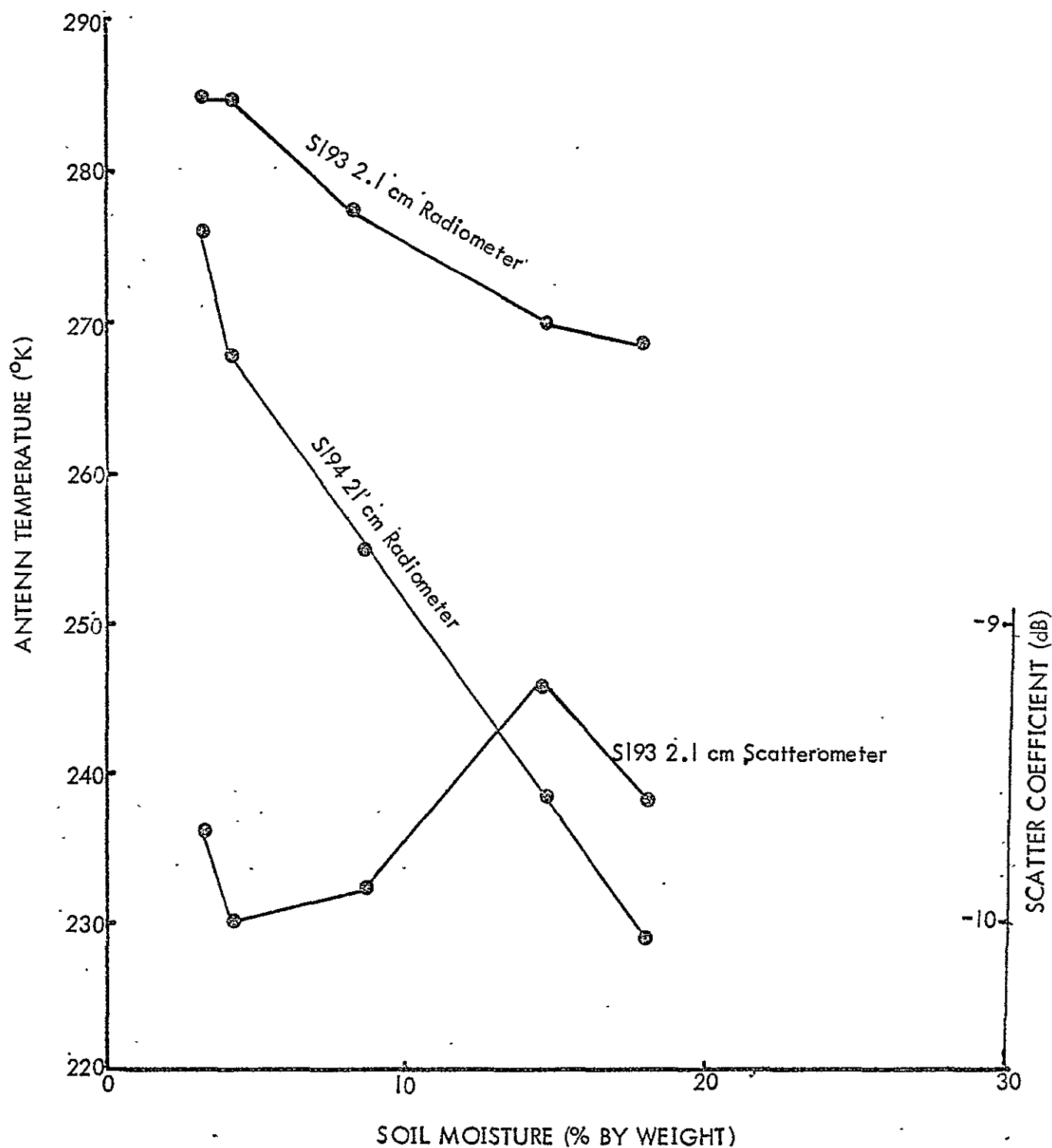
Figure 79 A comparison of the response of the two radiometers and the scatterometer to the soil moisture content when averaged for the same size resolution cell.

C.3

indicate that an angle of the order of 15° should have been much more sensitive to soil moisture than the 30+° angles used in the Skylab S193 experiment. This is particularly important when vegetation is fairly dense over the soil whose moisture is to be determined. Consequently, the moderate correlations observed with S193 are encouraging and consistent with ground-based measurements; and this leads to the conclusion that a scatterometer operating at a steeper incidence angle should give results much more like those of the radiometer.

Accuracy of Remotely Sensed Soil Moisture Data

The standard error of soil moisture estimated from radiometric data was computed as a measure of the expected accuracy of remotely sensed data. Table XI gives the standard error for individual passes where S194, S193 or aircraft radiometric data were available as well as the composite of five passes combined into one data set for the S194 sensor. The standard error was least (only 0.83% moisture) for the S194 data obtained on June 5, 1973. Thus, about two-thirds of new estimates of soil moisture based on this pass could be expected to fall within a range of only ±0.83% soil moisture. This would provide very accurate measurements of soil moisture from passive radiometers. However, when the S194 data are combined for various Skylab passes over different terrain the standard error increases to 3.05% soil moisture. This is still an acceptable accuracy considering all the advantages of a remote sensing system.

192

TABLE XI

The Standard Error of Estimate, Correlation Coefficient
and other Data for the Various Microwave Sensors.

Sensor	Regression equation	Correlation Coefficient	Standard Error	Range of Soil Moisture	Pass and Site
S194 RAD	SM=253.03-1.4898 AT&0 .0021AT^2	-0.96	3.05	1-34	Composite
S194 RAD	SM=124.36-0.4478 AT	-0.94	3.09	1-34	Composite
S194 RAD	SM=82.70-0.2930 AT	-0.99	0.83	2-19	5 Texas
S194 RAD	SM=188.75-0.6992 AT	-0.95	1.59	10-25	10 Kansas
S194 RAD	SM=93.50-0.3339 AT	-0.92	0.98	2-13	16 Texas
S194 RAD	SM=127.23-0.4571 AT	-0.97	0.88	3-14	38 Texas
S194 RAD	SM=409.49-1.7213 AT	-0.94	2.05	15-34	38 Kansas
S193 RAD	SM=185.63-0.6379	-0.91	2.42	1-23	5 Texas
S193 SCAT	SM=43.98-3.7182 SC	+0.53	4.75	1-23	5 Texas
S193 RAD	SM=64.47-0.2153 AT	-0.28	1.64	1-8	16 Texas
S193 SCAT	SM=4.6588+0.1290 SC	0.04	1.78	1-8	16 Texas
S193 RAD	SM=203.86-0.6994 AT	-0.69	2.86	3-17	8 Texas
S193 SCAT	SM=32.41+2.2829 SC	0.72	2.62	3-17	38 Texas
S193 RAD	SM=275.87-0.9316 AT	0.34	6.66	15-40	38 Kansas
S193 SCAT	SM=41.91 + 1.2453 SC	0.14	7.11	15-40	38 Kansas
Aircraft RAD	SM=241.79-0.7920 AT	-0.69	5.8	1-27	Texas

Chapter VII

ANALYSIS AND RESULTS OF THE
SNOW EXPERIMENT

Snow depth, water equivalent and water equivalent/snow depth were the principal parameters examined in this study. Quantitative areal mapping of these parameters was generated via the least squares surface contour mapping technique used in the soil moisture experiment.

Two of the three data sets for the snow experiment have been analyzed. These were the Skylab passes on January 11 and January 14, 1974. No analysis of the January 24 test site in South Dakota-Iowa was conducted. Of the 65 stations utilized in the test site area, 23 of them revealed snow depths from zero to one inch, 25 more from two to three inches. Thus, nearly 75% of the stations revealed snow depths three inches or less. Due to the possible error in measuring snow depths of these small magnitudes, the ground truth data is very questionable. Also, this was the 10th day of a prolonged melt period and any water equivalent data would be quite meaningless. For these reasons the analysis was not on the S194 data for the 24th of January. Therefore, the results of the analysis of the January 11 and 14 data follow.

Kansas: January 11, 1974 - Ground Truth

As previously mentioned, the January 11 test site area
extended from the Texas Panhandle into southern Iowa. The
Kansas and extreme northwest Missouri region was extensively
surveyed on January 11 through the efforts of the National
Weather Service. At each of the 24 station sites in Kansas
and four in Missouri, the snow depth and corresponding water
equivalent was measured. The ground truth for the remainder
of the test site area was generated from Climatological Data,
but only snow depth data was adequately available. In addi-
tion, S190B imagery was available for a portion of the test
site area; this included the Kansas and extreme northwest
Missouri region. The southern portion of the test area in
thr Texas Panhandle and Oklahoma as well as the northern por-
tion in Iowa were not included in the imagery. Inasmuch as
the most intensive data coverage coincided with the S190B
coverage, it was deemed advisable to focus the brunt of anal-
ysis upon the Kansas region of the test site area.

The meteorological weather factors operative during
the first 11 days of January 1974 resulted in cP/cA air
mass movement into the Central United States (for more

detail, see Chapter 1). Thus, mean temperatures in the Dansas test site area ranged from only 2-7°F., north to south, on January 11. Maximum temperatures there did not rise above 15°F. Snow depths generally ranged from 4-10 inches throughout Kansas.

Colorado-Nebraska: Pass 83, January 14,1974-Ground Truth

The January 14 test site area extended from Denver, Colorado to Mankato, Minnesota. Snow depth data collected from Climatological Data revealed amounts ranging from a trace at Colorado Springs, Colorado, to eleven inches at Cambridge and Culbertson, Nebraska. Thirty one weather ob-servations were employed to develop the snow contour field. Water equivalent data was extracted from contour maps ob-tained from the River Forecast Center Office in Kansas City, Missouri. In addition, S190A and B coverage was available for the entire test site area.

Chinook-type adiabatic warming on January 14 ushered in a pronounced warming trend throughout the remainder of Janu-ary. The western portion of the January 14 test site area revealed meximum temperature of 58°F. at Denver, Colorado, while Nebraska City, Nebraska, reported an overnight low of 8°F. Due to the variation in temperature over the January 14 test site area, the ground truth data was divided into two sets: subfreezing and superfreezing. Snow depths generally ranged 4-9 inches along the track, increasing northeastward.

196

Background for Radiometric Response to Snow

One of the principal objectives of the SL-4 mission centered upon the various sensors' potential capabilities in quantifying the moisture parameters in a snow field. As previously demonstrated by the soil moisture experiment, the 21 cm passive radiometer exhibits high correlations between percentage of soil moisture versus antenna temperature that is responsive to the emissivity. This dependence of emissivity upon soil moisture content stems from the role the dielectric constants of water, soil and air play.

Since emissivity = 1 - reflectivity (neglecting transmissivity), the more reflective mediums will exhibit the lower emissivities. The reflectivity, however, is directly dependent upon the dielectric constant. The contrast between the high dielectric constant of water as compared to air and soil is such that the presence of water is the principal factor which regulates changes in microwave response.

Yet Edgerton et.al., (1971) noted that "the relationship between microwave brightness temperature and snow water content bears no resemblence to that observed in soils". Whereas an increase in soil moisture results in a decrease in radiometric temperature for a soil medium they discovered that the microwave brightness temperatures rise with increasing water content of a snow medium. Their Dillon reservoir snow study also revealed that microwave brightness temperatures

remained unresponsive when moisture values (free water con-
tent) exceeded 2.5% by volume. In addition, Edgerton et al.,
(1971) indicated that the effective microwave emissivity
decreases with increasing snow depth under the conditions of
dry snow over frozen soil. These effects can be explained in
terms of attenuation in the snow and the small value of the
reflection coefficient at the snow-air interface.

It should be pointed out that air temperatures had aver-
aged well below freezing in Kansas since January 1. A thin
blanket of snow had also covered the state since that time
and one to two inches of fresh snow had fallen in the test
site area on January 9-10. Under the preceding and prevail-
ing meteorological conditions described, the ground possibly
was frozen and the snow definitely was quite dry. Thus, the
areal situation is similar to the two Edgerton studies.

S194 Radiometer Response - January 11, 1974

With regard to the above, the analysis of the S194 data
for the test area was conducted. Beginning in the southern-
most portion of central Kansas, antenna temperature measured
approximately 242 degrees Kelvin and declined to 223.6 in the
vicinity of Topeka, Kansas (Figure 80). A rapid reversal in
microwave response occurred there and emissivity increased
for the remaining portion of the track, ultimately reaching
the levels observed in the earliest portion of the run.

198
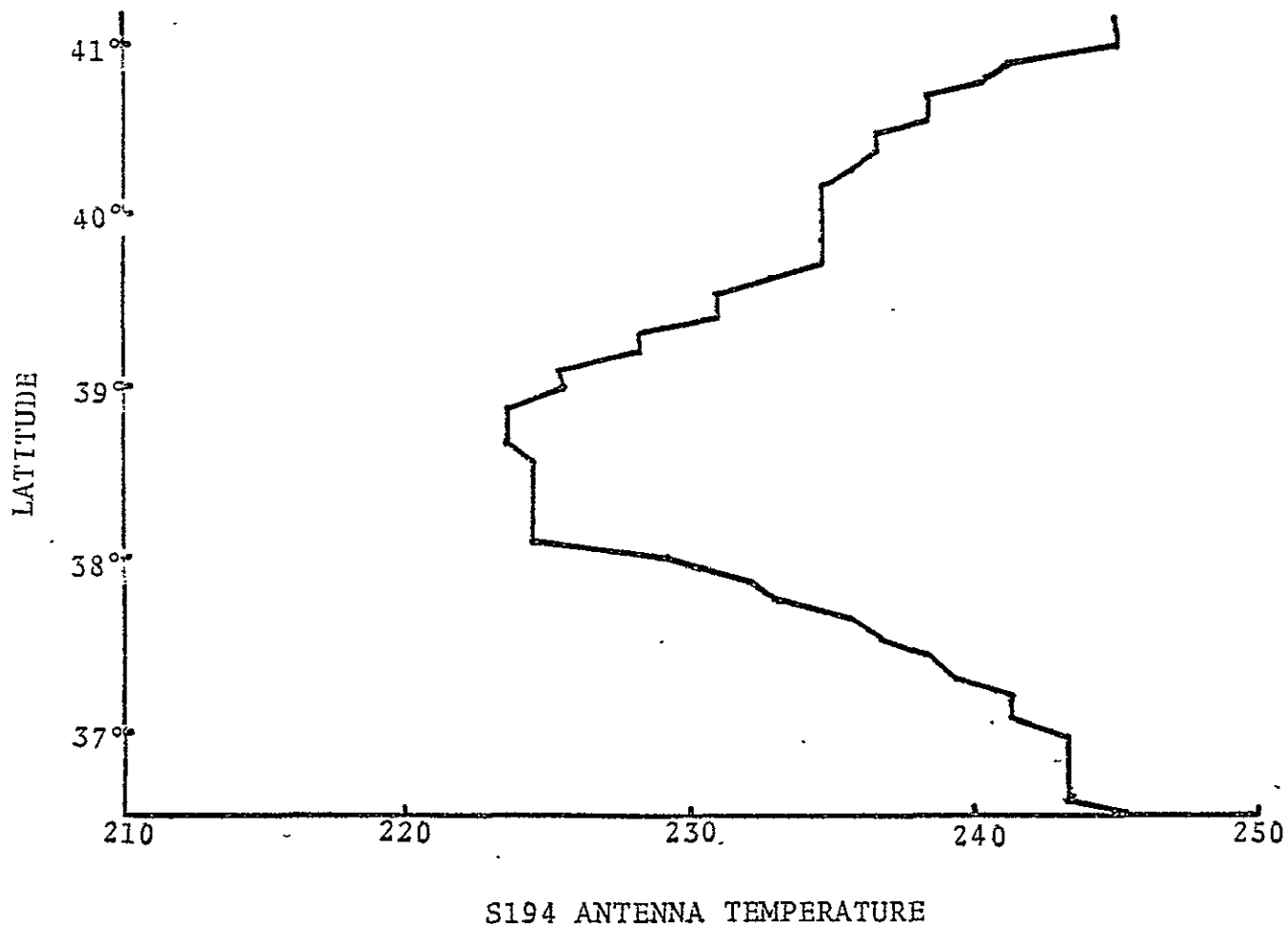
Figure 80 Variation of S194 brightness temperatures across the
snow test site in Kansas on January 11, 1974

A distinctly different type of ground cover in the Topeka area and northeastward is revealed by the S190B coverage. although Climatological Data indicates as much as 12 inches of snow existed in parts of Missouri and Iowa, significant areas of bare ground are apparent. Therefore, this area was not included in correlation analyses. Since the dielectric constant of ice is very low compared to that of water, frozen ground would yield higher microwave emissivities when compared to unfrozen ground. The increase in brightness temmperature from Topeka northeastward most likely was coused by the contribution of the frozen exposed ground to the L-band radiometer.

Utilizing the data obtained by the NWS survey in Kansas, contour maps of snow depth, water equivalent, and water equivalent/snow depth (WE/SD) were generated by the computer. Thirty S194 overlapping footprints were capable of resting inside the contoured surfaces. Overlap was employed, because only two completely independent footprints existed within the NWS survey area.

The correlation analysis utilizing the overlapping footprints must be viewed with caution because of the dependency that exists between the data points. However, even if they do not represent the true independent statistical values, they are indicative of trends in the data. Figures 81,82, and 83 do indicate a trend between the variables snow depth, water equivalent, and WE/SD and the S194 radiometric temperatures.

Figure 81   S194 brightness temperature as a function of snow depth on January 11, 1974.
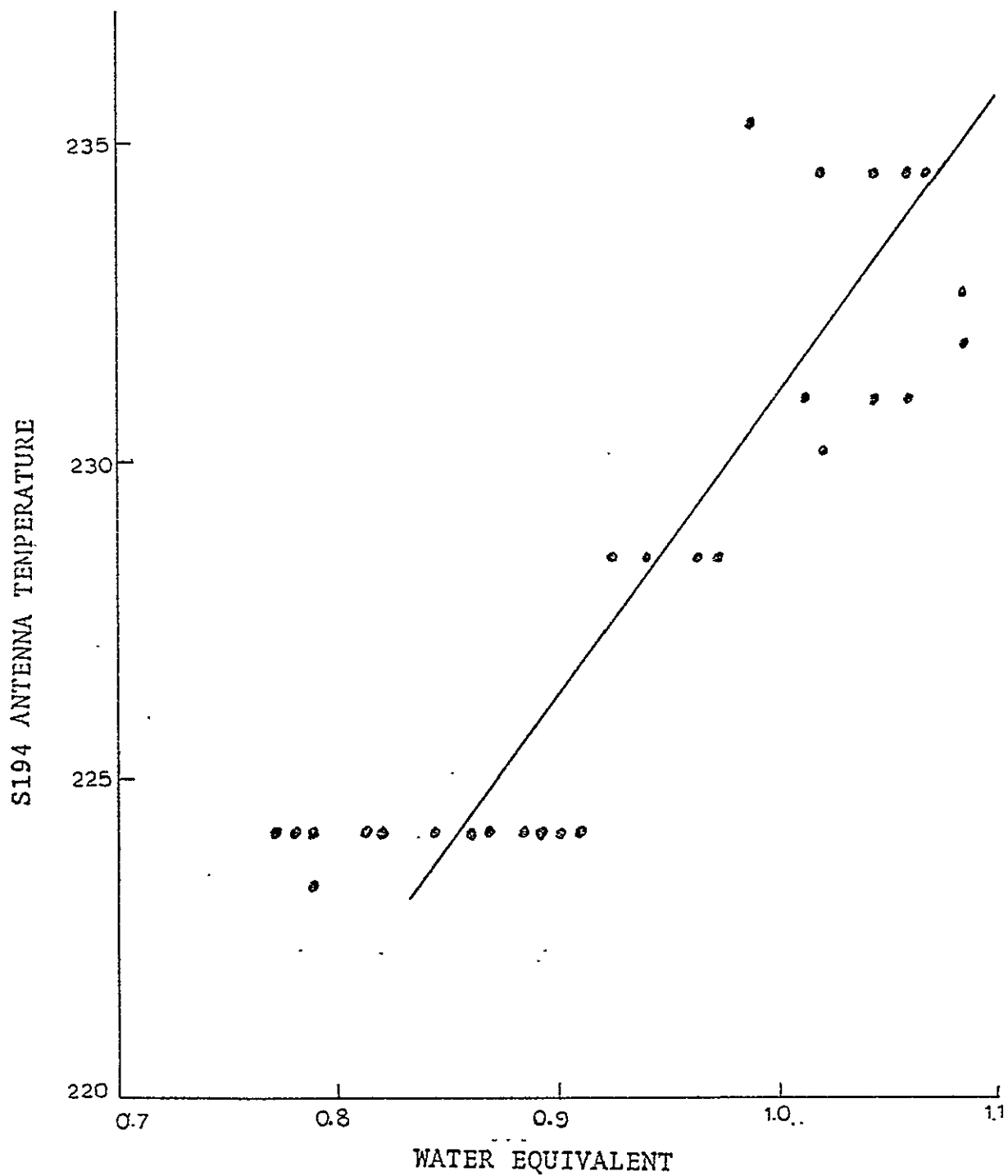
Figure 82   S194 brightness temperature as a function of
water equivalent on January 11, 1974.

Figure 83   S194 brightness temperature as a function of
water equivalent/snow depth on January 11, 1974.

In determining these trends, three important variables were not considered which potentially could alter the microwave response. These factors, subsequently analyzed, included ground temperature, snow surface temperature and soil moisture. Since measurements of these parameters were not recorded in the test site area at overpass time, indirect techniques were employed to estimate them.

Due to the season of the year, any possible variability in soil moisture in Kansas was entirely attributed to all potential contributions of melt water from the overlying snow cover. This index of melt water is termed the Antecedent Possible-melt Index (APMI) and is a modified version of the Antecedent Precipitation Index commonly utilized in various hydrologic investigations. The APMI is given by the following equation:

$$APMI = \overline{MP} \cdot k^t$$

where $\overline{MP}$ = melt water, k = recession constant and t = antecedent days before January 11. Any decrease in the water equivalent of the snow was attributed to melt and the melt was assumed to totally infiltrate the soil. Thus, an attempt was conducted to account for the maximum possible infiltration of melt water into the soil.

Water equivalent values were obtained from eight stations in Kansas, in addition to 39 others in Colorado, Nebraska, Iowa, South Dakota and Minnesota. The APMI values calculated for the eight Kansas stations, less one, equaled zero. This truly reflects the sub-freezing conditions (lack of melt) of

this period from January 1 to 11.

Another potential source of error centered upon the variation in snow surface temperature in the test site. Higher surface temperatures would result in greater emissivity. Temperature data was not available for the entire site at the overpass time. However, an analysis of the diurnal temperature range at Lawrence, Kansas on January 11 revealed the following:

maximum temperature = 11 degrees F @ 2:30 P.M.

minimum temperature = -3 degrees F @ 9:00 A.M.

temperature at overpass time = 3 degrees F @ 12:35 P.M.

mean temperature on 1/11/74 = 4 degrees F.

Assuming the diurnal variation of temperature in eastern and southern Kansas was similar to the Lawrence situation, the mean temperature appeared to be an excellent parameter to estimate snow surface temperature. The following equation was utilized to adjust the antenna temperature to reflect this variation in mean temperature:

Taw = Tac + 0.993 E(300-Tg)

Where: Taw = adjusted weighted antenna temperature

Tac = actual antenna temperature

E = emissivity of Snow

Tg = mean temperature of the air

The emissivity utilized was 0.6 which is similar of slightly lower than other studies would indicate. Figures 84-86 indicate the adjusted temperature variation along the test site track compared to snow depth, water equivalent, and WE/SD.

The correction for ground temperature proved to be the
most difficult. The only available source for ground temper-
atures in January was Climatological Data. A dearth of sta-
tions existed in Kansas, but Nebraska kept ground temperatures
for 5 stations. Under the snow cover present, the recorded
ground temperature measurements revealed no direct relation-
ship to the prevailing air temperature. The lack of suffi-
cient time precluded the possibility of estimating ground
temperature through the use of a model. Its contribution
to the microwave emission received by the L-Radiometer could,
therefore, not be estimated.
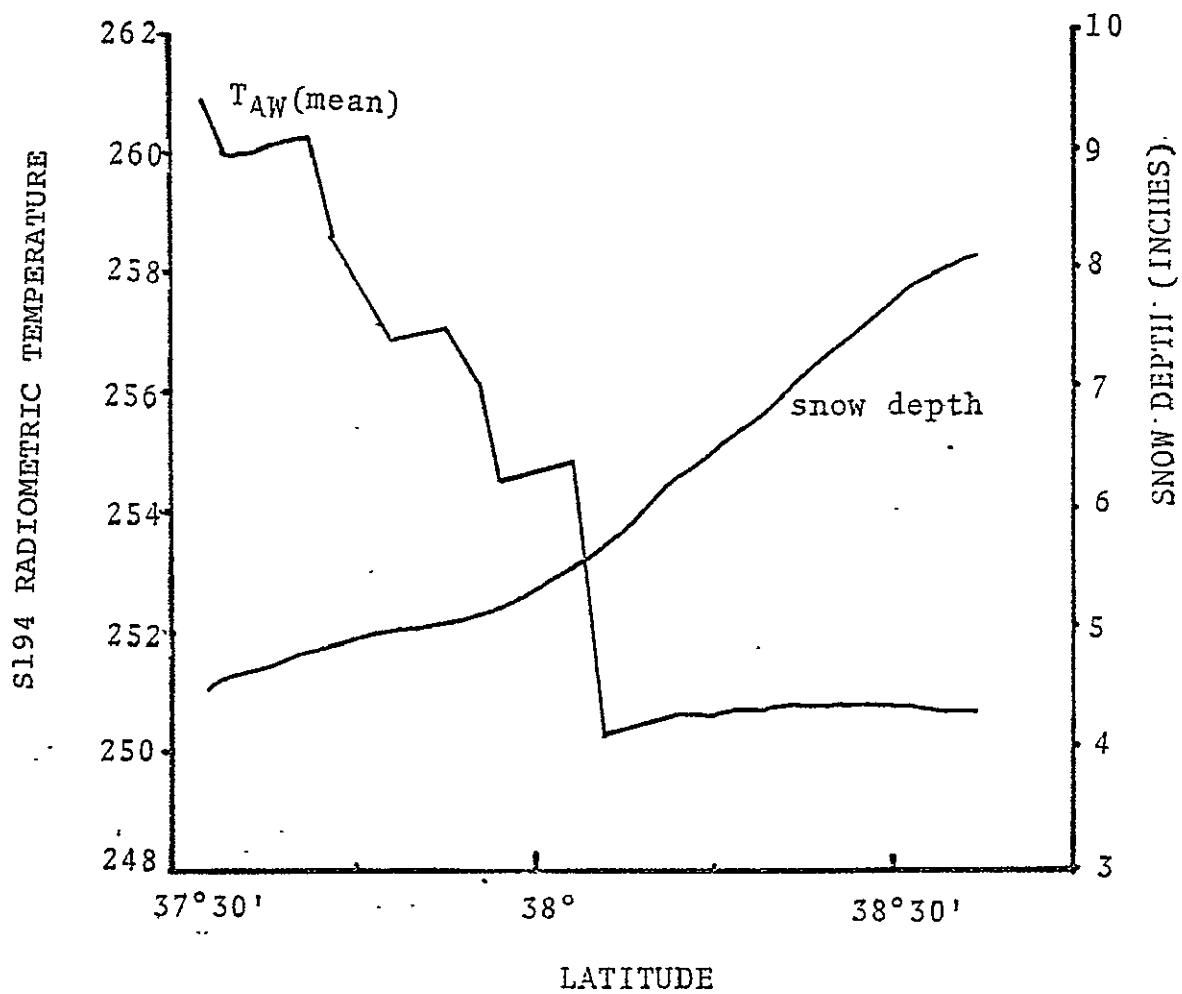
Figure 84   S194 antenna temperature and snow depth variations across the test area January 11, 1974.
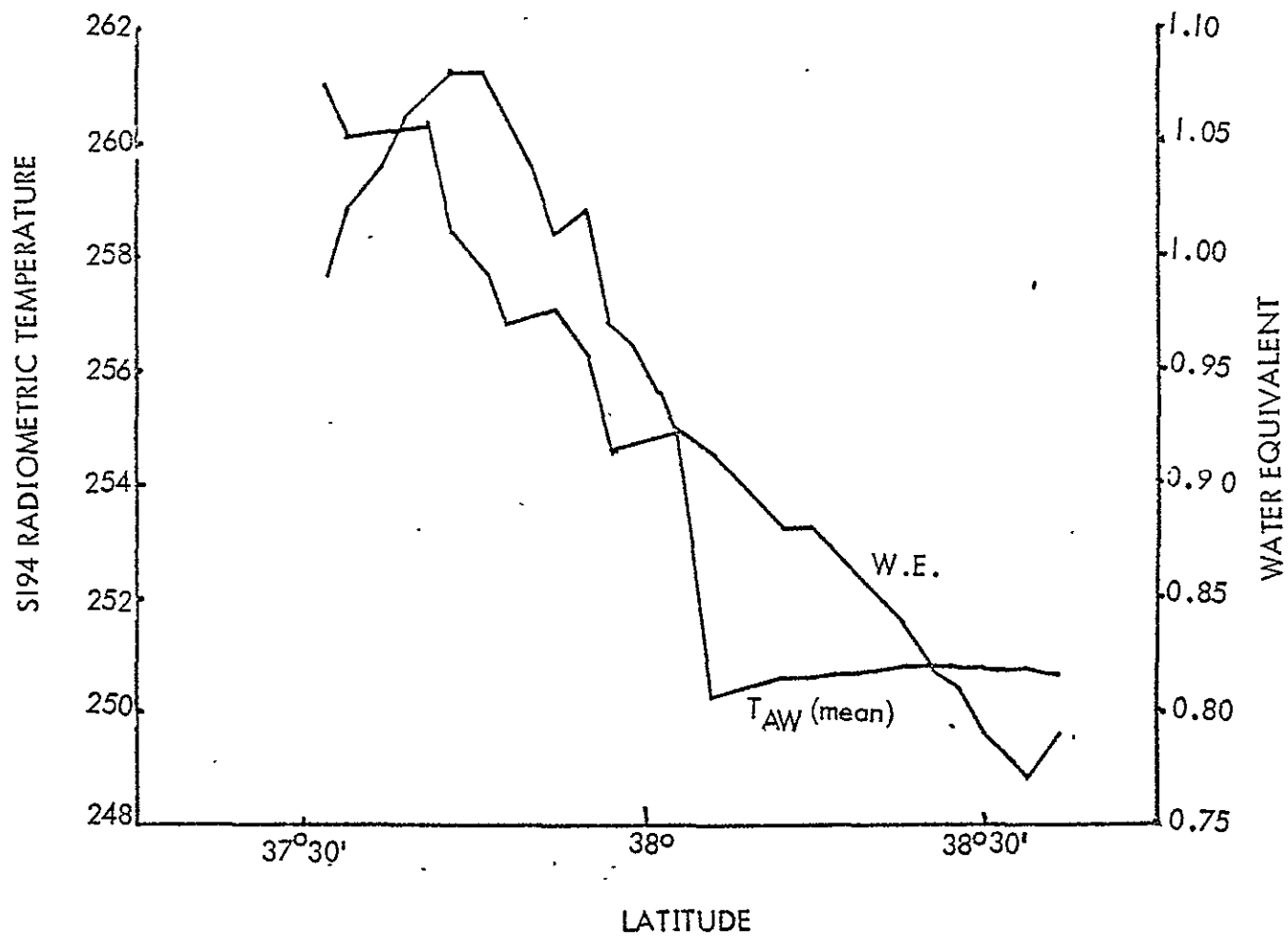
Figure 85   S194 antenna temperature and water equivalent variations across the test area January 11, 1974.
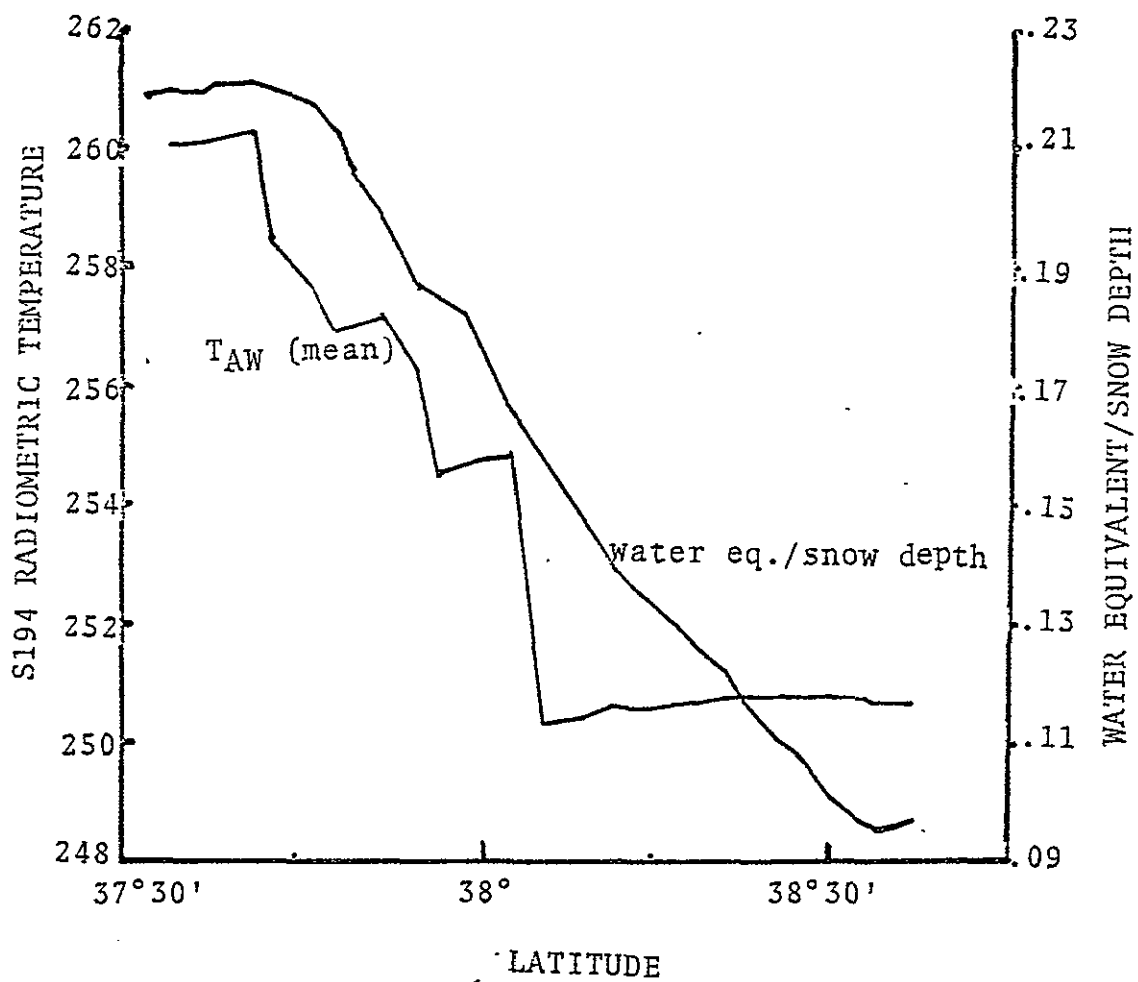
Figure 86 S194 antenna temperature and water equivalent/
snow depth variations across the test area,
January11, 1974.

The original S194 antenna temperature track across the test site revealed an extremely small range of temperature, i.e., 4.8°K. This makes difficult the justification of any trends discovered in this pass. The time of Skylab data collection corresponded with the initiation of a prolonged warming trend in the Central United States which persisted throughout the remainder of the month of January.

For the January 14 test site in Nebraska and Colorado, only 3 independent footprints of the S194 would have been available. Due to this factor, the type of correlation analysis performed on the 11th of January utilizing overlapping footprints was utilized. Again, the correlation coefficients are misleading and only trends can be inferred. Figures 87-89 indicate the relationships between the variables snow depth, water equivalent, and WE/SD and the S194 Radiometric Temperature.

Although low, these correlation trends are quite understandable. The melt condition of the snow pack is such that the free water content at the surface of the snow is probably greater than 2.5% by volume, a condition discovered by Edgerton, et.al. (1968) to affect 37 and 14 GHz sensors. More important, however, may be the non-equilibrium condition existing between absorptivity and emissivity. The basic conservation of energy equation $E = 1-R$ is predicated on the assumption that:
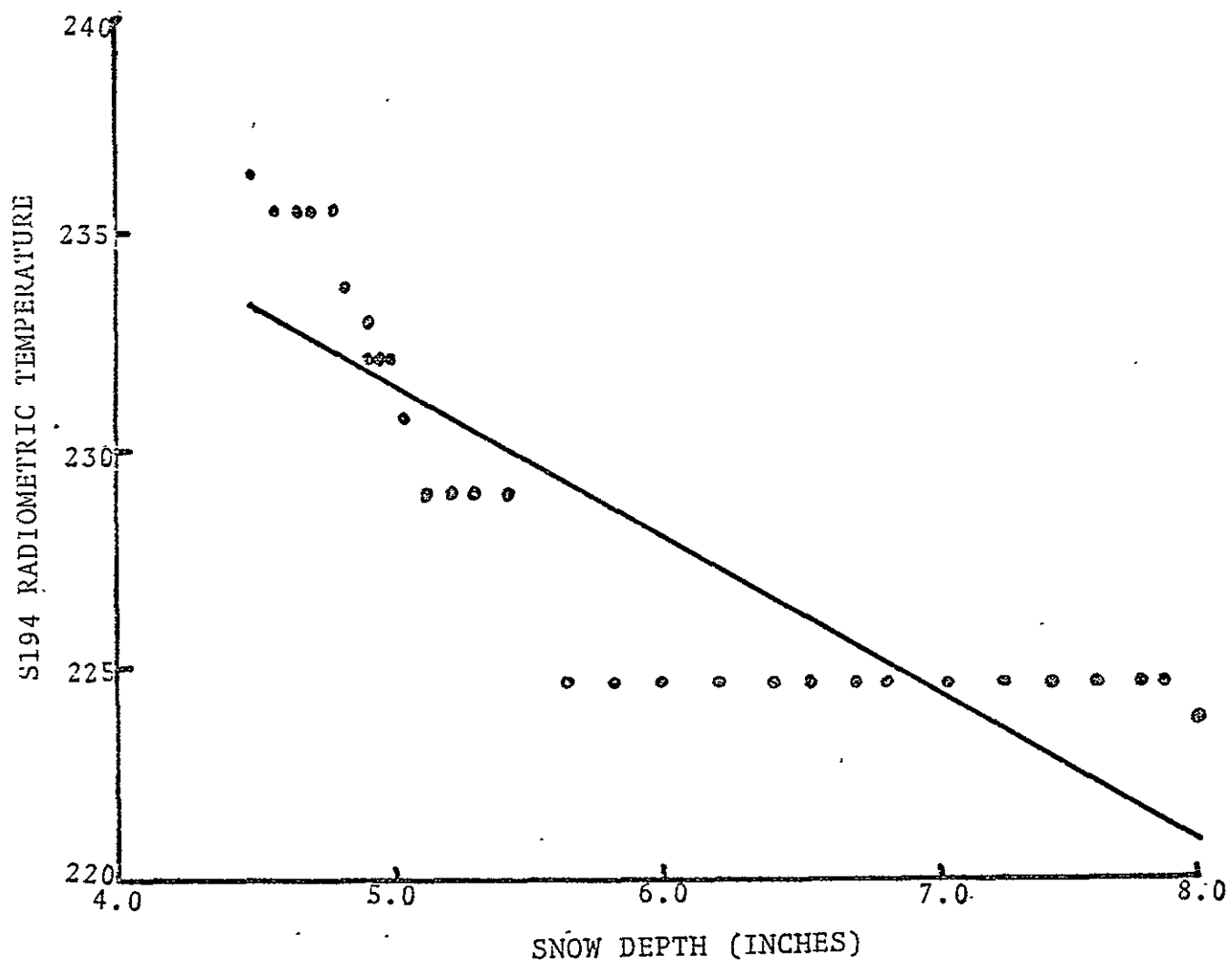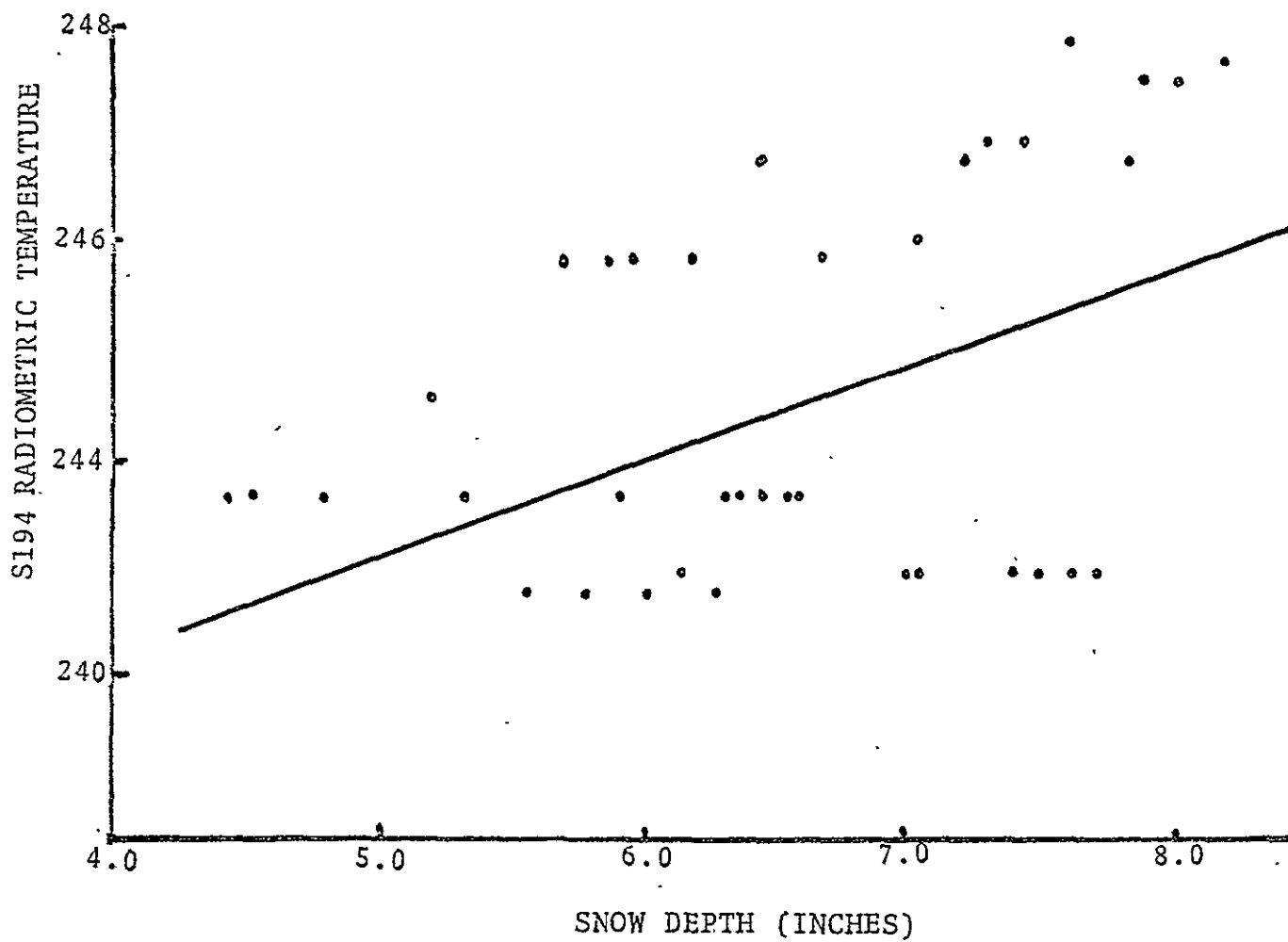
Figure 87 S194 brightness temperature as a function of snow depth on January 14, 1974.
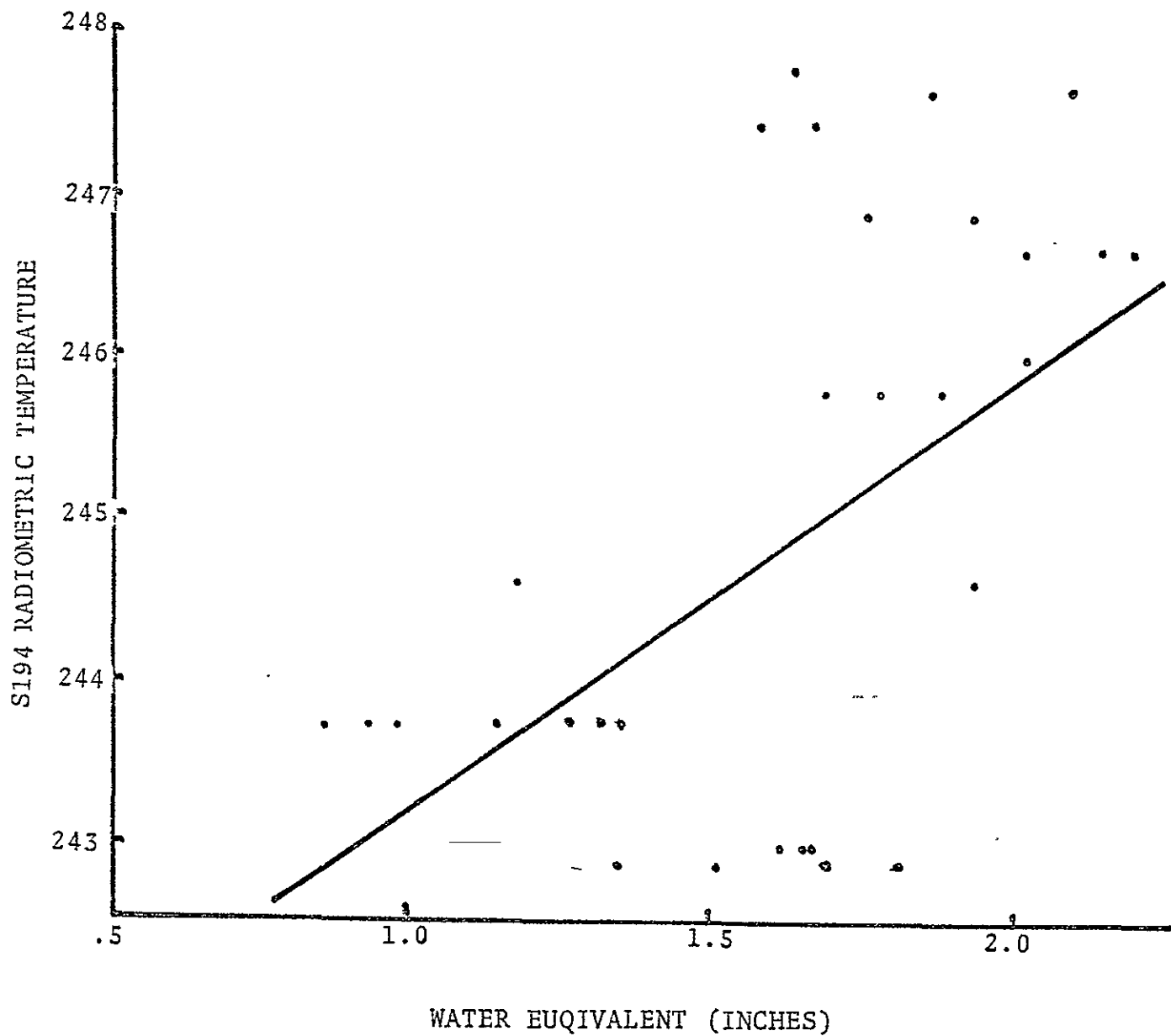
Figure   88   S194 brightness temperature as a function of water
equivalent on January 14, 1974.

212

Figure 89   S194 brightness temperature as a function of water
equivalent/snow depth on January 14, 1974.

1) an equilibrium exists between absorptivity and emis-
   sivity in the target material, and

2) the target material is sufficiently thick so that
   the amount of energy transmitted through the material
   is nill.

Although the second condition may well be satisfied, the first
probably isn't. According to Edgerton, et. al. (1968),
"It is not readily apparent that the assumed condition of
thermal equilibrium is valid for snow systems. Substantial
amounts of energy are used during phase changes (melting and
refreezing)". It is postulated that the incipient melt con-
ditions of January 14 upset the thermal equilibrium neces-
sary to satisfy the conservation of energy equation. Examina-
tion of the computed Taw for January 14 vs. snow depth and
water equivalent (Figures 90 and 91) reveals the complex
nature of the response pattern. Early portions of the Taw
vs. snow depth reveal opposing trends in Colorado, yet simi-
lar trends in Nebraska. Taw vs. water equivalent is more
varied than for snow depth.

The mean adjusted antenna temperature (Taw) accounting
for variations in air temperature (snow surface temperature)
in Colorado-Nebraska was calculated in a manner identical
to the January 11 data. The correlations between Taw and
snow depth, water equivalent, and water equivalent/snow depth
were poor.

One final analysis to account for melt conditions was
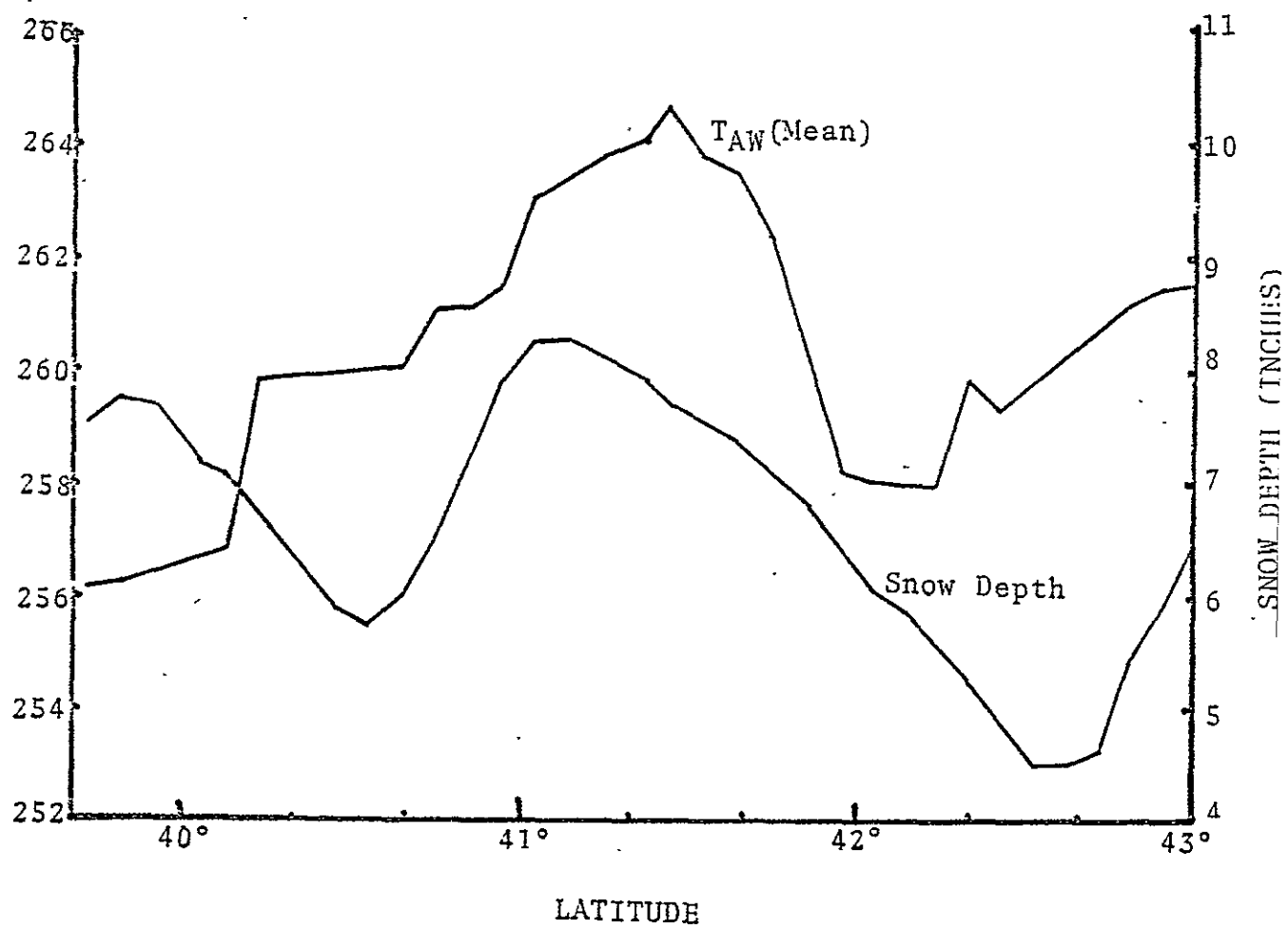
Figure 90 Variations of snow depth and S194 brightness temp-
erature on January 14, 1974.

215
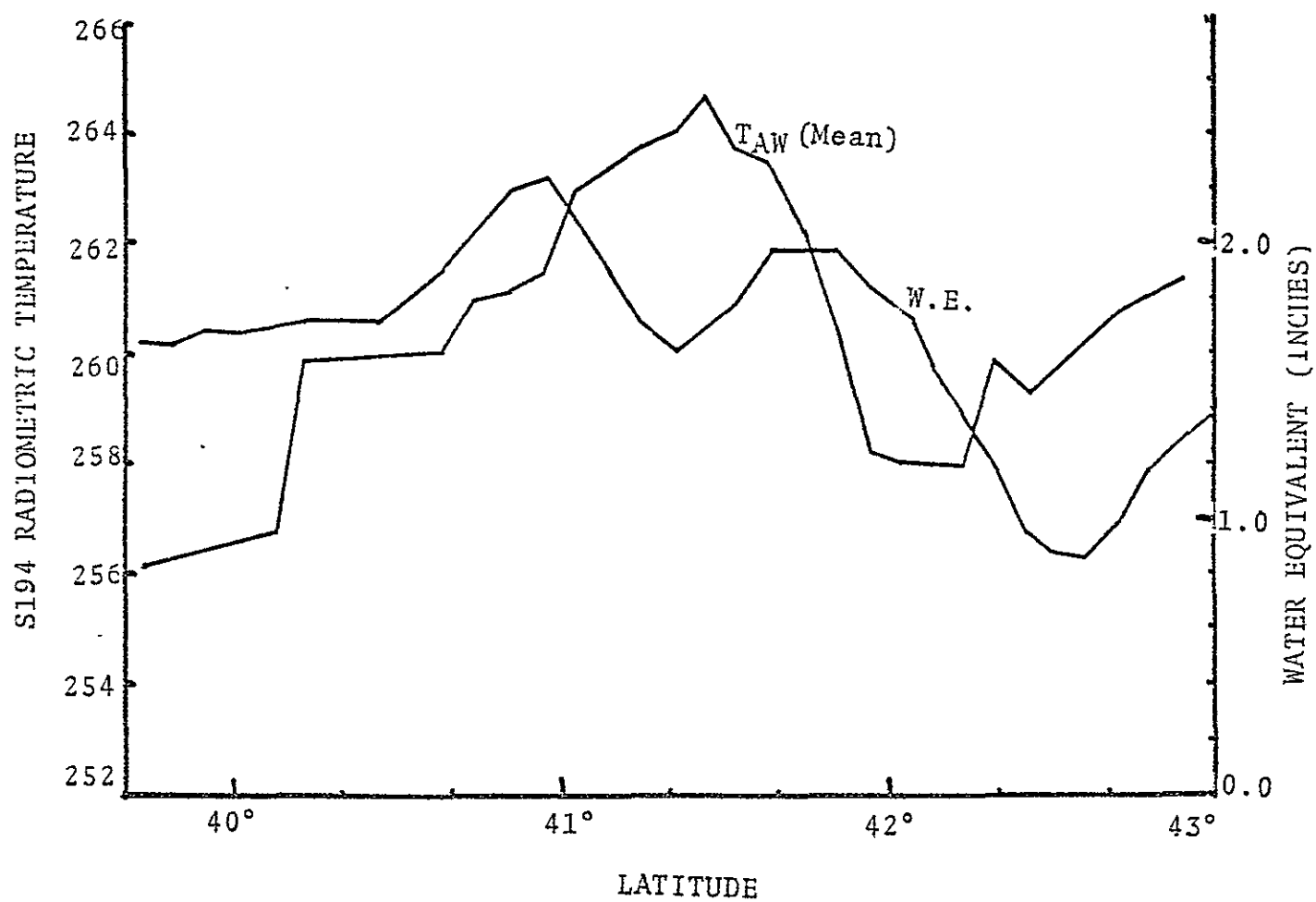
Figure 91 Variations of water equivalent and S194 brightness
temperature on January 14, 1974.

attempted. Since mean temperature eas available for each footprint, all footprints exhibiting mean temperatures above freezing were eliminated from consideration. This technique was employed to eliminate the effects of free water in the snow system. The remaining subfreezing S194 footprints were subsequently compared with the previously utilized snow parameters. The resulting trends are revealed in Figures 92-94. Note the high positive correlation between snow depth, and water equivalent vs. Taw(subfreezing footprints).

The remaining S194 footprints displaying above freezing (superfreezing) temperatures were similarly analyzed. The resulting trends were extremely poor.

Just prior to press time, one final adjustment to Taw was utilized; i.e., an emissivity of 0.9 was substituted for 0.6. The assumption was simply that 0.9 would probably be a closer approximation to the emissivities of freshly fallen snow at microwave wevelengths. This higher emissivity Taw (Tawhe) was subsequently correlated with snow depth in Kansas and Colorado. The resulting trends are indicated in Figures 95 and 96.
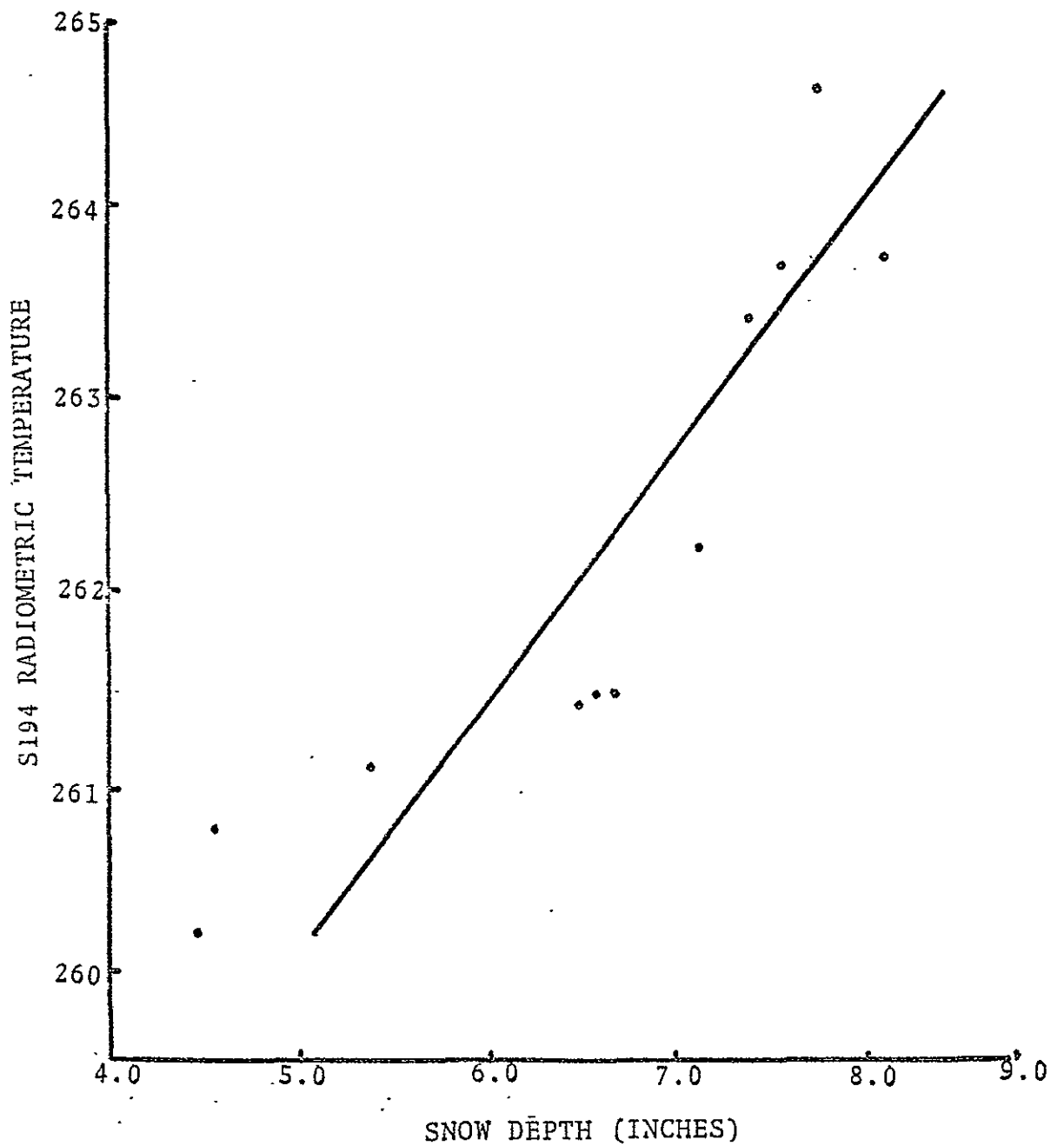
Figure 92 S194 brightness temperatures as a function of snow depth for subfreezing ground temperatures on January 14, 1974.
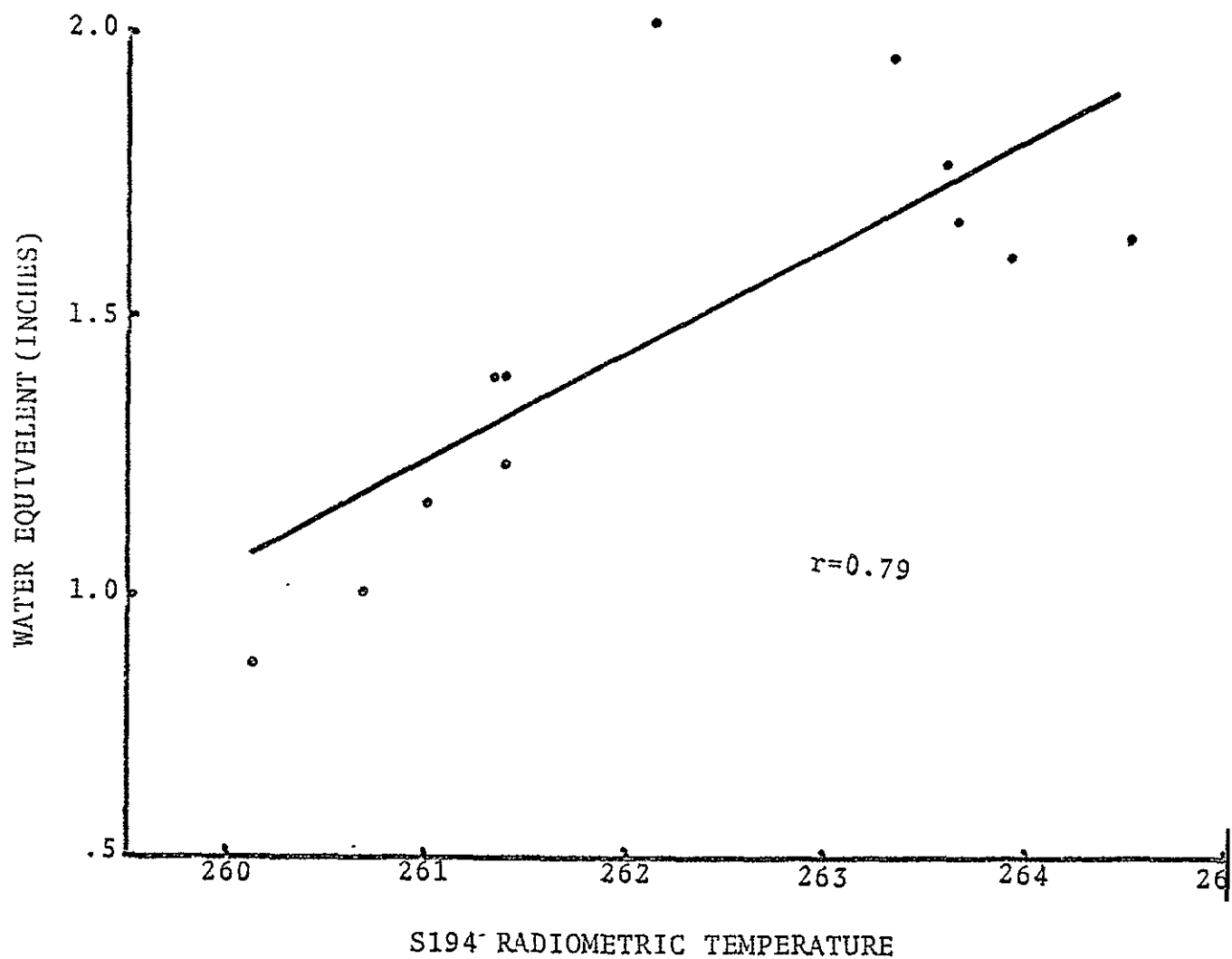
Figure 93   S194 brightness temperatures as a function of
water equivalent for subfreezing ground temp-
eratures on January 14, 1974.
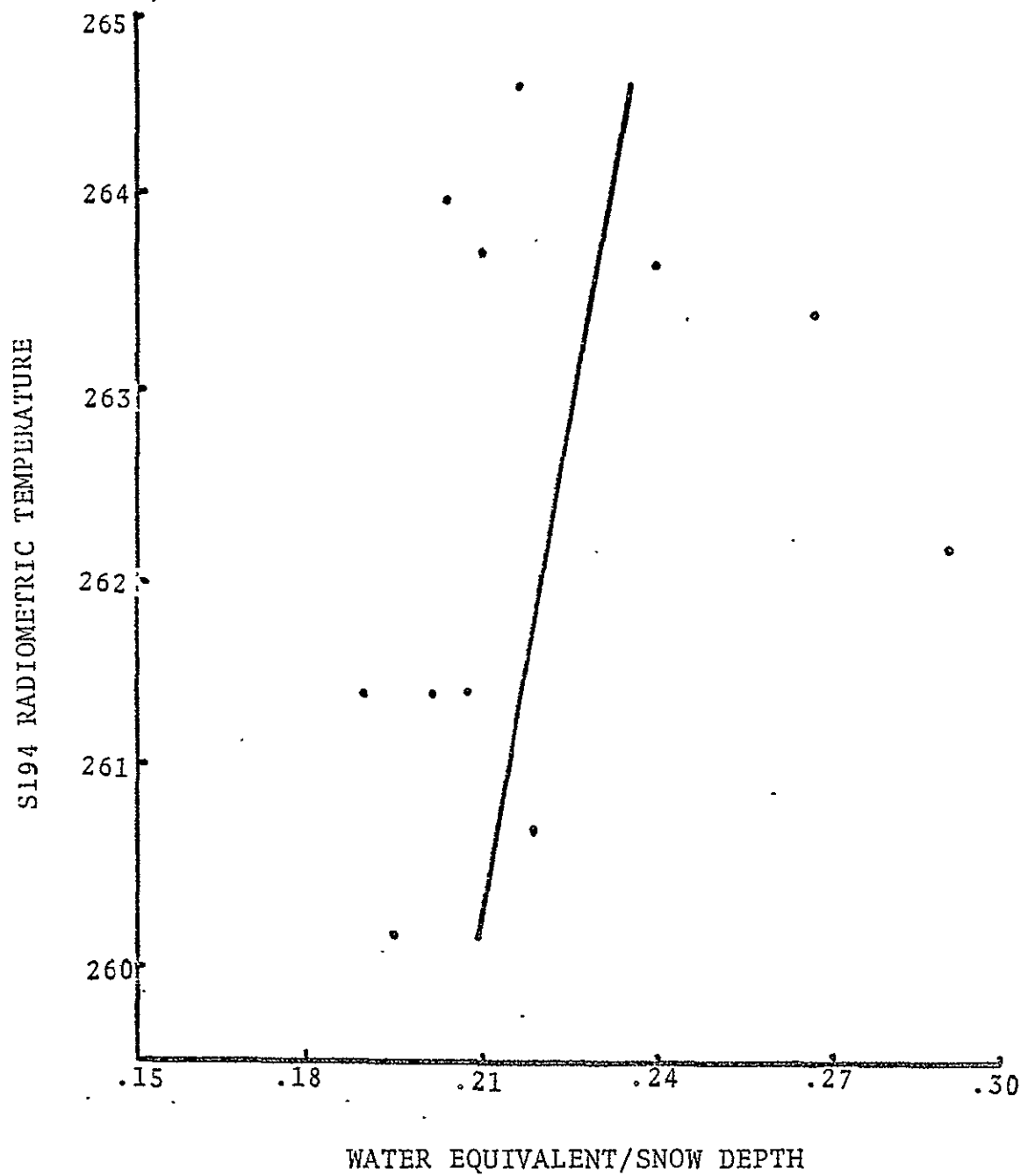
Figure 94 S194 brightenss temperatures as a function of water equivalent/snow depth for subfreezing ground temperatures on January 14, 1974.

220
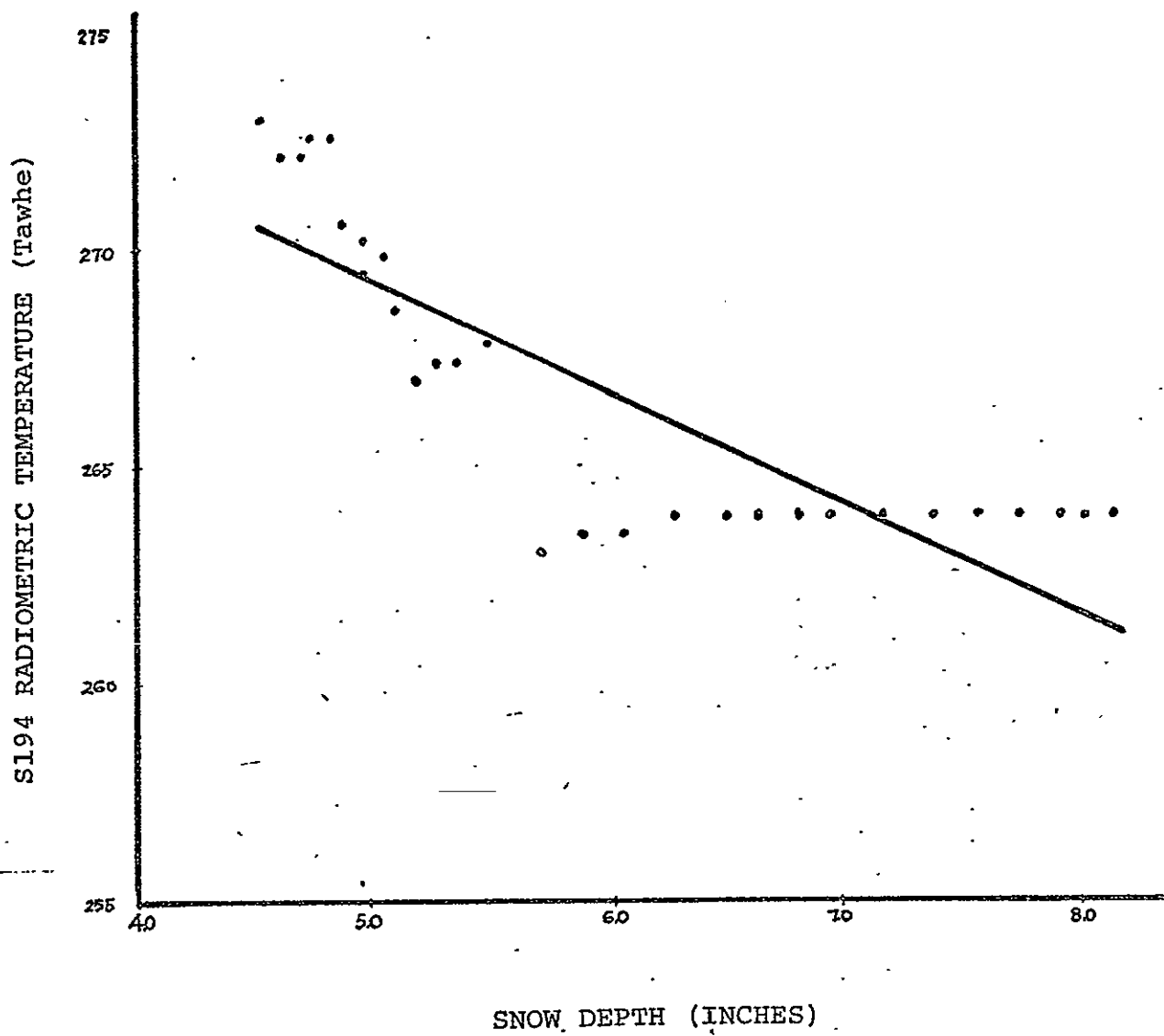
Figure 95 S194 brightness temperature (Tawhe) as a function of snow depth on January 11, 1974 in Kansas

221
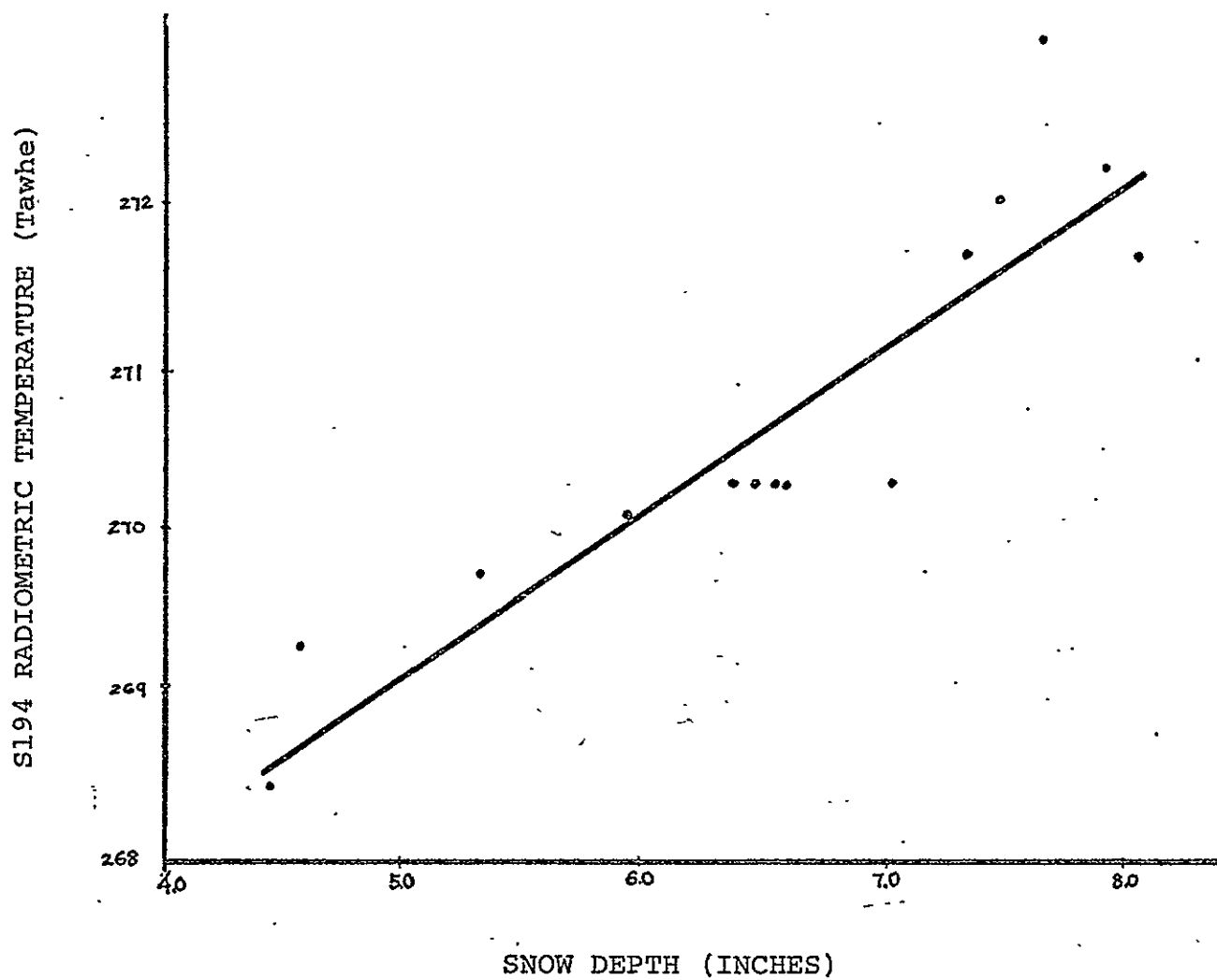
Figure 96   S194 brightness temperature (Tawhe) as a function of snow depth on January 14, 1974 in Colorado-Nebraska (subfreezing)

Conclusions; S194 Response to Snow

In the final analysis, any conclusions based upon findings derived from only two sites is tenuous at best. On the basis of these, however, it does appear that L-Band may possess the capability of locating the freeze-thaw line, and under certain circumstances reveal relative snow depth.

It is common knowledge that although the albedo of fresh snow at short wavelengths is high (0.8-0.9), snow's reflectivity at longer wavelengths (i.e., L-Band) is extremely low (0.005). With respect to longwave radiation, therefore, snow behaves almost like a black body. Due to the density of the emitting media, we suggest that S194 is more sensitive in determining soil moisture differences than snow depth variations. When the soil moisture freezes, however, the snowpack's black body influence may furnish the principal control over microwave emissivity received by the S194.

Thus, the high positive correlation between snow depth and Tawhe (subfreezing footprints) in Colorado-Nebraska sugfests that L-Band is responding to changes in snow depth rather than any moisture changes in the underlying soil. Since the soil moisture phass of the report conclusively demonstrated that S194 inversely responds to changes in soil moisture, it would appear that the ground was frozen. Thus, the radiometer directly responded to increasing snow depth.

. The S194's unresponsiveness (Tawhe) to snow depth located in superfreezing footprints must principally be a result of the violation of the conservation of energy equation; i.e., absorptivity $\neq$ emissivity during melt periods.

The high negative correlation between snow depth and Tawhe in Kansas indicates that the snowpack is not the principal contributor to longwave emission. If such was the situation, higher snow depths should result in higher emissivities. It appears, therefore, that L-Band is responding to soil moisture changes; i.e., the soil is unfrozen. Snow depth probably indicates the degree of wetness of the underlying soil. The sudden upswing of antenna temperature in Northeast Kansas may indicate that frozen ground has been encountered. The Climatological Data Bulletin has also indicated that up to 13 inches of snow had accumulated in portions of Northwest Missouri and Southern Iowa, which would contribute to the increase in antenna temperature.

Several constraints were operating upon the S193 mechanism in January, 1974. The displacement of the antenna cap and subsequent distortion of the footprint has previously been mentioned. In addition, the instrument's sweep mechanism had suffered extensive damage on the left(+) side. For these reasons, it was initially determined to utilize the right side (minus) readings at four distinct angles between nadir and 6 degrees, these being 0,1,3,and 5. These four categories were further subdivided according to the instrument direction of motion, i.e., left to right and right to left. This was employed because minor angle differences dependent upon the direction of motion were observed in each class. [At a later date the analysis was extended to include 9° and 12° (L-R)] During the January passes (except January 24), roll 0 pitch 0 was utilized.

Increased return is noted for the first four angles in the vicinity of 38 degrees north latitude (Figures 97-100). An increase in microwave response of this type has been observed by Schmugge, et. al. (1974)with a 1.55 cm. passive radiometer. They attributed this to an increase in liquid water content at the snow surface layer. The area of interest lies in the Flint Hills region of Kansas which is characterized by moderately undulating topography. The south-facing slopes in this area could augment a surface melt that may be responsible for the increased response. The corresponding S190B

225
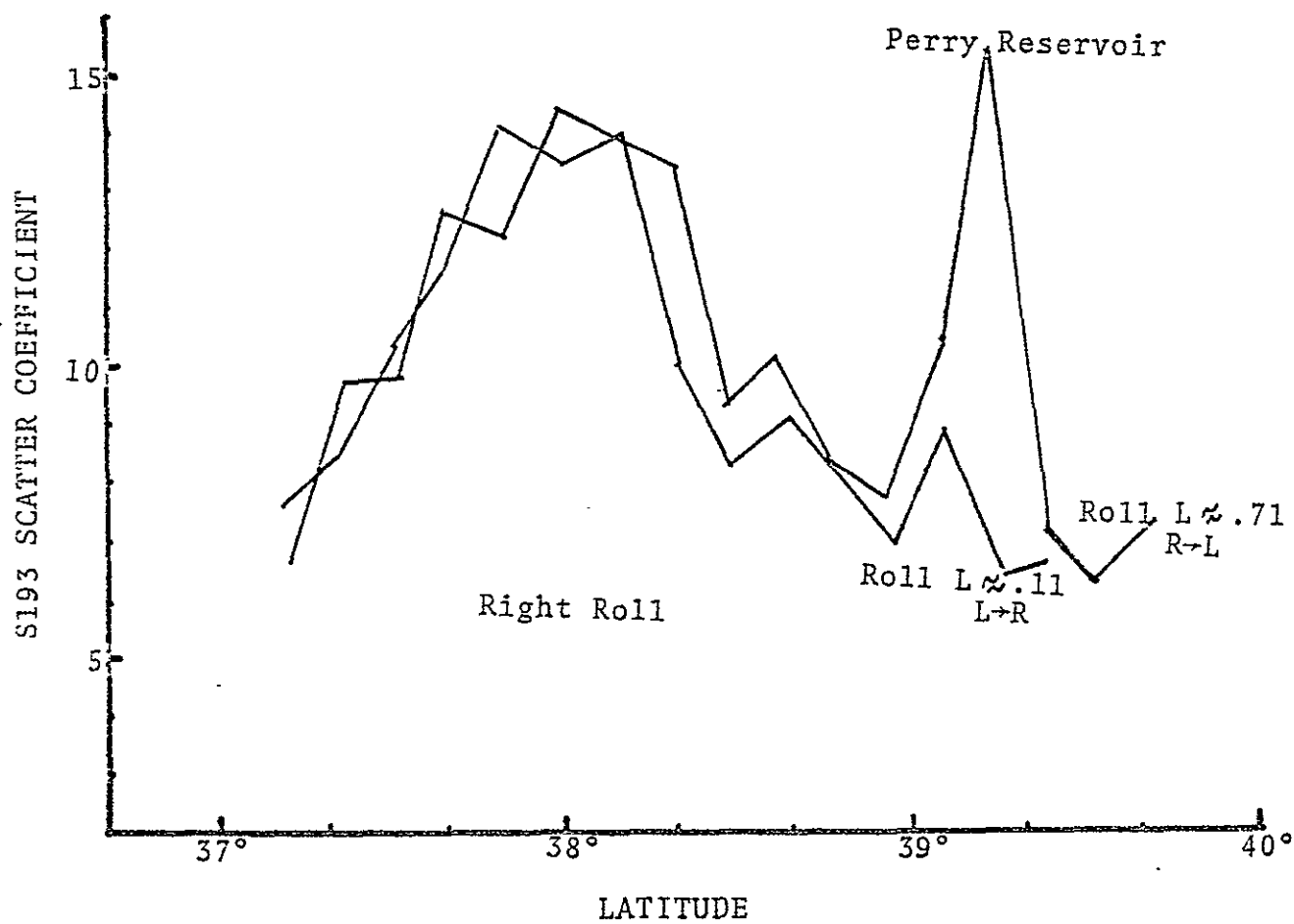
Figure 97   S193 scatter coefficient measured at angles near
zero degrees on January 11, 1974.
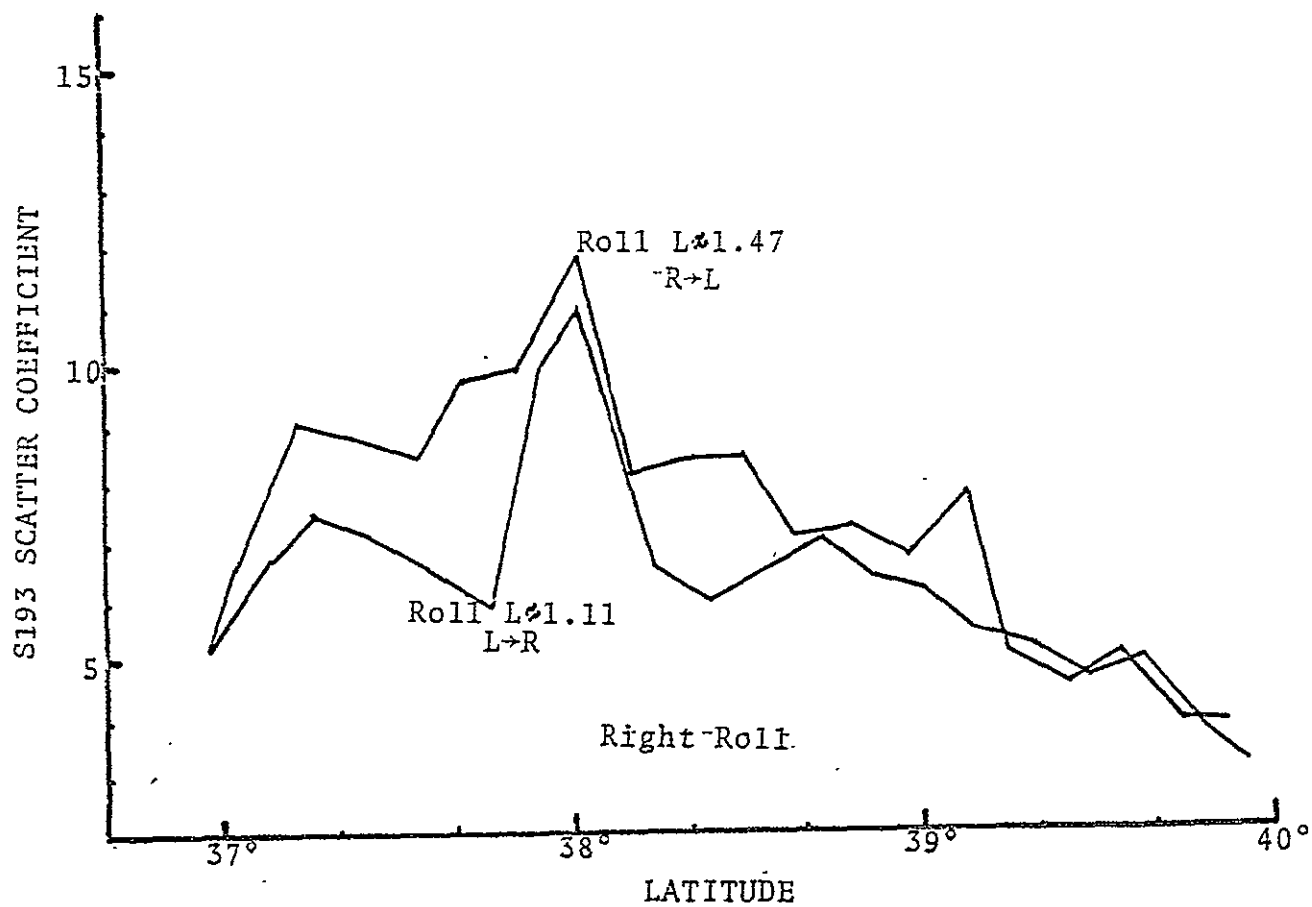
Figure 98 S193 scatter coefficient measured at angles near
one and one-half degrees on January 11, 1974.
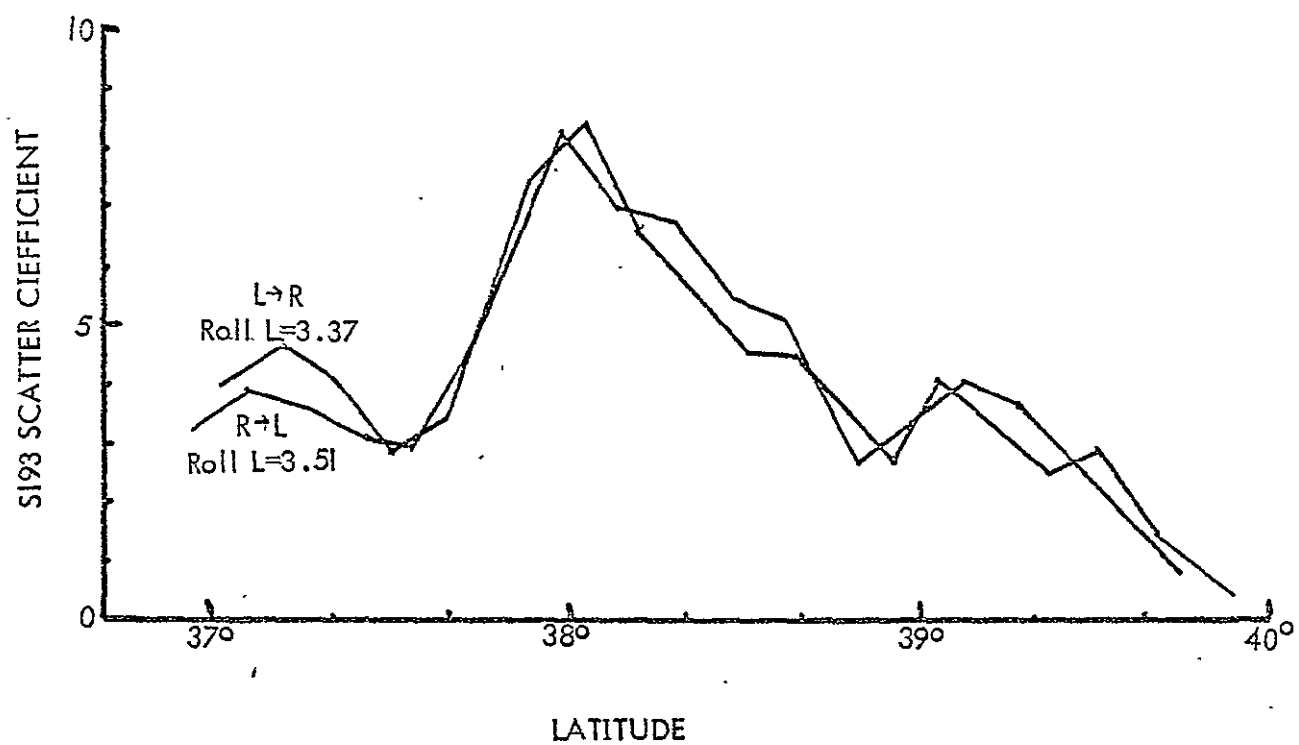
Figure 99 S193 scatter coefficient measured at angels near
three and one-half degrees on January 11, 1974..
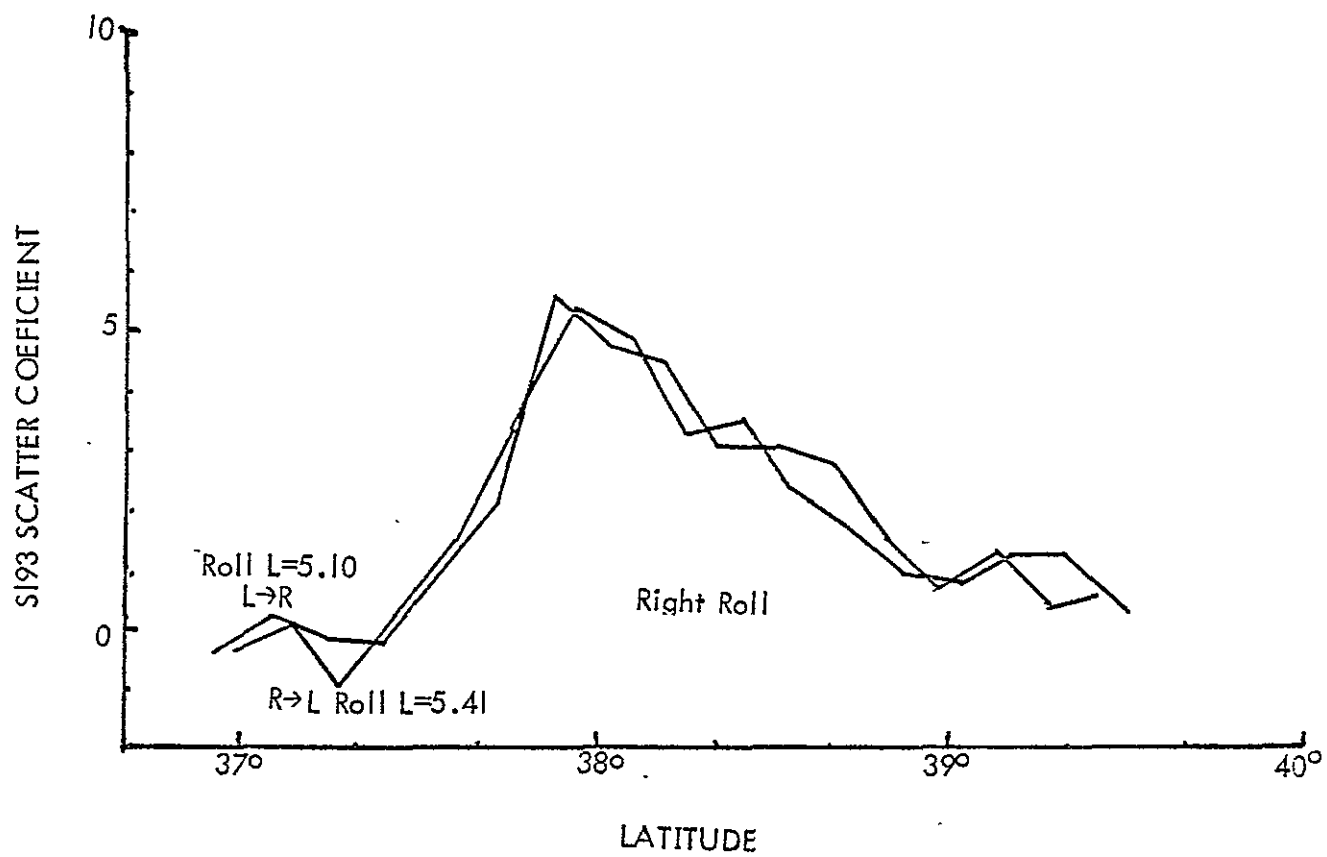
Figure 100 S193 scatter coefficient measured at angles near five degrees on January 11, 1974.

imagery reveals virtually 100% snow cover, although drainage patterns are quite evident.

The linear correlations between the S193 scatterometer data and snow depth, water equivalent, and water equivalent/ snow depth (WE/SD) have been computed for Kansas and are shown in Table 12 for different angles. In general, the correlations coefficients tended to increase as the look angle moved from nadir to 5 degrees. This is quite expected, because at angles near nadir (0-3 degrees) small errors in pointing accuracy result in greater interpretative problems. These near-vertical correlations should therefore be discounted. The correlations between snow depth or WE/SD are quite good for the 5° angle, and for snow depth at 9° as well. Some of these better relationships are shown in Figures 101-104.

S193 Scatterometer Response - January 14, 1974

Correlation coefficients in the Colorado-Nebraska test site area between S193 and various snow parameters are shown in Table 13, and Figures 105-108. These minimal correlations have previously been observed with the passive system.Edgerton et. al. (1968) stated that there is probably "...no hope of discovering any free moisture content data from 13.4 or 37 GHz microwave [passive,(author note)] studies when the free moisture exceeds 2.5%". It appears highly likely that a significant amount of free water existed in the snowpack on the 14th of January.
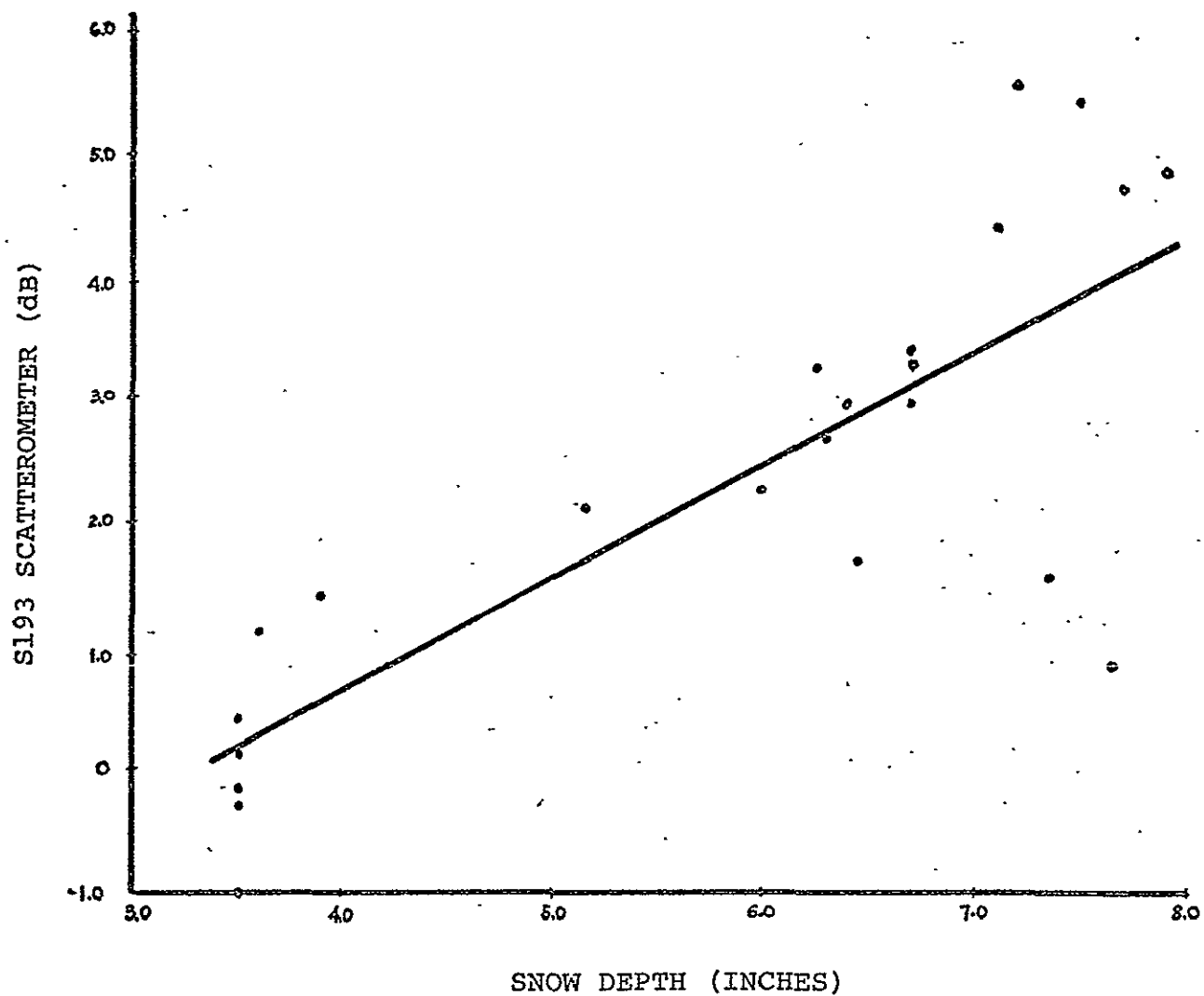
Figure 101 S193 scatterometer as a function of snow depth on January 11, 1974 in Kansas (5 degrees)
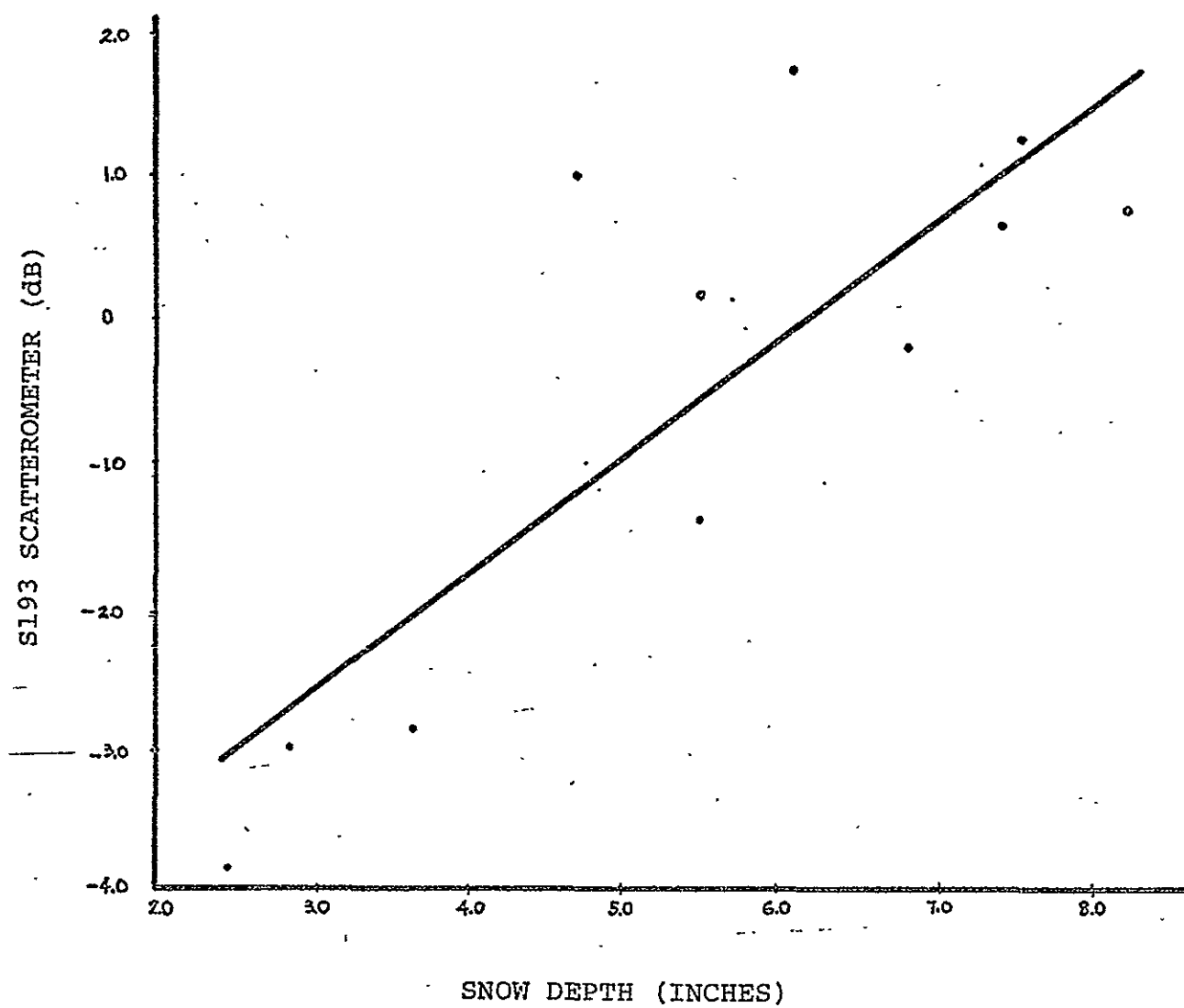
Figure 102. S193 scatterometer as a function of snow depth on January 11, 1974 in Kansas (9 degrees)

232
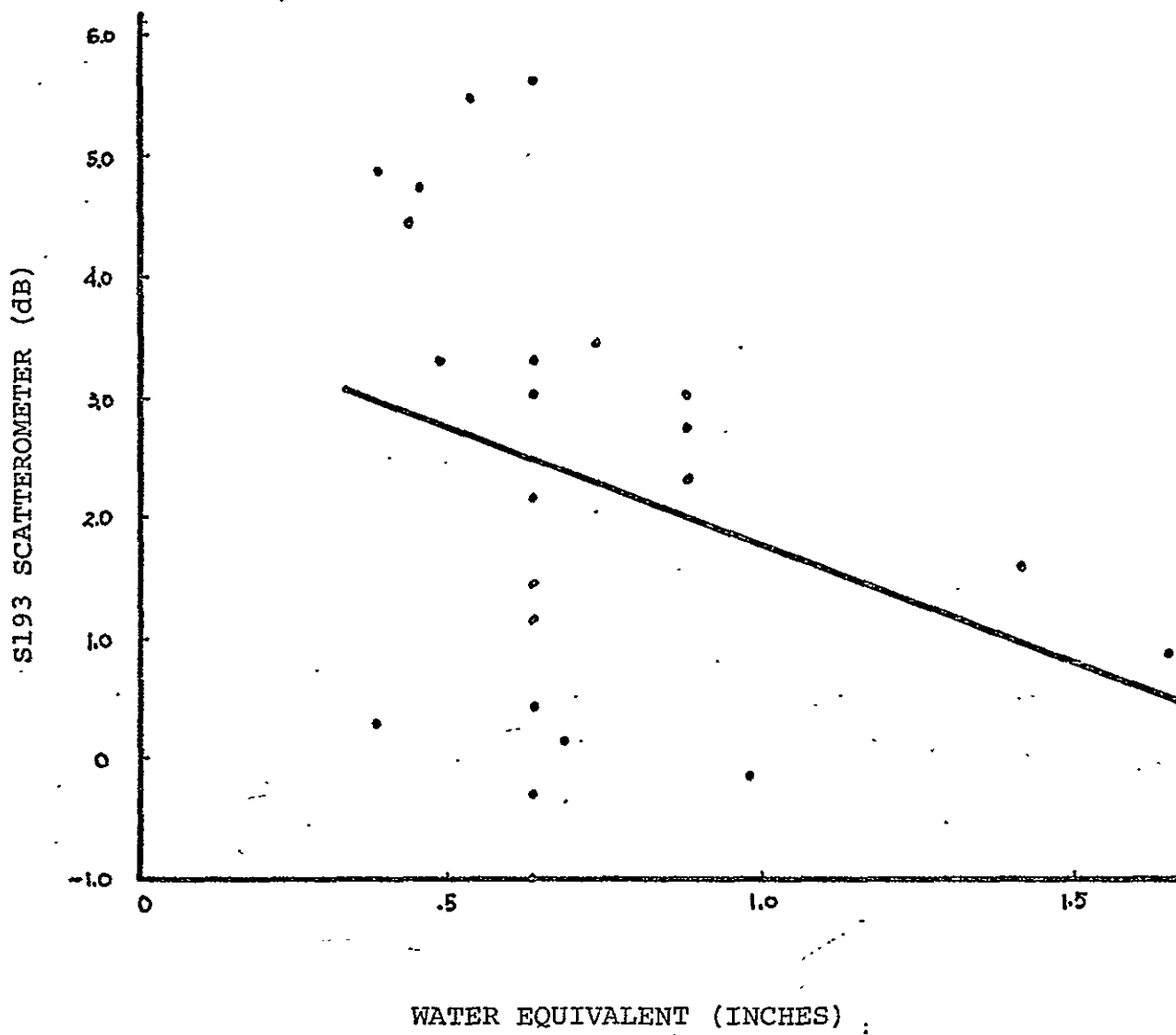
Figure 103 S193 scatterometer as a function of water equivalent on January 11, 1974 in Kansas (5 degrees)
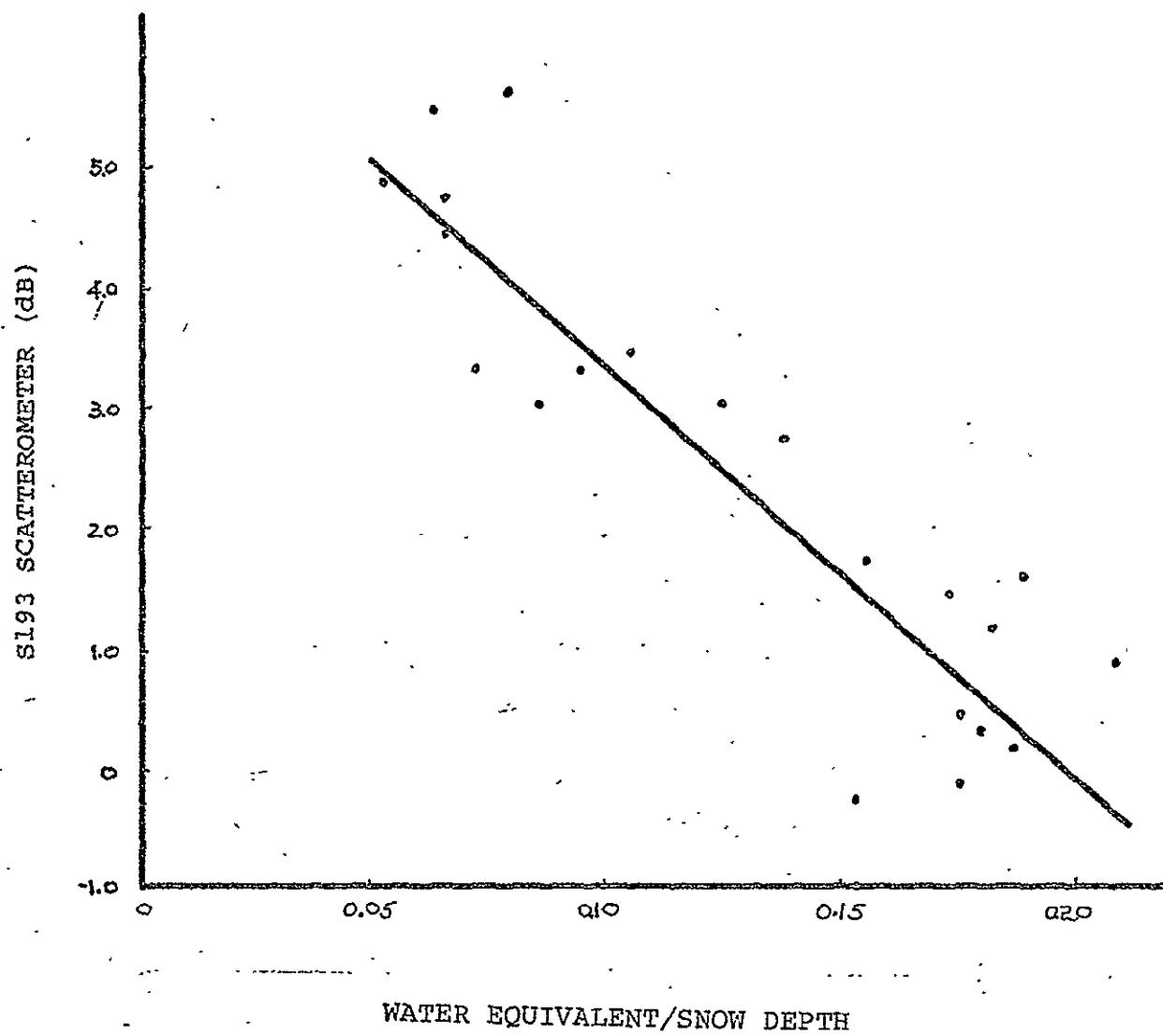
Figure 104 S193 scatterometer as a function of WE/SD on January 11, 1974 in Kansas (5 degrees)
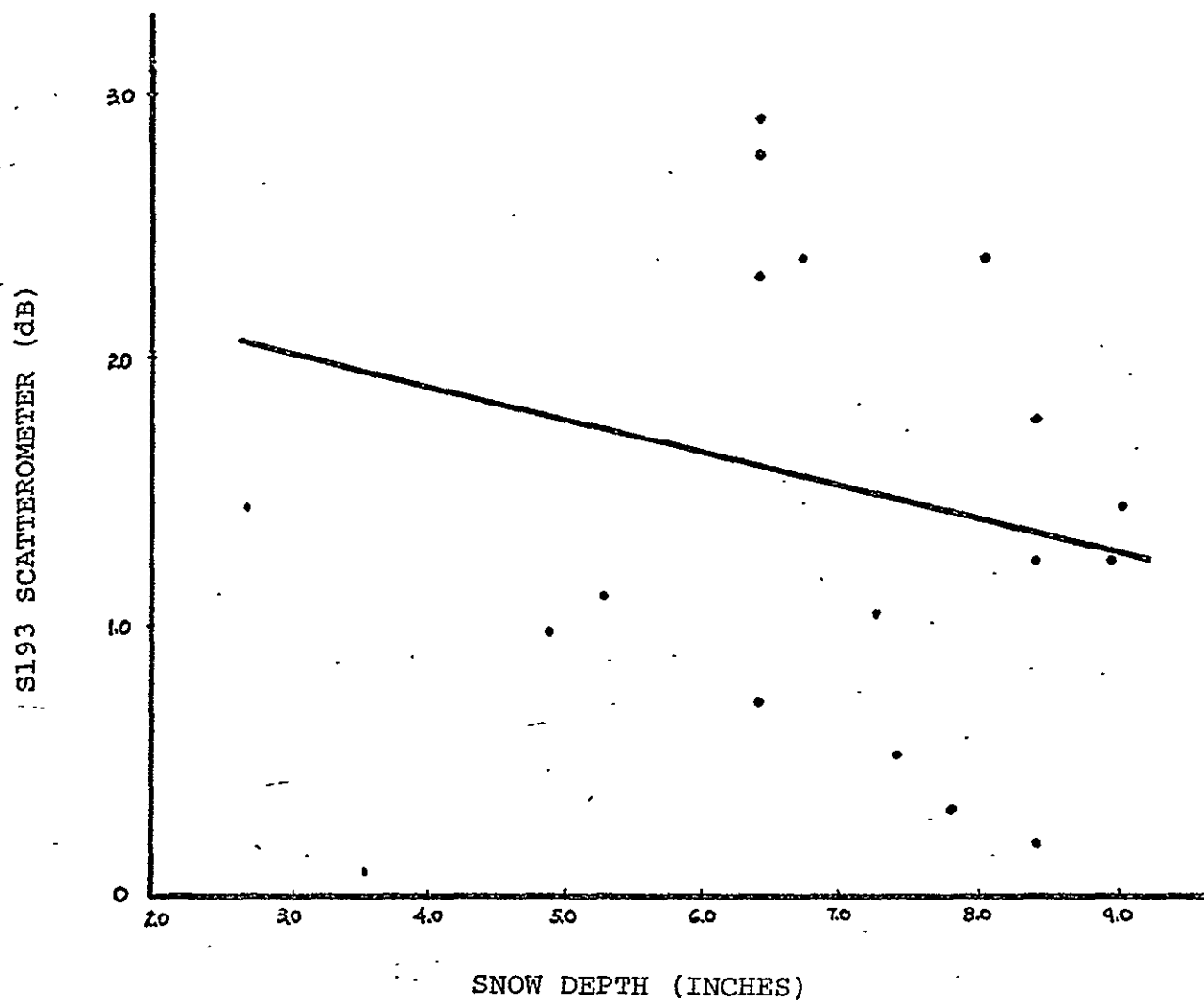
Figure 105   S193 scatterometer as a function of snow depth on January
              14, 1974 in Colorado-Nebraska (5 degrees)

Figure 106 S193 scatterometer as a function of snow depth on January 14, 1974 in Colorado-Nebraska (14 degrees)
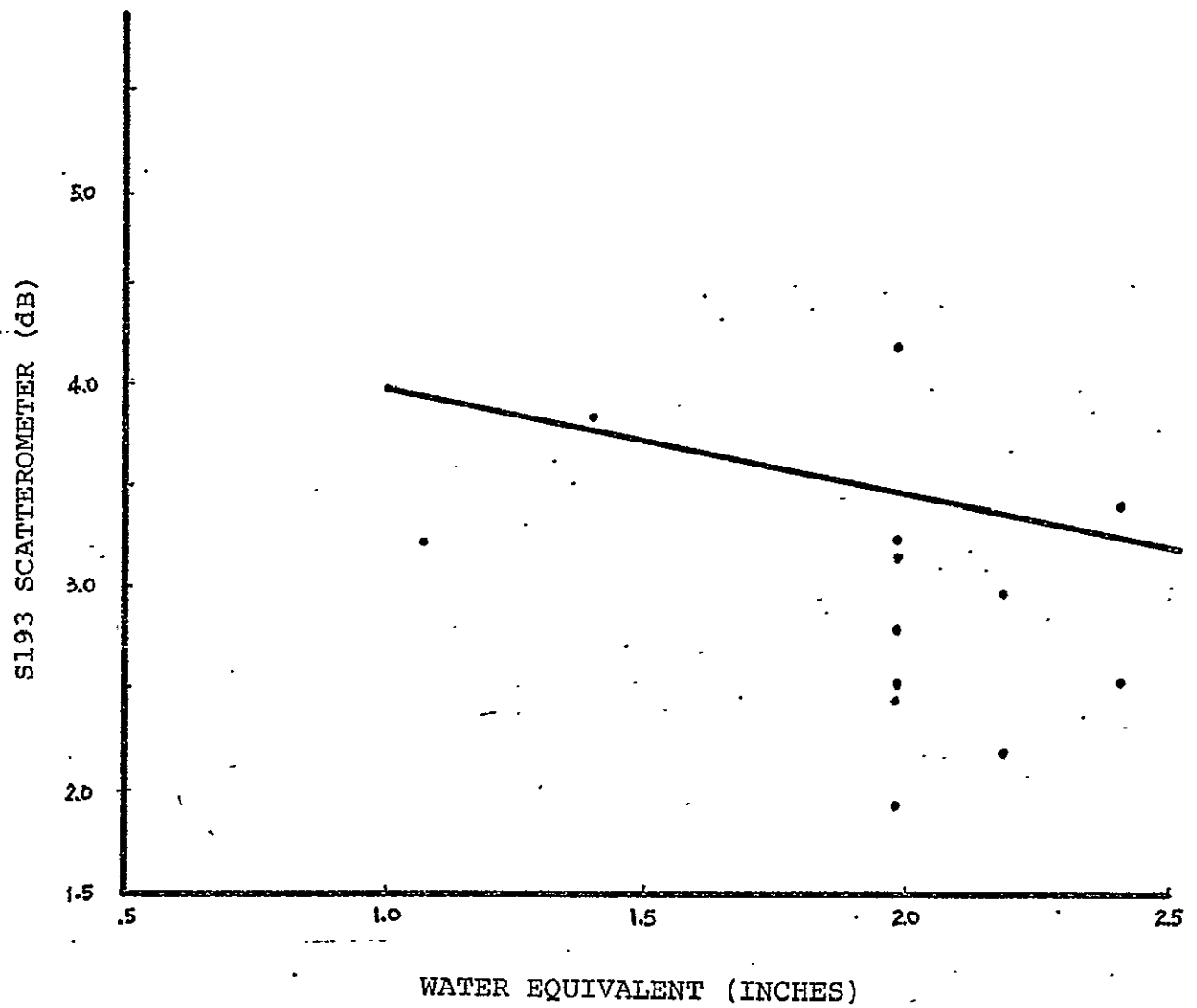
Figure 107 S193 scatterometer as a function of water equivalent on
January 14, 1974 in Colorado-Nebraska (3 degrees)
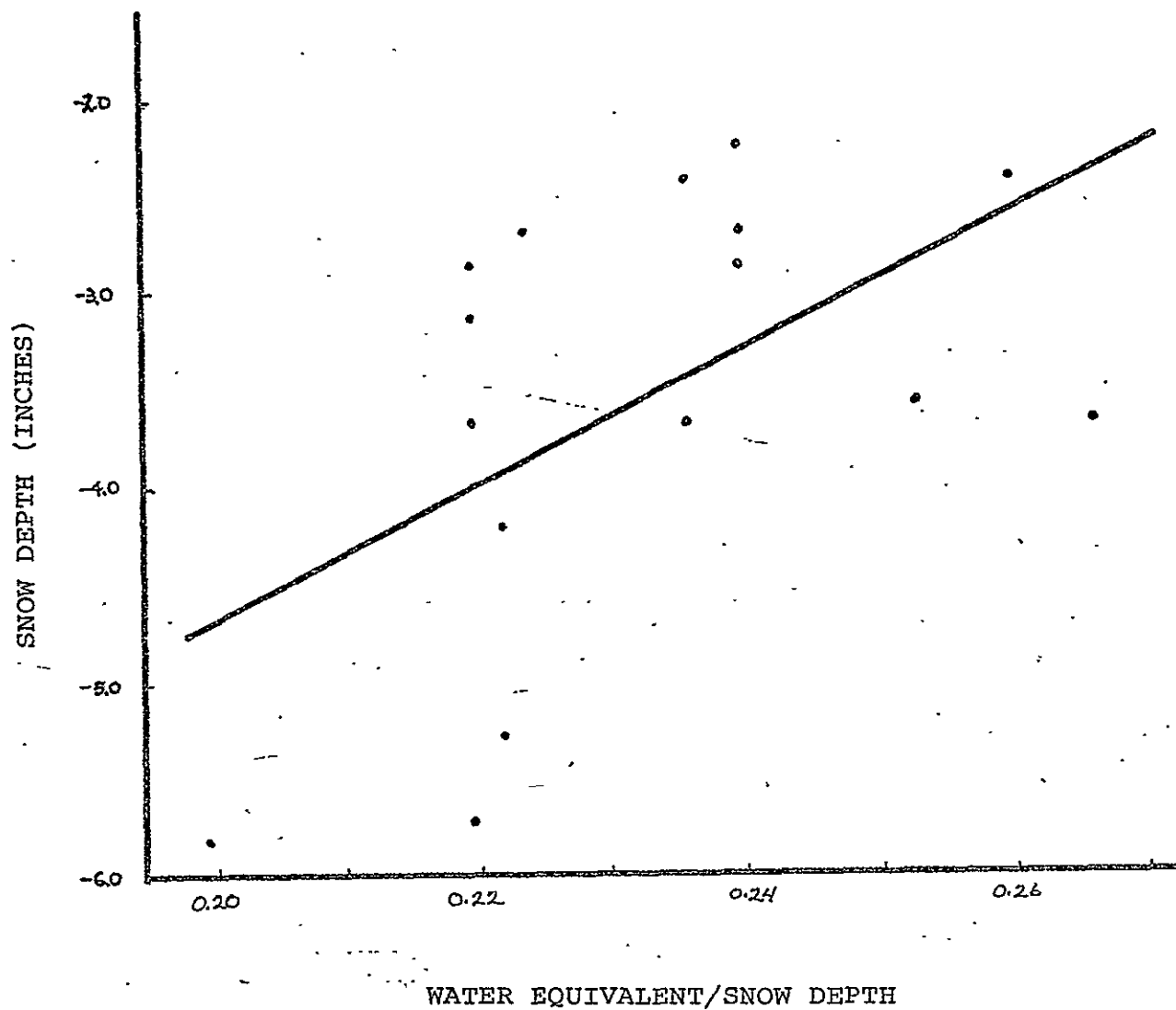
Figure 108   S193 scatterometer as a function of WE/SD on January
14, 1974 in Colorado-Nebraska (14 degrees)

Recall, however, the improved correlations obtained when S194 footprints were divided into subfreezing and super-freezing categories. Performing an identical division upon the S193 Scatterometer in Colorado-Nebraska produced an increase in correlation coefficient (see Tables 14-15 and Figures 109-112). Especially note the increased correlation upon snow depth and WE/SD as the angle increased to 14°.

In the Colorado-Nebraska test site area, we find that the range of snow depth is not very great for subfreezing footprints, at the most 2 inches. The question may well arise concerning the accuracy of the snow depth data when a range of only two inches exists. Thus, the correlation derived from this analysis may be suspect in that only a minute range of potential snow depths was examined. An attempt to determine the validity of these correlations was undertaken using the moment arm principle. Under the assumption the assumption that dry soil (i.e., zero snow depth) and frozen ground behave similarly (i.e., similar scattering coefficient), we introduced one zero intercept scatterometer value into each data set. These values were obtained from previous S193 analyses performed in the Texas Panhandle on January 11, 1974 (no snow condition). There is reasonable justification for using these zero intercept values for the January 14 run in Colorado-Nebraska. Even though soil types are different for the two sites, the terrain type is similar. Both exhibit flat or slightly rolling topography. The absence of living

Table 12

Correlation coefficients between the S193 scatterometer
and various snow parameters obtained across the
Kansas test area on January 11, 1974

Look Angle	0	1°	3°	5°	0°	1°	3°	5°
Movement	L to R	L to R	L to R	L to R	R to L	R to L	R to L	R to L
Linear Correlation Coefficients								
Snowdepth	−0.38	−0.30	0.29	0.86	−0.38	−0.62	0.37	0.78
Water Equivalent	0.09	−0.17	−0.51	−0.25	0.17	−0.41	−0.54	−0.36
WE/SD	0.53	0.06	0.79	0.87	0.47	0.25	−0.79	−0.87
Curvilinear Correlation Coefficients								
Snowdepth	0.40	0.50	0.29	0.89	0.45	0.76	0.37	0.79
Water Equivalent	0.12	0.34	0.51	0.39	0.18	0.56	0.57	0.57
WE/SD	0.53	0.14	0.79	0.88	0.54	0.28	0.80	0.90

Table 13

Correlation coefficients between the S193 scatterometer
and various snow parameters obtained across the Colorado-Nebraska
test area on January 14, 1974 with antenna movement from left to right.

Look Angle	0°	2°	3°	5°	9°	14°
Linear Correlation Coefficients						
Snowdepth	-0.03	0.26	0.25	-0.22	-0.66	-0.23
Water Equivalent	0.13	-0.32	-0.16	0.04	+-.32	
WE/SD	-0.05	0.19	0.24	0.07	0.78	0.52
Curvilinear Correlation Coefficients						
Snowdepth	0.25	0.33	0.28	0.33		
Water Equivalent	0.51	0.38	0.28	0.28		
WE/SD	0.18	0.29	0.29	0.37		

Table 14

Correlation coefficients between the S193 Scatterometer

(subfreezing footprints) and various snow parameters obtained

across the Colorado-Nebraska test site area on 1/14/74

Look Angle	0°	2°	3°	5°	9°	14°
Snow depth	0.68	0.36	0.10	0.59	-0.68	-0.89
Water Equivalent	0.03	-0.61	-0.80	0.11	0.47	--
WE/SD	0.08	-0.31	-0.79	-0.01	0.55	0.91

Table 15

Correlation coefficients between the S193 Scatterometer

(superfreezing footprints) and various snow parameters obtained

across the Colorado-Nebraska test site area on 1/14/74

Look Angle	0°	2°	3°	5°	9°	14°
Snow depth	0.27	0.50	0.35	0.06	-0.69	0.06
Water Equivalent	0.12	-0.32	-0.25	-0.27	-0.63	0.52
WE/SD	-0.27	0.29	0.45	0.34	0.02	-0.11

vegetation at this time of year is common to both sites, as well. We therefore assume that the winter return should be similar for both, even though we realize the possible significant differences in soil moisture or temperature which may exist.

The slope value thus obtained is termed moment arm one (MA1), because only one data point representing a zero snow condition was introduced. In addition, a second slope determination was calculated for Colorado-Nebraska using an equal number of data points and zero intercept points. It was deemed advisable to analyze such a data set due to the limited range of the original data set, and to equally weight the probable zero intercept value. Equally weighting these two data clusters would subsequently result in a balanced moment arm (MAx). [Note: The Kansas test site area was subject to the MA1) procedure only, because of the wider range of snow depth and scattering coefficient originally present]. Tables 16-22 and Figures 113-115 reveal the outcome of these proceedings.
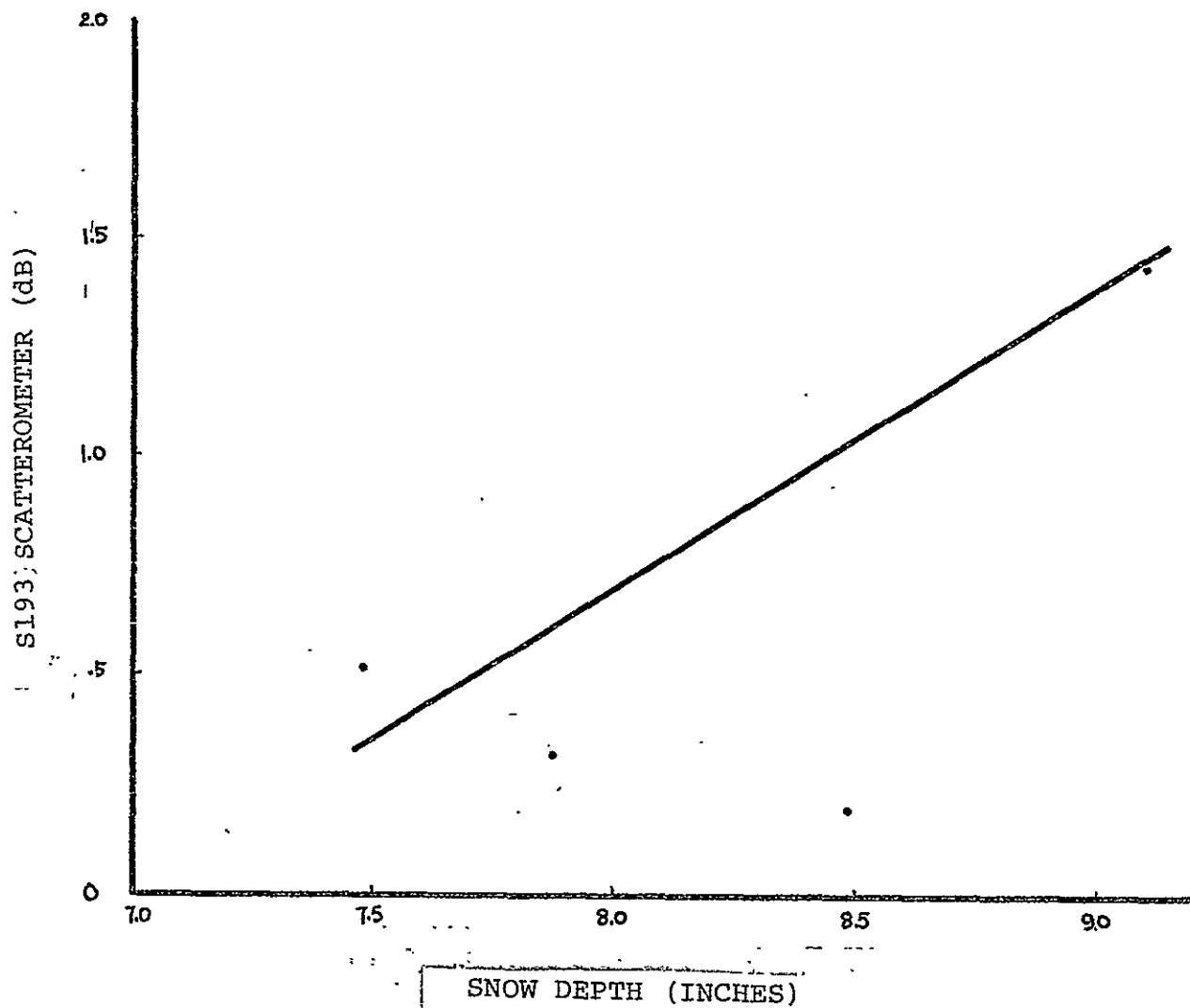
Figure 109   S193 scatterometer as a function of snow depth (subfreezing)
on January 14, 1974 in Colorado-Nebraska (5 degrees)

244
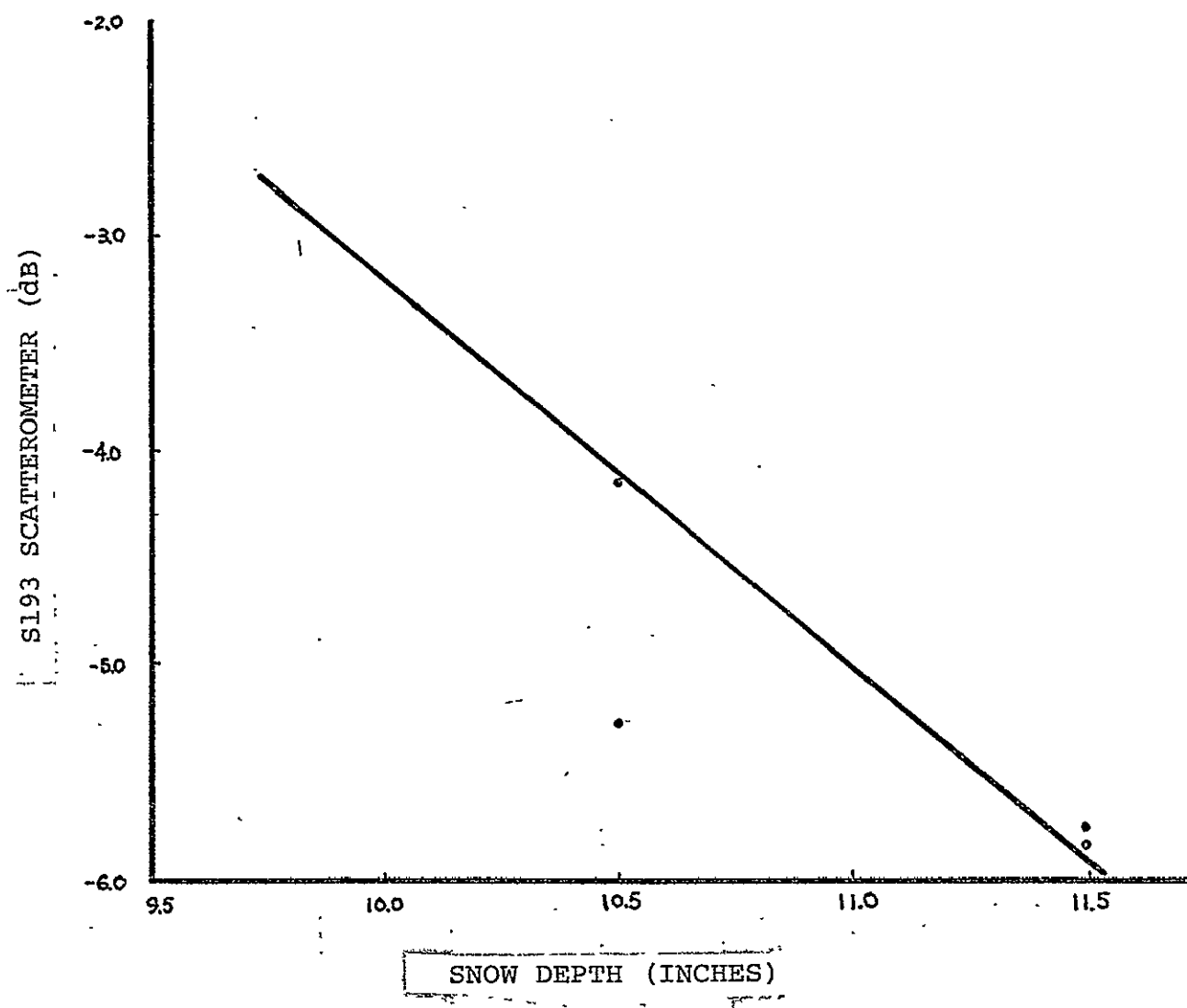
Figure 110   S193 scatterometer as a function of snow depth (subfreezing)
             on January 14, 1974 in Colorado-Nebraska (14 degrees)
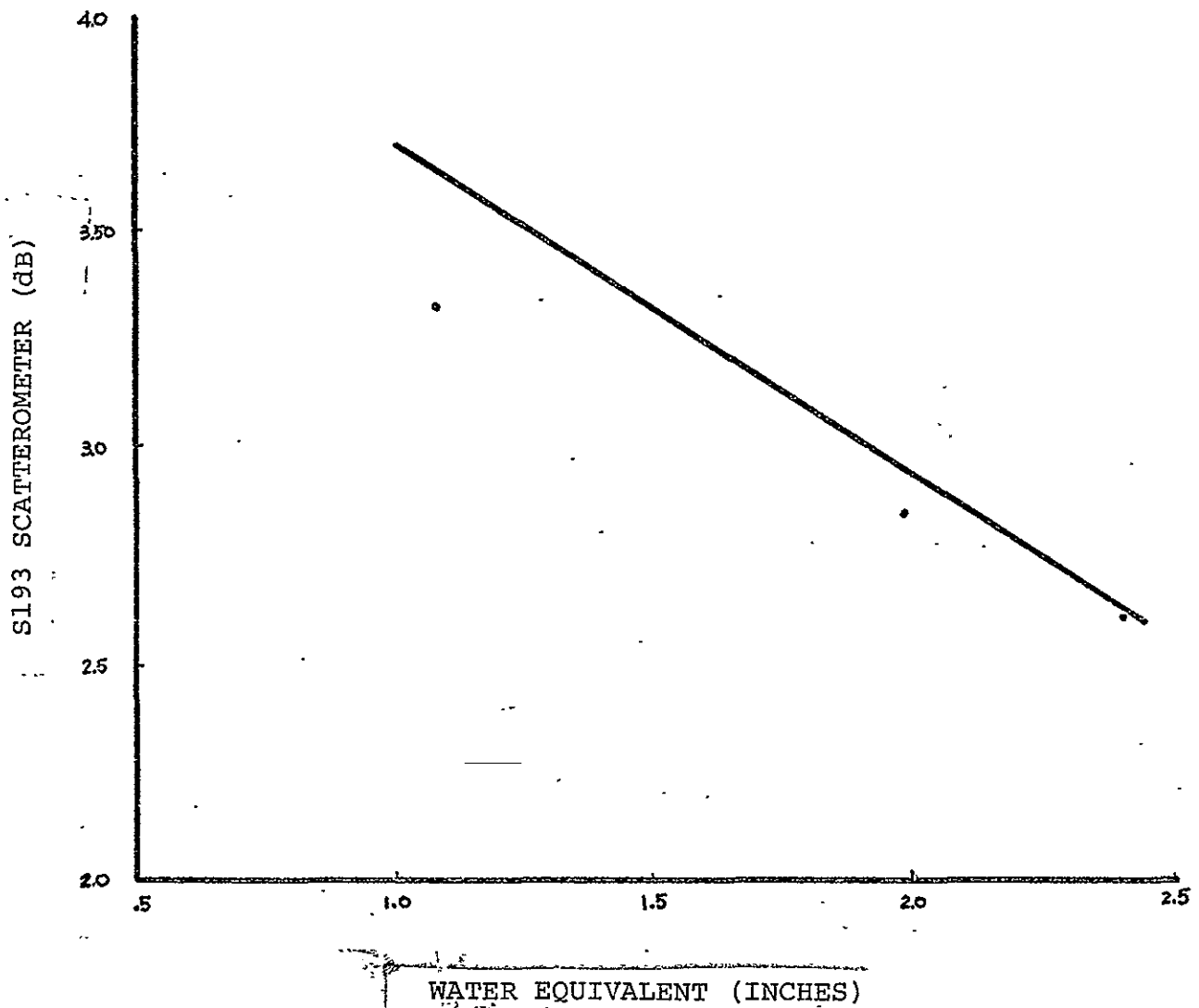
Figure 111 S193 scatterometer as a function of water equivalent (sub-freezing) on January 14, 1974 in Colorado-Nebraska (3 degrees)
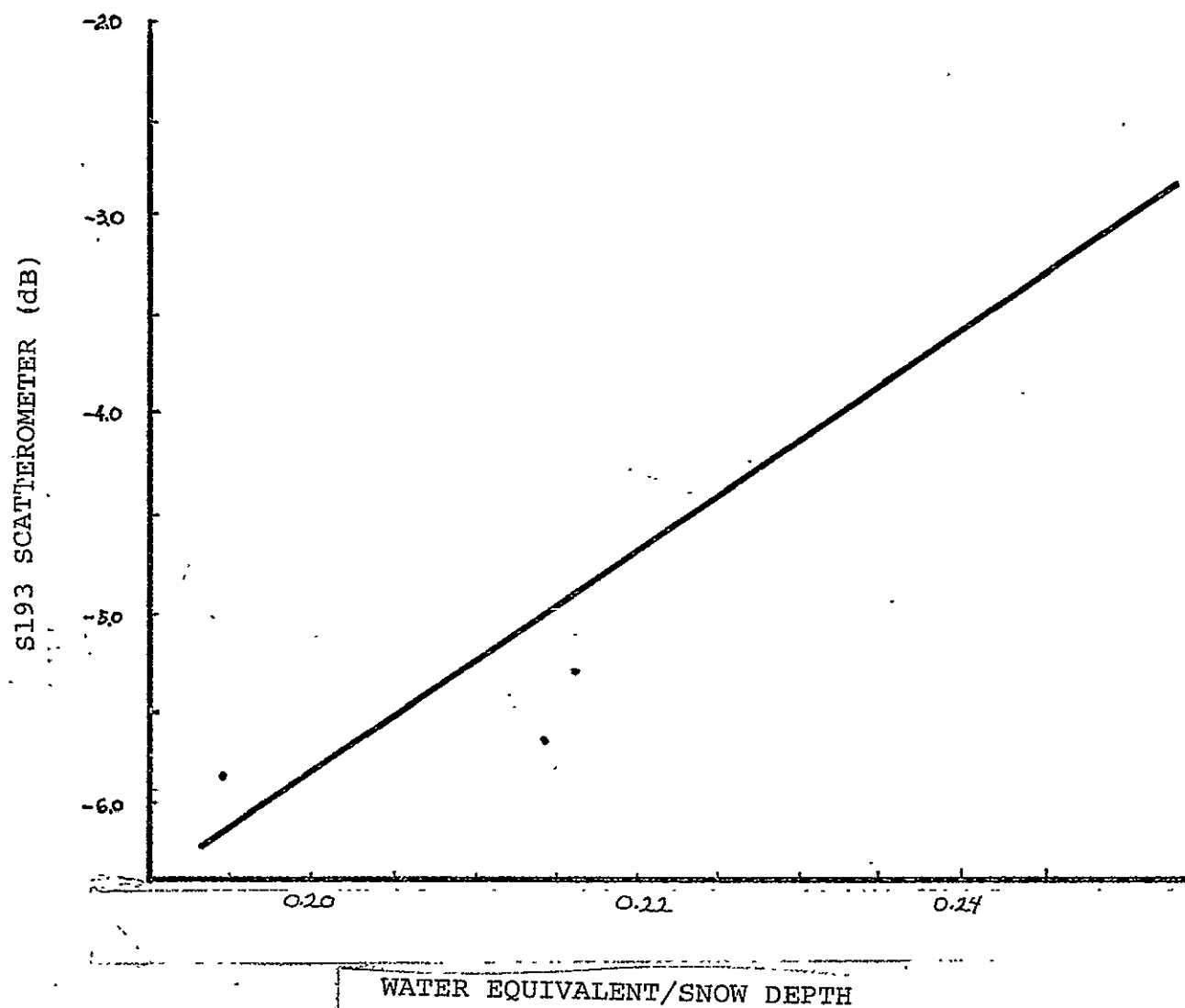
Figure 11.1   S193 scatterometer as a function of WE/SD (subfreezing) on January 14, 1974 in Colorado-Nebraska (14 degrees)

247

Table 16

Slopes calculated between the S193 Scatterometer and various
snow parameters obtained across the Kansas test site
area on 1/11/74 (sweep R-L)

Look Angle	0°	1°	3°	5°	9°
Snow depth	− .47	− .44	− 0.37	0.87	0.82
Water Equivalent	1.47	− 2.06	− 3.49	− 2.11	− 0.47
WE/SD	23.85	7.50	−30.95	−32.15	−19.41

Table 17

Slopes calculated between the S193 Scatterometer and various
snow parameters obtained across the Kansas test site
area on 1/11/74 (sweep L-R)

Look Angle	0°	1°	3°	5°
Snow depth	− 0.44	− 0.22	0.27	0.96
Water Equivalent	0.72	− 0.85	− 2.62	− 1.71
WE/SD	26.48	1.99	−31.20	−36.00

248

Table 18

Slopes calculated between the S193 Scatterometer and various
snow parameters obtained across the
Colorado-Nebraska test site area on 1/14/74

Look Angle	0°	2°	3°	5°	9°	14°
Snow depth	− 0.02	0.13	0.15	− 0.12	− 0.42	− 0.13
Water Equivalent	0.42	− 0.89	− 0.52	0.13	1.63	---
WE/SD	− 1.94	7.12	10.49	0.12	83.19	35.69

Table 19

Slopes calculated between the S193 Scatterometer
(subfreezing footprints) and various snow parameters obtained
across the Colorado-Nebraska test site area on 1/14/74

Look Angle	0°	2°	3°	5°	9°	14°
Snow depth	3.46	1.66	0.15	0.69	− 1.14	− 1.83
Water Equivalent	0.11	− 1.31	− 0.76	0.17	2.95	---
WE/SD	6.04	−13.63	−12.15	− 0.15	63.33	54.92

249

Table 20

Slopes calculated between the S193 Scatterometer
(superfreezing footprints) and various snow parameters obtained
across the Colorado-Nebraska test site area on 1/14/74

Look Angle	0°	2°	3°	5°	9°	14°
Snow depth	0.11	0.21	0.22	0.03	− 0.18	0.01
Water Equivalent	0.27	− 1.14	− 1.79	− 1.12	− 1.50	17.56
WE/SD	5.38	·9.89	32.47	33.15	3.80	− 4.22

Table ·21

Comparison among slopes (original, moment arm (1), moment arm (x));
S193 Scatterometer vs. snow depth obtained across
the Colorado-Nebraska test site area on 1/14/74

	Superfreezing			Subfreezing		
Slopes	·Orig	MA(1)	MA(x)	Orig	MA(1)	MA(x)
5°	0.03	0.16	0.23	0.69	0.10	0.08
9°	−0.18	−0.08	0.28	−1.14	0.03	0.06
14°	0.01	0.11	0.18	−1.83	0.01	0.03

Table 22

Comparison among slopes (original, moment arm (1), moment arm (x));
S193 Scatterometer vs. snow depth obtained across
the Kansas test area on 1/11/74

Slope	Orig	MA(1)	Correlation Coefficient	Orig	MA(1)
5°	.92	.73		.82	.78
9°	.82	.66		.82	.81
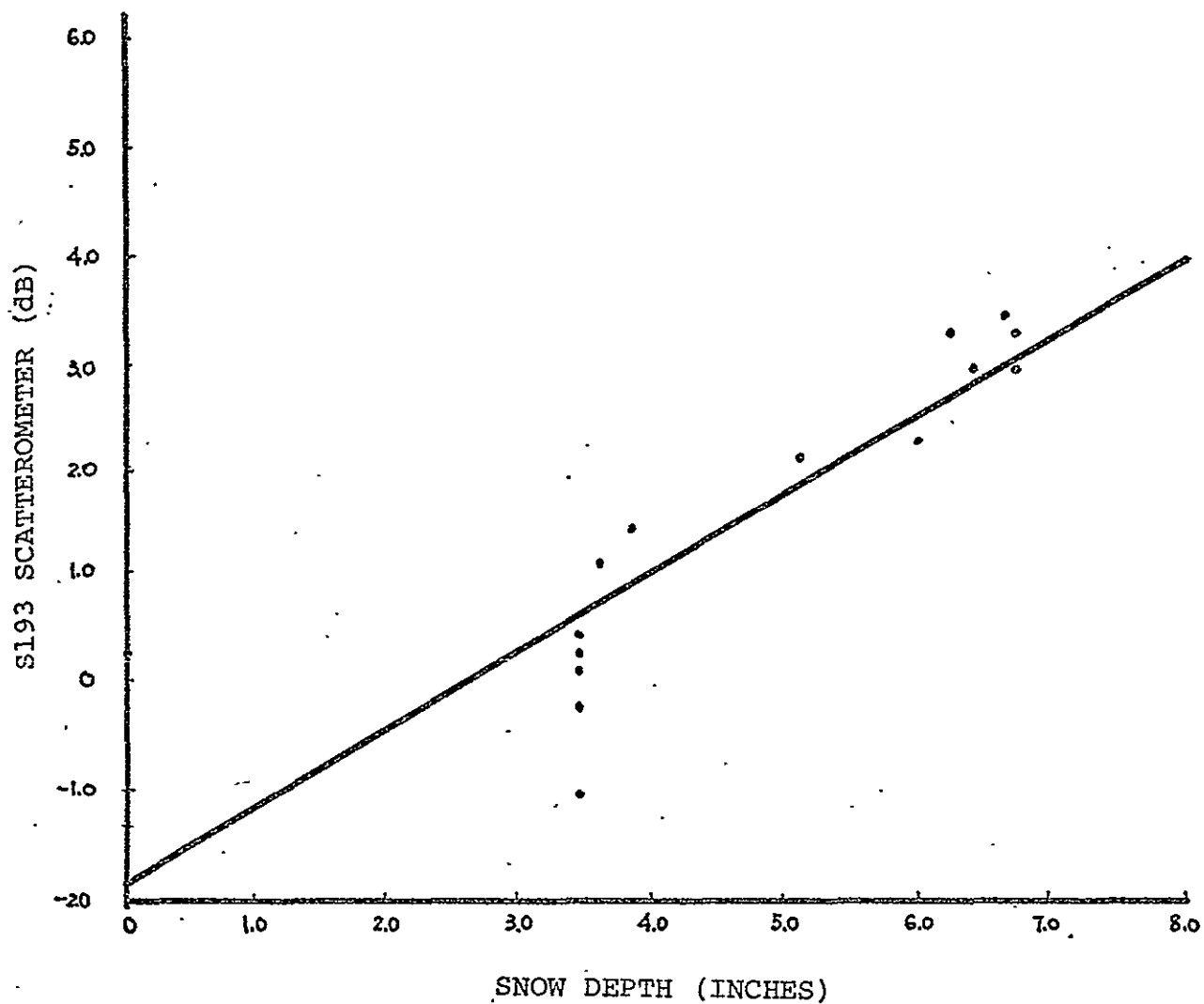
Figure 113 S193 scatterometer as a function of snow depth (moment arm 1)
on January 11, 1974 in Kansas (5 degrees)

252
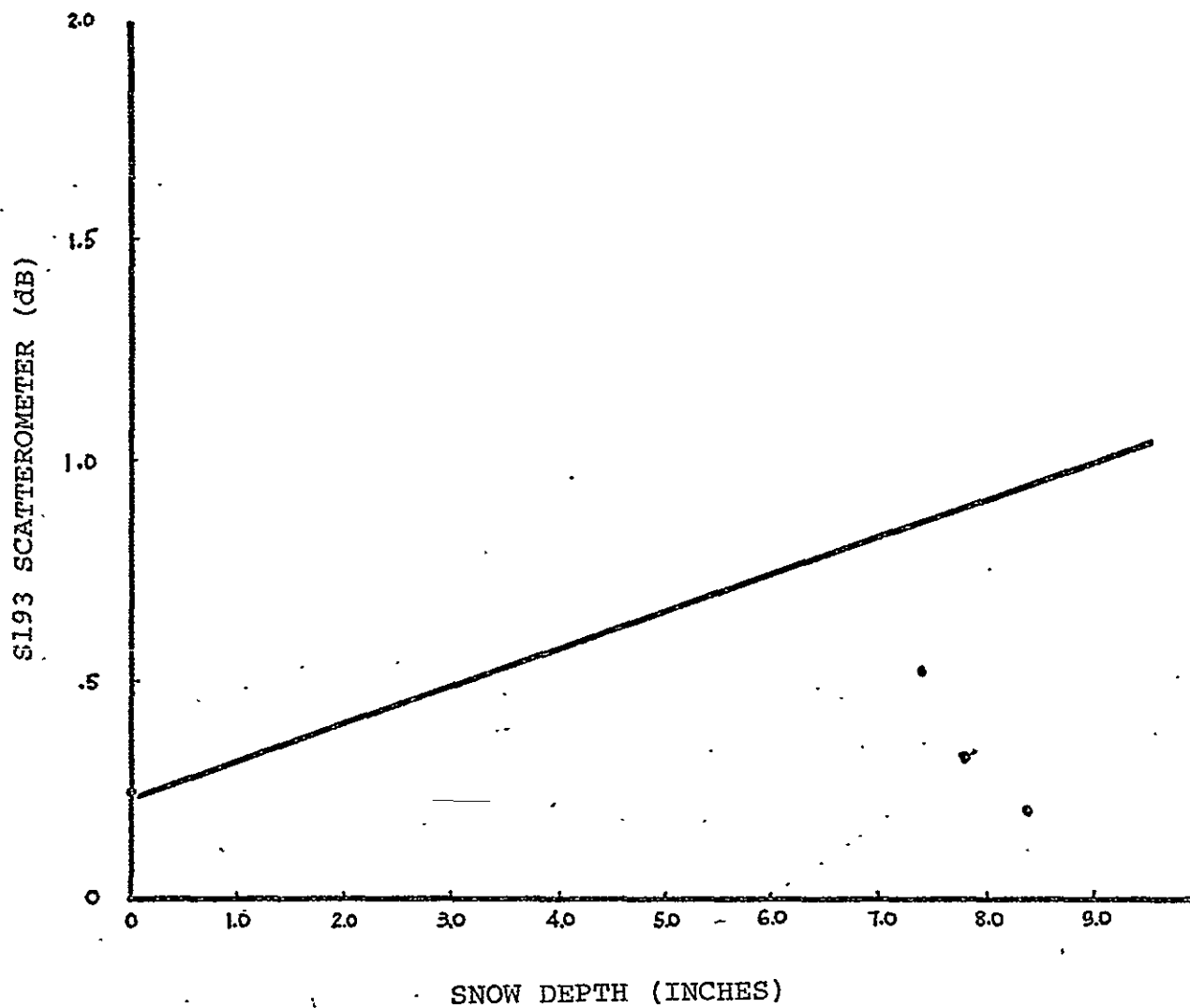
Figure 114   S193 scatterometer as a function of snow depth (moment arm X)
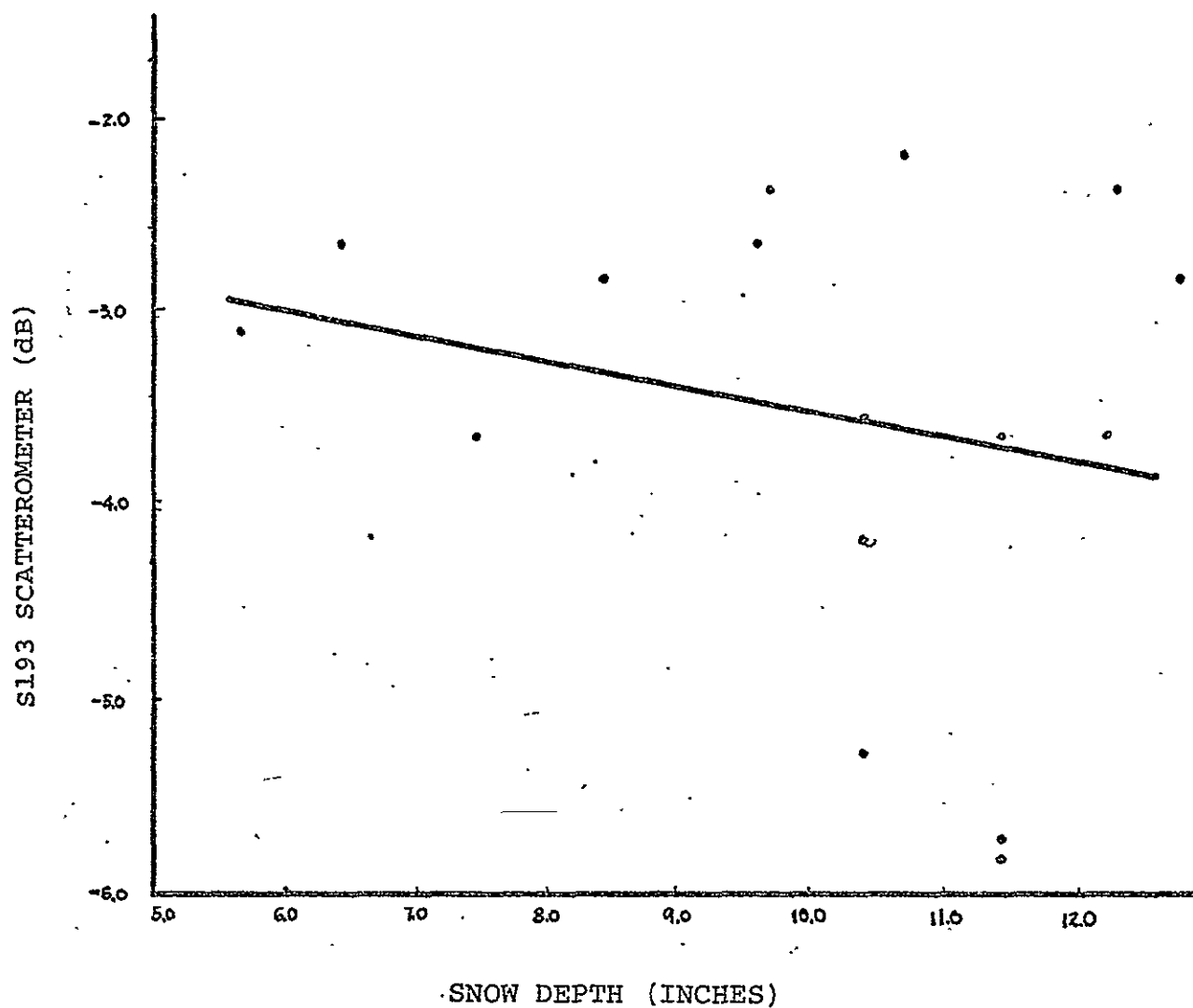   on January 14, 1974 in Colorado-Nebraska (subfreezing, 5 degrees)
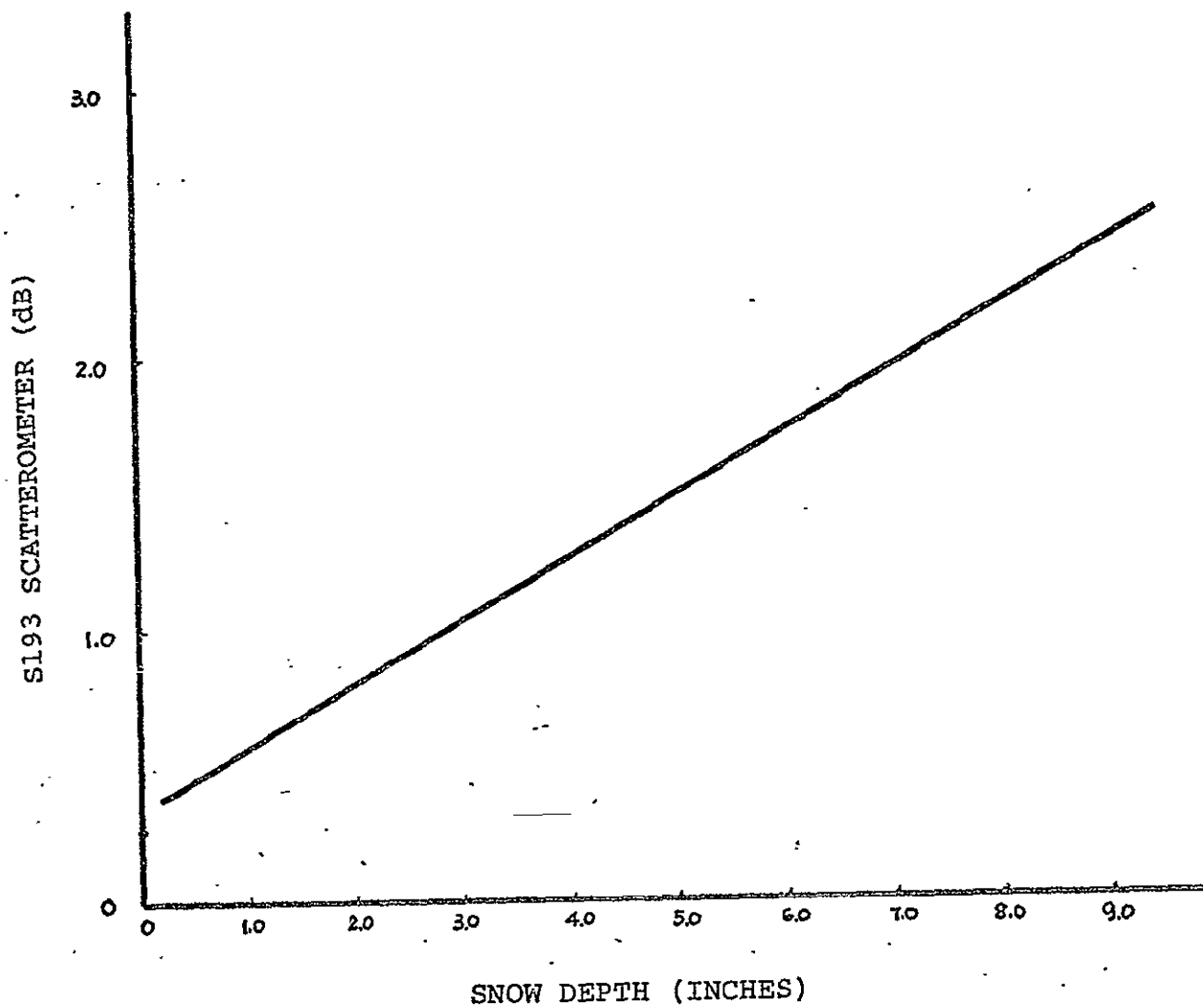
Figure 115 | S193 scatterometer as a function of snow depth (moment arm X)
on January 14, 1974 in Colorado-Nebraska (superfreezing,
5 degrees)

After the best possible corrections were made to the S193 scatterometer data sets, all data sets indicate a positive correlation between snow depth and scattering coefficient; the variability, however, of the relation seems so great that other factors are clearly important. The small size of the winter set severely hampered the attempts to determine the degree of correlation and almost completely precluded determining what other factors may be important. In the January 11 pass over Kansas, where a wide range of snow depths was available and the ground was cold and probably mostly frozen, the correlations at 5° and 9° seem quite good. In the Colorado -Nebraska pass on January 14, the correlations are not so consistent. In fact, if one uses the correlations based on only the small set of snow depths observed in the below-freezing part of the pass, the correlations are negative. This procedure, however, seemed inadequate because the lack of precision in snow depth estimates probably made the errors in these estimates as great as the spread of the data themselves. Consequently, a crude estimate, based on snowfree areas in the Texas panhandle was used to prepare a "best" value for the zero-snow-depth intercept to go with the deeper snow in Nebraska. Only when this value was used with a weight comparable to that assigned to the snow-covered areas did all the correlations become positive.

Thus, it appears that some snow-related quantity, perhaps

snow depth, is proportional to the scattering coefficient, so that future systems might be able to survey snow. In the Kansas area water equivalent/snow depth, a measure of per-unit density, also correlated positively with the scattering, but no meaningful correlation of this kind could be made in Nebraska, for the zero-snow value associated with this quantity would be indeterminate.

Although this first attempt at surveying snow from space with a radar is somewhat promising because of the positive correlations, the lack of sufficient data prevents drawing strong conclusions. More extensive experiments are clearly needed.

Since the S193 only operated at angles quite near vertical in these experiments, and because operational spacecraft imaging systems sill probably operate much farther from vertical, additional experiments in the other ranges of angle of incidence are particularly important. It is regrettable that difficulties with the scan mechanism on S193 prevented the planned experiments using about 30° incidence angle.

Chapter VIII

APPLICATIONS

Estimation of Soil Moisture
Using the S194 Radiometer

The composite relationship between the S194 bright-

ness temperature and soil moisture content for five different

Skylab passes across the two test sites shows that the

S194 L-band radiometer is quite sensitive to the moisture

content of soil. These passes were over different types

of terrain including variations in soil type, vegetation

type and amount, and soil moisture content; thus, these

data may be useful for the remote sensing of the soil mois-

ture content of large areas of the earth's surface. The

regression equation from Figure 61 is:

$$SM = 253.03 - 1.4898 \ T + 0.00210 \ T^2$$

where SM is soil moisture content in percent by weight and

T is the measured brightness temperature. This equation with

adjustments for differences in ground temperature was used

to estimate the distribution of soil moisture across the

United States along SL2 and SL3 tracks for several passes

(Figure 116). This figure illustrates the potential for

gaining quantitative information on the moisture content

of the earth's surface quite rapidly for large areas. The

values above 40% correspond to the Great Salt Lake and

257

June 13, 1973
August 8, 1973
September 13, 1973
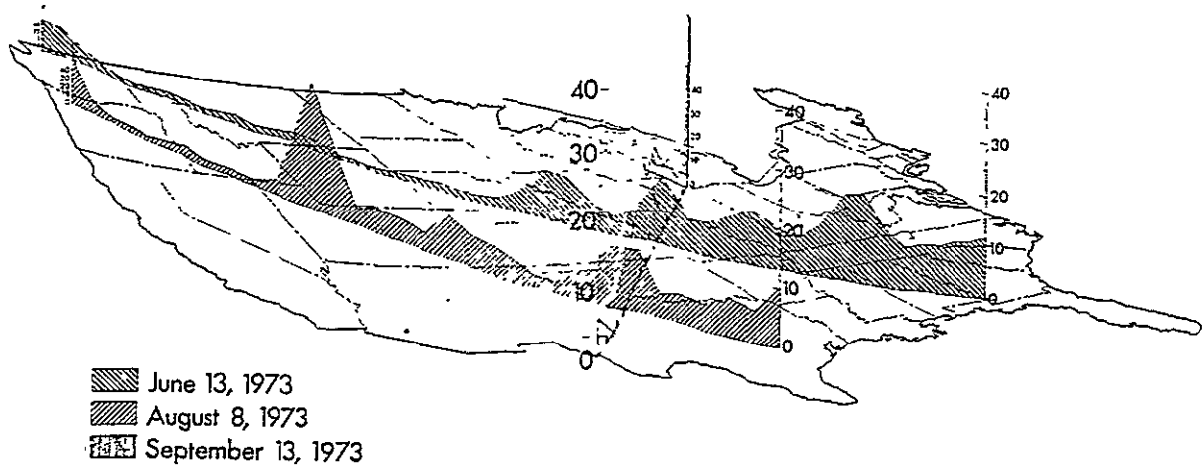
Figure 116   The distribution of soil moisture (% by weight)
              determined from Skylab's L-band radiometer for
              three passes across the United States.

Lake Michigan. The lowest values in the figure occur over the mountainous western states. These are the most questionable locations in this illustration, since roughness and slope of this magnitude may influence the results. However, the moistures indicated are similar to that anticipated from precipitation patterns. In fact, individual variations throughout the United States correspond closely to prior rainfall history.

These results indicate that an L-band radiometer operating from a satellite can be used for obtaining precise information on the near-surface moisture content. The implications are great in terms of utility to agricultural endeavors that depend on soil water resources, flood forecasting for large watersheds, as well as a host of other possible applications.

Estimation of Various Other Moisture Parameters
From S194 Data

The quantity of runoff produced by a storm depends on the moisture deficiency of the basin at the onset of rain and the storm characteristics, such as rainfall amount, intensity and duration. The storm characteristics can be determined from an adequate network of precipitation gages, but the direct determination of moisture conditions throughout the basin at the beginning of the storm is not feasible.

Because of the importance of this parameter, several indices have been used to establish the soil moisture conditions, i.e., ground water discharge, basin-accounting techniques from pan-evaporation or the climatic water balance, and the antecedent precipitation index (API). These approaches can only estimate relative values for soil moisture conditions. The microwave sensors have great potential for obtaining the soil moisture conditions of an area, since they responde to an average value of soil moisture content for the entire resolution cell which may be quite large.

An effort has been made to compare the S194 radiometric temperatures with several current estimation techniques for soil moisture, such as the API; calculated soil moisture content from the climatic water balance, and an aridity index. The weather stations, where both daily temperature and daily precipitation were recorded within 60 kilometers on either side of the Skylab track have been selected for pass 48 (Figure 117). There were a total of 150 weather stations for these calculations.

The most common index for initial moisture conditions for estimating the volume of storm runoff is based on antecedent precipitation. The form of characterizing the antecedent precipitation index (API) is:
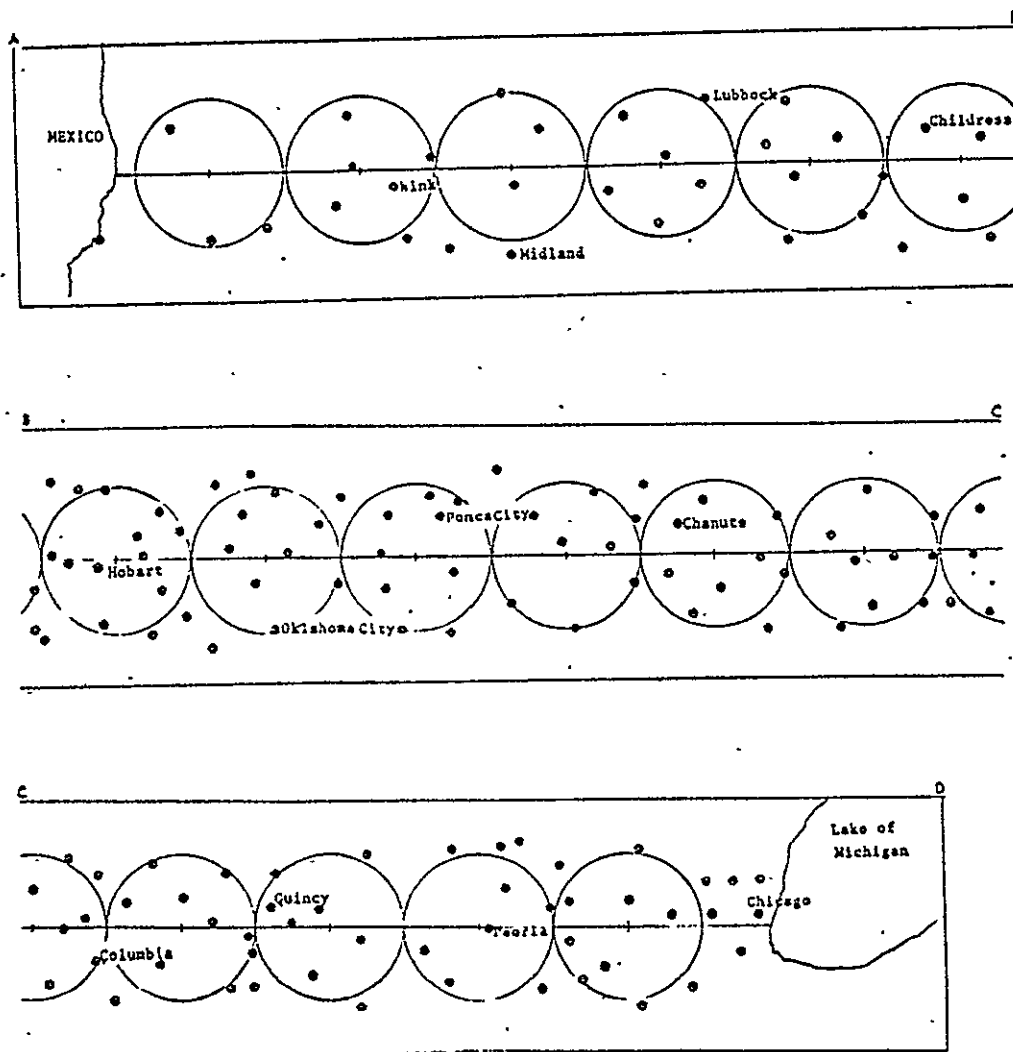
Figure 117   Location of the weather stations used in cal-
culations and corresponding S194 footprints.

$$API = \sum_{t=0}^{n} Pk^{t}$$

Where   k= Recession factor

               t= Number of days previous to the

                  Skylab pass

               p= Daily precipitation

The value of the index theorectically depends on precipitation over an infinite antecedent period, but the computed index will closely approach the true value within a few weeks. Thus the API has been computed for various antecedent periods. The value of k is related primarily to evapotranspiration. The actual evapotranspiration is a function of the potential value, the available moisture, soil type and vegetation cover.

The average API within the circular area of 115 km diameter was computed by the weighted factor of area for every 115 km from the border of Mexico to the Lake of Michigan along the track of pass 48. All footprints used in the analysis were independent in terms of the half-power resolution cell of the S194 radiometer. The average ground temperature in the half-power footprint ranged from 303 $^{\circ}$K to 288 $^{\circ}$K. The S194 radiometric temperatures were adjusted to a ground temperature of 293 $^{\circ}$K. The correlation coefficient and regression equations between average API and the S194 radiometric temperature are shown in Table 23. The k value of .9 and the 31-day antecedent period provided the best relationship (Figure 118) and will be used later for projections of this parameter.

Table 23
Correlation coefficients for the Skylab L-band radiometer
and various applications oriented soil moisture parameters

	k	t	Regression Equation	Standard Error	Correlation Coefficent
API	0.95	31	15.041 - 0.0546 AT	0.565	-0.82
	0.90	31	9.459 - 0.0343 AT	0.256	-0.90
	0.85	31	6.809 - 0.0249 AT	0.197	-0.88
	0.90	21	9.932 - 0.0364 AT	0.282	-0.89
	0.90	11	6.804 - 0.0250 AT	0.3007	-0.78
Estimated Soil Moisture	Eagleman's method		152.804 - 0.5550 AT	5.347	-0.84
	Thornthwaite's method		153.447 - 0.5555 AT	5.840	-0.82
AE/PE	0.90	31	32.518 - 0.11777 AT	0.833	-0.90
100(1-AE/PE)	0.90	31	-42.6764 + 0.2611 AT	3.472	0.75
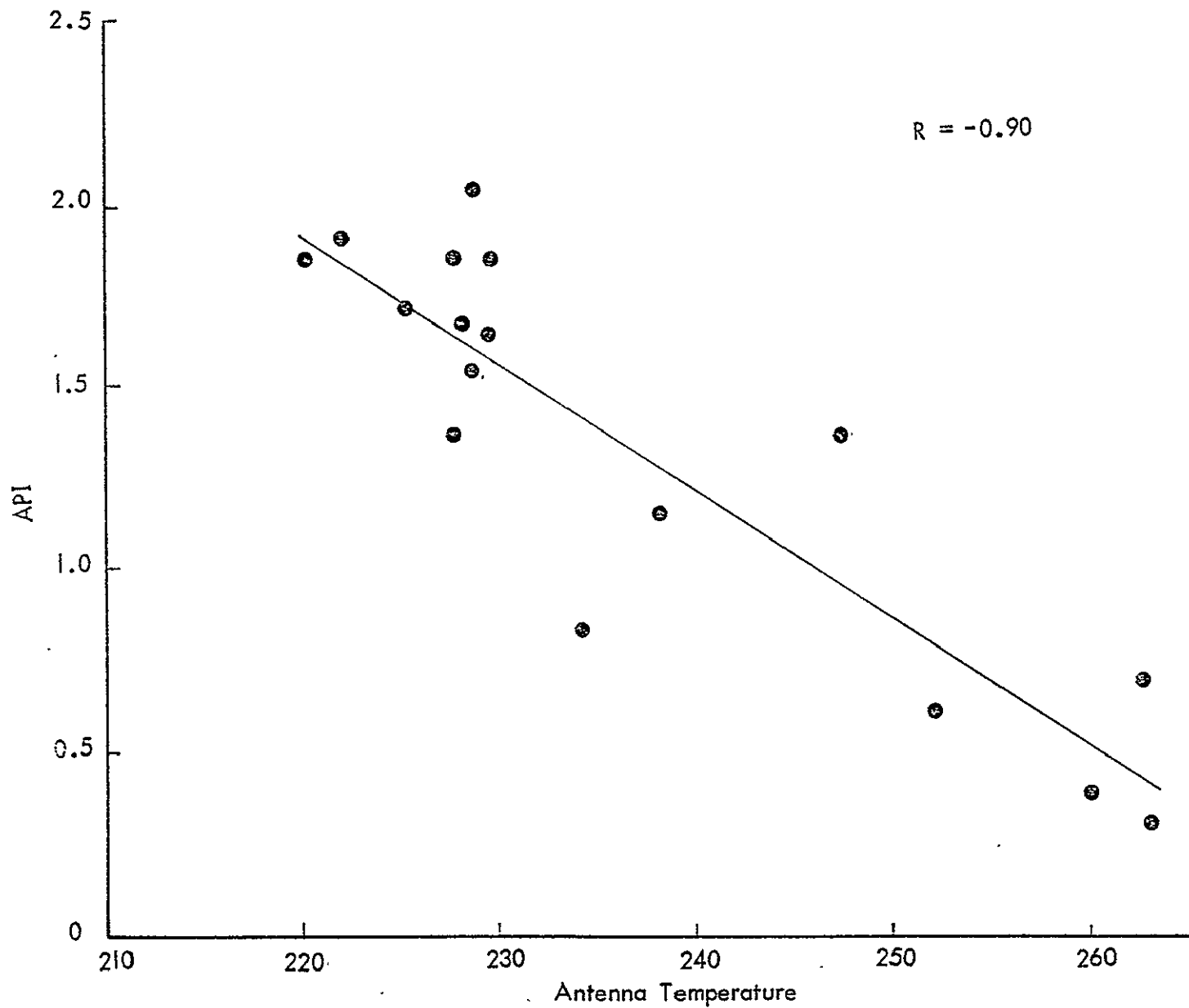
Figure 118   The relationship between the antecedent precipi-
tation index (API) and S194 antenna temperature.

The technique of calculating the water balance from climatic data on a daily basis provides a reasonably accurate estimate of soil moisture storage and can be used as an index to runoff and irrigation. This approach is laborious and it is difficult to collect the data of soil texture, vegetation cover and available water of the soil. This analysis used the Thornthwaite equation (1948) to estimate potential evapotranspiration (PE). The Thornthwaite-Mather method (1955) and the Eagleman method (1971) were used to estimate actual evapotranspiration (AE). The soil moisture content in percent by volume for the surface 15-cm layer was calculated for 150 stations. The average moisture content of each footprint was computed and related to the S194 antenna temperature. The correlation coefficient (-0.84) using Eagleman's method (Figure 119) was better than that for the Thornthwaite-Mather methods (-0.81) and was, therefore, used for projecting soil moisture from other Skylab passes. The available water of the soil was assigned on a regional basis depending on the soil type (Aandahl, 1972), since the specific available water for each station could not be obtained.

An aridity index (AI) was suggested by Eagleman (1975) which is defined:

$$AI = 100(1 - \frac{AE}{PE})$$

Where: AE = actual evapotranspiration

PE = potential evapotranspiration
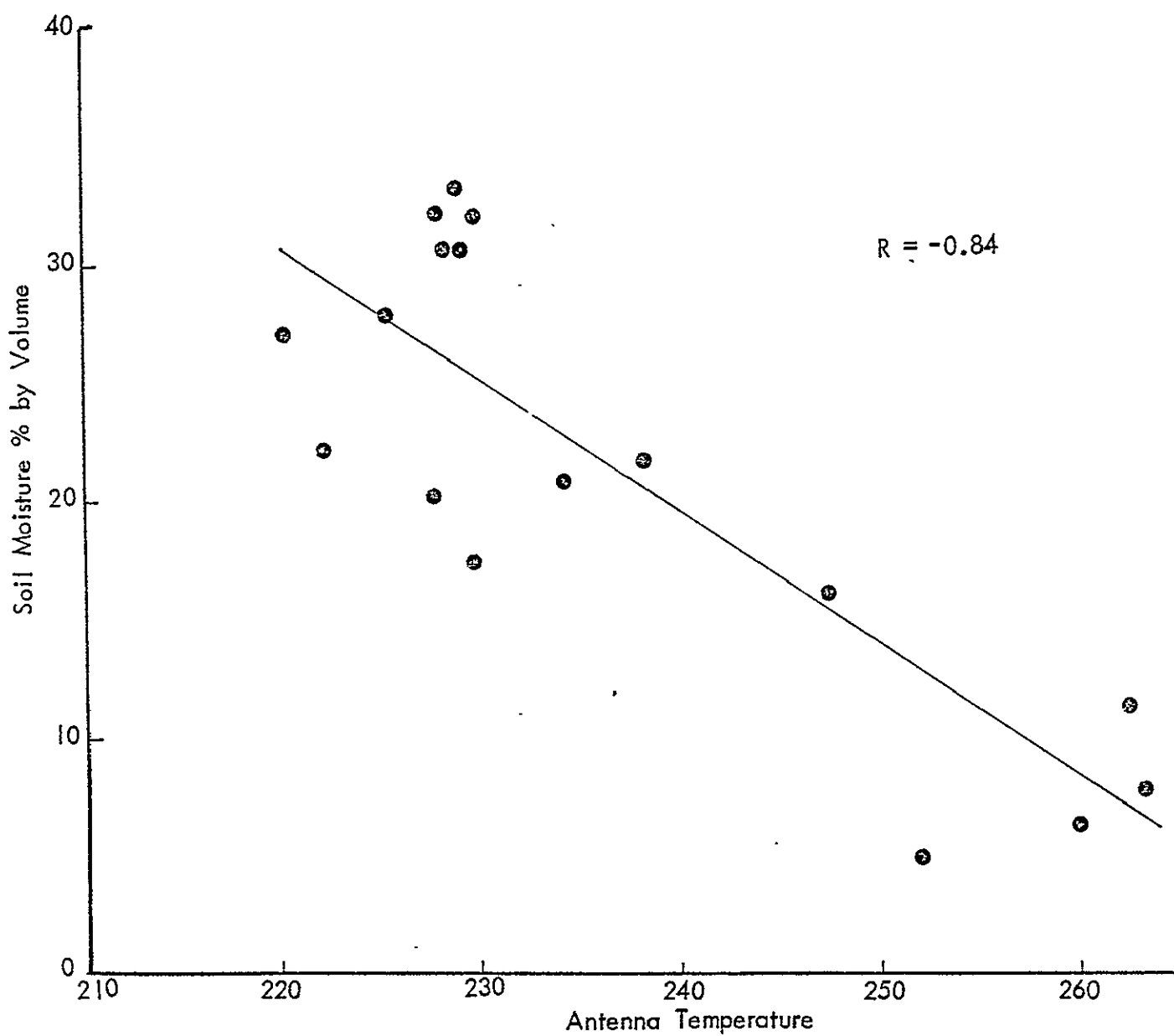
Figure 119   The relationship between the volumetric percentage
soil moisture calculated from climatic data and S194
antenna temperature.

Both AE and PE were calculated from the climatic water balance as described previously. The index provides a number between zero and one hundred which specifies the aridity of the location. An antecedent aridity index (AAI),

$$AAI = \sum_{t=0}^{30} AI\ 0.9^t$$

was used in this study to compare with the S194 antenna temperature. At the same time, a different antecedent aridity index (AAIX),

$$AAIX = \sum_{t=0}^{30} \frac{AE}{PE}\ 0.9^t$$

was also calculated. The correlation coefficient for AAI and the S194 antenna temperature was 0.75, and for AAIX was -0.90 (Figure 120).

The regression equations shown in Table XIV relating the S194 antenna temperature and the API using a k value of .9 and an antecedent period of 31 days, the soil moisture, percentage by volume, calculated by the methods of Thornthwaite (1948) and Eagleman (1971), and the antecedent aridity index were used, after adjustments for differences in ground temperature, to estimate distributions across the United States for passes 16 and 38. Soil moisture calculations are for the surface 15 cm layer. These distributions shown in Figures 121 and 122 illustrate the potential of the S194

267
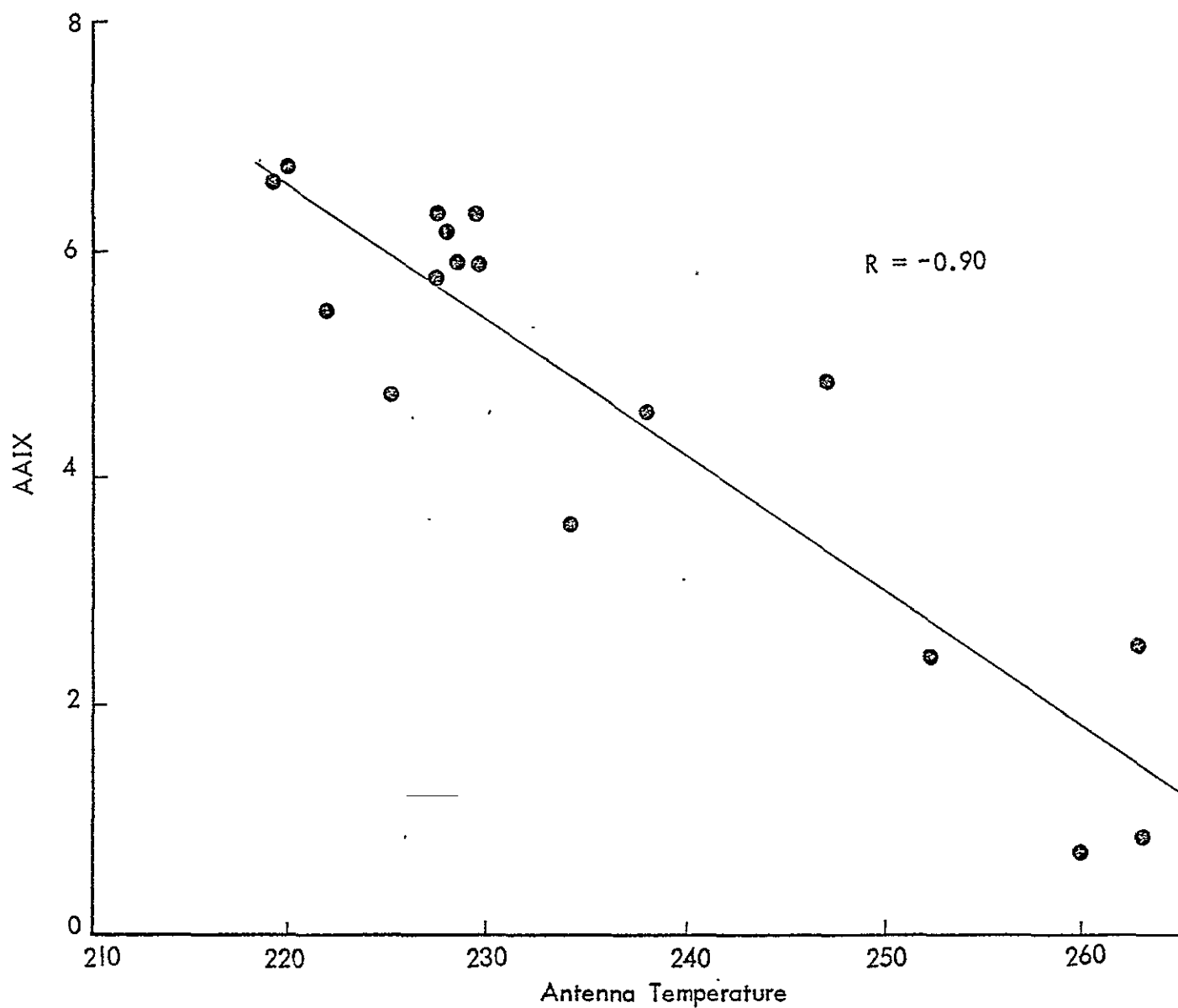
Figure 120 The relationship between the antecedent aridity
index (AAIX) and S194 antenna temperature.
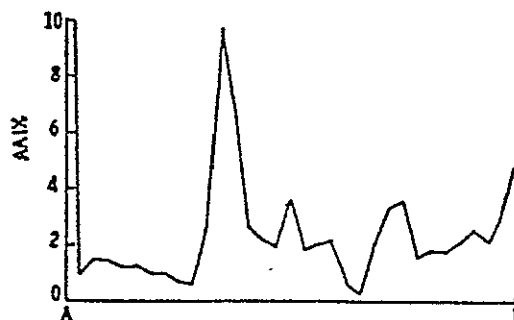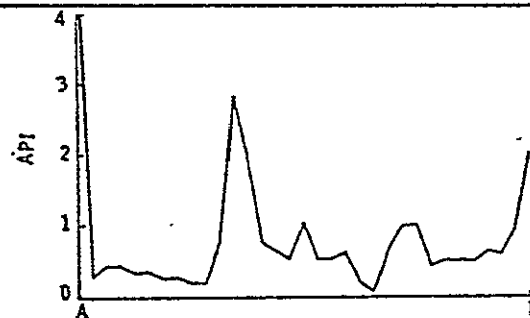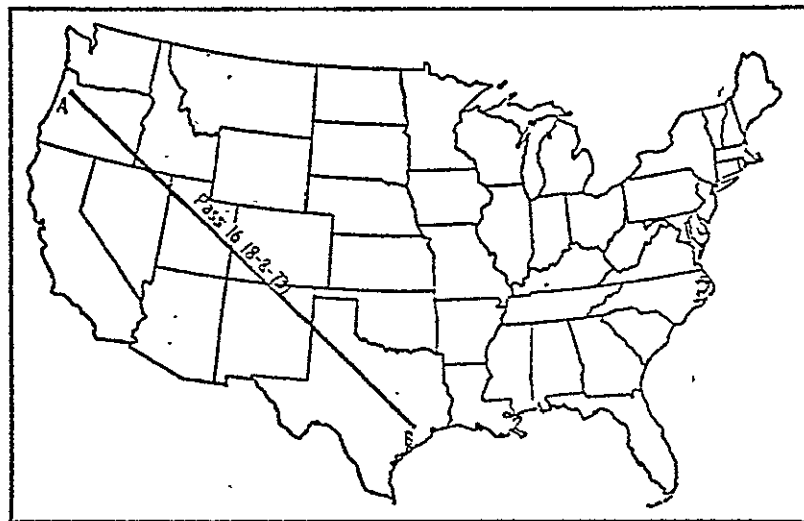
Figure 121   Calculated distributions of three different soil
moisture or aridity measures based on S194 antenna
temperature measured by Skylab pass 16.
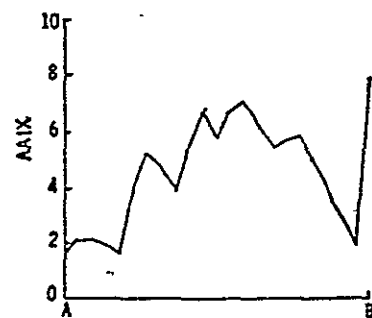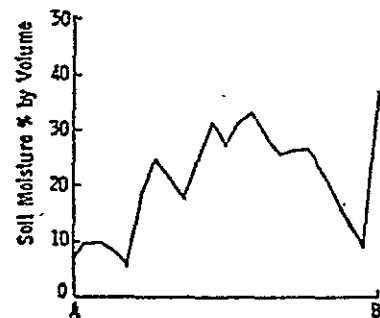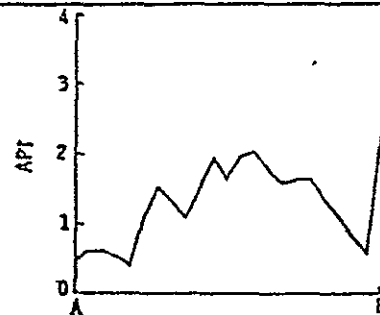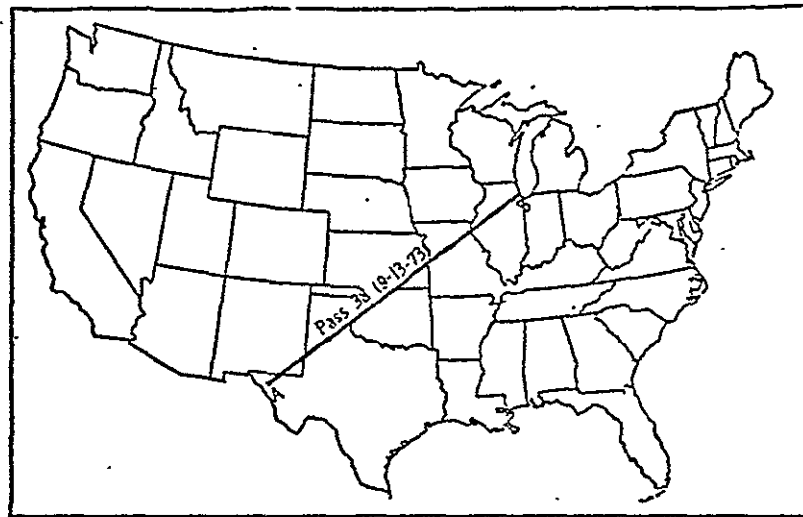
Figure 122 Calculated distributions of three different soil
moisture or aridity measures based on S194 antenna
temperatures measured by Skylab pass 38.

system for accessing regional moisture characteristics
whether the soil moisture parameter of interest is soil
moisture content, antecedent precipitation for flood fore-
casting or an aridity index describing the general dryness
of a region.

Economics of Remotely Sensed Soil Moisture Data

In addition to other disadvantages, direct measure-
ments of soil moisture are time consuming and costly. Our
experience in collecting the soil moisture data from the
field can be used for a comparison with the data collected
by Skylab. It required about 80 man hours in the field to
collect soil moisture information along 350 km of the Skylab
track. An additional 30 man hours were required in the
laboratory for weighing and drying the soil samples. Thus,
110 man hours were required for obtaining data along only
350 km of one of the Skylab tracks.

Consider the cost of obtaining direct soil moisture
measurements over the areas shown in Figure 101 for the
Skylab passes where the soil moisture content was determined
for three tracks across the United States. Skylab data
extended over about 9,210 km and would have required 2,894
man hours. At $5.00 per hour the cost would have been
$14,470 to obtain data by direct measurements for the area
covered in Figure 101. It should also be pointed out that
the coverage from the direct measurements would not be as

271

complete as the Skylab data since it correponds to the average soil moisture of a region; neither could the direct measurements all be taken at the same time. Add to this the potential for routinely measuring not only three strips across the United States but the whole area of the United States and it is easy to see why there is so much interest in remote sensing techniques.

Chapter IX

IMPLICATIONS FOR FUTURE SYSTEMS

The results of this study of the Skylab microwave sensors indicate that it is indeed possible to measure soil moisture over relatively large areas with reasonable precision by the use of microwave radiometers, and the precision is somewhat less with scatterometers, at least at 30° incidence angle and 13.9GHz, where the scatterometer data were available.

Surprisingly, when averaging is done over the kind of large area represented by the S194 footprint, the difference between 1.4 GHz of the S194 and 13.9GHz of the S193 radiometer response to soil moisture is not great. This was unexpected because it was thought that both the vegetation effects and the atmospheric effects would make the correlation between brightness temperature and soil moisture significantly poorer at the higher frequency. One may even assume that the results would be similar at the two frequencies if a correction were applied for the cloud and vegetation effects.

The use of the 29.4° pitch angle for the majority of the S193 scatterometer measurements of soil moisture was, in retrospect, unfortunate. At the time the angle was selected indications of the angular sensitivity of the scatterometer

soil moisture responses were based on a single measurement of irrigated and unirrigated fields (King and Moore, 1973); this experiment suggested that any angle out to about 40° would be satisfactory. Since that time, more extensive soil moisture measurements have been made (e.g., Ulaby, 1975) and it has been shown that angles of incidence should be kept under about 20° for soil moisture determination. Fortunately, the radiometer turns out to be less sensitive to angle of incidence, so the radiometric results at 30° were satisfactory.

Future systems that are to measure soil moisture must fall into at least two classes: those that determine soil moisture in very localized areas and those that are intended to provide the "big picture". Probably the first kind of measurement will be made with imaging radars because radiometers cannot be built to have fine resolutions at suitable frequencies. The results of the Skylab measurements show, however, that the second class of applications can be met with spaceborne radiometers.

Although the S194 demonstrated what can be done with a very poor resolution system, even with this resolution some sort of scanning would be needed for an operational system. If the operational system is to provide valid data, the repetition cycle should not exceed about six days, which means a swath width to be covered that is of the order of 600 km. In the case of a system with the resolution of the

S194 this means that the beam would have to have at least six positions across the track of the spacecraft to allow adequate coverage. Thus, a system as simple as the S194 itself would not be adequate even if this resolution were to be used.

The resolution cell for the S194 was too large to be of value for many applications, but it demonstrated the principle of sensing soil moisture and the smoothing effect in both ground truth and microwave data that comes from averaging over a large area. A cell about 1/4 the diameter of the S194 does however, appear to be useful for regional soil moisture studies, since it would be adequate to delineate regions about 25 km across and to identify boundaries between wet and dry soil regions to within a few kilometers. Thus, we recommend that a future soil moisture system have a resolution cell at least as good as 25 km across to the half-power points. A system may of course have much finer resolutions needed for other purposes and still be used for soil moisture measurement, either using its full resolution to produce a finer grain soil moisture map or averaging together many of its cells to produce a map of soil moisture like the one that would be produced using a 25 km diameter resolution cell.

For the radiometer the comparable quality of the results observed at 1.4 GHz and 13.8 GHz when the same resolution cell size was used indicates that the choice of microwave radiometer frequency for soil moisture measurement may not be as

critical as it was originally thought to be. Nevertheless,
the 13.9 GHz frequency is too high for such a sensor because
it is much more affected by the presence of clouds and rain
than a lower-frequency system would be. A frequency below
about 8 GHz seems called for because of the cloud and rain
effect. It will also be more useful in areas having heavier
vegetation than the test site for which S193 and S194 radio-
meters were compared with the same resolution cell size, since
part of the good performance of the S193 must surely have
been predicated on a less-than-lush vegetation cover, on the
average, over the large cells in Texas.

To produce a scanning radiometer requires either the
ability to scan a reflector or other antenna element mechani-
cally or the ability to scan an array electrically as with
the ESMR systems in Nimbus. A fixed antenna like that of
the S194 might be made large enough to give rather good
resolution even at 1.4 GHz, but a scanning antenna bigger
than about six meters square seems impractical. Thus, we
fix our attention on square arrays with electronic scanning
and with dimensions not to exceed six meters on a side. Table
24 shows the type of resolution that can be obtained normal
to the plane of an array of one, three or six meters on a
side at frequencies of 1.4, 5 and 14 GHz. These numbers
assume a spacecraft altitude of 500 km, and are scaled in
direct proportion to the altitude.

Table 24
500 Km, Resolution Cell Sizes at Vertical Incidence

Antenna size	14 GHz	5 GHz	1.4 GHz
1 m	10.7 km	30.0 km	107 km
3 m	3.6 km	10.0 km	36 km
6 m	1.8 km	5.0 km	18 km

The criterion of a 25 km diameter can be met at vertical by even a one meter antenna at 14 GHz, but it requires somewhat more than one meter at 5 GHz and it requires an antenna almost six meters on a side at 1.4 GHz. Of course the finer resolutions possible with the larger antenna could always be used to advantage. Hence, such a radiometer probably should have the largest antenna possible for a frequency of 1.4 or at the most, five GHz.

The design of a scatterometer for similar measurements cannot be predicated successfully on the data measured here. The correlation between scattering coefficient and soil moisture is definitely significant, but at the near-30° angles of incidence used in the passes analyzed, so many other factors entered into determining the return that the correlation is not high enough to justify such a sensor. The greater sensitivity of the scatterometer signal to vegetation at this angle of incidence is probably the culprit, for measurements on bare fields indicate that even at this angle, the correlation should be strong, and the correlation actually observed is high enough to indicate that this mechanism must indeed be working in a significant part of the data set.

Fortunately, since the beginning of the Skylab mission when the decisions were made regarding the parameters for S193 design and flight conditions, a great deal of information about soil moisture response of the scatterometer had been collected, for example, Ulaby (1975). The response is clearly quite strong under the right conditions; the conditions seem to be a frequency below about eight GHz, and an angle of incidence that is a function of the frequency but in any case should be under 20°, if possible.

A scatterometer for such a purpose could use a scanning antenna like that mentioned above for the radiometer, except that use of the two-way gain pattern would mean a reduction in illuminated diameter of about one third. On the other hand, radar systems need not use such large antennas. Thus, a radar can get by with an antenna large in only one dimension by using either a range measurement or a Doppler-frequency measurement to separate the cells in the direction along the beam. Since a radar may also use a synthetic aperture, it may achieve very fine resolutions not possible with a real aperture antenna. Thus, the greatest promise for the use of the active system lies not in duplicating a passive system with its bulky antenna but rather in taking advantage of the inherent ability of the radar to achieve resolution without as large a total aperture area as the radiometer needs.

As a consequence of these analyses of the situation, we believe that a future design for either an active or a passive

278

system should aim at the region near 1.4 GHz or 5 GHz at the most --the radiometer doing so to achieve reasonable resolution with a feasible antenna and the radar doing so because . this may be a near-optimum frequency when the various factors are considered. The radiometer design for such a system must have an antenna several meters in diameter with three meters being a good size for 5 GHz and six meters for the 1.4 GHz radiometer, to give resolutions comparable with those achieved by the S193. The scatterometer probably should not be a separate instrument, but rather should be included in a synthetic aperture imaging system that can produce resolutions fine enough to accomplish other water-resourse related tasks. Designs are presently being developed at Kansas University for a system that will be able to cover a wider swath than the usual synthetic-aperture system, this wider swath being important to obtain the frequently repeated coverage necessary for water problems.

Chapter. X

SUMMARY AND CONCLUSIONS

Although a number of interesting results have been
obtained by this investigation, the most significant result
is the good response of the passive radiometers, particularly
the L-band radiometer, to changing soil moisture conditions
near the surface of the earth. The Skylab soil moisture
experiment was designed to evaluate the ability of the various
microwave sensors on Skylab for their response to changing
soil moisture patterns on earth. The first step of the analysis
consisted of obtaining detailed soil moisture information
by direct measurement techniques on the ground at the time
Skylab was collecting data from space. Detailed soil moisture
information was collected from test sites in western Texas
and eastern Kansas for evaluating the response of the Skylab
microwave sensors. A total of 2,250 soil samples were collected
at 375 different sites and at six layers at each site so
that the moisture content of the surface to 15 cm was obtained
by 2.5 cm increments. The geographical distribution of soil
moisture patterns was obtained throughout the test sites
for comparison with the microwave sensors.

The response of the S194 L-band radiometer to changing
soil moisture conditions was very good for the five complete
data sets consisting of three passes across Texas and two
passes across Kansas. The comparisons between the L-band
radiometer and soil moisture content within the footprint

of the radiometer gave correlation coefficients ranging
from -0.99 to -0.95 for these five data sets. Two of these
passes were over the same general terrain of Texas so that
it could be established that the antenna temperatures were
responding to changing moisture conditions rather than some
other variable. The correlations between the L-band radiome-
ter and various layers beneath the surface was completed
for each of the 2.5 cm layers in order to evaluate the depth
of influence for the L-band radiometer. For these five
data sets the average moisture content within the top five
centimeters gave the best correlation with the antenna tem-
perature in one case. For all of the other four passes the
best correlation was obtained for the average moisture con-
tent in the top 2.5 cm of soil. This agreed very well with
skin depth calculations, and indicates that the effective
depth for determining the response of a radiometer is about
a third of the skin depth, a depth at which a plane wave
is attenuated to about half its power.

When data for the five different passes were combined,
the correlation between the S194 radiometric temperature
and soil moisture content remained quite high with a value
of -0.96. Therefore, these data indicate that the L-band
radiometer has a very high potential for being able to ac-
curately monitor the soil moisture content of the earth.
Using the established relationship between the L-band radiomet-
ric temperature and the moisture content of the surface

2.5 cm of soil, the soil moisture content variations across the United States were calculated, along with an aridity and antecedent precipitation index, for several different times during 1973 to illustrate the application of this instrument.

The performance of the S193 passive radiometer was less consistent than for the S194 L-band radiometer; however, one data set gave a very high correlation of -0.95. A further comparison between the two passive radiometers was conducted by averaging several of the S193 footprints so that the same area was compared with the soil moisture measurement as for the S194 footprint. For the same data the correlation between the S194 antenna temperature and the average moisture content was -0.996 in comparison to the S193 correlation which was -0.988 for this particular pass across Texas on June 5, 1973. It was therefore concluded that passive radiometers were quite sensitive to moisture content. This same comparison showed that the range in antenna temperatures was quite different for the two radiometers operating across the same test area. The longer wavelength S194 radiometer had a range in antenna temperature of 47°K compared to a range of only 16°K for the shorter wavelength S193 radiometer. Because of this response as well as the greater influence from clouds and vegetation upon the shorter wavelength radiometer, it would appear that the L-band radiometer would be the proper choice for a system designed

to measure the moisture content of the earth on an opera-
tional basis. For an operational system, an L-band radiometer
with a 15° conical scan would provide the ideal system for
earth monitoring from space, especially if the antenna could
be made large enough to give a smaller resolution cell than
for the Skylab radiometer. Although a resolution cell of
about 25 km would have considerable application in hydrology
and agriculture as well as in other areas, a smaller re-
solution of perhaps 10 km would be even better. An accurate
thermal radiation sensor should be a part of this system
in order to monitor, as accurately as possible, the surface
temperature during cloudless skies for comparisons between
areas with widely differing surface temperatures.

The scatterometer response to soil moisture at incidence
angles near 30° was not as good as for the radiometers.
Nevertheless, a correlation coefficient of 0.75 was obtained
when the effect of varying angle of incidence was removed.
In view of the more-recent ground-based measurements that
indicate a more suitable angle of incidence for the scatterome-
ter would have been in the neighborhood of 15°, and a lower
frequency would have been much better for soil moisture pur-
poses,the modest 0.75 correlation coefficient is encouraging,
but not conclusive, for the use of radar in soil moisture
determination since the only hope for obtaining fine resolution
is by using synthetic aperture radars.

The superior performance of the radiometers relative
to the radars for space observation of soil moisture, combined
with the possibility for finer resolutions only with radars,
suggests that future systems may well use combined radar-
radiometer systems in which the radiometer provides more
precise measures of the average soil moisture over larger
areas and the radar provides less precise moisture measure-
ment for small well defined points in space.

The analysis of Skylab photography has shown some
areas where the infrared bands of the S190A and S192 sensors
were able to segregate areas where soil moisture varied
significantly from adjacent areas. An area in Texas was
identified where a clay loam soil was surrounded by sandy
soils with a significantly different water holding capacity.
This area can be identified on the black and white infrared
and color infrared bands of the S190A and the black and
white infrared of the S192 system.

Direct measurements of subsurface soil moisture content
by optical and multispectral scanner data is impossible. Also
the presence of a vegetation cover completely shields any
soil moisture information by these methods. This means that
quantitative soil moisture information cannot be gathered
on a practical basis by optical or multispectral scanner
data. However, good quality high resolution optical and MSS
data can be used very effectively with microwave sensors
in order to increase the accuracy of soil moisture measure-
ments by using imagery as a means of providing vegetation

type and density information and by using a thermal band to collect and assemble surface temperature. The data would then supplement, effectively, data collected with microwave sensors.

The analysis of the aircraft data have shown that it is necessary to have ground truth information on an entirely different scale in order to calibrate or evaluate the aircraft sensor. For some applications it may be very important to have detailed variations of soil moisture in small areas. In this case, an L-band radiometer mounted in an airplane with the same angle and scanning system as for a satellite could provide important information because of the finer resolution system.

Two data sets were obtained for determining the microwave response to snow characteristics. The S193 scatterometer data indicated a positive correlation between snow depth and scattering coefficient; the variability, however, of the relationship seems so great that other factors are clearly important. The small amount of winter data severely hampered attempts to determine the degree of correlation and almost completely precluded determining what other factors may be important. Although this first attempt at surveying snow from space with a radar is somewhat promising the lack of sufficient data prevents drawing strong conclusions.

On the basis of the same two winter data sets it appears that the 21 cm passive radiometer possesses the capability

of locating the freeze-thaw line, and under certain circum-
stances reveals relative snow depth. However the S194
sensor is so sensitive to soil moisture differences that
snow depth variations may be secondary to changes in the
soil moisture beneath the snow. When the soil moisture
freezes, however, the snowpack's black body influence may
furnish the principal control over microwave emissivity
received by the S194 radiometer. If these microwave tech-
niques for determining the amount of snow pack can be
perfected they would be quite useful in river basin runoff
forecasting.

BIBLIOGRAPHY

Aandahl, Andrew R., 1972, "Soils of the Great Plains", University of Nebraska.

Barnes, J.C., C.J. Bowlye and D.A. Simmes, 1974, "Snow Studies Using Visible and Thermal IR Measurements from Earth Satellites", Advanced Concepts and Techniques in the Study of Snow and Ice Resources, National Academy of Sciences, pp 477-486.

Barnes, J.C., D.T. Chang and J.H. Willand, 1970, "Satellite Infrared Observation of Arctic Sea Ice", AIAA Paper no. 7-301, AIAA Earth Resources Observations and Information Systems Meeting, Annapolis, Maryland,.

Barnes, J.C., D.T. Chang and J.H. Willand, 1972a, "Image Enhancement Techniques for Improving Sea Ice Depiction in Satellite Infrared Data", Journal of Geophysical Research, Oceans and Atmospheric Edition, 77(3), pp. 453-462.

Benoit, Andre, 1968, "Signal Attenuation Due to Neutral Oxygen and Water Vapor, Rain and Clouds", the Microwave Journal, vol. 11, #11, pp 73-80.

Chen, S. and W. Peake, 1961, "Apparent Temperatures of Smooth and Rough Terrain", IRE Transaction on Antennas and Propagation, Col, AP-9, pp 567-572.

Cihlar, J. and F.T. Ulaby, 1974, "Dielectric Properties of Soil as a Function of Moisture Content", CRES Technical Report 177-47, University of Kansas Center for Research, Inc., Lawrence, Kansas..

Dickey, F., C. King, J. C. Holtzman, R. K. Moore, 1974, "Moisture Dependency of Radar Backscatter from irrigated and non-irrigated fields, IEEE Transactions on Geoscience Electronics, vol., GE-12 (1), pp 19-21.

Eagleman, Joe R., 1971, "An Experimentally Derived Model for Actual Evapotranspiration, Agricultural Meteorology, 8, pp 385-394.

Eagleman, Joe R., 1974, "Moisture Detection from Skylab", Proceedings, Ninth International Symposium on Remote Sensing, Environmental research Institute, Ann Arbor, Michigan, pp 701-705.

Eagleman, Joe R., 1975, Visualization of Climate, Lexington Books, Lexington, Mass. In Press.

Eagleman, J.R. and W. C. Lin, 1975, "Remote Sensing of Soil Moisture by an L-band Passive Radiometer", Submitted to Journal of Geophysical Research.

Eagleman, Joe R. and F. T. Ulaby, 1974, "Remote Sensing of Soil Moisture by Skylab Radiometer and Scatterometer Sensors", The Skylab Results, Advances in the Astronautical Sciences, vol. 31, The American Astronautical Society, Tarzana, California, p. 681.

Edgerton, A. T., R. M. Mandl, G. A. Poe, J.E. Jenkins, F. Soltis and S. Sakamoto, 1968, "Passive Microwave Measurements of Snow, Soils, and Snow-Ice-Water Systems", Technical Report # 4, Aerojet General Corp., El Monte, California.

Edgerton, A.T., A Stogryn and G. Poe, 1971, "Microwave Radiometric Investigations of Snowpack", Final Report No. 1285 R-4 for U.S.G.S. Contract No. 14-08-001-11828, Aerojet-General Corp., Microwave Division, El Monte, California.

Edgerton, A. T. and D. T. Trexler, 1970, "Passive Microwave Techniques Applied to Geologic Problems", Final Report 1361R-1 USGS Geological Division, Washington, D.C.

Evans, S., 1965, "Dielectric Properties of Ice and Snow", Journal of Glaciology, vol. 5, #42, pp 773-792.

Fung, A.K., 1965, "Scattering Theories and Radar Return", CRES Technical Report, 48-3, University of Kansas, Center for Research, Inc., Lawrence, Kansas.

Geiger, F.E. and D. Williams, 1972, "Dielectric Constants of Soils at Microwave Frequencies", Goddard Space Flight Center, Greenbelt, Maryland, 30 pp.

Hasted, J.B., 1961, "The Dielectric Properties of Water", Progress in Dielectrics, Vol. 3, New York, J. Wiley & Sons, Inc., pp 101-149.

Hipp, J.E.,1974, "Soil Electromagnet Parameters as a Function of Frequency, Soil Density and Soil Moisture", Proceedings of the IEEE, vol. 62, #1, pp 98-103.

Hoekstra, P. and A. Delaney, 1974, "Dielectric Properties of Soils at UHF and Microwave Frequencies", Journal of Geophysical Research, vol. 79, #11, pp 1699-1708.

Jean, R., 1971, "Selected Applications of Microwave Radiometric Techniques", Technical Report RSC-30, Remote Sensing Center, Texas A&M University, College Station, Texas.

Johnson, L.F., 1972, "On the Performance of Infrared Sensors in Earth Observations", Technical Report RSC-37, Remote Sensing Center, Texas A&M University, College Station, Texas.

Kennedy, J.M. and A.T. Edgerton, 1967, "Microwave Radiometric Sensing of Soil Moisture Content", IUGG, 14th General Assembly, September 27 to October 7.

King, C., 1973, "Agricultural Terrain Scatterometer Observations with Emphasis on Soil Moisture Variations",CRES Technical Report 177-44, University of Kansas, Lawrence, Kansas, 50 pp.

C, 4

King, C. and R.K. Moore, 1973,"A Survey of Terrain Radar Backscatter Measurement Programs", CRES Technical Report 243-2, University of Kansas, Lawrence, Kansas.

Lee, S.L., L974, "Dual Frequency Microwave Radiometer Measurements of Soil Moisture for Bare and Vegetated Rough Surfaces", Technical Report RSC-56, Texas A&M University, College Station, Texas, 211 pp.

Lundien, J.R., 1966, "Terrain Analysis by Electromagnetic Means", Technical Report 3-693, Report 2, US Army Engineer Waterways Experiment Station, Vicksburg, Mississippi, 55 pp.

MacDonald, H.C. and W.P. Waite, 1971, "Soil Moisture Detection with Imaging Radars, Water Resources Research, vol. 7, #1, pp 100-110.

Myers, V.I. et. al, 1970, "Soil,Water and Plant Relations, Remote Sensing with Special Reference ot Agriculture and Forestry, N.A.S., Washington, D.C., 424 pp.

NASA, 1971, EREP User's Handbook, Skylab A, NASA-S71-13209-F, Science Requirements and Operations Branch, Science and Applications Directorate, NASA Manned Spacecraft Center, Houston, Texas.

NASA, 1972, S193 Microwave Radiometer/Scatterometer Altimeter Flight Hardware Configuration Specification, Rev.C, General Electric Company, Spec. No. SVS 7846,

NASA, 1974, Sensor Performance Report, Vol 4 (S193 R/S), Skylab Program, Earth Resources Experiment Package, MSC-05528, NASA Lyndon B. Johnson Space Center, Houston, Texas.

NASA, 1974, "Sensor Performance Report, vol. 6, (S194), Skylab Program,", MSC-05528, Lyndon B. Johnson Space Center, Houston, Texas.

Newton, R.W., S.L. Lee and J.W. Ronse, Jr., 1974, "On the Feasibility of Remore Monitoring of Soil Moisture with Microwave Sensors", Proceedings of the Ninth International Symposium on Remote Sensing of Environment, Ann Arbor, Michigan, pp 725-738.

Palmer, W.C., 1965, "Meteorological Drought", Research paper no.45 US Dept. of Commerce, Weather Bureau, Government Printing Office, Washington, D.C. 58 p.

Peake, W.H., 1959, "Interaction of Electromagnetic Waves with Some Natural Surfaces", IRE Transactions on Antenna and Propagation, AP-7, pp S324-S329.

Poe, G.A., 1971, "Remote Sensing of the Near Surface Profile of Spectular Soils with Multifrequency Microwave Radiometer", Proceeding of Society of Photo-optical Instrumental Engineers, No. 27.

Poe, G.A. and A.T. Edgerton, 1971, "Determination of Soil Moisture Content with Airborne Microwave Radiometry", Final Tech. Report 4006R-1, US Dept. of Commerce, National Oceanic and Atmospheric Administration, National Environmental Satellite Service, Hill Crest Heights, Maryland.

Poe, G.A., A. Stogryn and A.T. Edgerton, 1971, "Determination of Soil Moisture Content Using Microwave Radiometry", Final Tech. Report 1684-1, Aerojet General Corp., El Monte, California.

Salter, P.J. and J.B. Williams, 1965, "The Influence of Texture on the Moisture Characteristics of Soils, II. Available-water Capacity and Moisture Release.Characteristics", Journal of Soil Science, 16(2), pp 310-317.

Schmugge, T., P. Gloersen, T. Wilhet and F. Geiger, 1974, "Remote·Sensing of Soil Moisture with Microwave Radiometers", Journal of Geophysical Research, #79, pp 137-323.

Schmugge, T., P. Gloersen, T. Wilheit, 1972, "Remote Sensing of Soil Moisture With Microwave Radiometers", Goddard Space Center, Greenbelt, Maryland, Preprint X-652-72-305.

Schmugge, T., T.T. Wilheit, P. Gloerson, M.F. Meier, D. Frankand I.Dirmhirn , 1974, "Microwave Signatures of Snow and Fresh Water Ice", Advanced Concepts and Techniques in the Study of Snow and Ice Resources, an Interdisciplinary Symposium, Asilomar Conference Grounds, Monterey, California, December 2-6, National Academy of Sciences, Washington, D.C..

Sibley, T.G., 1973, "Microwave Emission and Scattering from Vegetated Terrain", Technical Report RSC-44,,Remote Sensing Center, Texas A&M University, College Station, Texas, 148 pp.

Skolnik, M.I., 1962, Introduction to Radar Systems, New York, McGraw-Hill Book Co.

Skolnik, M.E., ed., 1970, The Radar Handbook, New York, McGraw-Hill Book Co.

Sobti, A., 1973, "A Simulation Study of the S193 RADSCAT in Orbit", CRES Technical Report 190-2, University of Kansas Center for Research, Inc., Lawrence, Kansas.

Stogryn, A., 1967, "Electromagnetic Scattering from Rough Finitely Conducting Surfaces", Radio Science, vol 2, pp 415-428.

Teschanskii, Y.I., G.N. Lebedeve and V.D. Shumilin, 1971, "Electricheskie Parametry peschanage i glimstage gruntav v diapagone santimetrouych, decimetrougab i metrorych redn. I zversiga Vysskikh Uchegorgh Zavedenig, Radiofiziko 14(40), pp 562-569.

Thornthwaite, C.W., 1948, "An Approach Toward A Rational Classification of Climate", Geographical Review, 38, pp 55-94.

Thornthwaite, C.W. and C.W. Mather, 1957, "Instructions and Tables for Computing Potential Evapotranspiration and Water Balance", Publications in Climatology, 10(3), pp 185-311.

Ulaby, F.T., 1975, "Radar Response to Vegetation", IEEE Transactions on Antennas and Propagation, vol. AP-23, pp 36-45.

Ulaby, F.T., 1974, "Radar Measurement of Soil Moisture Content", IEEE Transactions on Antennas and Propagation, vol AP-22, pp 257-265.

Ulaby, F. T., J. Cihlar, and R. K. Moore, 1974, "Active Microwave Measurements of Soil Water Content", Remote Sensing of Environment, vol. 3, pp. 185-203.

UNESCO, International Classification and Mapping of Vegetation, UNESCO, Paris, France, 1973, 93 p.

USDA, 1964, Cochran County, "Soil Conservation Service, Series 1960, No. 17, USGPO, Washington, D.C., 80 pp.

USDA, 1964, Yoakum County, Soil Conservation Service, Series 1960, No. 15, USGPO, Washington, D.C., 53 pp.

Waite, W.P. and H.C.MacDonald, 1970, "Snowfield Mapping with K-Band Radar", Remote Sensing of Environment, vol.1, no.2.

Ward, S.H., G.R. Jiracek and W. I. Linlor, 1969, "Some Factors Affecting Electromagnetic Detection of Lunar Subsurface Water", IEEE Transactions on Geoscience Electronics, vol GE-7, pp 19-27.

Wiebe, M.L., 1971, "Laboratory Measurements of the Complex Dielectric Constant of Soils", Technical Report RSC-23, Texas A&M University, College Station, Texas, 19p.

Wiesnet, D.R., 1974, "The Role of Satellites in Snow and Ice Measurements", Advanced Concepts and Techniques in the Study of Snow and Ice Resources, National Academy of Sciences, pp 447-456.

APPENDIX I

SOIL MOISTURE MEASUREMENTS

(See Figures 6 to·11 for site locations)

.

Field Measurements of Soil Moisture
In Percent by Weight
For Pass 5

Date	Site No.	0-2.5 cm	2.5-5.0 cm	5.0-7.5 cm	7.5-10 cm	10-12.5cm	12.5-15 cm
6/5/73	1	2.9	4.6	9.4	11.5	13.4	13.8
	2	5.9	13.3	14.8	14.9	15.0	15.1
	3	3.7	11.2	15.4	16.4	16.7	18.2
	4	21.1	23.6	26.2	22.7	20.7	21.71
	5	6.3	10.1	15.3	14.7	16.0	19.8
	6	5.1	9.7	12.0	15.6	I4.9	16.2
	7	5.3	13.3	17.1	17.3	17.7	18.1
	8	5.7	10.4	13.6	21.3	16.5	20.7
	9	4.0	10.6	13.3	15.0	16.9	17.4
	10	4.6	11.4	17.8	19.3	18.9	18.9
	11	0.7	1.7	2.7	8.9	8.3	7.7
	12	13.5	22.3	32.8	37.1	33.4	33.01
	13	2.5	4.4	9.2	10.0	9.8	10.3
	14	1.9	2.7	4.8	5.7	6.1	6.4
	15	2.6	5.9	7.5	6.6	8.8	10.5
	16	2.6	4.6	4.5	6.1	9.2	6.1
	17	2.4	3.1	5.0	8.9	9.6	9.7
	18	0.8	1.4	1.5	3.0	6.2	7.2
	19	1.1	1.9	3.4	7.9	9.7	10.6
	20	0.6	1.4	3.8	8.3	8.5	6.0
	21	0.4	0.6	0.7	1.0	2.6	3.0
	22	2.0	3.8	7.9	11.3	11.2	11.5
	23	1.2	3.0	5.7	7.2	6.8	6.6

Date	Site No.	0-2.5 cm	2.5-5.0 cm	5.0-7.5 cm	7.5-10 cm	10-12.5cm	12.5-15 cm
	24	1.3	4.5	6.2	6.7	7.8	8.0
	25	3.2	1.8	3.1	4.1	4.4	3.4
	26	5.0	8.2	10.4	10.8	10.5	11.2
	27	1.2	2.4	3.5	5.1	6.3	6.0
	28	1.8	4.6	6.7	9.3	13.2	13.8
	29	2.8	5.8	9.0	13.4	14.2	10.8
	30	1.8	6.5	11.1	14.6	15.8	14.4
	31	4.1	8.3	9.1	8.5	10.1	11.9
	32	2.2	7.8	11.7	11.1	11.2	10.5
	33	2.6	2.3	9.7	9.7	9.3	8.8
	34	2.2	5.0	10.7	6.2	]6.6	6.8
	35	9.3	14.2	16.1	16.9	16.7	15.5
	36	13.7	15.9	11.6	13.7	13.5	9.0
	37	4.9	14.9	16.2	16.6	16.8	16.1
	38	3.1	9.2	11.5	13.2	13.4	13.9
	39	3.1	9.3	12.2	12.2	11.7	12.6
	40	4.0	12.2	14.0	16.0	16.8	16.0
	41	8.2	7.5	7.2	8.1	9.4	9.6
	42	12.9	13.4	12.7	13.2	10.5	9.7
	43	4.7	6.2	4.3	4.1	4.0	4.0
	44	4.2	5.4	6.0	6.5	6.6	5.7
	45	2.4	4.7	4.1	5.1	4.3	5.9
	46	4.0	7.0	8.4	11.4	11.6	12.1
6/6/73	47	16.5	17.8	17.2	14.8	14.8	12.9
	48	35.0	28.6	26.6	25.9	26.0	24.61
	49	18.6	18.7	19.4	19.2	18.3	20.01

Date	Site No.	0-2.5 cm	2.5-5.0 cm	5.0-7.5 cm	7.5-10 cm	10-12.5cm	12.5-15 cm
	50	6.3	9.0	9.6	12.2	11.6	9.2
	51	8.4	21.8	9.4	10.6	10.7	9.4
	52	23.6	19.5	16.6	15.4	14.9	14.4
	53	4.8	5.0	4.7	3.6	4.3	4.8
	54	9.5	16.3	15.2	14.4	12.2	13.1
	55	13.6	15.8	15.2	15.8	15.7	17.8
	56	26.9	26.4	25.5	24.5	25.6	26.0
	57	7.7	10.8	9.9	11.7	10.0	9.3
	58	25.1	21.9	21.0	23.5	23.7	42.0
	59	13.9	13.1	13.5	14.9	15.6	15.8
	60	19.3	19.7	22.7	22.2	23.7	23.3
	61	17.2	17.1	15.6	16.7	17.9	19.3
	62	19.0	22.1	25.1	26.0	23.8	25.6
	63	34.2	34.3	33.3	36.3	36.5	36.1
	64	39.9	35.3	33.6	33.0	34.0	33.8
	65	23.5	23.6	22.0	22.6	22.5	22.5
	66	10.4	20.1	20.6	20.4	20.1	16.3

Field Measurements of Soil Moisture
In Percent by Weight
For Pass 10

Date	Site No.	0-2.5 cm	2.5-5.0 cm	5.0-7.5 cm	7.5-10 cm	10-12.5cm	12.5-15 cm
6/13/73	1	19.4	17.7	28.2	21.1	18.5	18.0
	2	28.7	29.3	24.0	24.6	24.8	24.8
	3	25.7	26.7	27.7	27.3	25.0	24.9
	4	22.6	23.6	22.9	20.1	19.8	20.1
	5	20.5	21.9	22.6	22.0	20.5	19.3
	6	19.1	20.9	19.6	18.1	20.2	18.7
	7	31.2	26.9	20.9	21.5	17.4	15.3
	8	41.0	40.4	32.3	30.7	29.4	25.4
	9	30.7	32.5	23.5	13.7	19.5	20.5
	10	30.4	24.7	22.8	22.8	18.1	16.5
	11	23.1	21.7	20.0	22.2	24.5	23.4
	12	20.6	7.2	8.6	8.6	8.6	7.8
	13	23.7	22.5	21.1	22.9	24.7	28.5
	14	27.4	30.8	27.5	29.8	29.0	30.0
	15	37.4	30.2	24.2	25.7	28.1	28.5
	16	39.7	39.8	36.0	32.2	28.6	19.5
	17	37.8	35.0	36.0	31.9	32.9	34.2
	18	36.1	34.8	34.3	32.4	34.2	36.8
	19	30.9	32.7	31.3	29.9	28.9	28.5
	20	44.3	42.2	41.1	41.1	38.8	37.9
	21	52.9	35.2	28.3	25.0	25.4	28.0
	22	17.0	23.4	26.1	26.6	28.0	27.3
	23	13.3	13.4	14.6	16.7	19.1	21.0

Date	Site No.	0-2.5 cm	2.5-5.0 cm	5.0-7.5 cm	7.5-10 cm	10-12.5cm	12.5-15 cm
	24	21.0	16.8	22.6	20.0	20.7	21.6
	25	7.2	10.9	17.9	18.8	18.3	17.9
	26	9.6	14.6	16.1	18.1	18.1	18.7
	27	10.0	16.8	19.2	19.1	20.1	22.1
	28	16.8	20.5	20.7	21.8	21.3	23.8
	29	19.9	12.8	24.0	25.6	26.5	27.1
	30	13.8	18.5	17.0	17.3	17.9	17.5
	31	7.0	12.0	14.7	15.5	15.5	15.6
	32	7.5	15.6	21.0	19.2	22.5	23.7
	33	12.9	14.0	17.9	19.2	19.3	22.9
	34	10.1	15.9	14.4	14.0	14.0	13.7
	35	12.1	19.3	24.2	35.9	47.4	49.7
	36	19.9	18.4	18.0	18.8	18.3	18.9
	37	6.0	13.3	29.3	27.8	30.9	30.8
	38	12.7	15.0	18.1	23.5	26.4	28.3
	39	5.7	8.6	16.7	18.9	21.2	21.8
	40	15.7	21.0	25.4	26.2	28.4	28.2
	41	32.2	39.3	37.7	35.5	33.6	32.2
	42	39.5	35.6	33.9	31.0	25.4	20.2

Field Measurements of Soil Moisture
In Percent by Weight
For Pass 16

Date	Site No.	0-2.5 cm	2.5-5.0 cm	5.0-7.5 cm	7.5-10 cm	10-12.5cm	12.5-15 cm
8/7/73	1	1.3	4.0	2.5	3.0	3.0	3.6
	2	7.3	19.6	21.8	24.0	28.2	28.1
	3	1.6	2.1	]2.7	3.6	4.0	5.0
	4	5.3	12.0	11.0	11.6	13.3	13.1
	5	2.9	3.6	4.4	6.3	7.6	8.1
	6	1.6	3.1	4.2	4.5	5.7	5.6
	7	0..7	1.8	2.1	3.2	3.6	3.8
	8	1.3	1.8	2.8	3.3	3.6	5.0
	9	1.3	1.5	2.1	] 2.6	2.8	2.6
	10	3.5	6.1	9.0	11.2	10.6	12.0
	11	2.8	8.7	13.8	15.0	15.9	18.3
	12	0.9	1.8	6.0	3.8	4.3	5.0
	13	1.6	2.2	3.6	4.6	4.9	4.9
	14	5.2	12.8	16.6	20.7	20.9	21.7
	15	3.3	13.3	17.3	17.4	18.9	19.7
	16	4.3	7.2	12.6	15.6	15.1	16.3
	17	1.3	2.3	4.8	7.0	9.4	8.1
	18	0.9	1.0	3.6	5.0	5.4	7.5
	19	1.1	1.9	2.9	5.0	6.7	6.8
	20	1.3	13.1	10.5	17.7	17.3	12.9
	21	2.5	4.0	7.6	8..8	9.5	9.7
	22	0.6	0..8	1.0	1.2	1.8	2.8
	23	2.0	1.4	1..8	4.8	5.9	6.0

Date	Site No.	0-2.5 cm	2.5-5.0 cm	5.0-7.5 cm	7.5-10 cm	10-12.5cm	12.5-15 cm
	24	2.4	3.8	5.0	5.9	7.1	6.5
	25	1.2	5.6	9.5	10.2	15.0	15.9
	26	2.6	5.6	11.4	15.9	18.6	19.9
	27	7.1	7.3	15.1	10.2	8.3	10.7
	28	2.2	3.4	4.7	5.1	5.2	5.2
	29	8.1	8.6	8.1	7.6	8.2	8.5
	30	7.1	1.3	1.8	3.4	5.3	5.8
	31	9.3	15.8	12.9	12.9	11.4	16.2
	32	3.6	9.9	11.9	12.9	13.8	15.6
	33	3.3	10.4	10.9	11.6	15.9	17.9
	34	1.3	3.7	4.2	4.4	5.2	5.8
	35	1.7	4.4	10.8	10.5	12.1	11.4
	36	2.8	5.6	6.6	6.5	6.4	6.4
	37	0.5	2.7	7.5	9.3	8.6	8.7
	38	1.7	5.1	8.5	15.4	16.0	17.4
	39	0.5	3.1	5.8	5.4	7.0	8.5
	40	0.3	1.0	2.7	4.5	5.0	6.0
	41	1.9	3.3	6.4	6.7	7.1	6.4
	42	0.5	0.9	3.6	4.1	4.8	4.5
	43	0.6	5.3	5.4	5.4	6.6	6.5
	44	0.3	0.5	2.0	2.7	7.2	5.7
	45	0.3	0.4	0.9	2.1	4.0	3.6
	46	0.1	0.8	0.4	3.1	3.4	3.4
	47	0.5	1.1	1.6	2.3	2.2	2.4
	48	0.3	0.6	1.1	1.6	2.6	3.0
	49	0.5	1.3	2.4	7.6	7.5	8.5

Date	Site No.	0-2.5 cm	2.5-5.0 cm	5.0-7.5 cm	7.5-10 cm	10-12.5cm	12.5-15 cm
	50	1.8	3.7	8.9	10.9	10.0	9.4
	51	1.1	2.4	5.3	6.0	10.3	20.4
	52	2.6	7.3	13.5	16.2	16.4	16.7
	53	1.3	2.4	3.9	6.7	7.6	8.8
8/8/73	54	11.0	10.6	10.0	9.2	8.8	8.4
	55	14.1	13.6	13.0	12.6	12.0	11.3
	66	17.5	15.4	13.6	13.7	13.5	12.5
	57	8.6	8.0	9.8	9 6	9.3	9.6
	58	10.5	8.9	10.2	10.8	9.6	8.7
	59	17.8	17.9	18.2	18.4	16.3	14.0
	60	15.5	14.2	12.5	10.8	10.3	10.1
	61	18.1	16.9	15.6	7.6	7.5	7.9
	62	2.1	1.0	1.2	2.2	2.3	4.9
	63	5.3	3.5	3.9	5.5	5.3	5.7
	64	1.2	0.4	0.4	0.3	1.0	0.9
	65	0.4	1.3	1.4	1.4	2.6	5.6
	66	2.5	3.0	3.9	4.6	6.0	7.1
	67	1.4	2.7	2.9	7.4	11.4	12.3
	68	4.0	8.9	15.4	16.1	16.6	17.2
	69	1.3	2.6	5.9	7.2	9.2	10.3
	70	1.1	2.0	2.5	3.5	5.3	5.3
	71	0.9	1.4	2.3	3.1	5.1	6.0
	72	0.3	0.2	2.3	2.2	3.0	3.2
	73	0.5	0.9	7.6	2.3	3.0	2.6
	74	0.2	1.1	1.7	3.0	3.4	5.0
	75	2.9	4.1	5.2	7.6	9.3	11.4

Date	Site No.	0-2.5 cm	2.5-5.0 cm	5.0-7.5 cm	7.5-10 cm	10-12.5cm	12.5-15 cm
	76	4.6	6.8	9.3	10.7	11.8	11.8
	77	1.6	5.2	6.7	9.3	10.5	10.9
	78	2.0	5.0	7.4	7.7	8.8	7.5
	79	4.8	10.3	12.5	13.7	12.7	13.5
	80	1.3	3.0	5.3	7.4	11.3	11.7
	81	2.1	4.4	7.0	10.6	13.2	14.0
	82	2.7	4.6	7.8	11.2	15.1	14.8
	83	20.4	20.1	25.0	24.2	27.1	22.6
	84	0.8	1.9	2.9	4.2	6.1	7.0
	85	1.5	5.1	6.7	9.3	17.3	15.5
	86	1.2	3.5	5.9	8.5	9.5	8.9
	87	13.8	16.7	17.2	18.0	17.5	17.6
	88	3.1	6.5	11.2	13.4	13.8	15.9
	89	2.8	6.5	11.8	13.8	13.0	13.4
	90	1.8	2.7	3.3	20.0	15.4	14.3
	91	3.6	5.8	8.0	10.8	10.7	10.0
	92	4.5	5.3	6.9	7.2	6.6	6.9
	93	3.1	6.7	8.2	9.2	9.7	11.1
	94	4.7	3.6	5.9	11.8	13.1	13.7
	95	4.0	6.4	9.2	9.7	10.2	10.7
	96	4.9	7.0	8.4	10.6	11.1	10.9
	97	7.7	7.9	8.3	8.2	8.9	9.1
	98	5.4	8.6	11.5	13.8	13.4	14.1
	99	13.6	14.0	12.6	10.8	10.1	11.2
	100	0.6	1.1	3.6	4.1	5.7	5.8
8/9/73	101	2.1	2.4	3.9	6.0	5.9	6.4

301

Date	Site No.	0-2.5 cm	2.5-5.0 cm	5.0-7.5 cm	7.5-10 cm	10-12.5cm	12.5-15 cm
	102	0.9	1.4	2.1	3.5	5.3	6.1
	103	0.5	1.5	3.0	4.5	5.8	6.2
	104	0.6	3.9	6.0	6.6	6.8	7.9
	105	1.0	1.8	3.2	4.2	5.5	6.4
	106	1.0	9.6	10.7	12.2	12.1	12.1
	107	2.1	5.1	9.9	12.6	13.0	12.0
	108	3.6	6.4	8.8	11.8	12.0	10.7
	109	2.4	3.0	5.0	6.3	7.1	8.7
	110	4.7	6.9	7.6	6.5	6.4	6.1
	111	1.1	2.3	3.4	4.1	4.3	4.6
	112	4.2	20.3	22.0	23.3	24.9	22.8
	113	4.3	7.7	11.4	16.8	20.8	19.6
	114	3.2	7.5	10.7	11.9	11.9	10.5
	115	1.9	2.7	4.9	6.5	7.7	9.0
	116	2.5	4.1	5.7	6.3	7.4	7.4
	117	3.2	5.7	6.8	8.7	4.4	7.7
	118	1.8	3.1	5.1	7.2	7.4	7.7
	119	4.1	6.8	12.4	15.0	15.7	15.5
	120	2.5	5.3	9.6	11.3	9.0	9.4

Field Measurements of Soil Moisture
In Percent by Weight
For Pass 38
Texas

Date	Site No.	0- 2.5 cm	2.5- 5.0 cm	5.0- 7.5 cm	7.5- 10 cm	10- 12.5cm	12.5- 15 cm
9/8/73	1	14.0	14.4	14.7	14.4	13.4	16.2
	2	17.4	17.6	17.2	16.8	18.3	18.1
	3	18.8	19.4	18.8	18.0	15.8	14.3
	4	12.3	13.1	13.1	13.2	14.6	17.0
	5	33.9	37.4	33.0	35.3	30.2	31.7
	6	17.2	17.5	17.5	17.7	17.7	16.8
	7	21.7	22.3	22.0	20.5	19.9	20.3
	8	21.8	19.2	18.9	17.6	17.8	15.8
	9	9.8	10.6	12.4	13.8	13.9	14.2
	10	11.0	11.7	12.1	11.9	11.4	7.8
	11	11.3	11.8	11.8	11.5	11.0	9.7
	12	10.0	11.2	11.1	10.5	8.5	7.1
	13	12.1	13.0	12.7	12.4	10.5	6.1
	14	9.4	9.8	8.8	5.0	5.8	6.0
	15	12.1	13.0	12.4	11.8	11.5	9.0
	16	12.0	14.5	13.9	13.6	6.5	7.7
	17	11.2	11.9	11.6	11.4	9.8	8.4
	18	11.0	11.6	11.4	8.7	8.7	10.3
	19	11.0	13.8	14.3	13.7	13.0	11.7
	20	11.0	11.8	12.6	12.5	12.2	11.6
	21	6.5	10.6	10.8	10.9	9.8	9.6
	22	3.8	6.1	6.5	7.7	8.1	8.9
	23	6.6	9.5	9.6	9.8	9.7	8.8

Date	Site No.	0-2.5 cm	2.5-5.0 cm	5.0-7.5 cm	7.5-10 cm	10-12.5cm	12.5-15 cm
	24	6.3	8.8	8.3	10.1	8.7	7.8
	25	7.5	7.5	6.0	3.3	2.5	2.5
	26	7.1	12.0	11.8	9.1	7.0	6.0
	27	5.9	7.2	7.9	7.9	9.0	7.7
	28	5.3	7.0	7.1	7.3	5.8	2.7
	29	3.9	4.4	6.3	6.9	6.0	5.9
	30	4.9	3.8	4.0	2.1	9.0	6.2
	31	5.5	6.2	6.7	7.0	7.3	7.4
	32	8.0	6.9	7.1	7.1	6.3	5.8
	33	0.8	2.4	0.6	2.1	2.1	2.0
	34	10.3	11.1	8.1	6.1	6.2	7.1
	35	11.8	12.5	10.5	7.8	5.7	5.9
	36	7.2	7.9	8.9	6.9	4.7	2.9
	37	7.8	10.7	11.4	11.5	11.3	11.2
	38	6.4	10.2	12.6	18.2	12.2	13.8
	39	6.8	9.8	11.1	10.0	10.0	10.3
	40	3.5	9.3	11.6	12.1	10.2	10.1
	41	14.6	15.0	13.9	12.6	11.6	12.2
	42	21.3	20.2	20.8	19.2	20.0	19.3
	43	7.3	8.9	9.6	10.8	10.3	9.5
	44	4.7	8.7	10.4	10.9	10.1	10.2
	45	8.3	6.5	7.1	7.1	7.4	6.8
	46	3.5	2.8	3.3	3.6	3.8	3.0
	47	3.1	5.7	6.5	6.1	6.6	8.8
	48	1.4	1.8	1.9	3.2	3.8	4.2
9/9/73	49	1.1	1.4	1.6	1.8	2.3	2.6

Date	Site No.	0-2.5 cm	2.5-5.0 cm	5.0-7.5 cm	7.5-10 cm	10-12.5cm	12.5-15 cm
	50	1.3	2.2	3.1	3.5	4.0	4.3
	51	0.9	2.0	1.5	2.9	1.9	2.0
	52	1.2	1.3	2.5	2.3	1.7	1.3
	53	0.4	0.8	1.3	1.6	0.9	1.0
	54	0.9	0.9	1.1	1.6	1.5	1.1
	55	0.6	0.8	0.9	1.4	1.9	1.2
	56	0.5	1.3	1.6	1.4	1.7	1.6
	57	0.3	1.2	2.0	1.7	1.4	1.2
	58	0.3	0.9	1.1	2.1	2.3	2.3
	59	0.5	0.8	1.1	1.9	2.1	1.6
	60	2.1	21.5	1.9	2.0	2.6	1.6
	61	1.4	2.9	4.9	5.3	5.0	5.1
	62	1.9	3.6	4.5	3.3	3.1	2.6
	63	1.6	6.2	6.1	6.3	5.9	5.2
	64	1.4	4.5	4.6	4.8	4.8	4.4
	65	3.3	4.4	4.8	4.4	3.3	3.8
	66	1.3	6.4	6.3	6.5	6.7	7.3
	67	2.1	4.3	9.2	5.9	4.9	4.7
	68	1.5	6.9	8.8	7.6	7.7	8.6
	69	2.7	5.6	5.8	5.5	5.8	5.3
	70	2.6	6.8	6.6	7.6	7.5	7.0
	71	1.4	4.4	6.9	4.5	4.2	3.9
	72	2.2	6.0	6.7	6.8	6.8	6.4
	73	2.1	5.4	6.7	7.5	6.0	5.0
9/10/73	74	2.7	2.6	3.6	3.5	2.8	2.2
	75	3.9	4.7	5.2	5.3	5.9	5.7

Date	Site No.	0- 2.5 cm	2.5- 5.0 cm	5.0- 7.5 cm	7.5- 10 cm	10- 12.5cm	12.5- 15 cm
	76	2.5	5.1	5.6	4.8	5.7	5.4
	77	2.6	4.2	5.4	6.7	6.4	11.0
	78	4.5	5.7	7.5	6.3	6.9	6.9
	79	5.7	8.5	11.3	12.6	8.8	11.8
	80	8.7	10.3	10.2	10.3	10.1	9.3
	81	3.7	7.4	8.4	8.6	8.7	8.2
	82	19.5	17.4	16.4	16.0	15.5	15.3
	83	14.6	12.6	12.5	10.0	9.8	9.8
	84	16.9	14.8	14.2	14.2	12.0	11.1
	85	8.6	10.7	12.0	11.6	11.8	12.0
	86	8.1	9.6	8.9	8.0	8.0	8.5

Field Measurements of Soil Moisture
In Percent by Weight
For Pass 38
Kansas

Date	Site No.	0-2.5 cm	2.5-5.0 cm	5.0-7.5 cm	7.5-10 cm	10-12.5cm	12.5-15 cm
9/13/73	1	37.0	30.8	25.8	24.0	25.0	24.8
	2	40.7	38.6	38.0	35.2	34.7	34.2
	3	32.4	30.9	30.6	29.6	29.3	26.4
	4	45.3	41.3	38.4	33.4	33.7	35.5
	5	42.0	39.9	36.4	32.0	32.2	30.8
	6	34.0	35.4	27.3	22.1	21.8	23.0
	7	38.6	29.8	27.2	27.5	26.3	27.7
	8	53.4	48.4	37.5	35.0	27.8	28.0
	9	32.4	26.0	24.0	23.0	23.8	24.6
	10	33.1	22.1	23.5	28.6	28.3	27.9
	11	42.6	39.5	37.1	36.9	30.2	28.5
	12	27.4	23.1	21.9	21.6	21.5	22.9
	13	55.2	47.6	43.8	38.2	39.5	38.4
	14	52.5	44.7	36.2	32.3	31.6	31.7
	15	43.3	38.9	31.2	27.4	27.9	26.6
	16	30.3	24.5	22.6	21.2	20.7	20.6
	17	27.0	23.3	22.7	21.6	21.2	21.1
	18	28.4	27.6	27.5	25.9	24.7	24.8
	19	33.5	30.1	30.4	31.1	32.0	32.6
	20	27.3	27.2	27.8	26.7	26.9	27.3
	21	35.2	35.0	35.8	36.8	32.4	31.2
	22	45.7	39.8	37.6	35.5	34.6	33.5
	23	41.5	33.8	30.4	27.4	27.4	28.9

Date	Site No.	0-2.5 cm	2.5-5.0 cm	5.0-7.5 cm	7.5-10 cm	10-12.5cm	12.5-15 cm
9/14/73	24	34.6	29.7	27.3	26.2	23.2	21.2
	25	26.3	24.0	23.0	19.9	16.4	18.2
	26	17.7	13.7	11.5	9.1	9.5	15.6
	27	14.3	20.2	19.0	20.2	20.5	19.5
	28	12.2	19.3	21.2	21.4	22.7	31.3
	29	12.7	16.7	18.8	18.3	20.1	20.0
	30	33.1	31.7	26.9	26.7	26.6	25.2
	31	22.6	20.5	21.2	21.2	21.0	22.6
	32	35.0	30.1	29.8	28.5	29.3	27.9
	33	38.3	35.0	31.5	31.1	30.7	30.1
	34	24.6	24.8	22.5	22.1	21.8	21.2
	35	9.3	16.9	18.8	18.0	16.0	14.5
	36	32.1	27.1	27.8	24.9	23.7	22.0
	37	24.1	23.9	22.5	20.8	21.1	18.3
	38	20.4	20.1	20.4	20.6	21.3	22.0
	39	17.3	16.3	15.9	15.9	15.8	15.9
	40	29.3	30.0	29.6	28.7	28.2	27.1
	41	25.7	24.1	22.9	22.5	23.1	22.4
	42	24.8	23.4	20.8	21.0	21.4	21.8
	43	41.9	31.9	29.2	26.4	24.9	22.5
	44	20.7	16.4	16.0	16.0	13.8	12.9
	45	24.1	22.8	23.6	23.4	24.0	25.3
	46	18.7	18.0	17.7	17.5	17.4	16.2
	47	33.0	32.7	29.0	27.3	29.6	30.0
	48	33.9	82.4	30.8	28.7	26.6	24.7
	49	37.4	32.4	29.3	30.5	24.8	27.5

Date	Site No.	0-2.5 cm	2.5-5.0 cm	5.0-7.5 cm	7.5-10 cm	10-12.5cm	12.5-15 cm
	50	37.7	32.3	31.0	29.5	29.0	27.6
	51	31.0	34.7	29.4	26.5	24.5	22.7
	52	23.9	23.4	22.3	23.3	23.7	23.2
	53	42.2	41.9	36.5	32.1	30.0	33.7
	54	33.0	25.0	23.6	23.7	24.3	24.6
	55	45.1	43.1	53.7	37.2	36.7	33.8
	56	43.4	39.2	34.5	31.9	28.8	27.1
	57	27.9	27.8	27.1	26.3	25.0	23.6
	58	29.1	30.7	29.3	30.5	29.8	28.8
	59	33.0	31.0	29.3	27.6	26.5	26.4